SORPTION AND EMULSION LIQUID MEMBRANES IN THE REMEDIATION OF METAL PROCESSING WASTE WATER EFFLUENTS USING RHODIUM, TRIOCTYLAMINE AND TRIHEXYLAMINE AS A MODEL

A thesis submitted in fulfilment of the requirements for the degree of

MASTER OF SCIENCE (PHARMACY)

of

RHODES UNIVERSITY

by

FRANCIS MOYO

JANUARY 2014

Faculty of pharmacy

RHODES UNIVERSITY

Grahamstown

South Africa

ABSTRACT

Two optimised ELMs were prepared with the diluent always being 30 % solution of toluene in kerosene. The first ELM contained 30.000 g/L (w/v) polyisobutylene, 10.870 g/L (m/v) of trioctyl amine and 51.001 g/L (m/v) of SPAN 80. The other optimised ELM was composed of 20.000 g/l of polyisobutylene, 10.268 g/l trioctyl amine and 50.024 g/l of SPAN 80. The stripping phase was always 2 M HNO_3 and the mixing ratios of organic phase to stripping phase were 1:1 and 2:1. The *t*-test was used to test for the difference between the mean micro-droplet sizes had a *p*-value of 0.3018 at 5 % level of significance, i.e. there was no statistically the mean micro-droplet size of the optimised ELMs. Demulsification was performed with polyethylene glycol with molecular weight of 400 g/mol at 50 ± 1 °C for 24 hours. The volumetric ratio of treated side-stream and the ELM was 5:1 and 98.7 to 108 % of the initial Rh amount was recovered in the stripping phase after chemical demulsification. Major carryover of the diluent components into the stripping phase observed was from trioctyl amine, toluene and polyethylene glycol was observed. The final spent side-stream should not be discharged into the environment based on the acute *Daphnia pulex* toxicity test. For sorption studies, the specific surface area of kaolin was 18.21 ± 0.8 m^2 g^{-1} and loss on ignition was 0.0086 ± 0.004 %. Removal efficiencies of trioctyl amine for 10 g of kaolin and particle size 65-100 µm and 101-400 µm were 18.1 % and 17.5 % respectively while sorption capacities were 0.92 g/g and 0.88 g/g respectively. The removal efficiency of 20 g of kaolin was 35.8 % and 33.3 % and sorption capacities were 0.93 g/g and 0.87 g/g respectively. For particle sizes 101-400 µm, the R^2 values obtained for Freundlich and Langmuir were 0.9757 and 0.9819 respectively. The *n* and K_f for Freundlich isotherm were 1.086 and 2.622. Removal efficiency for trihexyl amine for particle size 101-400 µm and 65-100 µm was 28.5 % and 29.3 % respectively while sorption capacities were 0.73 g/g and 0.75 g/g respectively. The R^2 values obtained for Freundlich and Langmuir for particle sizes 101-400 µm were 0.957 and 0.989 respectively. The *n* and K_f for Freundlich isotherm were 1.307 and 2.151 respectively. These results suggest that kaolinite could potentially be used in remediation of metal wastewaters containing hydrophobic extractants.

TABLE OF CONTENTS

LIST OF FIGURES

LIST OF TABLES

ACKNOWLEDGEMENTS

First and foremost, I thank my friend God for His presence in my life and for providing me with protection, strength and resolve to succeed throughout my studies. It is only through His grace, mercy and willingness that I was able to carry out and complete this work in a timely manner.

I would like to express my sincere gratitude to the following people and organizations:

My parents, Shadreck and Simangaliso Moyo for giving me a life that I have come to love and Cherish. I am forever grateful to my parents for the values, teachings and beliefs that they instilled in me as well as for the sacrifices and decisions that they made to support my education. In addition my immediate and extended family members for their encouragement, love, support and understanding throughout my years as a student. Special thanks to my uncles Khumbulani and Chido Gumbo for having played a major role in my upbringing.

My supervisor Dr Roman Tandlich for giving me the opportunity to be part of his research group and for his support, patience, guidance and assistance throughout the course of my studies and during the preparation of this thesis and also for providing me with laboratory facilities and financial assistance. In addition, many thanks to Dr R. Tandlich for giving me the opportunity to attend the International Symposium on "Emerging Pollutants in Irrigation Waters: Origins, Fate, Risks, and Mitigation", 25-28 November 2013, Gammarth, Tunisia.

The Head and Dean, Professor R.B. Walker and the staff of the Faculty of Pharmacy, Rhodes University for use of the facilities in the Faculty and for their support and friendship during my time as a postgraduate student in the Faculty.

Mr. Dave Morley, Mr. Tichaona Samkange, Mr. Leon Pardon, Mr. Collin Nontyi, Ms Linda Emslie, Ms Tanya Kent and Mrs Morley for their technical assistance during my studies at

Rhodes University. Special thanks to Mr Sean James Bosman for proof reading this manuscript in a timely manner.

My colleagues, friends, past and present fellow postgraduate students in the Environmental Health and Biotechnology Research Group in the Faculty of Pharmacy and Rhodes University at large who have been a source of support and sometimes just laughter that kept me going throughout my research experience:

Ms. Asive Linyana, who has always been there for me through thick and thin and a special source of inspiration throughout my academic life in South Africa, for her unfailing love, support, encouragement and understanding, in addition to always showing interest in my research work. Many thanks Asive!

Finally, The Research Committee of Rhodes University and the Institute of water research (IWR) of Rhodes University for financial assistance during my studies.

ACRONYMS AND ABREIVATIONS

BLM	bulk liquid membranes
$CaCl_2$	Calcium chloride
COD	Chemical Oxygen Demand
D2EHPA	Di (2-ethylhexyl) phosphoric acids
EDS	Emulsion droplet size
EGME	Ethylene glycol mono-ethyl
ELM(s)	Emulsion Liquid Membrane(s)
HCl	Hydrochloric acid
HLB	Hydrophilic-lipophilic balance
HLM	Hybrid liquid membranes
HFLM	Hollow fiber liquid membranes
HFRLM	Hollow fiber renewal liquid membranes
FLM	Flowing liquid membranes
ICP	Induced coupled plasma
ILM	Immobilized liquid membranes
IR	Infra-red
KHP	Potassium hydrogen phthalate
KBr	Potassium Bromide
LD	Laser diffraction
LM(s)	Liquid membranes
LOD	Limit of detection
LOI	Loss on ignition

NAPL(s)	non-aqueous phase liquid(s)
O/W	Oil in water emulsion
O/W/O	Oil in water in oil emulsion
PCS	photon correlation spectroscopy
PEG	Polyethylene glycol with molecular weight of 400
PGM(s)	Platinum Group Metal(s)
PI	poly-dispersity index
PIB	Polyisobutylene
Rh	Rhodium
SEM	Scanning electron microscopy
SLM	Supported liquid membranes
SSA	specific surface area
TBP	Tributylphosphate
THA	Trihexyl amine
TOA	Trioctyl amine
TOPO	Tri-n-octylphosphine oxide
TVC	Taylor vortex column
W/O	Water in oil emulsion
W/O/W	Water in oil in water emulsion
XRD	X-ray diffraction
ZP	Zeta potential

CHAPTER 1
INTRODUCTION AND SCOPE OF THE STUDY

1.1. RHODIUM

Rhodium is part of the platinum group metals (PGMs) (Zimmermann, Menzel et al. 2003, Bernardis, Grant et al. 2005). These are six closely related metals with similar physical and chemical properties, namely palladium (Pd), platinum (Pt), osmium (Os), rhodium (Rh), iridium (Ir) and ruthenium (Ru) (Ravindra, Bencs et al. 2004, Rao, Trivedi 2005). They are classified as noble metals due to their high resistance to corrosion and oxidation (Rao, Trivedi 2005), high mechanical strength and good ductility (Ravindra, Bencs et al. 2004). They are known as good catalysts for various electrochemical reactions. For example, in metal nano- or micro-particles electrocatalysis, platinum-ruthenium ($Pt_{0.5}Ru_{0.5}$) nano particles are used in the oxidation of methanol in the direct methanol fuel cell (DMFC) (Rao, Trivedi 2005). PGMs are also used as catalysts in motor vehicles to reduce the emission of carbon monoxide, hydrocarbons and nitrogen oxide (Zimmermann, Menzel et al. 2003, Ravindra, Bencs et al. 2004). About 99 % of rhodium produced is used for catalysis (Ravindra, Bencs et al. 2004). PGMs have been used in many important industrial synthetic processes. These include reforming reactions in the petroleum refining industry, hydrogenation and dehydrogenation reactions in the pharmaceutical industry, organic and inorganic oxidation reactions (Bernardis, Grant et al. 2005). They are also used in jewellery, in dentistry as alloys and, in medicine, as treatment drugs for cancer (Ravindra, Bencs et al. 2004).

1.2. STUDY RATIONALE

Global production of PGMs has increased exponentially over the last century and this has, to some extent, reflected the growth in the number of applications of PGMs (Bernardis, Grant et al. 2005, Rao, Trivedi 2005). Known platinum reserves have decreased (Guibal, Von Offenberg Sweeney et al. 2002, Ravindra, Bencs et al. 2004) and this has raised concerns about the long

term ability to supply PGMs to meet future technological needs (Gordon, Bertram et al. 2006) and concerns on the significant environmental and social impacts such as water pollution (Curtis 2008, Rajak 2008, Mnwana, Akpan 2009). With known reserves decreasing as well as the steadily increasing demand and the increasing value of PGMs, the appreciable amount lost in wastewater streams needs to be recovered. Alternative extraction methods with low capital costs, low reagent or energy requirements and methods that are environmentally favorable need to be researched and employed.

Emulsion liquid membranes (ELMs) have been used in the processing of various chemical classes of compounds such as organic acids and base metals. Their advantages compared to classical solvent extractions include faster kinetics of extraction and the performance of extraction and metal stripping in a single step (Kislik 2009, Tandlich 2010). These features make them highly attractive for PGM processing, but no such applications have been documented in scientific literature/the public domain to date. The scope of this research is to address this knowledge gap with Rh as the model PGM. The choice of Rh is due to the fact that it is generally the last metal extracted from PGM-bearing materials, and its solution chemistry is the most complicated of all the PGMs. Commercial use of ELMs in extraction processes is often hindered by the instability of the stripping phase micro-droplets due to the absorption of water from the feed phase into the ELM matrix. The classical solution is to increase the surfactant concentration in the ELM. This increases the stability of micro-droplets, but also leads to decreased mass transfer rates during metal extraction. Thus a novel solution must be found to address this problem. One of the solutions proposed in literature for the extraction of base metals is the use of non-Newtonian liquids as ELMs. The simplest way to construct a non-Newtonian ELM is the addition of a polymer such as polyisobutylene (PIB) to an ELM diluent. The shear stress is further decreased by the extraction contactor - the Taylor-vortex column.

The use of reagents (such as organic solvents and extractants) that ensure higher efficiencies in the mining process have led to increased environmental pollution (Sales, Magriotis et al. 2013). Use of trioctyl amine (TOA) and other tertiary amines as extractants or carriers in liquid membrane (LM) studies in the extraction of metals from metal waste water effluents has been suggested (Kumbasar 2008, Kumbasar 2009, Ahmad, Kusumastuti et al. 2012). If mining waste water is accidentally released into the environment with TOA, it may lead to environmental

pollution. There is thus a need to investigate and develop methods to reduce the impact of hydrophobic organic chemicals released into the environment from the mining metallurgical industry and metal processing waste water effluents. This study focuses on the removal of TOA using sorption. For comparison, sorption of another tertiary amine, trihexyl amine (THA), will also be studied.

1.3. PURPOSE OF THIS STUDY

This study set out to investigate the application of emulsion liquid membranes (ELMs) in PGMs from the aqueous by-products of PGM refining. The by-products are generated as side-streams which require storage and reprocessing. Of the PGMs, rhodium (Rh) is one of the more inert and therefore difficult to extract (Lee et al. 2009).

1.3.1. Study Aims

The main aims of the study were to:

1. Formulate and manufacture an ELM which could be used in the extraction of rhodium in the remediation of metal processing waste water effluents. The study examines the aqueous chemistry of rhodium extracted from chloride solutions and considers the use of an emulsion liquid membrane technique for rhodium extraction. The system was based on the formation of a rhodium chloride feed solution used as a model of mining waste water effluent from mining and metal refineries. Rhodium-chloro complexes were formed using 0.01 M HCl (pH 2) and 0.001 M HCl (pH 3) to form a 7 mg/L concentration of rhodium. This was followed by the extraction of rhodium using the tertiary amine TOA as the extractant in a Taylor vortex column. The stripping stage is where rhodium is transferred from the organic phase back to an aqueous solution. Nitric acid (HNO_3) was used as the multiple cross-current stripping phase. In summation, the whole process consists of three main steps, namely: a) the formation of rhodium-chloro complexes using HCl, called the rhodium feed pre-treatment; b) the extraction process in a Taylor vortex column; and c) stripping. Further study of the effect of temperature on the ELM and the extraction process of rhodium was undertaken, as described in Chapter 4.

2. To investigate the feasibility of using a combination of the Taylor-vortex column and emulsion liquid membranes in the extraction of rhodium (Rh) from the model metal refinery side-streams.

3. To investigate the use of kerosene and TBP/toluene as diluents for the ELMs and TOA as an extractant in the emulsion liquid membrane.

4. To investigate the scale-up of the optimised system to an industrial scale.

5. To investigate the sorption of the extractant TOA and another tertiary amine, THA, using kaolinite, a low-cost adsorbent from kerosene. This is due to the risks of TOA being accidentally released from the mining side stream into the environment. This may lead to environmental contamination.

Aim 3 was accomplished, but limited success using the original diluent was observed. Modifications to the diluent were undertaken throughout the process. The pH of the aqueous phase was found to influence the extraction efficiency. Temperature of extraction showed a strong influence on the ELM's stability. Scale-up considerations were only accomplished in the theoretical domain, but temperature of extraction and the chemical de-emulsification were optimised for upgrade in the future. The complete extraction of Rh from the model side-stream (mining waste water generated after the processing of the minerals has been completed) has been achieved, and thus Aims 1 to 3 of the research have been satisfied. The pursuit of Aim 4 was contingent upon positive, conclusive results generated in preceding aims. Since the results are conclusive but not positive, Aim 4 could not be completed. Aim 5 was partially achieved. The maximum sorption obtained of TOA and THA were 35 %and 29 % respectively.

1.3.2 Objectives of the Study

1. To design a model mining and metal refinery waste water.

- The system was based on the formation of a rhodium chloride feed solution used as the mining and metal refinery effluent. Rhodium-chloro complexes were formed using 0.01 M HCl (pH 2) and 0.001 M HCl (pH 3) to form a concentration of 7 mg/L of rhodium.

2. To assess and optimise ELM composition and micro-droplet size.
3. To optimise de-emulsification of the emulsions.
4. To use Induced Coupled Plasma (ICP) to assess the amount of rhodium extracted from the aqueous phase after demulsification.
5. To determine the chemical oxygen demand (COD) of the aqueous phase after de-emulsification of the ELM so as to assess the carry-over of ELM components into the stripping phase, as this affects the efficiency of the extraction process.
6. To investigate the effect of temperature on the ELM and on the extraction of rhodium.
7. To assess the toxicity of the waste water effluent using *Daphnia pulex.*
8. To investigate adsorption principles and the application of low-cost adsorbent material kaolinite to remove the tertiary amines TOA (extractant) and THA.

1.4. THESIS ORGANISATION

Chapter 1: provides the overall structure of the study; starting by summarising the importance of rhodium as a part of the platinum group metals and its uses. The study rationale, aims and objectives of the study are outlined.

Chapter 2: This chapter presents a literature review of emulsion liquid membranes supporting the experimental procedures presented in Chapters 3 – 5. It focuses on the general description of ELMs as well as on the types available, the ELM process and the importance of micro-droplet diameter. It also explores problems associated with ELMs and proposed solutions to these, as well as the extraction of various metals from waste waters using Emulsion Liquid Membranes.

Chapter 3: The main focus of this chapter is to develop methods to track the concentration of the components of the ELM throughout the extraction process. This includes preparation of the

model metal refinery side-stream and quantification of the concentration of the ELM components in it.

Chapter 4: focuses on the emulsification, the optimisation of micro-droplet globule size and the de-emulsification of the emulsions after extraction. Chemical oxygen demand for the stripping phase was assessed after de-emulsification.

Chapter 5: This chapter examines the extraction of rhodium from a model of metal processing waste water effluent and the effects of temperature on the ELM and extraction, using the Taylor-vortex column.

Chapter 6: In this chapter, further work on the eco-toxicity of rhodium using *Daphnia pulex* was carried out on the waste water effluent remaining (side stream) after rhodium extraction. This was to assess the toxicity of the rhodium which remains un-extracted from the waste water.

Chapter 7: Sorption of the extractants TOA and THA using kaolinite as a sorbent matrix was investigated in this chapter.

Chapter 8: Presents the conclusions for this study and recommendations for future work.

References: A list of references cited in this thesis, according to the Harvard style of referencing, is presented at the end of each chapter.

Appendices: Additional comments from experimental events and secondary data are provided in the appendix section. Data which are not analytical results but need to be included to allow interrogation of the results are also appended.

REFERENCES

AHMAD, A.L., KUSUMASTUTI, A., DEREK, C.J.C. and OOI, B.S., 2012. Emulsion liquid membrane for cadmium removal: Studies on emulsion diameter and stability. *Desalination,* **287**, pp. 30-34.

BERNARDIS, F.L., GRANT, R.A. and SHERRINGTON, D.C., 2005. A review of methods of separation of the platinum-group metals through their chloro-complexes. *Reactive and Functional Polymers,* **65**, pp. 205-217.

CURTIS, M., 2008. Precious Metal: The impact of Anglo Platinum on poor communities in Limpopo, South Africa. *ActionAid, Johannesburg, South Africa,* .

GORDON, R.B., BERTRAM, M. and GRAEDEL, T., 2006. Metal stocks and sustainability. *Proceedings of the National Academy of Sciences of the United States of America,* **103**, pp. 1209-1214.

GUIBAL, E., VON OFFENBERG SWEENEY, N., VINCENT, T. and TOBIN, J., 2002. Sulfur derivatives of chitosan for palladium sorption. *Reactive and Functional Polymers,* **50**, pp. 149-163.

KISLIK, V.S., 2009. *Liquid membranes: principles and applications in chemical separations and wastewater treatment.* Elsevier Science, Amsterdam, Netherlands

KUMBASAR, R.A., 2009. Extraction and concentration study of cadmium from zinc plant leach solutions by emulsion liquid membrane using trioctylamine as extractant. *Hydrometallurgy,* **95**, pp. 290-296.

KUMBASAR, R.A., 2008. Selective separation of chromium (VI) from acidic solutions containing various metal ions through emulsion liquid membrane using trioctylamine as extractant. *Separation and Purification Technology,* **64**, pp. 56-62.

LEE, J., RAJESH KUMAR, J., KIM, J., PARK, H. and YOON, H., 2009. Liquid–liquid extraction/separation of platinum (IV) and rhodium (III) from acidic chloride solutions using tri-iso-octylamine. Journal of Hazardous Materials, vol. 168, no. 1, pp. 424-429.

MNWANA, S. and AKPAN, W., 2009. Platinum Wealth, Community Participation and Social Inequality in South Africa's Royal Bafokeng community—A Paradox of Plenty, *Proceeding 4th International Conference on Sustainable Development Indicators in the Minerals Industry–SDIMI* 2009, pp. 283-290.

RAJAK, D., 2008. 'Uplift and empower': The market, morality and corporate responsibility on South Africa's platinum belt. *Research in Economic Anthropology,* **28**, pp. 297-324.

RAO, C.R.K. and TRIVEDI, D.C., 2005. Chemical and electrochemical depositions of platinum group metals and their applications. *Coordination Chemistry Reviews,* **249**, pp. 613-631.

RAVINDRA, K., BENCS, L. and VAN GRIEKEN, R., 2004. Platinum group elements in the environment and their health risk. *Science of The Total Environment,* **318**, pp. 1-43.

SALES, P.F.D., MAGRIOTIS, Z.M., ROSSI, M.A.D.L.S., TARTUCI, L.G., PAPINI, R.M. and VIANA, P.R.M., 2013. Study of chemical and thermal treatment of kaolinite and its influence on the removal of contaminants from mining effluents. *Journal of environmental management,* **128**, pp. 480-488.

TANDLICH, R., 2010. Chapter 8 - Application of Liquid Membranes in Wastewater Treatment. In: VLADIMIR S. KISLIK, ed, *Liquid Membranes.* Elsevier, Amsterdam, Netherlands pp. 357-400.

ZIMMERMANN, S., MENZEL, C.M., STÜBEN, D., TARASCHEWSKI, H. and SURES, B., 2003. Lipid solubility of the platinum group metals Pt, Pd and Rh in dependence on the presence of complexing agents. *Environmental Pollution,* **124**, pp. 1-5.

CHAPTER 2

LITERATURE REVIEW: EMULSION LIQUID MEMBRANES

2.1. INTRODUCTION

A membrane is a thin, film-like structure that separates two phases (Kislik 2010). It is semi-permeable (Kislik 2010), meaning it is a selective barrier. It allows some particles or chemicals to pass through but remains impermeable to specific particles, molecules, or substances (Davis 1997). Membranes are used to separate mixed components in two different phases by the different rates at which these components move through the membrane. The advantage of using membranes is that they are easy to scale up for industrial purposes. Their simplicity in concept, operation and their low energy consumption makes them cost effective (Kislik 2010).

The concept of membranes has been extended to include liquids (Kislik 2010). Liquid membrane systems in wastewater treatment consist of three main components: the source (feed), also called the external phase; the liquid membrane which is normally made up of an organic diluent such as kerosene; and the receiving (stripping) phase emulsified in the liquid membrane (Kislik 2010, Tandlich 2010). The liquid membrane is immiscible with the source. An extracting reagent solution may be added to the system. It is also immiscible with the source. Extracting reagent solutions either flow between the feed and the receiving phases or it are stationary. The liquid membrane technique has been studied in the removal of heavy metals and organic pollutants in wastewater treatment (Kislik 2010).

There are three types of liquid membranes. These are bulk liquid membranes (BLM), emulsion liquid membranes (ELM) and supported or immobilized liquid membranes (SLM or ILM) (Kislik 2010, Tandlich 2010, Peng, Jiao *et al.* 2012a). The BLM is made up of a water immiscible phase (liquid membrane) which separates the stripping and the feed phases, preventing them from mixing. In some models of BLM the feed and stripping phases are one (Daugulis 2001), where the hydrophobicity character of the solute will allow it to partition in the hydrophobic diluent overlying the aqueous phase (Tandlich 2010). Systems using the principle of an organic membrane preventing the mixing of the aqueous feed phase and the stripping phase

are incorporated under the BLM such as hybrid liquid membranes (HLM) (Kislik, Eyal 1996, Mortaheb, Zolfaghari *et al*. 2010, Yongquan, Ming *et al.* 2012), hollow fiber liquid membranes (HFLM) (Guha, Majumdar *et al*. 1992), hollow fiber renewal liquid membranes (HFRLM) (Ren, Zhang *et al*. 2010, Ren, Yang *et al.* 2013), flowing liquid membranes (FLM) (Teramoto, Takeuchi *et al.* 2002), membrane contactor systems (Drioli, Romano 2001) and pertraction (Zhivkova, Dimitrov *et al.* 2004). In SLM or ILM, the liquid, which is usually organic and hydrophobic, is immobilized and supported by a polymeric or inorganic micro porous support and is held by capillary action. The structure serves as the membrane (Dzygiel, Wieczorek 2000). Emulsion liquid membranes (ELM) will be discussed in detail below.

2.2. EMULSION LIQUID MEMBRANES.

2.2.1. General description of Emulsion liquid membranes

An emulsion is a dispersion consisting of at least two immiscible phases, one of which is finely subdivided and uniformly dispersed as globules (dispersed phase) throughout the other liquid phase (continuous phase) (Remington 2006). This is achieved using mechanical agitation of the two immiscible liquids. Usually one liquid in an emulsion is essentially polar (e.g. aqueous) while the other is relatively non-polar (e.g. an oil). The liquid usually used is water to which water-immiscible organic solvents are added. Emulsions are thermodynamically unstable and are turbid in appearance. Thus a third component, the emulsifying agent (surfactant), is required to stabilize the emulsion (Allen, Popovich 2005, Remington 2006) . In oil in water emulsion (O/W), the oil phase is dispersed as globules throughout an aqueous continuous phase, while in the water in oil (W/O) emulsions, the oil serves as the continuous phase with water being the disperse phase. An emulsion liquid membrane results from combining the concepts of liquid membranes to those of emulsions.

Emulsion liquid membrane separation technique was invented by Li in 1968 (Patnaik 1995, Wan, Zhang 2002b, Kargari, Kaghazchi *et al*. 2004). This is an emerging technique which can be used in environmental and pharmaceutical engineering, hydrometallurgy and the food industry

(Wan, Zhang 2000). ELMs are the most effective technique used for extraction of very low concentrations (Fouad, Bart 2008). Therefore it could be used for the recovery of heavy metals (Patnaik 1995, Fouad, Bart 2008) such as copper, zinc, nickel and cadmium (Fouad, Bart 2008) from mining refinery waste water. ELMs can also be used in the purification of metal ions (Kargari, Kaghazchi *et al*. 2004) and the removal of organic contaminants such as organic acids and amines (Kargari, Kaghazchi *et al.* 2004), phenol, chlorophenol, and nitrophenol in industrial water treatment (Fouad, Bart 2008).

ELMs are a three-phase dispersion system (Fouad, Bart 2008). They are made up of the internal phase (stripping phase) which is emulsified in an immiscible organic phase (membrane phase) (Kargari, Kaghazchi *et al*. 2004). The membrane phase contains the extractant and the surfactant, which stabilizes the emulsion droplets (Fouad, Bart 2008). This is then dispersed in the external phase (Feed Phase) by agitation. Oil in water in oil (O/W/O) or water in oil in water (W/O/W) emulsions form depending on the internal or external phase (Kargari, Kaghazchi *et al.* 2004).

2.2.2. Types of ELMs and extraction mechanisms

There are two types of ELM systems, namely type 1 and type 2 systems. This is dependent on the presence or absence of a carrier/extractant (Chanukya, Rastogi 2013). The chemical potential difference between the external phase and the stripping phase is the driving force of solute transfer (Ho, Sirkar 1992).

2.2.3.1. ELM type 1 system

In this system the solute is soluble in all three phases: the feed phase, oil membrane phase and internal stripping phase. This leads to the easy diffusion of the solute from the feed phase down its concentration gradient through the membrane into the stripping phase. Once in the stripping phase, the solute is converted to an insoluble molecule by reaction with the stripping phase agent, making it difficult for the solute to diffuse back into the membrane. Due to this conversion of the solute in the stripping to an insoluble substance, the concentration of the solute remains

zero in the stripping phase. The concentration gradient thus remains high from the feed into the stripping phase (Park 2006, Chanukya, Rastogi 2010, Chanukya, Rastogi 2013).

2.2.3.2. ELM type 2 system

In this system a solute is insoluble in the membrane phase and hence requires a carrier/extractant to facilitate its movement across the membrane into the stripping phase. The first reaction occurs at the feed/membrane interphase, where the solute reacts with the carrier/extractant to form the solute/carrier complex. This complex diffuses into the membrane and, at the membrane/stripping phase interphase, the solute dissociates from the carrier and enters the stripping phase. Thus the carrier is regenerated to be reused to chelate another solute (Park 2006).

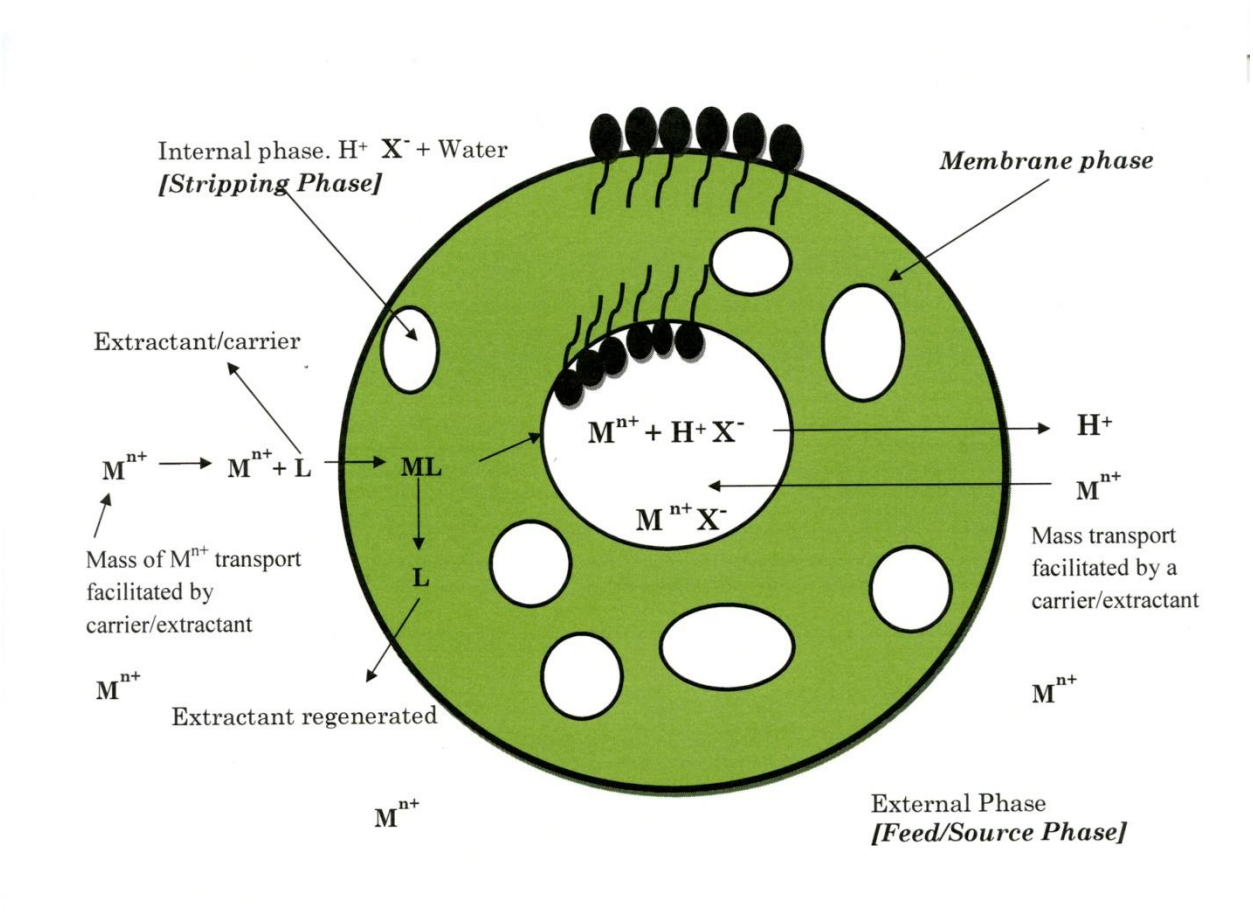

Figure 2.1: *Schematic representation of extraction of metal M using ELMs in type 2 ELM systems [Adapted from Park, 2006]*.

The following reaction takes place at the feed/membrane interphase (Park 2006):

$$\mathrm{M}^{2+}(ep) + 2\mathrm{RL}(mp) = \mathrm{MRL}_2(mp) \qquad (2.1)$$

And the following equation takes place at the membrane/stripping interphase (Park 2006).

$$\mathrm{MRL}_2\,(mp) + \mathrm{H}^{+}\mathrm{X}^{-}\,(sp) = \mathrm{M}^{2+}(\mathrm{i}p) + 2\mathrm{X}^{-}(ip) + 2\mathrm{RL}(mp) + \mathrm{H}^{+}(mp) \qquad (2.2)$$

Where M^{2+}represents a metal of interest, RL represents the liquid membrane containing the extractant L, MRL_2 is the metal liquid membrane and extractant complex, H^+X^- is the acid contained in the stripping phase. *Mp, sp, ip* and *ep* indicates the phase in which the species will be found i.e. mp (membrane phase), sp (stripping phase), ex (external phase) and ip (internal phase).

Liquid membranes (LM) are an alternative to the solvent extraction process. Therefore the extractants used in solvent extraction have been developed to be carriers in the LM transport process. Carriers are water immiscible and are dissolved in the LM, which is also water immiscible. These carriers selectively interact with the solute to form a carrier-solute complex. This is called carrier-facilitated coupled transport. This system has enhanced the selective separation and concentration of the solute in dilute concentrations (S Kislik 2010).

The carrier properties influence the LM performance. The carrier should be highly selective to the solute, meaning that it can easily form the carrier-solute complex. (Kislik 2009) This enables the carrier to extract the solute from the feed into the liquid membrane phase at the feed-LM interface (Kislik 2009). This means the carrier should have a high partition, extraction or distribution constant. Decomplexation of the carrier-solute complex at the LM-strip phase should be easy so the carrier is easily regenerated for the continuity and success of the extraction. The diffusion kinetics of the complex should be rapid for successful extraction. The carrier should have suitable viscosity, density and surface tension. It should not react with other components of the LM (Kislik 2009).

Carriers are divided into different classes. There is a group of amines (secondary, tertiary and quaternary) and their derivatives. These are proton acceptors. Tri-octyl-amine (TOA) a tertiary amine has been used in the separation of cobalt and nickel from acidic leach solutions by emulsion liquid membranes (Kumbasar, Tutkun 2008). Another group is of large organic acids and their derivatives. These are extractants such as di-(2-ethylhexyl) phosphoric acid (DEHPA). DEHPA has been used successfully by Fouad et al. (2008) in the extraction of zinc using ELMs and a hollow fiber contactor. A third class includes extractants with solvating and electron donor or acceptor properties. These include tri-n-octylphosphine oxide (TOPO) which has been used in the removal of chromium from aqueous waste solution using ELMs (Hasan, Selim *et al. 2009)*. Included in this group are carbon-oxygen compounds such as ketones, ethers and amides. Methyl *iso*-butyl ketone has been used in batch extraction of gold (III) ions from aqueous solutions using ELMs (Kargari, Kaghazchi *et al*. 2004).

2.3. EMULSION LIQUID MEMBRANE PROCESS

There are four main steps involved in the emulsion liquid membrane process: emulsion preparation, solute extraction, emulsion separation and demulsification. The membrane phase is largely composed of hydrophobic aliphatic diluents such as kerosene and is prepared first. It contains the extractant/carrier agent (in cases of type 2 emulsion), surfactant and the polymers for modification of viscosity (Ho, Sirkar 1992). The following factors should be considered when choosing a solvent: (1) low solubility in the external feed phase and the internal stripping phase in order not to lose the solvent during emulsion preparation and solute extraction; (2) compatibility with surfactant and the extractant dissolved; (3) moderate viscosity balancing the membrane stability and permeability; (4) enough density difference from the aqueous phase for the fast process of emulsion separation; (5) low cost of production and (6) low toxicity because of environmental concerns (Ho, Sirkar 1992).

The following should be considered when selecting an extractant (Park 2006): (1) the extractant should thermodynamically favour the formation of the extractant/solute complex from the feed phase; (2) the extractant should react fast enough to form this complex for fast solute extraction and (3) the complex should easily dissociate at the stripping phase. In this study, Tri-n-octylamine was used as an extractant. It has been successfully used in various studies as an extractant (Kumbasar 2008, Kumbasar 2009b, Ahmad, Kusumastuti *et al*. 2012,).

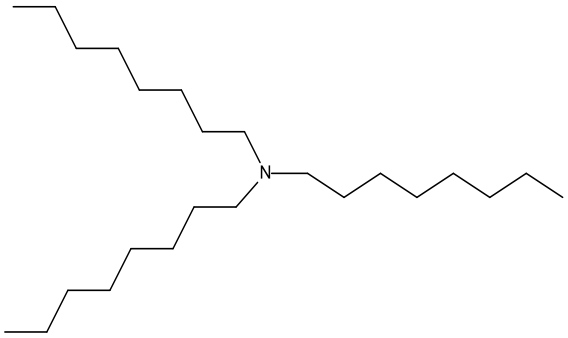

Figure 2.2: *Schematic representation of tri-n-octylamine*

2.3.1. Preparation of the emulsion and Droplet diameter

High pressure homogenisation, mechanical agitation, rotor stator devices (e.g., colloid mills), ultrasonic and static mixer techniques have been used for emulsification of the two immiscible phases because of their ability to produce small sized droplet (Mohan, Narsimhan 1997). In the emulsification process the internal/stripping phase is introduced to the membrane phase prepared (see above section 2.3). High speed agitators with stirring rates up to 20 000 rpm and ultrasonic emulsifiers are used to achieve the required droplet size of the desired emulsion (Park 2006). The internal phase contains a stripping agent which is thermodynamically favourable for the stripping process and exhibits a fast reaction with a solute-extractant complex for successful stripping (Park 2006). The droplet diameter is also important for high extraction efficiency and high stability of the membrane (Ahmad, Kusumastuti *et al.* 2011). Large droplet diameters produce poor extraction efficiency, resulting in poor membrane stability (Li, Cahn *et al*. 1983). Emulsions of good stability and rapid extraction have droplets in the range of 0.3 - 10 µm, although the most preferable range is 0.8 - 3 µm (Li, Cahn *et al*. 1983, Chanukya, Rastogi 2013). Smaller droplets have higher extraction efficiency as well as a better breaking resistance compared to larger droplets (Li, Cahn *et al*. 1983). Large droplets cause membranes to rapture easily due to easy coalescence, resulting in poor stability and poor extraction efficiency (Patnaik 1995). Figure 2.4 shows the size of the stripping phase micro-droplet diameter and the globule diameter of the emulsion globules in the feed phase after agitation.

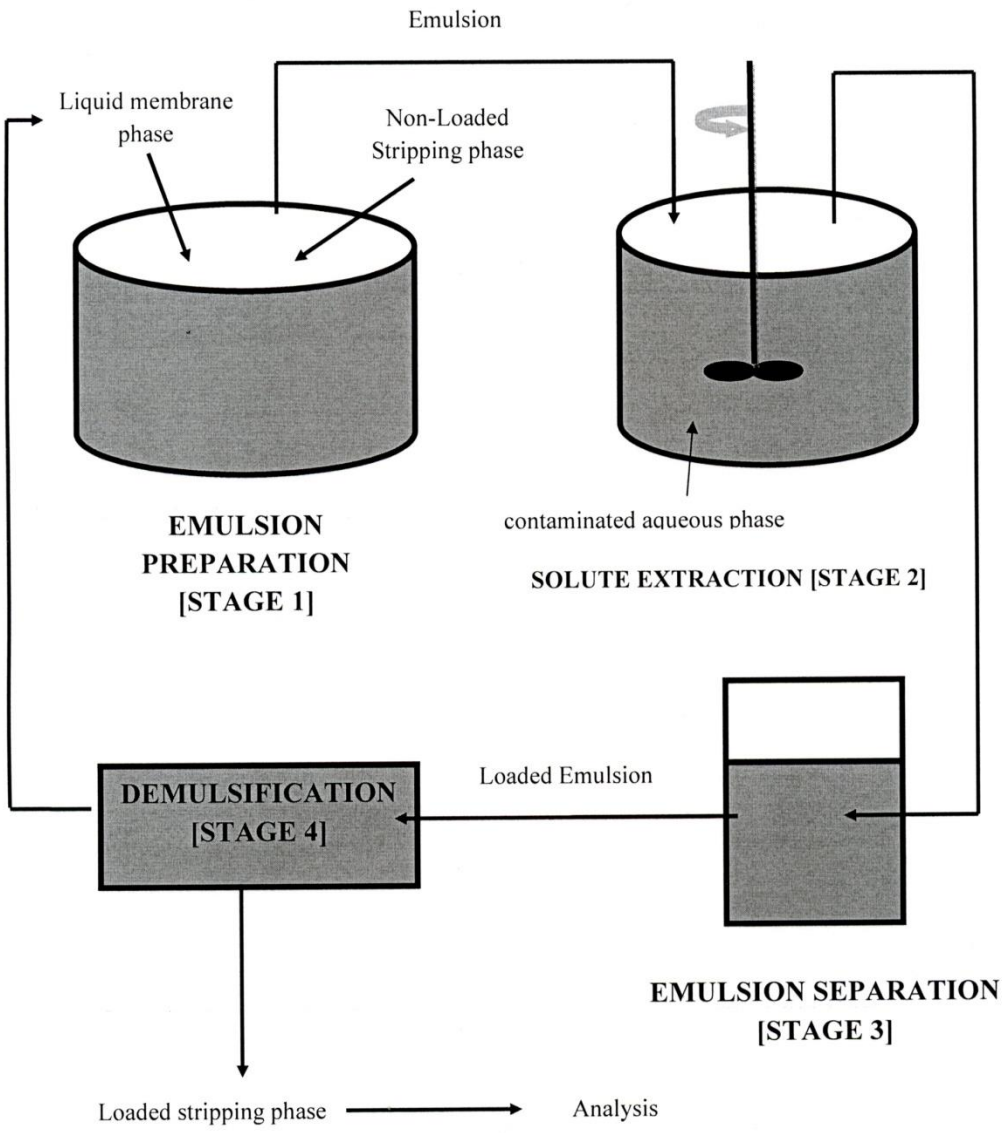

Figure 2.3: *The stages of the emulsion liquid membrane process [Adapted from Park, 2006].*

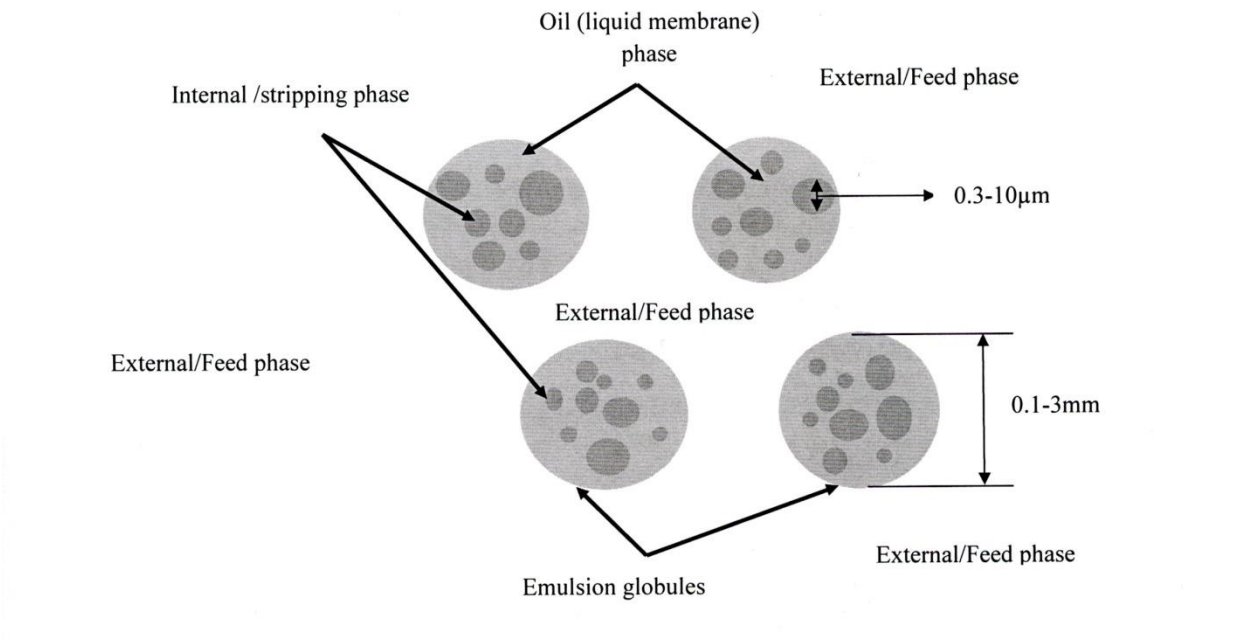

Figure 2.4: *The emulsion liquid membrane system showing the size of the stripping phase micro-droplet diameter and the globule diameter of the emulsion globules in the feed phase after agitation [Adapted from Park, 2006].*

2.3.2. Solute extraction

This process commences by introducing the prepared emulsion into the feed phase. These emulsions are mixed or agitated in the mixing reactor, leading to the dispersion of the emulsion form globules of 0.1 - 3 mm in diameter (Park, Skelland *et al*. 2006, Chanukya, Rastogi 2013). Speed of agitation is important. This should be high enough to form the required size globules for efficient extraction but should be low enough to reduce shear rate and shear stress, the main causes of emulsion instability leading to emulsion rapture and reducing the extraction efficiency. Therefore optimum speed of agitation is required in this stage.

2.3.3. Emulsion separation (setting)

Agitation is stopped after solute extraction and the system is left to rest. The emulsion separation/setting from the treated feed phase is governed by the density (Park 2006).

2.3.4. Demulsification

This is an important stage in the emulsion liquid membrane process (Park 2006). During this process the membrane phase is separated from the stripping phase, which now has a high concentration of the solute e.g. metal (Sun, Duan *et al*. 1998). The processes involved in demulsification are: coagulation or agglomeration of the droplets followed by coalescence of the agglomerated droplets (Kim, Wasan 1996, Al-Sabagh, Nasser *et al.* 2013). Coagulation is the coming together of the disperse medium in the emulsion, reducing the interfacial area, while coalescence is the coming together of agglomerated droplets to form bigger droplets, leading to the destabilization of the emulsion (Sun *et al.* 1998). There are two major demulsification approaches - physical treatment and chemical treatment. Three physical characteristics of the internal/stripping phase affect demulsification. These are the surfactant concentration, droplet size, and oil viscosity (Sun *et al.* 1998). This enhances the coalescence of the water droplets. Drawbacks of chemical demulsification are that the addition of the chemical will alter the properties of the membrane phase meaning that the membrane cannot be reused (Park 2006). Studies have revealed that nonionic surfactants such as tweens are good chemical demulsifiers and that surfactants with a high number of hydrophilic groups are good as demulsifiers (Shetty, Nikolov *et al.* 1992, Bhardwaj, Hartland 1998). This is because the hydrophilic groups of these surfactants form hydrogen bonds with water, making them good demulsifiers (Roodbari *et al.* 2011). Roodbari *et al.* (2011) studied the effect of TWEEN 40, TWEEN 60, TWEEN 80 and TWEEN 85 as demulsifiers on the heavy crude oil in water emulsions. They concluded that tweens have a greater effect as demulsifiers with the increase of Hydrophilic-lipophilic balance (HLB) values. Various studies have shown that chemicals have been successfully used as demulsifiers in chemical demulsification (Wang, Hu *et al.* 2010, Roodbari, Badiei *et al*. 2011, Tong, Zhang *et al*. 2013). Sometimes combinations of chemical and physical approaches are necessary for successful demulsification to take place (Sun, Duan *et al*. 1998). The physical approach involves heat, centrifugation, porous glass, ultrasonics, electrostatic enhancement and microwave radiation (Al-Sabagh, Nasser *et al*. 2013). Studies have shown that W/O emulsions are broken using these methods (Eow, Ghadiri 2002, Park 2006).

In this study a combination of the chemical approach and the physical approach was used. The chemical demulsifier used was poly ethylene glycol 400 (shown in figure 2.5 with CAS Number

25322-68-3 (PEG 400) with an HLB value of 11.6. Its molecular mass ranges from 370 - 430 g/mole.

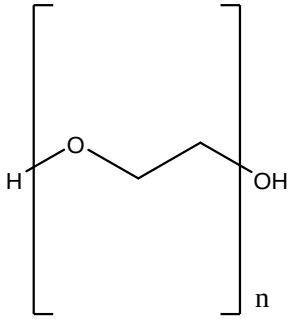

Linear Formula $H(OCH_2CH_2)_nOH$

Figure 2.5: *Schematic representation of PEG 400*

Figure 2.3 above shows all the four main steps involved in the emulsion liquid membrane process as outlined in sections 2.3.1, 2.3.2, 2.3.3 and 2.3.4.

2.4. PROBLEMS OF ELMS AND PROPOSED SOLUTIONS

2.4.1. Problems of ELMS

The main problems in the stability of ELMs are swelling and leakage (Sun, Duan *et al*. 1998, Kukizaki, Goto 2008, Mousavichoubeh, Ghadiri *et al.* 2011, Peng, Jiao *et al.* 2012b, Hosseini, Shahavi 2012). Stability of the membrane is defined as its ability to resist leakage or rapture in the process of solute extraction in the contactor (Patnaik 1995, Ahmad, Kusumastuti *et al.* 2011). Leakage is normally due to the high shear stress generated in the process of solute extraction (Park, Forney *et al*. 2004). Leakage is the most serious problem pointed out by researchers. It can prevent extraction from taking place because the stripping phase and extracted solutes leak back into the source phase (Park, Forney *et al*. 2004),rendering the ELM ineffective.

Swelling occurs when the external phase is incorporated into the emulsion, leading to an increase in the volume of the internal phase, causing several obstacles to the process of solute extraction. The drawbacks associated with swelling (Borwankar, Chan e*t al.* 1988, Bhowal, Datta 1997, Bandyopadhyaya, Bhowal *et al*. 1998) are: (1) the reduction of membrane thickness; (2)

viscosity of the ELM is compromised, impeding the extraction process from the feed phase (Wan, Zhang 2000, Park, Forney *et al*. 2004) and (3) it leads to the dilution of the final concentration of the solute (Park, Forney *et al*. 2004). Swelling is a result of pH, temperature, difference in ionic strength, viscosity of diluents, water volume fraction in W/O emulsion, by surfactant, carrier, acidity and salinity of aqueous phase and droplet size (Wan, Zhang 2000) and is also due to entrainment and osmosis (Ahmad, Kusumastuti *et al*. 2011). In entrainment swelling, the feed phase is drawn into the stripping phase as a result of coalescence of emulsion globules during the extraction process (Wan, Zhang 2000). In osmotic swelling, the pressure difference between the stripping phase and the external phase is the driving force. Osmotic swelling may be caused by a surfactant which moves back and forth through the membrane (Wan, Zhang 2000). Hydration of the surfactant takes place at the external phase/membrane phase interphase where the hydrophilic polar head of the surfactant forms a complex with a water molecule (Colinart, Delepine *et al*. 1984). The other process by which osmotic swelling occurs in the liquid membranes is the formation of the reversed micelles (Ho, Sirkar 1992). In the reversed micelle formation the hydrophilic heads of the surfactants are attracted by the aqueous core and they face each other or aggregate, creating a water or hydrophilic core, as shown in figure 2.6, while the hydrophobic tails of the surfactant are attracted by the hydrophobic phase - the liquid membrane (Park 2006). Water is easily solubilized in the hydrophilic core and hence the reversed micelles then transport the water into the internal phase (Ghosh 2011, Mohd-Setapar, Mohamad-Aziz *et al*. 2012).

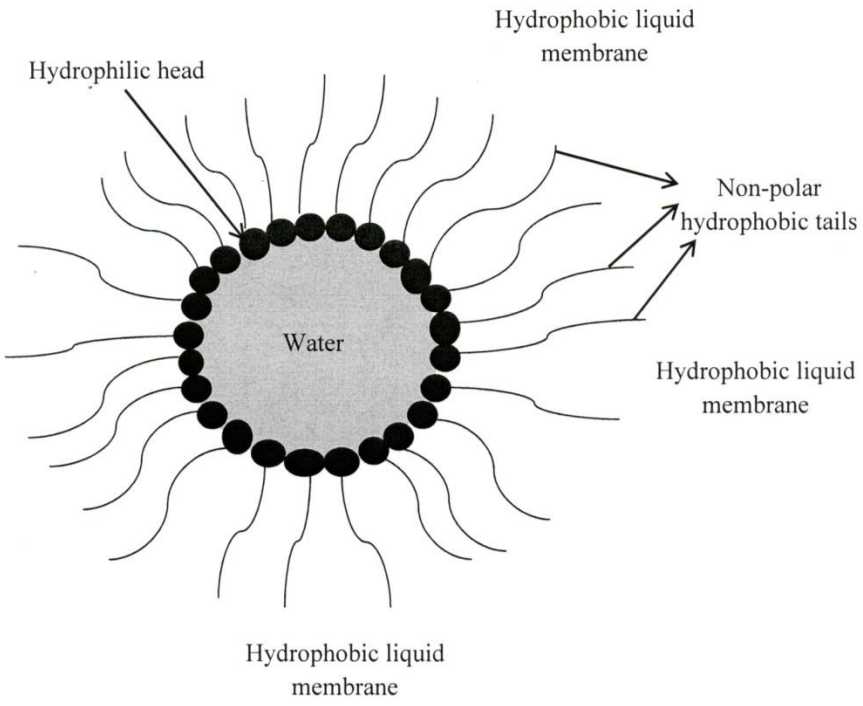

Figure 2.6: *Schematic representation of a reversed micelle.*

The use of ELM method in the removal and recovery of heavy metals is limited. It has been successfully used in extraction of zinc but, because of emulsion stability problems such as membrane swelling, coalescence and membrane leakage, its commercial use in the removal of other heavy metals is limited (Ho, Sirkar 1992, Malik, Wani *et al*. 2012). Swelling, coalescence and membrane leakage lead to the reduced extraction efficiency of the globules (Ahmad, Kusumastuti *et al*. 2011). The stability depends on composition of the membrane; therefore an understanding of the behaviour of the carrier, stripping agent, surfactant, and diluents during preparation is important in the selection process of the ELM constituents. Stability also depends on the shear produced by agitation which leads to the rupturing of the ELM (Gu, Ho *et al.* 1992). The internal droplet size may also contribute to membrane stability problems (Stroeve, Varanasi 1984, Patnaik 1995). The surface active agents, shear, occlusion and the extractant may cause swelling (Völkel, Halwachs *et al*. 1980, Stroeve, Varanasi 1984, Patnaik 1995). Addition of

hydrocarbons reduces swelling (Patnaik 1995). Addition of 5 % cyclohexanone reduced swelling by half (Gadekar, Mukkolath *et al.* 1992).

2.4.2. The proposed solutions of membrane instability

Stability of ELMs may be improved by increasing the concentration of surfactants (Gadekar, Mukkolath *et al*. 1992), the use of membrane diluent with high viscosity (Li 1971) and the use of non-Newtonian modifiers for the membrane phase. These are high molecular weight polymers such as polyisobutylene. These are dissolved in the membrane phase, causing the membrane to behave like a non-Newtonian fluid i.e, pseudo-plastic (Terry, Li *et al*. 1982, Skelland, Meng 1996). Optimizations of the operational conditions such as stirring speed, composition of emulsion and temperature have been investigated in order to try and improve ELM stability (Skelland, (Michael) Meng 1999).

2.4.2.1. Importance of Surfactant and the effects of its concentration

The selection of a surfactant is important because it will influence the swelling and breakage of the emulsion (Pfeiffer, Bunge *et al*. 1992, Correia, de Carvalho 2003, Chakraborty, Bhattacharya *et al*. 2004). Poor selection may lead to an ineffective ELM process (Wan, Zhang 2000). Surfactants are amphipathic compounds, meaning that they are composed of a hydrophilic polar part, which is the head, and a hydrophobic non-polar part, which is the tail (Gu, Ho *et al*. 1992, Wan, Zhang 2000, Ahmad, Kusumastuti *et al.* 2011). This makes them soluble in both water and organic solvents (Allen, Popovich 2005). Its major role results from its ability to reduce the interfacial tension between oil and water. As it decreases the mass transfer resistance, it is also an important constituent in the formulation of an emulsion (Chakraborty, Bhattacharya *et al*. 2010). If two immiscible liquids are agitated together so that one of the liquids is dispersed as small droplets in the other, in most cases the liquids separate rapidly into two clearly defined layers. This is because the cohesive force between the molecules of the individual liquids is greater than the adhesive force between the two liquids. The cohesive force of the individual phases is manifested as an interfacial energy or tension at the boundary between the liquids (Wan, Zhang 2000, Ahmad, Kusumastuti *et al*. 2011). Interfacial tension is reduced by the adsorption of the surfactant at the liquid-liquid interface (Aulton, Wells 2002). This is due to the formation of the

interfacial film around dispersed internal droplets precluding or delaying the process of coagulation and flocculation. They help in the maintenance of emulsion stability (Chakraborty, Bhattacharya *et al.* 2010). Apart from maintaining the stability of emulsion, other factors to consider are mass transfer resistance, water solubility and osmosis, which all lead to swelling. Various studies have showed that the choice of surfactant affects the stability of the emulsion (Basualto, Poblete *et al*. 2006, Kakoi, Goto *et al.* 1996).

Interfacial tension is inversely proportional to the concentration of surfactant (Nakashio, Goto *et al*. 1988, Kakoi, Goto *et al.* 1996, Wan, Zhang 2002). It decreases as the concentration of surfactant increases which leads to the formation of smaller droplets and hence a more stable emulsion. This will reduce the internal leakage of the membrane (Chakraborty, Bhattacharya *et al*. 2010). But increased concentration of the surfactant leads to the increase in swelling (Gasser, El-Hefny *et al*. 2008). Surfactant concentration also affects the viscosity of the ELM (Yan, Pal 2001, Wan, Zhang 2000, Yan, Pal 2004, Sengupta, Sengupta *et al*. 2006). Viscosity increases with increased surfactant concentration. Increases in viscosity of the membrane phase lead to a mechanically stable ELM (Ahmad, Kusumastuti *et al*. 2011). However it has its drawbacks. It leads to a decrease in the diffusion and mass transfer coefficients, resulting in a decrease in the extraction efficiency of the ELM (Li, Liu *et al.* 1997, Chakravarti, Chowdhury *et al*. 2000, Kumbasar 2009a). This can be explained using the Eyring-Stokes-Einstein equation (Lacks, Rear *et al*. 2007) below

$$D = \frac{KT}{\eta\lambda} \tag{2.3}$$

Where D is the molecular diffusivity or the diffusion coefficient of the solute extracted from wastewater in the membrane phase of the ELM in question ($m^2.s^{-1}$), and k is the Boltzmann constant, i.e. 1.38 x 10^{-23} ($J.K^{-1}$), T is the thermodynamic temperature (K), λ is the jump distance for a diffusive event (a solute property; m), and η is the dynamic viscosity of the membrane phase of the ELM (Pa.s). From the equation it can be noted that the increase in viscosity of the membrane phase leads to the decrease in the diffusion coefficient D of the solute inside the ELM leading to reduced extraction rates of the ELM (Terry, Li *et al*. 1982).

Therefore the concentration of the surfactant is vital to the ELM process. Optimum concentrations need to be determined for the success of the ELM process, two to five weight percentage (wt%) has been shown to be the optimum concentration of the surfactant (Terry, Li *et al.* 1982, Wang, Bunge 1990, Park, Forney *et al*. 2004). For a successful ELM process, the surfactant must be insoluble in the feed and the stripping phases and must be soluble in the membrane phase so as to prevent the loss of the surfactant during the whole process. It should not react with the extractant and should be stable in the presence of the stripping phase, which is likely to be either a base or an acid. Its resistance to mass transfer should be low and, finally, the demulsification process must not be hindered by the surfactant (Ahmad, Kusumastuti *et al.* 2011). The hydrophile–lipophile balance (HLB) value is also important when choosing a surfactant. They determine the type of emulsion formed. HLB is a scale of numbers whereby surfactants with HLB of 1-10 are more soluble in oil and those rated from 10 to 20 are more soluble in water. These tend to make water in oil emulsions and oil in water emulsions respectively (Park 2006) as shown in table 2.1. Hydration capacity of the surfactant is also important as well as molecular weight for a suitable surfactant. High molecular weight leads to low diffusivity of the surfactant. This and low hydration capacity are preferred for a stable surfactant (Kislik 2009).

Table 2.1: HLB values of surfactants and emulgents (Wan, Zhang 2000).

HLB range	use
1-3	Anti-forming agents
3-6	w/o emulsifying agents
7-9	Wetting agents
8-16	o/w emulsifying agents
13-15	detergents
15-18	Solubilising agents

In this study SPAN 80 (sorbitan mono-oleate CAS-No. 1338-43-8), a non-ionic emulsifying agent (Remington 2006), was used as the surfactant. Its HLB value is 4.2 and provides relatively stable w/o emulsions compared to SPAN 20 (HLB 8.6) (sorbitan monolaurate), SPAN 40 (sorbitan monopalmitate), SPAN 60 (HLB 4.7) (sorbitan monostearate), SPAN 65 (HLB 2.1)

(sorbitan tristearate) and ECA 4360 (a non-ionic polyamine) (Draxler *et al*. 1986, Nakashio *et al*. 1988, Venkatesan *et al*. 2009a). A stable emulsion will have very little coalescence of globules, minimum swelling and leakage, making it more efficient in the extraction of metals. SPAN 80 has been used successfully in various studies in the ELM extraction techniques below (Venkatesan, Meera Sheriffa Begum 2009b, Venkatesan, Meera Sheriffa Begum 2009c, Rajasimman, Karthic 2010, Goyal, Jayakumar *et al*. 2011, Chanukya, Rastogi 2013).

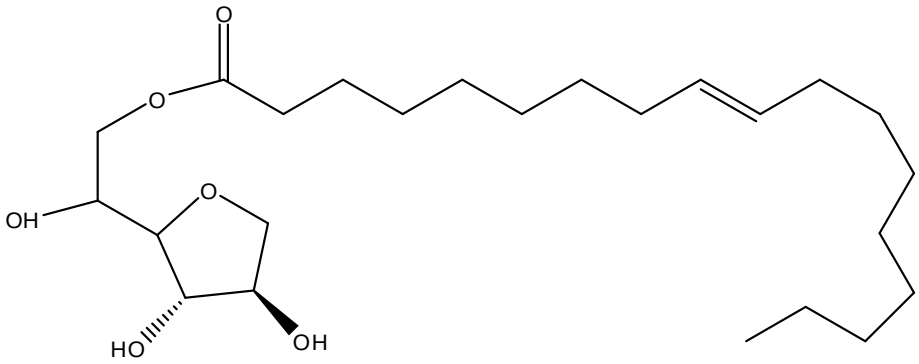

Figure 2.7: *Schematic representation of SPAN 80*

2.4.2.2. Newtonian and Non- Newtonian fluids

In Newtonian fluids, shear stress and shear rate are directly proportional, as shown in equation 2.6 (Aulton, Wells 2002, Allen, Popovich 2005, Remington 2006);

$$\sigma = \eta\gamma \tag{2.4}$$

Where σ is shear stress, γ is shear rate and η is the constant of proportionality which is also known as the coefficient of dynamic viscosity or simply as viscosity. It is a linear relationship. The constant of proportionality is viscosity. Viscosity can then be made the subject as shown in equation 2.5 below

$$\eta = \frac{\sigma}{\gamma} \tag{2.5}$$

The non-Newtonian liquid is used to modify the viscosity of the liquid membranes. Below the critical concentration and at low shears, the viscosity of the resulting mixture increases, thus increasing the ELM stability (Aulton, Wells 2002). In non-Newtonian fluids, the constant coefficient of viscosity cannot be defined. Therefore the diffusion coefficient of the extracted solute is independent of the ELM viscosity (Park 2006). This is only applicable below the critical concentration (the concentration of the polymer used in the ELM, at which the molecules of the polymer start undergoing intermolecular interactions with each other) of the non-Newtonian fluid (Skelland 1967). Increase in viscosity due to non-Newtonian liquid improves the process of extraction by reducing coalescence and movement of the ELM droplets, leading to a more stable and more efficient ELM (Skelland, (Michael) Meng 1999). This reduces the concentration of the surfactant used, hence leading to the lower affinity for water of the ELM, reducing the rates of swelling (Skelland, (Michael) Meng 1999).

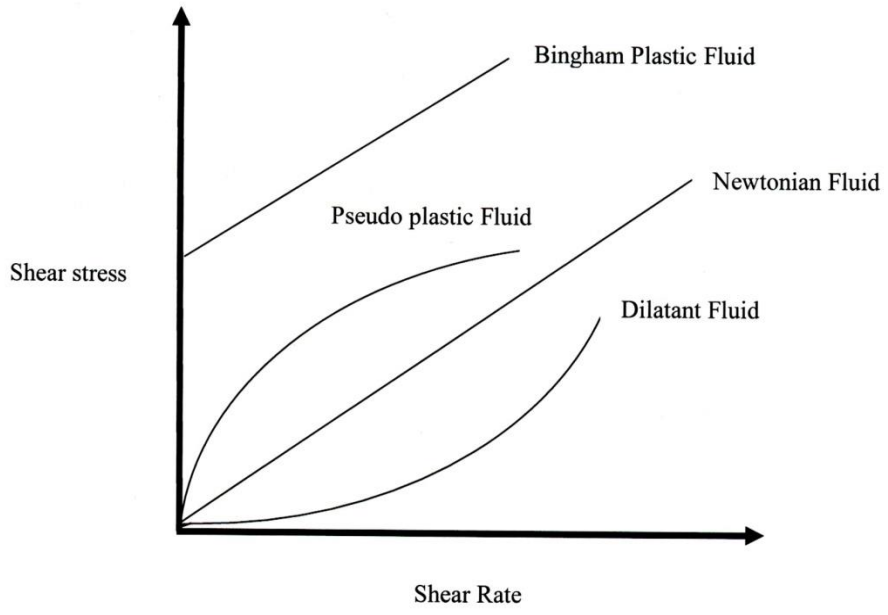

Figure 2.8: *Graph showing the flow of Newtonian and non-Newtonian fluids in relation to shear stress and shear rate.*

The Newtonian diluent is modified to a non-Newtonian polymer by the dissolution of an appropriate polymer with a high molecular weight such as polyisobutylene (Tandlich 2010). But

the critical concentration of the polymer in the diluent is important as it controls the viscosity of the resulting diluent and has a bearing on the extraction efficiency of the ELM (Skelland, (Michael) Meng 1999). The critical concentration can be calculated using equation 2.6 below, derived by Skelland and Meng (1996).

$$C_{critical} = \frac{228\,(M_{sru})^{\frac{5}{3}}}{V_{sru}(M_p)^{\frac{2}{3}}} \tag{2.6}$$

Where M_{sru} is the molecular weight of the pure liquid monomeric unit of the polymer (single repeat unit; g/mol), V_{sru} is the molar volume of the pure liquid monomeric unit of the polymer at its respective normal pressure and boiling point (cm^3/mol), M_p stands for the average molecular weight of the polymer (g/mol) (Park 2006).

The non-Newtonian liquid's effectiveness was first investigated by Skelland and Meng (1999) in their study of extraction of benzoic acid, phenol and ammonia from simulated wastewater. The diluent used was isoparaffinic oil with chain length ranging from C_{13} to C_{17} (Phillips Petroleum, USA). The non-Newtonian modifiers were Polyisobutylene (molecular weight = 1 250 000), polystyrene and polybutadiene (molecular weight = 940 000 g/mol, Exxon, USA) (Skelland, Meng 1996). SPAN 80 was used as a surfactant.

2.4.2.3. Non-Newtonian liquid based ELMs and Taylor vortex column

The Taylor vortex column consists of two cylinders, namely the outer static cylinder and the inner rotating cylinder. The flow patterns, which are described by the Taylor number (T_a) in the annular gap, are dependent on the rotating speed of the rotating cylinder (Skelland, (Michael) Meng 1999). The desired flow in the Taylor vortex is the Couette flow which is achieved at low T_a numbers. When a critical T_a number is exceeded, undesirable flow patterns - such as laminar Taylor-vortex flow and azimuthal wavy motion - are encountered and may lead to turbulent flow when T_a continues to increase (Richter, Hoffmann *et al*. 2008).

$$T_a = \frac{2\pi\, N\, (R_{rotor})^{\frac{1}{2}}\, (d_{ag})^{\frac{3}{2}}}{V} \tag{2.7}$$

Where R is the radius of the rotor (m), N is the rotational speed (s^{-1}), dg is the annular gap width (m), and v is the kinematic viscosity of the liquid inside the Taylor-vortex column ($m^2.s^{-1}$).

The Taylor vortex column is advantageous over the continuously stirred tanks which have been used in most ELM studies. The disadvantages of continuously stirred tanks are drag and large shear around the impeller surface (Richter, Hoffmann *et al*. 2008). This leads to the breakage of emulsion droplets due to the turbulences created around the impeller (Groeneweg, van Dieren *et al.* 1994). These turbulences are a result of the unequal dissipation of volumetric energy in the reactor. Most volumetric energy dissipation occurs near the impeller tips (Groeneweg, van Dieren *et al*. 1994). Forney *et al.* (2002) concluded that shear increases with the increase in the size of the contactor and that more electrical energy is required in scale-up devices used in industry (Park 2006). The Taylor vortex column nullifies these disadvantages by distributing the power evenly per unit volume throughout the volume of the contactor and the rotor and tank stirrers are roughly equal in diameter (Forney, Skelland *et al*. 2002). The Taylor vortex column produces the Taylor-Couette flow pattern, reducing the maximum shear stress by one to two orders of magnitude compared to a stirred tank**.** This reduction leads to an increase in the area inside the contactor exposed to constant maximum shear based on the friction drag on the large cylindrical surfaces near the boundaries of the Taylor-Couette flow (Park 2006)**.** One other major advantage of Taylor-column type extraction devices is the simplicity of the potential scale-up, as it only requires the constant value of the dimensionless Taylor number (Forney, Skelland *et al.* 2002, Richter, Hoffmann *et al*. 2008).

The use of Taylor vortex columns instead of conventional mixing reactors has also improved the stability of the ELMs (Forney, Skelland *et al*. 2002). Taylor vortex columns as contactors and non-Newtonian fluid have been used in the extraction of benzoic acid (Park, Forney *et al.* 2004), phenol and substituted phenols (Park, Forney *et al.* 2004), of Zn, Pb, Ni and Cd (Park, Skelland *et al*. 2006) from model industrial wastewater. Park (2006) used the shrinking core mathematical model of Liu and Liu (2000) for quantitative description of the mass transfer kinetics of the process (Park 2006).

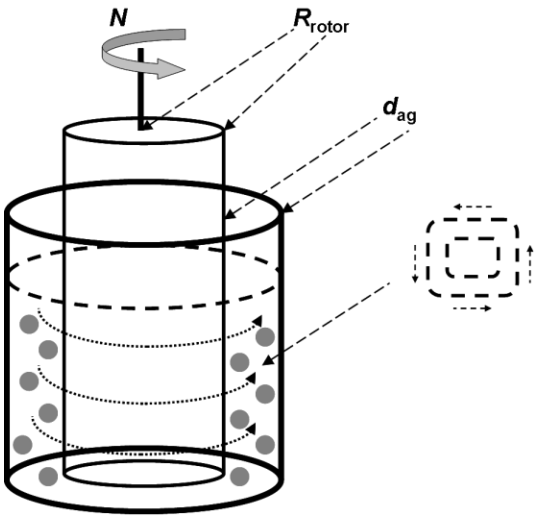

Figure 2.9: *The Taylor-vortex column. In the picture, R_{rotor} stands for the radius of the inner cylinder (vortex or rotor part of the Taylor-vortex column), d_{ag} is the diameter of the angular gap (the space between the inner and the outer cylindrical part of the Taylor-vortex column. N stands for the rotational speed of the rotor or inner cylinder. The membrane globules (●) are dispersed in the feed phase of the system via the rotation of the inner cylinder of the Taylor-vortex column. Near the walls of the outer cylinder, the energy distribution due to mixing leads to the flow pattern that are depicted by the dashed lines on the right-hand side of the depiction. The dotted lines represent the stirring pattern due to the rotation of the inner cylinder, and point out the even distribution of energy in the entire volume of the ELM wastewater mixture (Tandlich, 2010).*

2.5. EXTRACTION OF METALS FROM WASTE WATERS USING EMULSION LIQUID MEMBRANES.

ELM technique is a potential replacement of precipitation of heavy metals from wastewater. It has been used in the recovery of copper, zinc, nickel and cadmium (Reefy, Selim *et al.* 2003) among others metals. The method shows some advantages in the recovery of PGMs from mining waste water. In ELMs there is simultaneous purification and concentration of the solute because the processes of extraction and stripping are combined in one stage (Tandlich 2010) as compared to traditional methods such as solvent extraction, where separate contactors for extraction and stripping processes are required. ELM processes could be up to 40% cheaper than those of

solvent extraction (Ahmad, Kusumastuti *et al*. 2011). Other advantages over liquid-liquid extraction are improved kinetics, selection of species to be removed and decreases in the volume ratio of organic phase to aqueous feed solution necessary (Ahmad, Kusumastuti *et al.* 2011).

Fouad and Bart (2008) studied the recovery of Cr (VI) using the ELMs. Approximately 98 % of chromium (VI) was extracted and preconcentrated from the feed phase, which contained 50 ppm of Cr (VI) by the ELM. The feed phase used contained 0.01M hydrochloric acid. The components of the membrane were Tri-octylphosphineoxide (TOPO) as the liquid membrane, cyclohexane as the diluents and sodium hydroxide as the stripping phase. It was chosen on the basis of conventional liquid–liquid extraction studies. SPAN 80 was used as the emulsifying agent. This study found that hydrogen ion concentration in the external aqueous phase, the stirring speed during the mixing of the two phases and the concentration of the extractant affected the permeation of Cr (VI) through the liquid membrane. The effects of these parameters were also studied by Othman *et al.* (2006*).*They used Cyanex 302 as the extractant and kerosene as the diluents in the separation of silver from liquid photographic waste (Hasan, Selim *et al*. 2009). It was discovered that the relationship between concentration of extractant and permeation of Cr (VI) was directly proportional. Cr (VI) permeation through the ELM increased with increased extractant concentration (Othman, Mat *et al*. 2006). It was also discovered that increasing concentration of the extractant leads to a decrease in the stripping reaction rate. This is because the metal remains in the complex form in the membrane phase (Hasan, Selim *et al. 2009).* For successful extraction, there is an optimum carrier concentration which should be in the membrane. In the experiment done by Othman *et al* it was 0.05M of Cyanex 302 (Othman, Mat *et al*. 2006).

The concentration of the surface active agent is important in the stability and swelling of the emulsion and de-emulsification (Othman, Mat *et al*. 2006). Breakup of the emulsion is dependent on the concentration of the surfactant. In the study done by Othman *et al* (2006), it was discovered that an increase in the concentration of SPAN 80 lead to a decrease in the breakage of the emulsion, thereby improving the stability of the membrane. This led to an increased extraction of silver. However continued increase of the surfactant may lead to a reduced rate of extraction (Othman, Mat *et al*. 2006). In the study of the recovery of copper ions, it was reported that the surfactant can be increased to a certain extent for optimum extraction (Valenzuela,

Fonsec*a et al.* 2005). This is because of the generation of a higher interfacial resistance leading to the reduction in metal extraction efficiency. Resistance at the interface can be attributed to an increase in viscosity of the liquid membrane phase (Valenzuela, Fonseca *et al*. 2005). Surfactant concentration affects the viscosity of the ELM (Yan, Pal 2001, Wan, Zhang 2000, Yan, Pal 2004, Sengupta, Sengupta *et al*. 2006). The viscosity increases with increased surfactant concentration. Increase in viscosity of the membrane phase leads to a mechanically stable ELM (Ahmad, Kusumastuti *et al*. 2011). This reduces diffusion of the metal complex in the membrane phase (Othman, Mat *et al*. 2006), leading to the mass transfer resistance caused by the surfactant film (Valenzuela, Fonseca *et al*. 2005).

The complexation rate is dependent on the H^+ concentration of the feed solution (Kumbasar, Tutkun 2008). It was discovered that the increase in hydrogen ion decreased the permeation of Cr (VI). This could be due to the competition between the hydrogen ions at the membrane–feed interface with the Chromium ions. Low concentrations of hydrogen ions also favour the metal/carrier complex formation at the membrane–feed interface, resulting in the increase of concentration gradient of the metal/carrier complex in the membrane phase leading to an increase in the permeation rate of chromium ions (Kargari, Kaghazchi *et a*l. 2004). Kumbasar *et al* (2008) concluded that increasing the pH of the feed increases the extraction of cobalt to a certain point and, after that, the rate of extraction decreases. The pH for the optimum extraction of cobalt was 4.5 (Hasan, Selim *et al*. 2009). Reduction in pH of the feed leads to an increase in the extraction efficiency (Kumbasar, Tutkun 2008). It is therefore important to identify the optimum pH for the high extraction efficiency. Taguchi analysis was used to determine optimal conditions for the extraction of gold (III). 99.9 % of gold ions were extracted (Kargari, Kaghazchi *et al*. 2004). The variables used were the concentration of carrier, which was methyl *iso*-butyl ketone $(CH_3)_2CHCH_2COCH_3$ (MIBK), pH of the feed, speed of agitation and the concentration of the stripping phase. Liquid paraffin was used as the membrane phase.

REFERENCES

AHMAD, A.L., KUSUMASTUTI, A., DEREK, C.J.C. and OOI, B.S., 2011. Emulsion liquid membrane for heavy metal removal: An overview on emulsion stabilization and destabilization. *Chemical Engineering Journal,* **171**, pp. 870-882.

AHMAD, A.L., KUSUMASTUTI, A., DEREK, C.J.C. and OOI, B.S., 2012. Emulsion liquid membrane for cadmium removal: Studies on emulsion diameter and stability. *Desalination,* **287**, pp. 30-34.

ALLEN, L.V. and POPOVICH, N.G., 2005. *Ansel's pharmaceutical dosage forms and drug delivery systems.* Lippincott Williams & Wilkins, New York. USA; pp. 383-405.

AL-SABAGH, A.M., NASSER, N.M. and ABD EL-HAMID, T.M., 2013. Investigation of Kinetic and Rheological Properties for the Demulsification Process. *Egyptian Journal of Petroleum,* **22**, pp. 117-127.

AULTON, M.E. and WELLS, T., 2002. Pharmaceutics: The science of dosage form design. 2nd ed. Churchill Livingstone, New York, USA, pp. 41-86.

BANDYOPADHYAYA, R., BHOWAL, A., DATTA, S. and SANYAL, S.K., 1998. A new model of batch-extraction in emulsion liquid membrane: Simulation of globule–globule interaction and leakage. *Chemical Engineering Science,* **53**, pp. 2799-2807.

BASUALTO, C., POBLETE, M., MARCHESE, J., OCHOA, A., ACOSTA, A., SAPAG, J. and VALENZUELA, F., 2006. Extraction of cadmium from aqueous solutions by emulsion liquid membranes using a stirred transfer cell contactor. *Journal of the Brazilian Chemical Society,* **17**, pp. 1347-1354.

BHOWAL, A. and DATTA, S., 1997. Facilitated transport through liquid surfactant membrane: Analysis of breakage model. *Journal of Membrane Science,* **135**, pp. 245-250.

BORWANKAR, R., CHAN, C., WASAN, D., KURZEJA, R., GU, Z. and LI, N., 1988. Analysis of the effect of internal phase leakage on liquid membrane separations. *AIChE Journal,* **34**, pp. 753-762.

CHAKRABORTY, M., BHATTACHARYA, C. and DATTA, S., 2004. Study of the Stability of W/O/W-Type Emulsion During the Extraction of Nickel via Emulsion Liquid Membrane. *Separation Science and Technology,* **39**, pp. 2609-2625.

CHAKRABORTY, M., BHATTACHARYA, C. and DATTA, S., 2010. Chapter 4 - Emulsion Liquid Membranes: Definitions and Classification, Theories, Module Design, Applications, New Directions and Perspectives. In: VLADIMIR S. KISLIK, ed, *Liquid Membranes.* Amsterdam: Elsevier, pp. 141-199.

CHAKRAVARTI, A., CHOWDHURY, S. and MUKHERJEE, D., 2000. Liquid membrane multiple emulsion process of separation of copper (II) from waste waters. *Colloids and Surfaces A: Physicochemical and Engineering Aspects,* **166**, pp. 7-25.

CHANUKYA, B. and RASTOGI, N.K., 2010. Extraction of alcohol using emulsion liquid membrane consisting of paraffin oil as an organic phase and lecithin as a surfactant. *Journal of Chemical Technology and Biotechnology,* **85**, pp. 243-247.

CHANUKYA, B.S. and RASTOGI, N.K., 2013. Extraction of alcohol from wine and color extracts using liquid emulsion membrane. *Separation and Purification Technology,* **105**, pp. 41-47.

COLINART, P., DELEPINE, S., TROUVE, G. and RENON, H., 1984. Water transfer in emulsified liquid membrane processes. *Journal of Membrane Science,* **20**, pp. 167-187.

CORREIA, P.F.M.M. and DE CARVALHO, J.M.R., 2003. Recovery of phenol from phenolic resin plant effluents by emulsion liquid membranes. *Journal of Membrane Science,* **225**, pp. 41-49.

DAUGULIS, A.J., 2001. Two-phase partitioning bioreactors: a new technology platform for destroying xenobiotics. *Trends in biotechnology,* **19**, pp. 457-462.

DAVIS, R.H., 1997. Microfiltration and ultrafiltration: Principles and applications: Leos J. Zeman and Andrew L. Zydney, Marcek Dekker, New York, 1996. *Journal of Membrane Science,* **134**, pp. 273-274.

DRAXLER, J. and MARR, R., 1986. Emulsion liquid membranes part I: phenomenon and industrial application. *Chemical Engineering and Processing: Process Intensification,* **20**(6), pp. 319-329.

DRIOLI, E. and ROMANO, M., 2001. Progress and new perspectives on integrated membrane operations for sustainable industrial growth. *Industrial & Engineering Chemistry Research,* **40**, pp. 1277-1300.

DZYGIEL, P. and WIECZOREK, P., 2000. Extraction of amino acids with emulsion liquid membranes using industrial surfactants and lecithin as stabilisers. *Journal of Membrane Science,* **172**, pp. 223-232.

EOW, J.S. and GHADIRI, M., 2002. Electrostatic enhancement of coalescence of water droplets in oil: a review of the technology. *Chemical Engineering Journal,* **85**, pp. 357-368.

FORNEY, L., SKELLAND, A., MORRIS, J. and HOLL, R., 2002. Taylor vortex column: large shear for liquid–liquid extraction. *Separation Science and Technology,* **37**, pp. 2967-2986.

FOUAD, E.A. and BART, H.-., 2008. Emulsion liquid membrane extraction of zinc by a hollow-fiber contactor. *Journal of Membrane Science,* **307**, pp. 156-168.

GADEKAR, P.T., MUKKOLATH, A.V. and TIWARI, K.K., 1992. Recovery of nitrophenols from aqueous solutions by a liquid emulsion membrane system. *Separation Science and Technology,* **27**, pp. 427-445.

GASSER, M., EL-HEFNY, N. and DAOUD, J., 2008. Extraction of Co (II) from aqueous solution using emulsion liquid membrane. *Journal of hazardous materials,* **151**, pp. 610-615.

GHOSH, S., 2011. Comparative studies on brij reverse micelles prepared in benzene/surfactant/ethylammonium nitrate systems: Effect of head group size and polarity of the hydrocarbon chain. *Journal of colloid and interface science,* **360**, pp. 672-680.

GOYAL, R.K., JAYAKUMAR, N.S. and HASHIM, M.A., 2011. Chromium removal by emulsion liquid membrane using $[BMIM]^{+}[NTf2]^{-}$ as stabilizer and TOMAC as extractant. *Desalination,* **278**, pp. 50-56.

GROENEWEG, F., VAN DIEREN, F. and AGTEROF, W.G.M., 1994. Droplet break-up in a stirred water-in-oil emulsion in the presence of emulsifiers. *Colloids and Surfaces A: Physicochemical and Engineering Aspects,* **91**, pp. 207-214.

GU, Z., HO, W.S.W. and LI, N., 1992. Emulsion liquid membranes: Design considerations. *IN: Membrane Handbook.Van Nostrand Reinhold,* New York, pp. 656-700.

GUHA, A.K., MAJUMDAR, S. and SIRKAR, K.K., 1992. Gas separation modes in a hollow fiber contained liquid membrane permeator. *Industrial & Engineering Chemistry Research,* **31**, pp. 593-604.

HASAN, M.A., SELIM, Y.T. and MOHAMED, K.M., 2009. Removal of chromium from aqueous waste solution using liquid emulsion membrane. *Journal of hazardous materials,* **168**, pp. 1537-1541.

HO, W. and SIRKAR, K.K., 1992. *Emulsion liquid membrane application: Membrane Handbook.* Van Nostrand Reinhold, New York, USA, pp 701-717.

HOSSEINI, M. and SHAHAVI, M.H., 2012. Electrostatic Enhancement of Coalescence of Oil Droplets (in Nanometer Scale) in Water Emulsion. *Chinese Journal of Chemical Engineering,* **20**, pp. 654-658.

KAKOI, T., GOTO, M. and NAKASHIO, F., 1996. Separation of platinum and palladium by liquid surfactant membranes utilizing a novel bi-functional surfactant. *Journal of Membrane Science,* **120**, pp. 77-88.

KARGARI, A., KAGHAZCHI, T., SOHRABI, M. and SOLEIMANI, M., 2004. Batch extraction of gold(III) ions from aqueous solutions using emulsion liquid membrane via facilitated carrier transport. *Journal of Membrane Science,* **233**, pp. 1-10.

KISLIK, V.S., 2009. *Liquid membranes: principles and applications in chemical separations and wastewater treatment.* Elsevier Science, Amsterdam, Netherlands.

KISLIK, V. and EYAL, A., 1996. Hybrid liquid membrane (HLM) and supported liquid membrane (SLM) based transport of titanium (IV). *Journal of Membrane Science,* **111**, pp. 273-281.

KISLIK, V.S., 2010. Chapter 1 - Introduction, General Description, Definitions, and Classification. Overview. In: VLADIMIR S. KISLIK, ed, *Liquid Membranes.* Amsterdam: Elsevier, pp. 1-15.

KUKIZAKI, M. and GOTO, M., 2008. Demulsification of water-in-oil emulsions by permeation through Shirasu-porous-glass (SPG) membranes. *Journal of Membrane Science,* **322**, pp. 196-203.

KUMBASAR, R.A., 2009a. Cobalt–nickel separation from acidic thiocyanate leach solutions by emulsion liquid membranes (ELMs) using TOPO as carrier. *Separation and Purification Technology,* **68**, pp. 208-215.

KUMBASAR, R.A., 2009b. Extraction and concentration study of cadmium from zinc plant leach solutions by emulsion liquid membrane using trioctylamine as extractant. *Hydrometallurgy,* **95**, pp. 290-296.

KUMBASAR, R.A., 2008. Selective separation of chromium (VI) from acidic solutions containing various metal ions through emulsion liquid membrane using trioctylamine as extractant. *Separation and Purification Technology*, **64**, pp. 56-62.

KUMBASAR, R.A. and TUTKUN, O., 2008. Separation of cobalt and nickel from acidic leach solutions by emulsion liquid membranes using Alamine 300 (TOA) as a mobile carrier. *Desalination,* **224**, pp. 201-208.

LACKS, D.J., REAR, D.B. and VAN ORMAN, J.A., 2007. Molecular dynamics investigation of viscosity, chemical diffusivities and partial molar volumes of liquids along the $MgO–SiO_2$ join as functions of pressure. *Geochimica et Cosmochimica Acta,* **71**, pp. 1312-1323.

LI, N.N., 1971. Separation of hydrocarbons by liquid membrane permeation. *Industrial & Engineering Chemistry Process Design and Development,* **10**, pp. 215-221.

LI, N., CAHN, R., NADEN, D. and LAI, R., 1983. Liquid membrane processes for copper extraction. *Hydrometallurgy,* **9**, pp. 277-305.

LI, Q., LIU, Q., LI, K. and TONG, S., 1997. Separation study of cadmium through an emulsion liquid membrane. *Talanta,* **44**, pp. 657-662.

LIU, X. and LIU, D., 2000. Mass transfer resistance analysis of L-tryptophan extraction in an emulsion liquid membrane system. *Separation Science and Technology,* **35**, pp. 2707-2724.

MALIK, M.A., WANI, M.Y. and HASHIM, M.A., 2012. Microemulsion method: a novel route to synthesize organic and inorganic nanomaterials: 1st nano update. *Arabian Journal of Chemistry,* **5**, pp. 397-417.

MOHAN, S. and NARSIMHAN, G., 1997. Coalescence of protein-stabilized emulsions in a high-pressure homogenizer. *Journal of colloid and interface science,* **192**, pp. 1-15.

MOHD-SETAPAR, S.H., MOHAMAD-AZIZ, S.N., HARUN, N.H. and MOHD-AZIZI, C.Y., 2012. Review on the Extraction of Biomolecules by Biosurfactant Reverse Micelles. *APCBEE Procedia,* **3**, pp. 78-83.

MORTAHEB, H.R., ZOLFAGHARI, A., MOKHTARANI, B., AMINI, M.H. and MANDANIPOUR, V., 2010. Study on removal of cadmium by hybrid liquid membrane process. *Journal of hazardous materials,* **177**, pp. 660-667.

MOUSAVICHOUBEH, M., GHADIRI, M. and SHARIATY-NIASSAR, M., 2011. Electro-coalescence of an aqueous droplet at an oil–water interface. *Chemical Engineering and Processing: Process Intensification,* **50**, pp. 338-344.

NAKASHIO, F., GOTO, M., MATSUMOTO, M., IRIE, J. and KONDO, K., 1988. Role of surfactants in the behavior of emulsion liquid membranes--development of new surfactants. *Journal of Membrane Science,* **38**, pp. 249-260.

OTHMAN, N., MAT, H. and GOTO, M., 2006. Separation of silver from photographic wastes by emulsion liquid membrane system. *Journal of Membrane Science,* **282**, pp. 171-177.

PARK, Y., 2006. Development and Optimization of Novel Emulsion Liquid Membranes Stabilized by Non-Newtonian Conversion in Taylor-Couette Flow for Extraction of Selected Organic and Metallic Contaminants.

PARK, Y., FORNEY, L.J., KIM, J.H. and SKELLAND, A.H.P., 2004. Optimum emulsion liquid membranes stabilized by non-Newtonian conversion in Taylor–Couette flow. *Chemical Engineering Science,* **59**, pp. 5725-5734.

PARK, Y., SKELLAND, A.H.P., FORNEY, L.J. and KIM, J., 2006. Removal of phenol and substituted phenols by newly developed emulsion liquid membrane process. *Water research,* **40**, pp. 1763-1772.

PATNAIK, P.R., 1995. Liquid emulsion membranes: Principles, problems and applications in fermentation processes. *Biotechnology Advances,* **13**, pp. 175-208.

PENG, W., JIAO, H., SHI, H. and XU, C., 2012a. The application of emulsion liquid membrane process and heat-induced demulsification for removal of pyridine from aqueous solutions. *Desalination,* **286**, pp. 372-378.

PENG, W., JIAO, H., SHI, H. and XU, C., 2012b. The application of emulsion liquid membrane process and heat-induced demulsification for removal of pyridine from aqueous solutions. *Desalination,* **286**, pp. 372-378.

PFEIFFER, R., BUNGE, A., CHEUNG, H. and SHERE, A., 1992. Corrected analysis of the effect of preparation parameters on leakage in liquid surfactant membrane systems. *Separation Science and Technology,* **27**, pp. 753-763.

RAJASIMMAN, M. and KARTHIC, P., 2010. Application of response surface methodology for the extraction of chromium (VI) by emulsion liquid membrane. *Journal of the Taiwan Institute of Chemical Engineers,* **41**, pp. 105-110.

REEFY, S., SELIM, Y., HASSAN, M. and ALY, H., 2003. Assessment of liquid emulsion membrane for clean up of aqueous waste effluents from hazardous elements, *WM'03 conference, Arizona* 2003, pp. 23-27.

REMINGTON, J.P., 2006. *Remington: The science and practice of pharmacy.* 21st ed. Lippincott Williams & Wilkins, New York, USA, pp. 331-338.

REN, Z., YANG, Y., ZHANG, W., LIU, J. and WANG, H., 2013. Modeling study on the mass transfer of hollow fiber renewal liquid membrane: Effect of the hollow fiber module scale. *Journal of Membrane Science,* **439**, pp. 28-35.

REN, Z., ZHANG, W., MENG, H., LIU, J. and WANG, S., 2010. Extraction separation of Cu(II) and Co(II) from sulfuric solutions by hollow fiber renewal liquid membrane. *Journal of Membrane Science,* **365**, pp. 260-268.

RICHTER, O., HOFFMANN, H. and KRAUSHAAR-CZARNETZKI, B., 2008. Effect of the rotor shape on the mixing characteristics of a continuous flow Taylor-vortex reactor. *Chemical Engineering Science,* **63**, pp. 3504-3513.

S KISLIK, V., 2010. Chapter 2 - Carrier-Facilitated Coupled Transport Through Liquid Membranes: General Theoretical Considerations and Influencing Parameters. In: VLADIMIR S. KISLIK, ed, *Liquid Membranes.* Amsterdam: Elsevier, pp. 17-71.

SENGUPTA, B., SENGUPTA, R. and SUBRAHMANYAM, N., 2006. Process intensification of copper extraction using emulsion liquid membranes: Experimental search for optimal conditions. *Hydrometallurgy,* **84**, pp. 43-53.

SKELLAND, A. and MENG, X.M., 1996. A new solution to emulsion liquid membrane problems by non-Newtonian conversion. *AIChE Journal,* **42**, pp. 547-561.

SKELLAND, A.H.P., 1967. *Non-Newtonian flow and heat transfer.* Wiley New York.

SKELLAND, A.H.P. and (MICHAEL) MENG, X., 1999. Non-Newtonian conversion solves problems of stability, permeability, and swelling in emulsion liquid membranes. *Journal of Membrane Science,* **158**, pp. 1-15.

STROEVE, P. and VARANASI, P.P., 1984. An experimental study on double emulsion drop breakup in uniform shear flow. *Journal of colloid and interface science,* **99**, pp. 360-373.

SUN, D., DUAN, X., LI, W. and ZHOU, D., 1998. Demulsification of water-in-oil emulsion by using porous glass membrane. *Journal of Membrane Science,* **146**, pp. 65-72.

TANDLICH, R., 2010. Chapter 8 - Application of Liquid Membranes in Wastewater Treatment. In: VLADIMIR S. KISLIK, ed, *Liquid Membranes.* Amsterdam: Elsevier, pp. 357-400.

TERAMOTO, M., TAKEUCHI, N., MAKI, T. and MATSUYAMA, H., 2002. Ethylene/ethane separation by facilitated transport membrane accompanied by permeation of aqueous silver nitrate solution. *Separation and purification technology,* **28**, pp. 117-124.

TERRY, R.E., LI, N.N. and HO, W.S., 1982. Extraction of phenolic compounds and organic acids by liquid membranes. *Journal of Membrane Science,* **10**, pp. 305-323.

VALENZUELA, F., FONSECA, C., BASUALTO, C., CORREA, O., TAPIA, C. and SAPAG, J., 2005. Removal of copper ions from a waste mine water by a liquid emulsion membrane method. *Minerals Engineering,* **18**, pp. 33-40.

VENKATESAN, S. and MEERA SHERIFFA BEGUM, K., 2009a. Emulsion liquid membrane pertraction of benzimidazole using a room temperature ionic liquid (RTIL) carrier. *Chemical Engineering Journal,* **148**, pp. 254-262.

VENKATESAN, S. and MEERA SHERIFFA BEGUM, K.M., 2009b. Emulsion liquid membrane pertraction of benzimidazole using a room temperature ionic liquid (RTIL) carrier. *Chemical Engineering Journal,* **148**, pp. 254-262.

VENKATESAN, S. and MEERA SHERIFFA BEGUM, K.M., 2009c. Emulsion liquid membrane pertraction of imidazole from dilute aqueous solutions by Aliquat-336 mobile carrier. *Desalination,* **236**, pp. 65-77.

VÖLKEL, W., HALWACHS, W. and SCHÜGERL, K., 1980. Copper extraction by means of a liquid surfactant membrane process. *Journal of Membrane Science,* **6**, pp. 19-31.

WAN, Y. and ZHANG, X., 2000. Swelling determination of W/O/W emulsion liquid membranes. *Journal of Membrane Science,* **196**, pp. 185-201.

WANG, C. and BUNGE, A., 1990. Multisolute extraction of organic acids by emulsion liquid membranes. I. Batch experiments and models. *Journal of Membrane Science,* **53**, pp. 71-103.

YAN, J. and PAL, R., 2004. Effects of aqueous-phase acidity and salinity on isotonic swelling of W/O/W emulsion liquid membranes under agitation conditions. *Journal of Membrane Science*, **244**, pp. 193-203.

YAN, J. and PAL, R., 2001. Osmotic swelling behavior of globules of W/O/W emulsion liquid membranes. *Journal of Membrane Science*, **190**, pp. 79-91.

YONGQUAN, D., MING, W., LIN, C. and MINGJUN, L., 2012. Preparation, characterization of P(VDF-HFP)/[bmim]BF4 ionic liquids hybrid membranes and their pervaporation performance for ethyl acetate recovery from water. *Desalination*, **295**, pp. 53-60.

ZHIVKOVA, S., DIMITROV, K., KYUCHOUKOV, G. and BOYADZHIEV, L., 2004. Separation of zinc and iron by pertraction in rotating film contactor with Kelex 100 as a carrier. *Separation and purification technology*, **37**, pp. 9-16.

CHAPTER 3

ANALYTICAL TECHNIQUES

3.1. INTRODUCTION

In order to investigate the applicability of the TVC and non-Newtonian ELMs in the solvent extraction of PGMs, with Rh as the model compound, the first task of the study was to develop the relevant methods for the quantification of the components of a model metal refinery side-stream. The aim of this chapter is to develop methods to track the concentration of the components of the ELM throughout the extraction process. This includes a description of the preparation of the model metal refinery side-stream and the quantification of the concentration of the ELM components in it. The model side-stream is based on the preliminary stability of the Rh solution and the nature of its water chemistry (Barbosa et al. 2007). In this case, Rh will only be soluble in aqueous environments if the pH of the aqueous phase is equal to 4.00 or lower. At the same time, the presence of chloride anions is essential to the stabilization of the Rh cations in solution (see Chapter 5). Thus the model Rh refinery effluent was modelled as the Rh solution in HCl (hydrochloric acid). Simultaneously, the model metal refinery effluent will be assessed on the premise that the Rh metal refinery works on the principle of zero discharge, i.e. no metal or organic species leave the production/metal refinery facility in question.

The exact amount of each of the components of the ELM that are used and lost in any Rh extraction process must be known. Therefore validated methods of quantitative analyses must be available for each ELM component. Such methods are developed in the current chapter and will be used throughout the remainder of the study. Due to the complex nature of the treated side-stream, a combination of colorimetry, gas chromatography, non-aqueous titration and the atomic absorption spectroscopy was chosen. Colorimetric methods were used to quantify chemical oxygen demand (COD). Non-aqueous titration with perchloric acid as the titrant was used to quantify trioctylamine (TOA). Gas chromatographic methods were used for the quantification of TBP, toluene and kerosene. Rh concentrations were determined using induced-coupled plasma spectroscopy (ICP) and atomic absorption spectroscopy.

3.2. CHEMICALS AND CONSUMABLES

The following items and consumables were purchased from Merck (Pty) Ltd. (Johannesburg/Cape Town, South Africa): non-aqueous titrant of perchloric acid in acetic acid, nitrate kit (catalogue number: 1.09713.0001), chloride kit (catalogue number: 1.14897.0001), reagent A (catalogue number: 1.14679.0495) and B (catalogue number: 1.14679.0495) for the determination of COD in the ranges of 100-2000 and 500-10000 mg/L, KNO_3, potassium hydrogen phthalate (KHP), NaCl, toluene, acetic acid and HCl. The following items and consumables were purchased from Sigma-Aldrich (Johannesburg, South Africa): tributylphosphate (TBP), kerosene, TOA, ethanol, n-hexane, 2.0 ml clear glass GC vials with PTFE-lined silicone septa and the rhodium standardised solution.

3.3. MEASUREMENT OF CHEMICAL OXYGEN DEMAND

Chemical oxygen demand (COD) was measured using the closed-reflux colorimetric method (APHA, 1998) in the concentration ranges from 100 to 2000 and from 500 to 10000 mg/L. The KHP was used as the standard to prepare solutions and the COD values were converted into KHP concentrations (mg KHP eq/L) where eq/L refers to equivalent per litre based on Equation (3.1).

$$K\,C_8H_5O_4 + 7.5\,O_2 \rightarrow \quad KOH + 8\,CO_2 + 2\,H_2O \tag{3.1}$$

Digestions were performed according to the manufacturer's instructions using the TR 300 thermoreactor (Merck Ltd., Johannesburg/Cape Town, South Africa). After completion of the digestions, the respective solutions were cooled and the spectrophotometric measurements were performed using a Shimadzu UV-1601 spectrophotometer (Shimadzu, Johannesburg, South Africa). Six concentration levels with three replicates each were measured to construct the calibration curve. This was then plotted as the dependence of the absorbance at 600 nm on the COD concentration in mg KHP eq/L. The calibration curve for the COD measurements is shown in Figure 3.1.

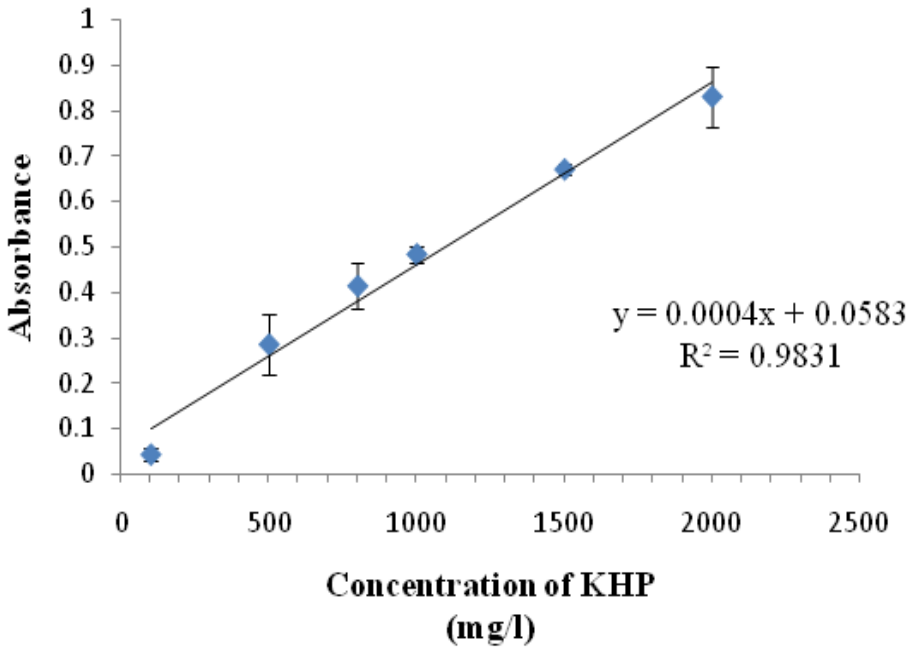

Figure 3.1: *The COD calibration curve with a range of 100-2000 mg/L potassium hydrogen phthalate (KHP) as the standard solution*

3.4. QUANTITATION OF TBP, TOLUENE AND KEROSENE

The method for the quantitation of TBP and kerosene is a combination of liquid-liquid extraction and gas chromatography. For gas chromatography, the external standard method was used for quantitation of both components. For the preparation of the stock solution of both compounds, 40 ml of n-hexane was poured into a 50 ml volumetric flask. Accurate amounts of TBP and kerosene were then weighed analytically on the PA1214 analytical balance (Pioneer™, Ohaus Corporation, Johannesburg, South Africa) and spiked into the layer of n-hexane in the 50 ml volumetric flask. The amount of each compound was adjusted to prepare a stock solution containing approximately 1.20 g/L of kerosene and 1.47 g/L of TBP. The flask was immediately stoppered and the contents mixed thoroughly by hand-shaking. Volume was filled up to the mark with n-hexane. Calibration solutions were then prepared in 2.0 ml GC vials by pipetting the required amount of the stock solution into n-hexane to obtain 1.5 ml of the respective calibration solution. The concentrations' ranges of the calibration curves were as follows: 20-100 mg/L for TBP and 8.0-80 mg/L for kerosene. The calibration curves were constructed as the dependence of the peak area for a given compound on its concentration.

Peak areas were obtained by a splitless injection of 1.0 µL of each of the calibration solutions using a 7693 auto sampler attached to a 7890 gas chromatograph (Agilent, Johannesburg, South Africa) equipped with a DB 5 capillary GC column (30 m × 0.32 µm × 0.25 mm; Agilent, Johannesburg, South Africa) and a flame-ionisation detector. Helium was used as the mobile phase at a flow rate of 1.0 ml/min. The injector and detector temperatures were set to 300 °C, and the oven temperature programme was as follows: initial temperature 40°C hold for 3 min, ramp to 180°C at 2.5 °C/min, ramp to 250°C at 20°C/min and hold for 3 min. All gases were purchased in instrument grade from Afrox-Linde (Port Elizabeth, South Africa). The calibration curve for TBP is shown in Figure 3.2, and shows that the independent variable, i.e. the TBP concentration, explains 96.8 % of the variability in the area of its chromatographic peak. Therefore the method can be deemed appropriate for analytical purposes in the scope of the ELM extraction. The calibration curve for kerosene followed a similar pattern and the R^2 value was equal to 0.998. Later in the study, toluene was used as the modifier in the ELM in the place of the TBP. This was caused by the acid hydrolysis of the TBP molecule, which led to the decrease in ELM stability. The same gas chromatographic programme was used for toluene and the R^2 value of the calibration curve was equal to 0.993. The limit of detection (LOD) values ranged from 1 to 5 mg/L for TBP, toluene and kerosene. At the same time, the respective limit of quantification (LOQ) values were equal to 5.7, 8.2 and 10.5 mg/L for TBP, toluene and kerosene.

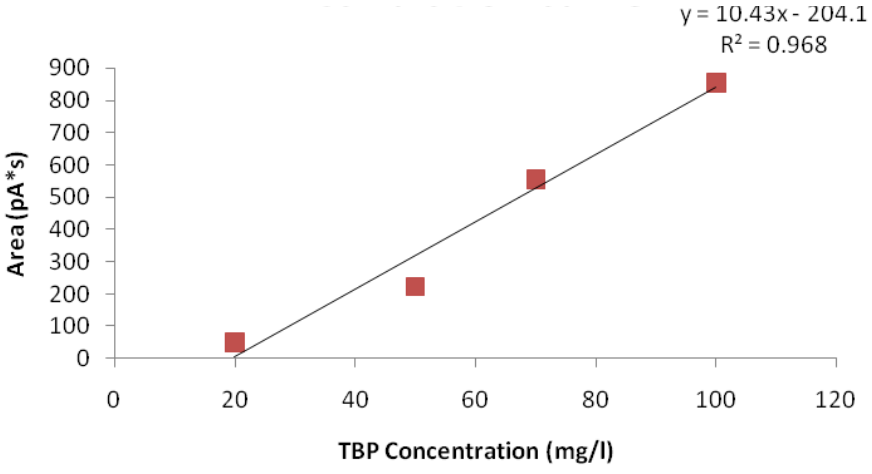

Figure 3.2: *Calibration curve for TBP analysed using gas chromatography.*

3.5. QUANTIFICATION OF RHODIUM

Calibration solutions were prepared by dilution of the standardised Rh stock solution with the concentration of 999 ± 5 mg/L (Sigma-Aldrich, Johannesburg, South Africa). Calibration curves were prepared by dilution of the certified stock solution with 0.01 and 0.001 M HCl (diluted from the 32 % commercially available solution; Sigma-Aldrich, Johannesburg, South Africa). Calibration range concentrations varied from 1 to 10 mg/L and the solutions were filtered through a 0.45 μm cellulose acetate filter (Spellbound, Port Elizabeth, South Africa) prior to analyses. The samples were analysed for Rh using the signal at 2334 nm and the Thermo/Finnagan ICP 7600 (Chemistry Department, Rhodes University). All readings were taken in triplicate. The calibration curves are shown in Figures 3.3 and 3.4.

As can be seen, the R^2 values were equal to 0.997 in 0.01 M HCl and 0.999 in 0.001 M HCl. Simultaneously, the sensitivities of the analysis (slopes of the calibration curves) were independent of the pH value of the hydrochloric acid, as the slope of the calibration curve was equal to 466.8 nml mg^{-1} in 0.01 M HCl and to 486.0 nml mg^{-1} in 0.001 M HCl. Standard deviations of the individual concentration level signals were always below 5 %. Thus the ICP method developed was deemed suitable for the determination of Rh concentrations in the extraction experiments. The LOD values were equal to 1.05 and 1.23 mg/L at pH = 2 and 3, respectively. At the same time, the LOQ values were equal to 2.61 and 3.11 mg/L. Due to maintenance and performance issues with the ICP instrument, some of the samples were analysed using the commercial laboratory at the Chemtech Lab (Pretoria, South Africa). Here only the LOQ value was provided and it was equal to 0.058 mg/L.

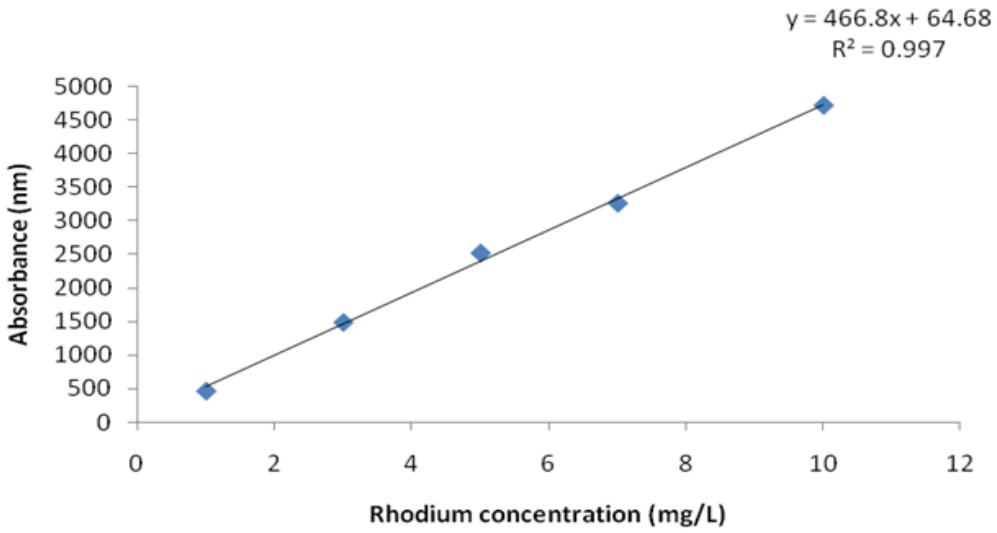

Figure 3.3: *Calibration curve for Rh in 0.01 M HCl at a range of 1 - 10 mg/L at the 2334 nm signal.*

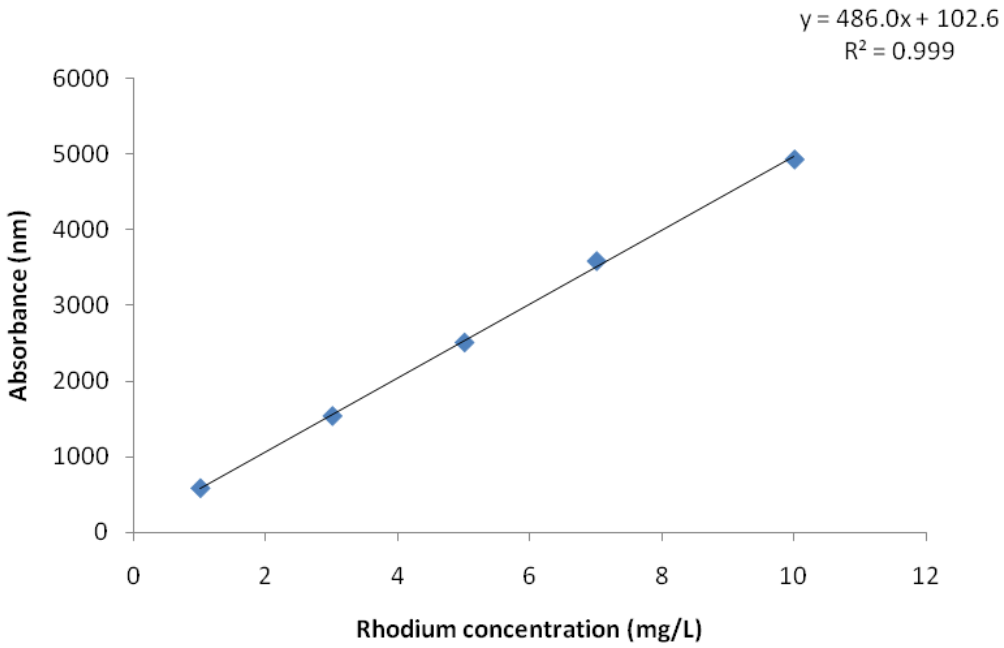

Figure 3.4: *Calibration curve for Rh in 0.001 M HCl at a range of 1 – 10 mg/L at the 2334 nm signal.*

3.6. QUANTIFICATION OF TRIOCTYL AMINE

The titration method by Kar (2007) was used as the basis for the quantification of TOA. First the standardisation of the approximately 0.1 M perchloric acid solution was performed against KHP. For this, 2.0400 g of KHP was accurately weighed using a PA1214 Pioneer™ analytical balance (Ohaus Corporation, Johannesburg, South Africa) and the powder was transferred quantitatively into a clean 100 ml volumetric flask. The KHP was quantitatively dissolved in 100 ml glacial acetic acid to give a solution with a concentration of 0.1000 M. Before bringing the solution to the final volume with acetic acid, the flask content was heated to achieve complete dissolution of KHP crystals. Then 25 ml of this solution was transferred into a 250 ml titration flask and three drops of 0.5 % crystal violet (Sigma-Aldrich, Johannesburg, South Africa) in glacial acetic acid was added to the solution. Aliquot of the KHP solution was then titrated with 0.1 M perchloric acid (solution in acetic acid) until the blue colour of the solution changed to a green/yellow colour. All titrations were performed in triplicate and the respective calculations were done according to Equation (3.4).

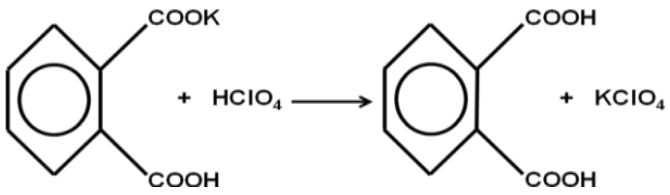

(3.4)

After standardisation of the titrant, TOA solutions with concentrations of 0.01 and 0.10 M were prepared in a simulated ELM, i.e. a 10 % solution of TBP in kerosene or the 30 % toluene solution in kerosene. These solutions are termed the test samples in the text below and were prepared as follows. Eighty millilitres of the simulated ELM was transferred into a 100 ml volumetric flask using a 250 ml graduated cylinder. This was placed onto a PA1214 Pioneer™ analytical balance and the balance was tared. The volumetric flask was then removed and 3.5367 g of the neat liquid TOA was pipetted into the volumetric flask and into the ELM diluent by submerging the pipette tip and dispensing the TOA into the diluent layer. The volumetric flask was stoppered and the outside was wiped clean with a paper towel to ensure that neither excess

TOA nor the simulated ELM contaminate the exterior of the volumetric flask. The flask was then placed onto the PA1214 Pioneer™ analytical balance and the accurate weight of TOA was recorded.

The solution inside the flask was mixed thoroughly by hand-shaking and the volume was made up to the 100 ml mark by a 10 % TBP in kerosene solution. To prepare 0.01 M TOA solution, 10 ml of the previous test sample was pipetted accurately into a clean 100 ml volumetric flask and diluted to volume with the simulated ELM. Next the test samples were assayed, as with the standardisation (see previous paragraph), and the exact concentration of the TOA solutions was calculated based on the stoichiometry in Equation (3.5).

$$HClO_4 + N(C_8H_{17})_3 \rightarrow ClO_4^- + N(C_8H_{17})_3H^+ \qquad (3.5)$$

Standardisation of three individual batches of the perchloric acid titrant showed that the average concentration was equal to 0.0950 ± 0.0017 M with a coefficient of variation of 1.8%. Analysis of the test samples showed at 0.10 M solution of TOA, the measured concentration was equal to 0.0950 ± 0.0039 M, while at the 0.01 M level the actual concentration was recorded at 0.0120 ± 0.0028 M. This gives precision of 4.1 % and 23 %; and accuracy values were equal to 95 and 120 % respectively. Volume expansion of the titrant had no influence on the independence of the results of the TOA determination between 20 and 35 °C (Kar, 2007). With the negative control (a 10 % solution of TBP in kerosene or 30 % solution of toluene in kerosene), the diluent did not interfere with the TOA determination.

REFERENCES

APHA, AWWA and WEF (1998). American Public Health Association, American Water Works Association and Water Environment Federation. Standard Methods for the Examination of Water and Wastewater. 20th ed, WEF, Washington, D.C., USA.

BARBOSA, V., TANDLICH, R. and BURGESS, J., 2007. Bioremediation of trace organic compounds found in precious metals refineries' wastewaters: A review of potential options. *Chemosphere*, vol. 68, no. 7, pp. 1195-1203.

KAR, A., 2007. Pharmaceutical drug analysis. New Age International, New Delhi, India.

CHAPTER 4

EMULSIFICATION, MICRO-DROPLET SIZE OPTIMISATION AND DEMULSIFICATION OF THE ELMs

4.1. INTRODUCTION

Emulsification is the process of dispersing one liquid in a second immiscible liquid (Matos, Suárez et al. 2013). This forms thermodynamically unstable ELMs which, due to certain factors, tend to destabilise. Emulsification is a two-way process: (a) deformation and disruption of droplet, thereby increasing the emulsion's specific surface area; (b) stabilization of this fresh interface by emulsifier to prevent re-coalescence of the newly formed droplets (Tesch, Schubert 2002, Floury, Legrand et al. 2004, Perrier-Cornet, Marie et al. 2005). Due to the thermodynamic instability of the newly formed droplets, re-coalescence might occur (Jafari, Assadpoor et al. 2008). Coalescence is the main cause of destabilisation of ELMs. This occurs when droplets fuse together to form larger droplets, due to the collision, resulting from the relative Brownian motion of the droplets and the high-intensity turbulence associated with emulsification (Jafari, Assadpoor et al. 2008). Coalescence can be reduced by the addition of a surfactant (Lambrich, Schubert 2005). This process is described in Chapter 2 Section 2.4.2.1. It can also be reduced by increasing the viscosity of the continuous phase (Behrend, Ax et al. 2000, Tesch, Schubert 2002). Re-coalescence might occur due to incomplete covering of the interface by emulsifier molecules (Jafari, Assadpoor et al. 2008). But it must be noted that the collisions between droplets do not always lead to coalescence (Mohan, Narsimhan 1997)

Emulsification methods are also paramount when it comes to improving emulsification. High pressure homogenisation, rotor stator devices (e.g. colloid mills), ultrasonic and static mixer techniques have been used for emulsification because of their ability to produce small sized droplets (Mohan, Narsimhan 1997). It is difficult to produce an emulsion of uniform droplet sizes, hence most ELMs are polydispersed, meaning that droplet sizes are different (Hiemenz, Rajagopalan 1997). Emulsion droplet size (EDS) is important for emulsion properties such as rheology and stability (Jafari, Assadpoor et al. 2008). In extraction using the emulsion liquid

membrane, small sized micro-droplets are necessary. ELMs of good stability and rapid extraction have droplet sizes in the range of 0.3-10 μm although the preferable range is 0.8-3 μm (Li, Cahn et al. 1983, Chanukya, Rastogi 2013) . Micro-droplet size is dependent on various factors: (a) the time taken for the emulsification process, as this enables the emulsifying agent to adsorb to all the interfacial surfaces of the droplets and reduce interfacial tension; (b) the viscosity of the emulsion, as increasing the viscosity of the continuous phase decreases the movement of the micro-droplets and reduces chances of coalescence; (c) the concentration of the emulsifier should be enough to cover the oil–water interface, which already exists, and the fresh interface resulting from the continued emulsification; (d) adsorption rate and efficiency refer to the emulsifier's ability to adsorb the oil–water interface as quickly as possible to prevent the process of coalescence (Jafari, Assadpoor et al. 2008). In this chapter, emulsification was optimised in order to generate stable micro droplets by attaining an appropriate ratio between the dispersed and continuous phase to form a stable emulsion.

The process of extraction using ELMs is largely dependent on the demulsification of the ELM. It is a key step in the ELM process (Sun, Duan et al. 1998). The process of demulsification has been fully described in Chapter 2 Section 2.3.4. In this chapter, demulsification studies were done to try and break the ELMs. A combination of chemical and physical demulsification was studied.

4.2. EMULSIFICATION AND MICRO-DROPLET GLOBULE SIZE OPTIMISATION

Composition of the ELM and the preparation procedure has significant influences on the micro-droplet size (Tandlich 2010). Concentrations of the individual components first need to be optimised before any extraction experiment is attempted. In this section, various protocols of ELM preparation are used and their influence on the micro-droplet diameter evaluated. Differences in the individual protocols originate from the use of mechanical shaking and sonication and varying concentrations of TBP, polyisobutylene (PIB), TOA and SPAN 80 used. The subsections will be titled based on the composition of the diluent/organic phase of the ELM and the method of the ELM preparation used.

4.2.1. Apparatus and chemicals

Kerosene, PIB and TOA were purchased from Sigma Aldrich (Johannesburg, South Africa); nitric acid was purchased from SAARCHEM PTY LTD (Krugersdorp, South Africa), SPAN 80 and toluene from Fluka analytical. An Olympus UCMAD3 microscope mounted with an Olympus ultra 20 soft imaging system UTVX-2 was used for all microscopic work (Institute for Water Research, Rhodes University, South Africa). Absorbances for chemical oxygen demand (COD) were measured using a UV spectrophotometer model UV-1201 Shimadzu Corporation Japan. The Labcon COD thermo reactor model D60 was used for COD (Merck Pty. Ltd., Johannesburg, South Africa) unless stated otherwise. All glassware was purchased from Sigma-Aldrich (Johannesburg, South Africa). All mass weighing was done analytically using the PA1214 analytical balance (Pioneer™, Ohaus Corporation, Johannesburg, South Africa). Sonication was done using the BRANSON 8510 ultrasonication bath (LASEC SA, Port Elizabeth, South Africa). Orbital shaking was done using the Chiltern orbital shaker SS70 (Slough, Berkshire, Chiltern Scientific, United Kingdom).

4.2.2. Methods

4.2.2.1. Kerosene-TBP diluent and sonication

The diluent was prepared as follows: 10 ml of TBP was put in a 100 ml volumetric flask. Kerosene was added to the 100 ml mark to make a 100 ml solution of 10 % TBP in kerosene. The diluent was then mixed with 2 M nitric acid in the ratios 1:1 (20 ml of nitric acid: 20 ml of the diluent), 1:2 (20 ml of nitric acid: 40 ml of the diluent) and 1:3 (20 ml of nitric acid: 60 ml of the diluents). The mixtures were sonicated for 10 minutes and they were left to stand. Sonication was repeated for the same preparations for 20 minutes.

4.2.2.2. kerosene-TBP-PIB-TOA-SPAN 80 diluent and sonication

The diluent was prepared as follows: 5 g PIB was weighed and transferred quantitatively into a 250 ml volumetric flask. It was completely dissolved in 150 ml of kerosene. Twenty five

millilitres (25 ml) of TBP was added and 2.5670 g of TOA was weighed out and the entire amount of the extractant was quantitatively dissolved in the diluent components. The entire content of the flask was homogenised by hand-shaking. The surfactant, 12.506 g of SPAN 80, was added. After dissolution of the surfactant, kerosene was added to the 250 ml mark to make 20 g/l of PIB, 10.268 g/l TOA and 50.024 g/l of SPAN 80. The diluent was mixed with 2 M nitric acid in the ratios 1:1, 1:2 and 1:3, as above, and sonicated for 10 minutes. The mixtures were left to stand at 21 ± 2 °C.

4.2.2.3. kerosene-TBP-PIB-TOA-SPAN 80 diluent and orbital shaking 1

The diluent was prepared in the same manner as the ones in 4.2.2.2. It was mixed with 2 M nitric acid in the ratios 1:1, 1:2 and 1:3 (as above). Instead of sonication, the mixtures were shaken using an orbital shaker at 600 rpm to make the ELMs for varying periods of time.

4.2.2.4. kerosene-Toluene-PIB-TOA-SPAN 80 diluent and orbital shaking 2

In this experiment, the diluent with extractant contained 5 g PIB which was dissolved in 100 mL of Kerosene inside a 250 ml volumetric flask. To it, 45 ml of toluene was added, together with 2.5390 g of TOA and 12.4936 g of SPAN 80. Both TOA and SPAN 80 were completely dissolved in the kerosene-toluene mixture. Then Kerosene was used to make up the volume to 250 mL to obtain the final ELM concentrations as follows: 30 % of Toluene in kerosene, 20.000 g/L (m/v) of PIB, 10.156 g/L (m/v) TOA and 49.972 g/L (m/v) of SPAN 80. Toluene had to be used instead of TBP in the ELM development because the dissolution of PIB in the Kerosene/TBP combination took more than 12 hours.. It was mixed with 2 M nitric acid in the ratios 1:1, 1:2, 1:3 and 1:4 (as above). These were shaken for 20 minutes using an orbital shaker at 600 rpm. They were then examined under the microscope using a magnification of 400x. Mixtures were left to stand, and the time for phase separation to occur was noted. The ELMs were reconstituted and refrigerated at 5 ± 2 °C for 24 hours. The ELMs were re-shaken and the micro-droplet size was re-examined. The point of this experiment was to investigate the reusability of the ELM between extractions and possible storage in the refrigerator on different days.

4.2.2.5. Micro-droplet size analysis

The average micro-droplet size of the emulsion was measured using photon correlation spectroscopy (PCS) using the Nano-ZS Zetasizer (Malvern Instruments Ltd, Worcestershire, United Kingdom). Before the PCS was done, 30 µl of each sample was diluted using 10 ml of double distilled water in order to obtain a suitable scattering intensity. Ten PCS measurements were performed on each sample at an angle of 90° at 25 °C. The measuring range of the Zetasizer is from approximately 6 nm to 6 µm (Kovacevic, Savic et al. 2011). Since the presence of particles not in the nano range in dispersion has to be eliminated, it is recommended that PCS be used in combination with laser diffraction (LD), allowing visualization of these particles. LD determines particle size based on detection of diffracted light from the radius of the particles' surface (Heurtault, Saulnier et al. 2003, Kovacevic, Savic et al. 2011). In the current study, it was used in conjunction with optical microscopy. The Olympus UCMAD3 microscope mounted with an Olympus ultra 20 soft imaging system UTVX-2 makes it possible to measure bigger droplet sizes manually. The ELMs were then examined under the microscope above at the magnification of 400x. Fifteen (15) micro-droplets were examined for each emulsion in ratios of 1:1, 1:2, 1:3 and 1:4 (see section 4.2.2.1 for details of emulsion manufacture). The size of each micro-droplet was manually measured using the optical microscope, the average size, the mode and standard deviation were calculated and results are shown in Appendix I.

4.2.2.6. kerosene-Toluene-PIB-TOA-SPAN 80 diluent and orbital shaking 3

The diluent was prepared as described in section 4.2.2.4.

a) The diluent was mixed with 2M nitric acid in the ratios 1:1 (10ml of the nitric acid: 10 ml of diluent) and 1:2 (10 ml of nitric acid: 20 ml of the diluents). These were shaken for 20 minutes using an orbital shaker at 600 rpm. Micro-droplet size was measured as described in section 4.2.2.5. The ELMs were then examined under the microscope at the magnification of 400x. The ELMs were left to stand at 21 ± 2 °C and monitored for phase separation. The time when significant phase separation occurred was noted. The ELMs were re-made as above and put in the fridge at 5 ˚C to examine the effect of temperature and the time for phase separation to occur was noted.

b) A new set of ELMs was prepared as above. They were then shaken for 40 minutes using an orbital shaker at 600 rpm. Micro-droplet size was measured as described in section 4.2.2.5. The ELMs were then examined under the microscope at the magnification of 400x. The ELMs were re-made and put in the fridge at 5 ˚C to examine the effect of temperature and the time for phase separation to occur was noted.

4.2.2.7. Emulsification with diluent containing 30 g/l PIB (kerosene-toluene-PIB-TOA-SPAN 80 diluent and orbital shaking 4)

The diluent was prepared as follows: 3.000 g of PIB was dissolved in a mixture of 50 ml kerosene and 30 ml toluene, 1.087 g of TOA and 5.1001 g of SPAN 80 were added. Kerosene was then added to the 100 ml mark to make 30 g/l (m/v) of PIB, 10,870 g/l (m/v) of TOA and 51.001 g/l (m/v) of SPAN 80. The diluent was mixed with 2 M nitric acid in the ratios 1:1 (10 ml of the nitric acid: 10 ml of diluent) and 1:2 (10 ml of nitric acid: 20 ml of the diluents). These were shaken for 40 minutes using an orbital shaker at 600 rpm (see model in section 4.2.1). Micro-droplet size was measured as described in section 4.2.2.5. The ELMs were then examined under the microscope at the magnification of 400x. The ELMs were left to stand at 21 ± 2 ˚C and monitored for phase separation. The time taken for significant phase separation to occur was noted. The ELMs were re-made and put in the fridge at 5 ± 2 ˚C to examine the effect of temperature and the time for phase separation to occur was again noted.

4.3. DEMULSIFICATION OF THE ELMS

4.3.1. Thermal demulsification at 35.0 ± 0.5°C

The diluent containing 20 g/l of PIB was prepared like the ones in 4.2.2.4 and the diluent containing 30 g/l PIB was prepared in the same way as the one in 4.2.2.7. The ELMs were prepared as follows:

a) The diluent with 30 g/l of PIB was mixed with 2 M nitric acid in the ratios 1:2 (20 ml of the nitric acid: 40 ml of diluent) to form two 1:2 ELMs in separate 250 ml Erlenmeyer

flasks. One flask was shaken for 20 minutes and the other for 40 minutes using an orbital shaker at 600 rpm.

b) The diluent with 20 g/l of PIB was mixed with 2 M nitric acid in the ratios 1:2 as above. Two 1:2 ELMs were formed and treated as above.

All four ELMs were put in the incubator at 35 ˚C for 24 hrs. Unless stated otherwise, all incubations in Chapter 4 were performed in one of the following incubators: a Labcon incubator Model FSIM B (Labmark, Johannesburg, RSA), a TS 606/3-I incubator (WTW, Weilheim, Germany), a Labcon low temperature incubator LTIE 10 (Labmark, Johannesburg, RSA); and/or a Heraeus Model FT 420 (Heraeus Kulzer GmbH, Dormagen, Germany).

4.3.2. Thermal demulsification at 45.0 ± 0.5 °C

The above experiment was repeated with 4 new ELMs - two had the PIB concentration of 20.000 g/l (m/v) and two contained 30.000 g/l (m/v) of PIB. These were placed in the UFE 700 oven (Memmert, Schwabach, Germany) at 45.0 ± 0.5 °C for 24 hours for de-emulsification.

4.3.3. Combination of chemical and thermal demulsification at 70.0 ± 0.5 °C

4.3.3.1. Emulsification and addition of Polyethylene glycol 400

The diluent containing 20 g/l of PIB was prepared like the ones in 4.2.2.4 and the diluent containing 30 g/l PIB was prepared like the one in 4.2.2.7. ELMs were prepared as follows:

a) A diluent with 20 g/l of PIB was mixed with 2 M nitric acid in the ratios 1:2 (20 ml of the nitric acid: 40 ml of diluent) to form 1:2 ELMs in 150 ml Erlenmeyer flasks. The flask was shaken for 40 minutes using an orbital shaker at 600 rpm. Five more ELMs were prepared in the same way. Polyethylene glycol with a molecular weight of 400 g/mol (PEG) was added, as shown in Table 1, to the 6 ELMs. The flasks were shaken at 600 rpm on the orbital shaker for 75 minutes.

Table 4.1: The amount of PEG added to each emulsion.

Emulsion	PEG added (g)
1	**0**
2	**1**
3	**2**
4	**4**
5	**6**
6	**10**

The ELMs containing 30.000 g/l of PIB were prepared in an analogical fashion and the same amounts of PEG were added (as in Table 4.1). This resulted in 12 ELMs which were subsequently statically and chemically demulsified using a UFE 700 oven, with the demulsification temperature set to 70 ± 1.0 °C and the incubation period equal to 24 hours. The bottom layer was pipetted and COD was carried out to determine how much of the diluent is in the aqueous phase.

4.3.3.2. ELM carry-over

After chemical de-emulsification, organic (diluent) layer from the given ELM was removed using a 10 ml glass pipette. Then the bottom/stripping layer from each ELM was transferred into a clean COD tube and was centrifuged at 3 000 rpm using an Allegra X-15 bench top centrifuge (Beckman Coulter, Johannesburg, South Africa). Once the centrifugation was finished, the COD concentration was measured in the stripping phase (bottom layer; see Section 4.3.3.3 for details and Chapter 3 Section 3.3). The aim of the measurement was to determine carry-over of the diluent components, extractant and the SPAN 80 into the stripping phase. Subsamples of the stripping phase were removed and examined for the presence of trace emulsion globules under a microscope with the magnification of 400x. This provides an indication of the completeness of phase separation, i.e. the effectiveness of the demulsification process.

The structures and aqueous solubilities of the individual ELM components were first examined to identify which of the ELM components were responsible for the COD concentrations measured in the stripping phase. SPAN 80 is otherwise known as sorbitan mono-oleate and it is only dispersible and practically insoluble in water. At the same time, kerosene contains mostly

hydrocarbons with limited or negligible aqueous solubility. This was proven by extraction of the stripping phase and measurement of kerosene levels below the LOD of the gas chromatographic method. Given the structure of TOA and the highly acidic pH of the aqueous phase, it is possible for TOA molecules to partition into the stripping phase by formation of ion pairs with nitrate anions from HNO_3 molecules. Molecules of toluene have been shown to undergo hydrogen bonding with molecules of water and its aqueous solubility has been shown to be around 526 mg/l (Tandlich, Zuma 2012). These two compounds are therefore most likely to contribute significantly to any carry-over of ELM components into the stripping phase during de-emulsification.

The following experiment was performed to measure the actual contribution of TOA and toluene to the COD in the stripping phase after de-emulsification. A fresh batch of the ELM mentioned above was prepared and demulsified in the same fashion. Next, the aqueous phase was placed in a 250 ml separating funnel and 20 ml of n-hexane was added. The contents of the funnel were vigorously hand-shaken for 5 minutes to achieve extraction of organic components. The funnel was left to stand until phase separation was observed and the n-hexane layer was collected into a 100ml volumetric flask. This was then stoppered and extraction was repeated twice with fresh 20 ml aliquots of n-hexane. The three n-hexane extracts were combined and dried with 2.00 g of anhydrous $MgSO_4$ (Sigma-Aldrich, Johannesburg, South Africa). Then 20 ml of the organic extract was pipetted into a clean 250 ml Erlenmeyer flask and the solution was titrated for the TOA content (see section 3.6 for details). The remainder of the organic extract was concentrated under a gentle stream of nitrogen to 1 ml and transferred into a 2 ml GC vial. The content of toluene was determined using GC analysis (see section 3.4 for details).

4.3.3.3. Chemical oxygen demand (COD)

For COD analysis, 3 ml of the aqueous samples were pipetted into the COD test tubes. Then 0.3 ml of reagent A (catalogue number: 1.14679.0495) purchased from Merck (Pty.) Ltd. (Johannesburg/Cape Town, South Africa) and 2.3 ml of reagent B (catalogue number: 1.14679.0495) purchased from Merck (Pty.) Ltd. (Johannesburg/Cape Town, South Africa) were added to each test-tube. The COD test tubes were tightly closed with a screw cap and the contents were mixed using a vortex machine. The samples were incubated at 148 ˚C in a TR-300

thermoreactor for 2 hours. After 2 hours the samples were allowed to cool at 21 ± 2 °C for 15 minutes. Absorbance readings were taken at 600 nm.

4.3.3.4. Combination of chemical and thermal demulsification at 50.0 ± 1 °C

The diluents from above in 3.3.4 were used in this experiment. The diluent with 20 g/l of PIB was mixed with 2M nitric acid in the ratios 1:2 (20 ml of the nitric acid: 40 ml of diluent) to form 1:2 ELMs in 150 ml Erlenmeyer flasks. The flask was shaken for 40 minutes using an orbital shaker at 600 rpm. Ten grams (10 g) of PEG was added and the emulsion was shaken at 600 rpm on the orbital shaker for 75 minutes. Emulsion containing 30 g/l of PIB was made and treated with PEG in the same way. The two ELMs were placed in an oven at 50 ± 1 ˚C for 24 hrs. The bottom layer was pipetted and chemical oxygen demand (COD) was carried out to determine how much of the diluent is in the aqueous phase.

4.4. RESULTS

4.4.1. Emulsification and micro-droplet globule size optimisation

4.4.1.1. Kerosene-TBP diluent and sonication

After 20 minutes of shaking, the two phases did not mix completely. Some aqueous phase mixed with the diluent to form a whitish, small emulsion which was very unstable in terms of phase separation. After leaving it to stand, complete separation was observed. The diluent floated above the aqueous phase.

4.4.1.2. kerosene-TBP-PIB-TOA-SPAN 80 diluent and sonication

Whitish ELMs were formed. There was some aqueous phase which did not mix with the organic/diluent phase. It took 167 minutes for a distinct separation of the two phases in the 1:1 preparation and it took 92 minutes for distinct separation of the two phases in the 1:2 preparation and it took 55 minutes to form in the 1:3 preparation. Sonication and the diluents from sections

4.2.2.1 and 4.2.2.2 were not suitable for application in extraction of Rh from side-streams (see section 4.5.1.1 for explanation).

4.4.1.3. kerosene-TBP-PIB-TOA-SPAN 80diluent Orbital shaking 1

The aqueous phase and the diluent (organic) phase mixed completely to form milky white ELMs. The ELMs were stable for 3 hours before phase separation began.

4.4.1.4. kerosene-Toluene-PIB-TOA-SPAN 80 diluent and orbital shaking 2

Here ELM stability and micro-droplet diameters are described for the diluents and preparation by orbital shaking as outlined in sections 4.2.2.3 and 4.2.2.4. The aqueous phase and the diluent (organic) phase mixed completely to form milky white ELMs. After the first round of shaking, all ELMs remained stable for 12 hours before phase separation took place. Re-emulsification occurred after the shaking was repeated. The 1:1 and 1:2 ELMs subsequently remained stable for 12 hours before phase separation reoccurred. The 1:3 and the 1:4 ELMs remained stable for 10 hours, after which separation occurred. No ELMs were stable beyond 24 hours when stored at 5 ± 2°C. Thus the ELMs for extraction will have to be prepared on the extraction day, and as close to the start of the Rh extraction as possible. The average micro-droplet size distribution, as determined using optical microscopy, is shown in Figure 4.1. The average globule diameters of 1:1, 1:2, 1:3 and 1:4 were as follows (µm): 10.8 ± 2.8; 4.0 ± 1.6; 11.4 ± 4.6 and 14.6 ± 6.7. Shaking was done for 20 minutes. This was outside of the optimum 1-3 µm range and therefore the mass transfer characteristics of these ELMs would not be favourable for Rh extraction from metal refinery side-streams.

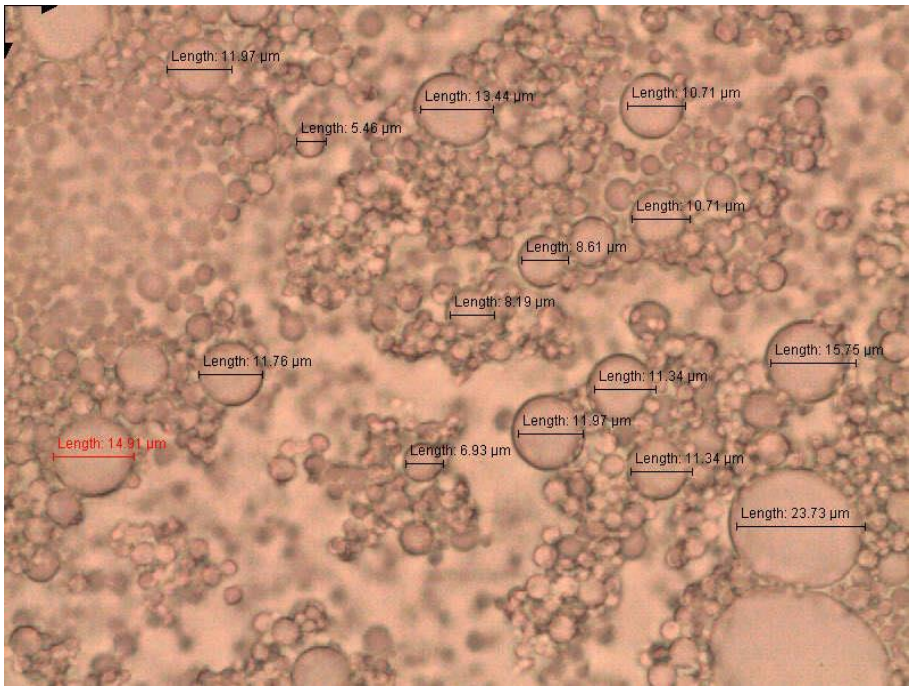

(a)

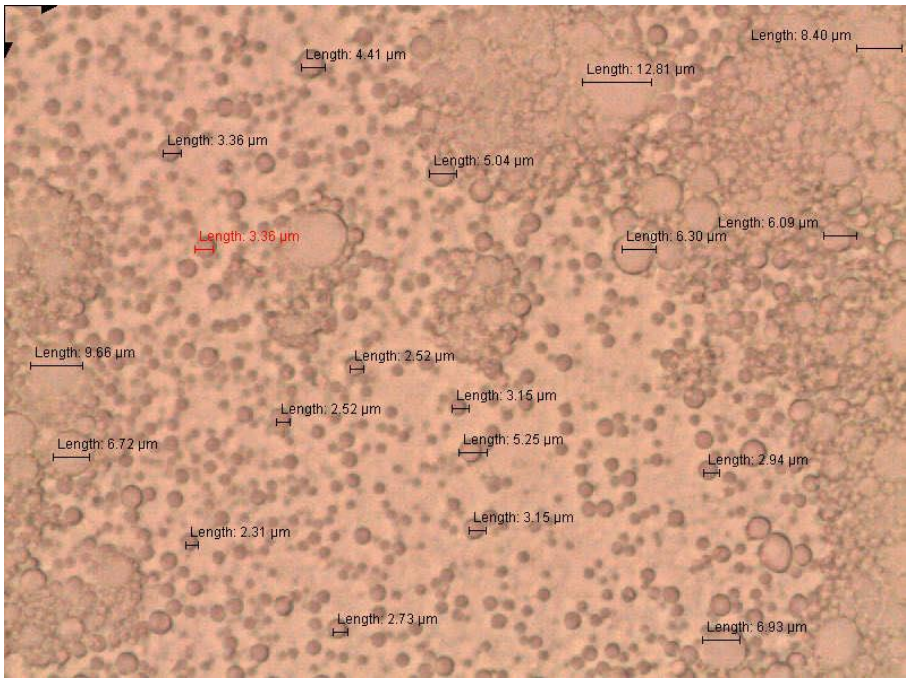

(b)

Figure 4.1: *(a) Globule sizes of a 1:1 emulsion; (b) Globule sizes of a 1:2 emulsion (c) Globule sizes of a 1:3 emulsion (d) Globule sizes of a 1:4 emulsion after 20 minutes of shaking*

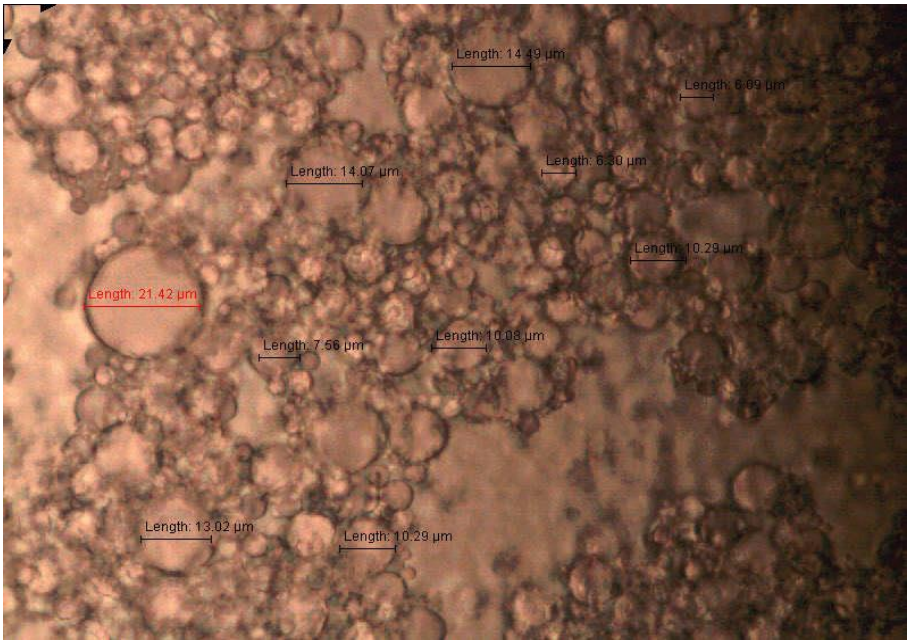

(c)

(d)

Figure 4.1 (Continued): *(a) Globule sizes of a 1:1 emulsion; (b) Globule sizes of a 1:2 emulsion (c) Globule sizes of a 1:3 emulsion (d) Globule sizes of a 1:4 emulsion after 20 minutes of shaking.*

The Zeta potential (ZP), poly-dispersity index (PI) and micro-droplet sizes as determined using the Zetasizer of the 1:1, 1:2, 1:3 and 1:4 ELMs are shown in Table 4.2 below.

Table 4.2: The ZP, PI and micro-droplet sizes as determined using the Zetasizer of the ELMs after 20 minutes of shaking.

Emulsion	Average Micro-droplet size (µm)	ZP (mV)	PI
1:1	5.93 ± 2.8	+ 45	0.65
1:2	4.66 ± 1.9	+ 35	0.57
1:3	5.31 ± 3.7	+ 55	0.70
1:4	5.69 ± 2.9	+ 67	0.53

4.4.1.5. kerosene-Toluene-PIB-TOA-SPAN 80 diluent and orbital shaking 3

a) After 20 minutes

Micro-droplet size distribution indicated that the average diameters, as determined using optical microscopy, of the 1:1 ELMs were 5.8 ± 1.5 µm after storage at 22 ± 1 °C after 12 hours. This value was 5.8 ± 2.9 µm after re-shaking and storage at 5 ± 2 °C for up to 24 hours (see section 4.2.2.6 for details). The average diameters of the micro-droplets with the 1:2 ELMs were 3.4 ± 1.0 µm and 3.3 ± 0.8 µm. The first value is reported for the ELM storage at 22 ± 1 °C after 12 hours, while the second describes the micro-droplet size distribution after re-constitution of the ELMs through the second shaking for 20 minutes and storage at 5 ± 2 °C for up to 24 hours.

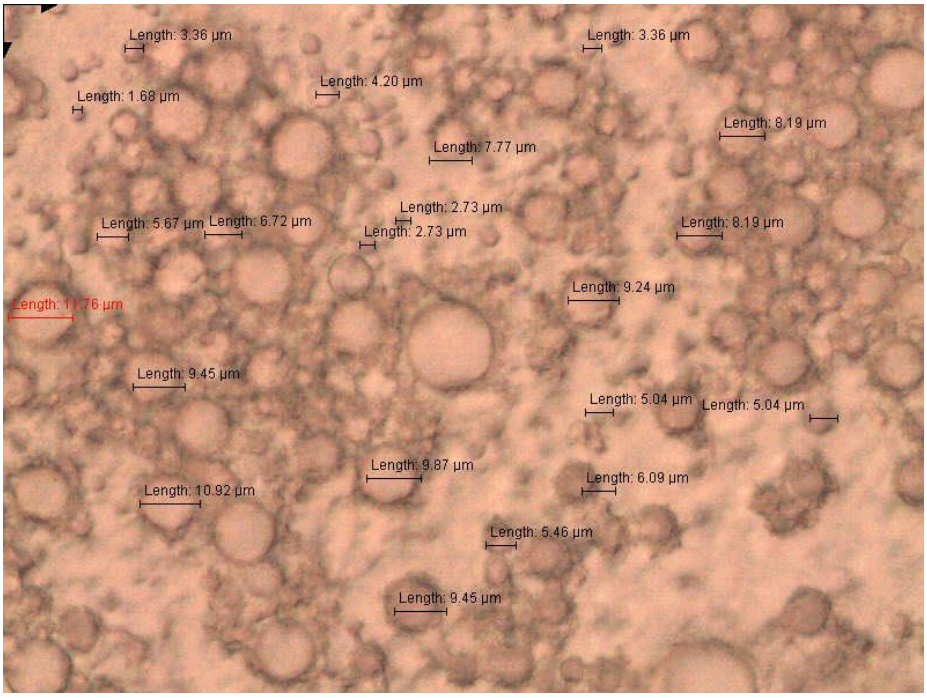

(a)

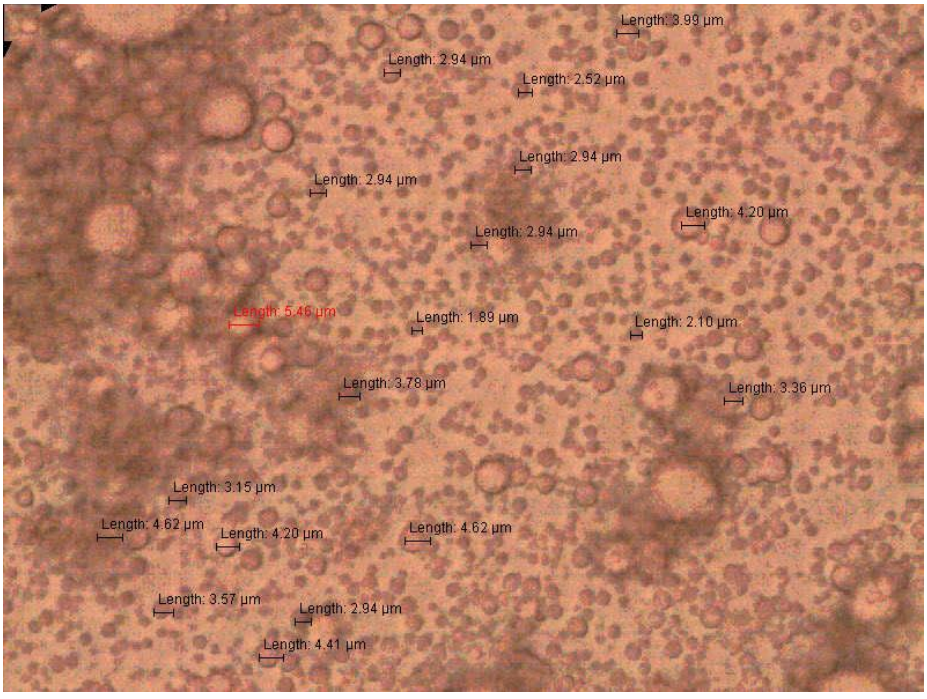

(b)

Figure 4.2: *a) Globule size of a 1:1 emulsion after 20 minutes of shaking. (b) Globule size of a 1:2 emulsion after 20 minutes of shaking.*

b) After 40 minutes

The 1:1 and 1:2 ELMs were stable. There was no phase separation after 12 hours in 21 ± 2 °C. Figure 4.3 shows images of the ELMs under a microscope with magnification of 400x. From the images shown below, the 1:1 emulsion tends to form globules of a similar size to the 1:2 after increased shacking time. The average globule diameters, as determined using optical microscopy, of the 1:1 ELMs were 3.1 ± 0.8 µm and 3.5 ± 1 µm. The average diameters of the globules of the 1:2 ELMs are 3.3 ± 0.5 µm and 2.9 ± 0.9 µm (Appendix I). In both cases, the first average value is reported for ELM storage at 22 ± 1 °C after 12 hours, while the second describes the micro-droplet size distribution after re-constitution of the ELMs through the second shaking for 40 minutes and storage at 5 ± 2 °C for up to 24 hours.

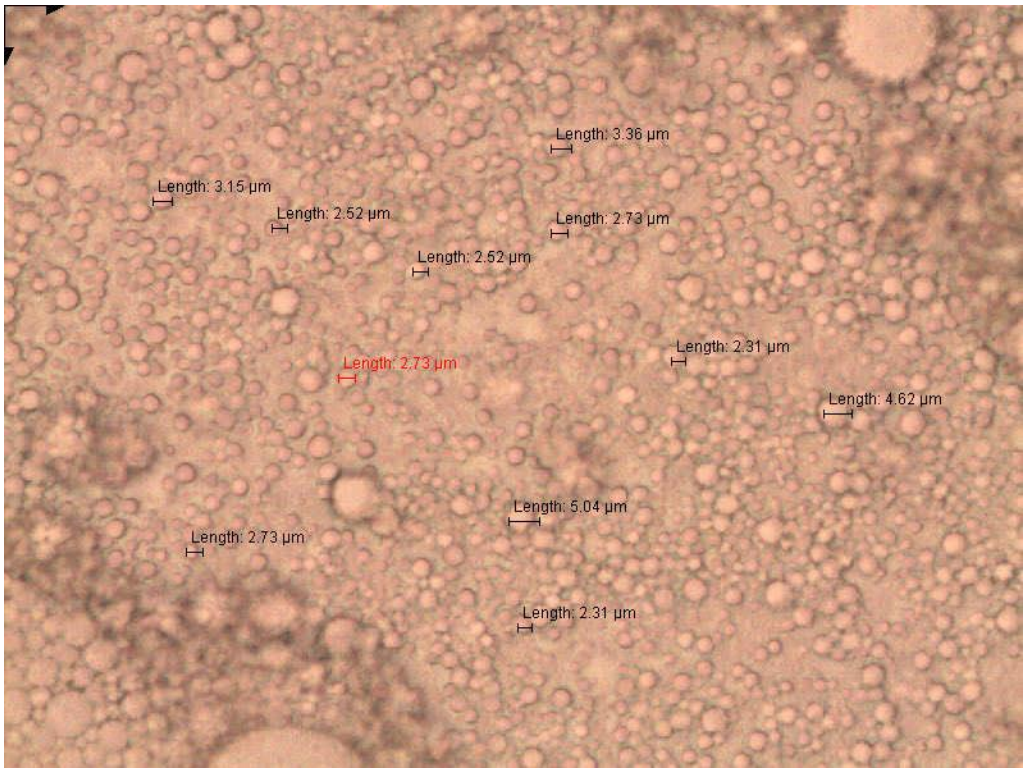

(a)

Figure 4.3: *Optical microscope photographs of ELMs containing 20 g/l of PIB after 40 minutes of shaking. a) Globule sizes of a 1:1 emulsion. (b) Globule sizes of a 1:2 emulsion.*

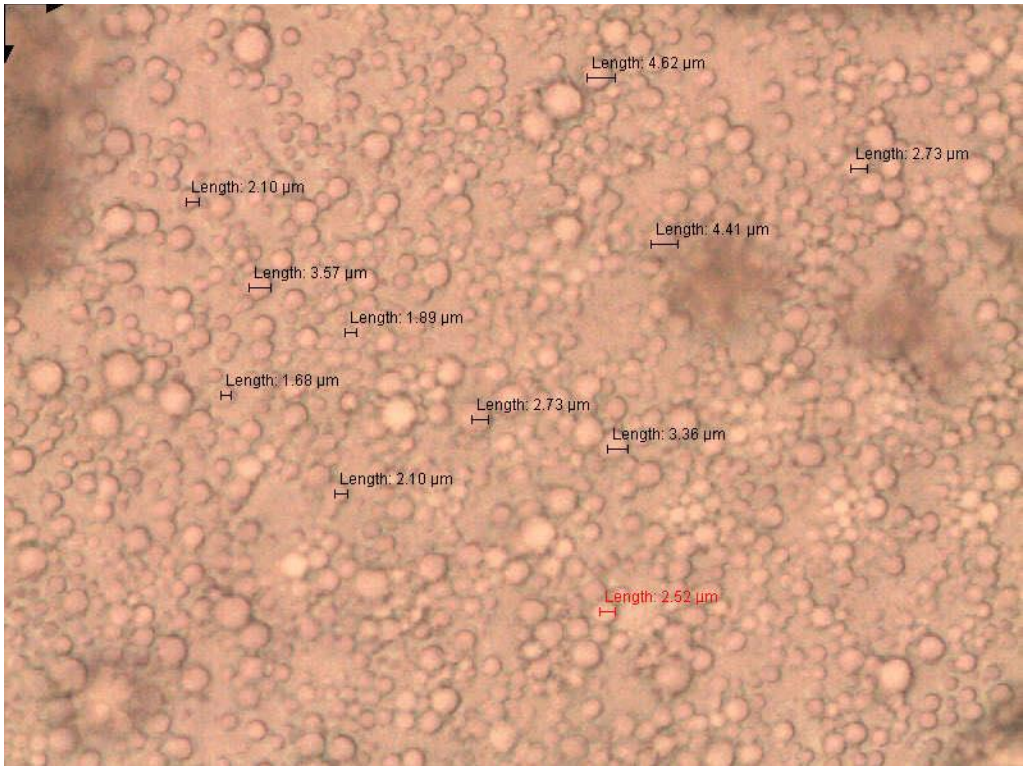

(b)

Figure 4.3 (Continued): *Optical microscope photographs of ELMs containing 20 g/l of PIB after 40 minutes of shaking. a) Globule sizes of a 1:1 emulsion. (b) Globule sizes of a 1:2 emulsion.*

The ZP, PI and micro-droplet sizes as determined using the Zetasizer of the 1:1 and 1:2 ELMs containing 20 g/l PIB after shaking for 20 minutes and 40 minutes are shown in Table 4.3 below.

Table 4.3: The ZP, PI and micro-droplet sizes as determined using the Zetasizer of the 1:1 and 1:2 ELMs after 20 minutes and 40 minutes of shaking.

Time of shaking	**20 minutes**		**40 minutes**	
Emulsion	**1:1**	**1:2**	**1:1**	**1:2**
ZP (mV)	+ 55	+ 43	+ 47	+ 45
PI	0.54	0.53	0.43	0.47
Average micro-droplet size (µm)	5.31 ± 2.6	4.93 ± 1.0	3.83 ± 0.8	2.34 ± 1.1

4.4.1.6. kerosene-Toluene-PIB-TOA-SPAN 80 diluent and orbital shaking 4

For the 1:1 ELMs, average micro-droplet diameters as determined using optical microscopy ranged from 3.0 ± 0.6 µm, 3.2 ± 0.5 µm and 4.1 ± 0.7 µm. The respective values for the 1:2 ELM (see section 4.2.2.7) stood at 3.0 ± 0.5 µm; 2.8 ± 0.4 µm and 2.9 ± 1.0 µm. For both types of ELMs, the first average diameter represents the microdroplet size distribution right after the 12 hour storage at 21 ± 2 °C. The second diameter indicates the microdroplet size distribution after the 12 hour storage at 21 ± 2 °C and reconstitution of the ELMs. The last diameter described the changes of the microdroplet diameter distribution after storage of the reconstituted ELM at 5 ± 2 °C for 24 hours. Diluent containing 30.000 g/l (w/v) PIB, 10.870 g/l (m/v) of TOA and 51.001 g/l (m/v) of SPAN 80 when mixed with 2 M HNO_3 in volumetric ratios of 1:1 or 1:2 leads to the formation of stable ELMs which can be used for up to 12 hours without requiring reconstitution. Storage in the refrigerator is possible after reconstitution and reuse is feasible on two different days.

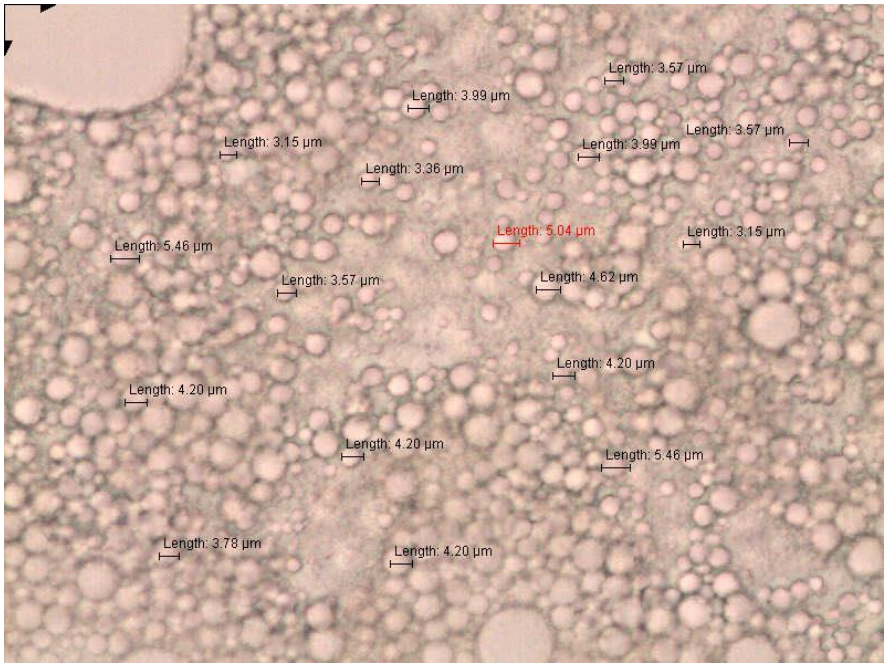

(a)

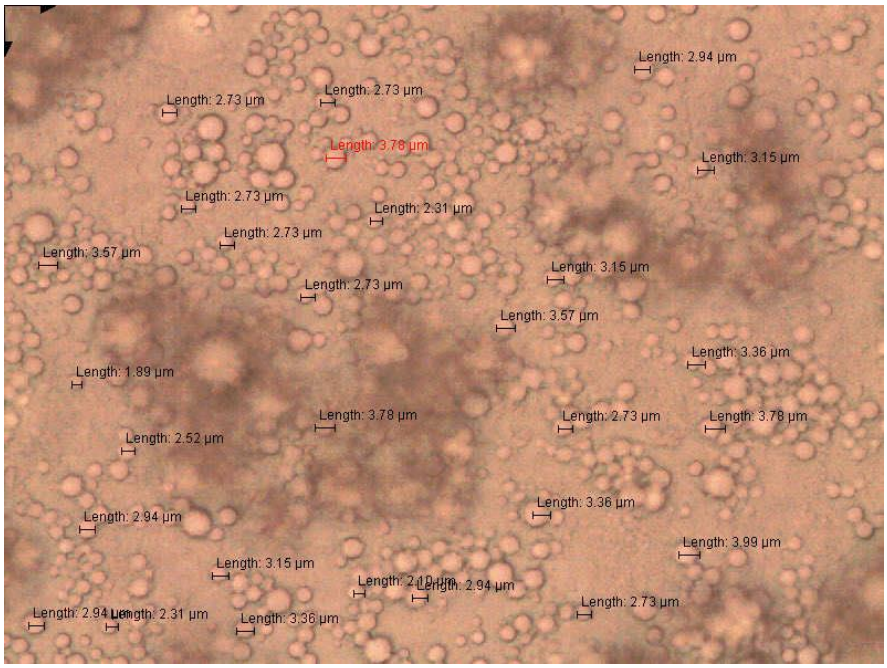

(b)

Figure 4.4: *Optical microscope photographs of ELMs containing 30 g/l of PIB. a) Globule size of a 1:1 emulsion after 40 minutes of shaking. (b) Globule size of a 1:2 emulsion after 40 minutes of shaking*

The ZP, PI and micro-droplet sizes as determined using the Zetasizer of the 1:1 and 1:2 ELMs containing 30 g/l PIB after shaking for 20 minutes and 40 minutes are shown in Table 4.4 below.

Table 4.4: The ZP, PI and micro-droplet sizes as determined using the Zetasizer of the 1:1 and 1:2 ELMs after 40 minutes of shaking.

Time of shaking	**40 minutes**	
Emulsion	**1:1**	**1:2**
ZP (mV)	+ 35	+ 40
PI	0.65	0.55
Average microdroplet size (µm)	3.36 ± 0.6	2.84 ± 1.0

4.4.2. De-emulsification

4.4.2.1. Thermal demulsification

Examples of ELMs after thermal demulsification at 35 ± 0.5°C and 45 ± 0.5°C are shown in Figures 4.5 and 4.6. Limited or no phase separation was observed after 24 hours. This was after shaking for 10 and 20 minutes.

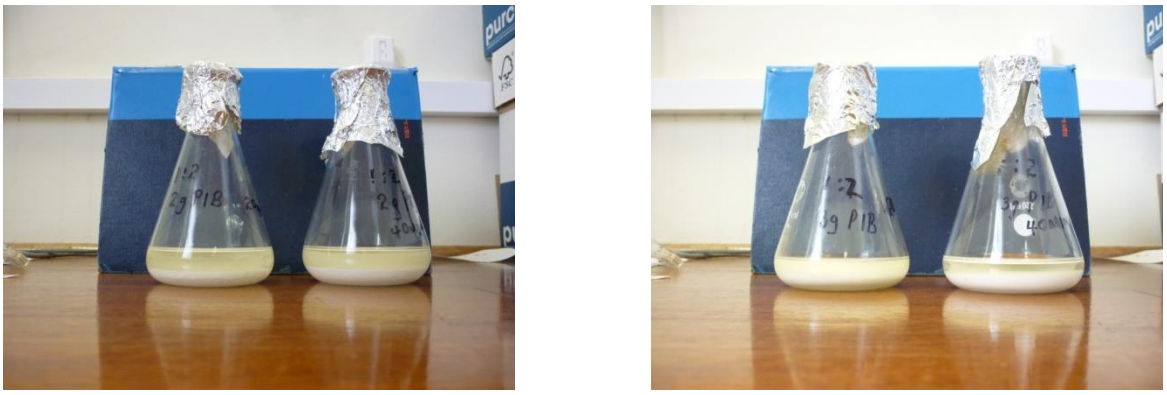

(a) (b)

Figure 4.5: *Incubations at 35 ± 0.5 ºC a) 1:2 ELMs after incubation for 24 hours with 20.000 g/l PIB. b) 1:2 ELMs after incubation for 24 hours with 30.000 g/l PIB*

(a) (b)

Figure 4.6: *Incubations at 45 ± 0.5 ºC a) 1:2 ELMs after incubation for 24 hours with 20.000 g/l PIB. b) 1:2 ELM after incubation for 24 hours with 30.000 g/l PIB*

4.4.2.2. Combination of chemical and thermal demulsification

Twelve milky white w/o ELMs were formed after 40 minutes of shaking. After the addition of the required amount of PEG and shaking for 75 minutes, the ELMs remained milky white. Figure 4.7 shows six of the milky white ELMs formed.

Figure 4.7: *ELMs after the addition of PEG and shaking for 40 minutes.*

Phase separation was achieved after the PEG 400 addition and heating of the ELM at 70°C for 24 hours (examples can be seen in Figure 4.8).

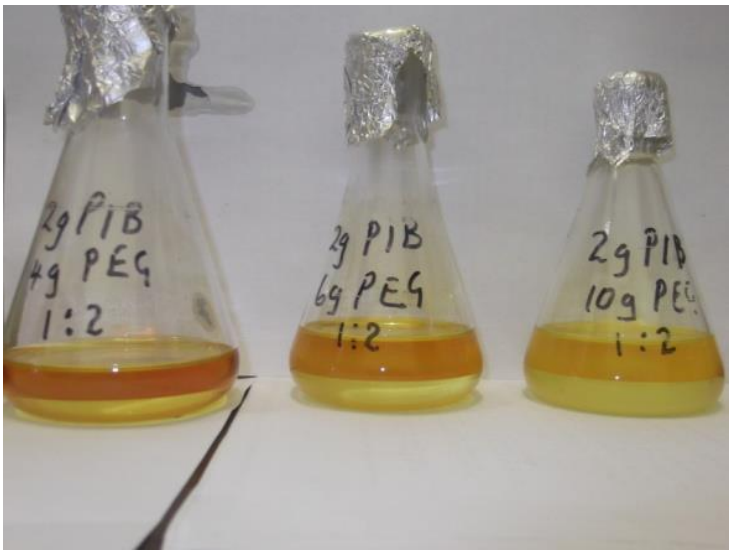

(a)

Figure 4.8: *(a) Chemical demulsification at 70°C for 24 hours when the diluent contained 20.000 g/l PIB (b) and when the diluent contained 30.000 g/l.*

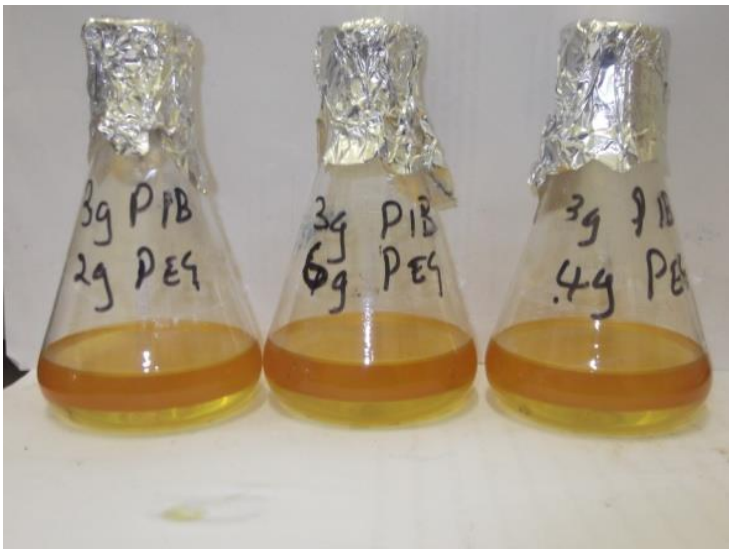

(b)

Figure 4.8 (continued): *(b) and when the diluent contained 30.000 g/l.*

4.4.2.3. Chemical oxygen demand

There was significant carry-over of ELM diluent components into the stripping phase, as demonstrated by the stripping phase COD concentrations shown in figure 4.9. The tables of absorbances are shown in Appendix II (Tables 3 and 4). At the same time, no emulsion droplets were detected microscopically in either the stripping phase or the diluent layer.

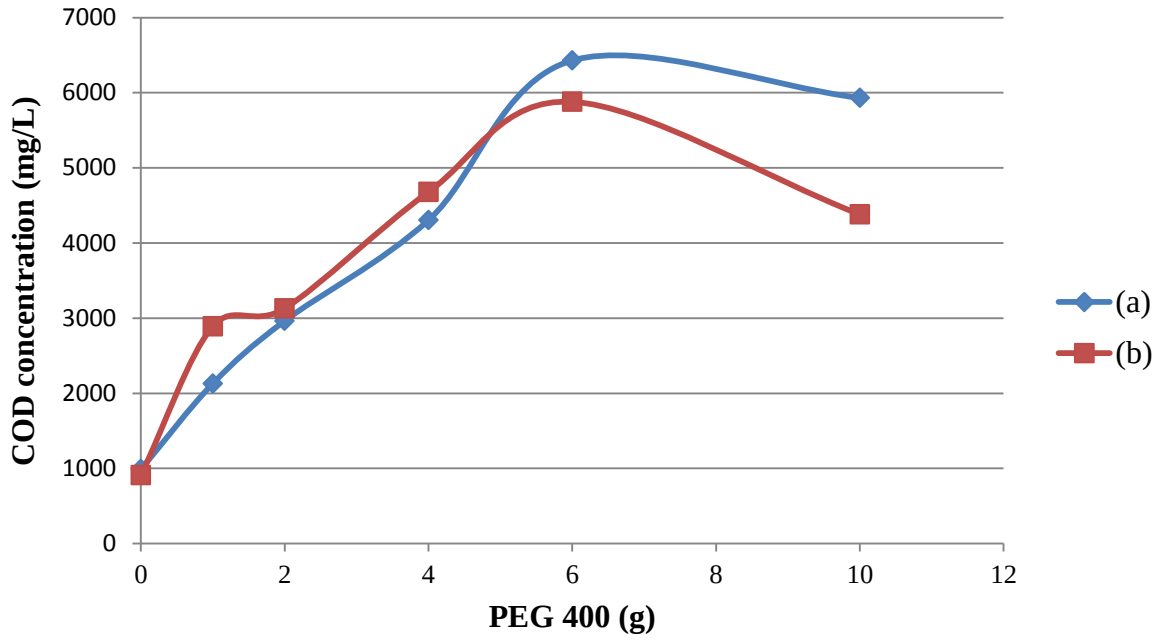

Figure 4.9: *The COD values obtained from the aqueous phase of the demulsified ELMs in relation to the amount of PEG 400 added as a chemical de-emulsifier: (a) COD graph of the aqueous phase of the ELMs containing 20g/l PIB and (b) COD values of the aqueous phase of the ELMs containing 30 g/l PIB.*

4.4.2.4. Combination of chemical and Thermal demulsification at 50.0 ± 1 °C

When the chemical demulsification was performed by shaking at 600 rpm for 75 minutes and incubations at 50 ± 1°C, the ELMs lost stability and complete phase separation was observed, as shown in Figure 4.10. No ELM micro-droplets were observed in the stripping phase or the diluent.

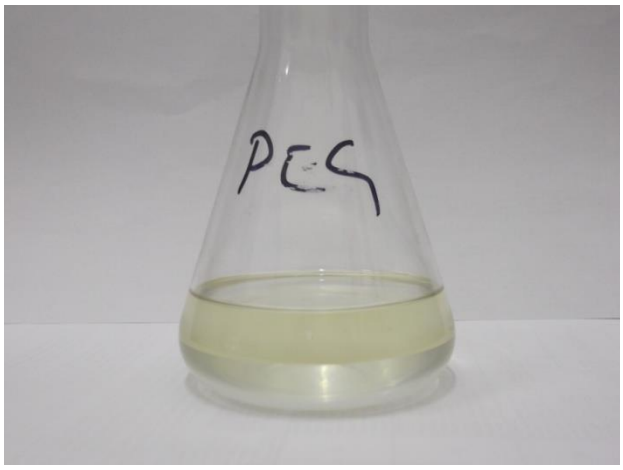

Figure 4.10: *1:2 emulsion with 10 g of PEG after incubation for 24 hours at 50 ˚C with 20 g/l PIB*

Figure 4.11 below shows the differences in appearance of the ELMs de-emulsified at 70 ˚C and at 50 ˚C. Both ELMs contained 20 g/l PIB and 6 g of PEG.

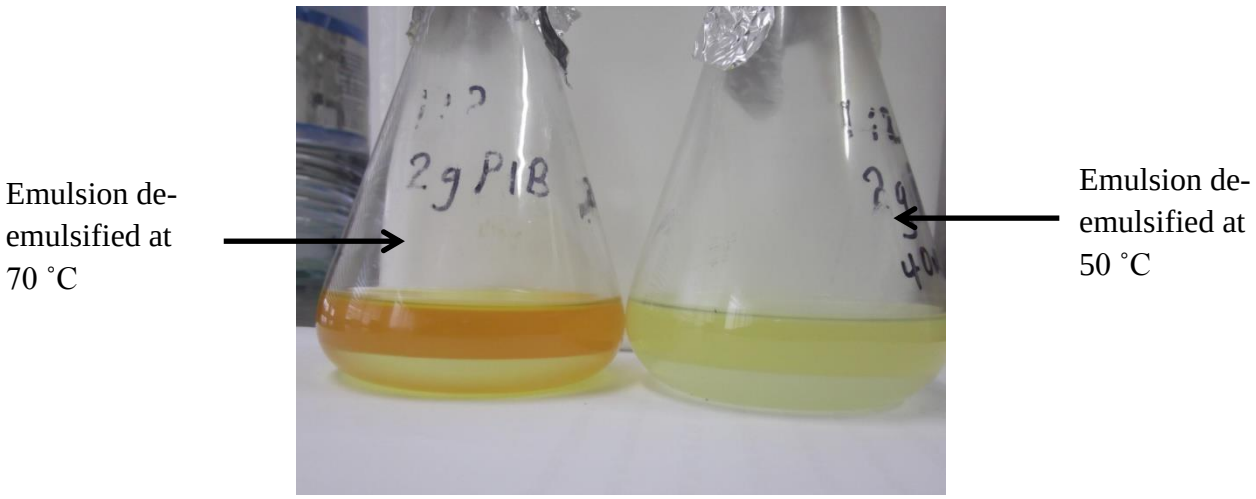

Figure 4.11: *Comparison of demulsification at 50 ˚C and 70 ˚C of ELMs containing 6 g of PEG*

4.4.2.5. ELM carryover

Average TOA concentration in the stripping phase was equal to 0.172 g/l. The contribution of these TOA levels to the measured COD concentrations can be estimated using the stoichiometry of the TOA molecule during the COD digestion as shown in Equation 4.1:

$$(C_8H_{17})_3N + 36O_2 \rightarrow NH_3 + 24CO_2 + 24H_2O \qquad (4.1)$$

The average volume of stripping phase after demulsification was equal to 15 ml. Combining Equation 4.1 with the molecular weights of TOA (353.68 g/mol) and O_2 (32 g/mol), the relationship between the TOA concentration and the COD contribution from TOA can be derived to obtain Equation 4.2.

$$COD = 3.257 \times C(TOA) = 560\, mg/l \quad (4.2)$$

The concentration of TOA is unlikely to be influenced by the weights of the PEG added to the ELM prior to demulsification as this compound is miscible with water and TOA is highly hydrophobic. The average toluene concentration in the stripping phase was equal to 450 mg/l, but the concentrations varied by up to 30 %. Toluene contribution to the measured COD concentrations can be estimated using the stoichiometric Equation 4.3:

$$C_7H_8 + 9O_2 \rightarrow 7CO_2 + 4H_2O \quad (4.3)$$

The average volume of stripping phase after demulsification was equal to 15 ml. Combining Equation 4.3 with the molecular weights of toluene (92.14 g/mol) and O_2 (32g/mol), the relationship between the stripping phase concentration of toluene and the respective COD levels takes the form of Equation 4.4.

$$COD = 3.126 \times C(toluene) = 1\,410\, mg/l \quad (4.4)$$

4.5. DISCUSSION

4.5.1. Emulsification and micro-droplet globule size optimisation

4.5.1.1. Emulsification without a surfactant

Emulsification without a surfactant leads to formation of a very unstable emulsion, as described in Section 4.4.1.1. This was due to re-coalescence of the droplets resulting from very high interfacial tension between the water and oil phases. These are adhesive forces between the liquid phase of one substance and either a solid, liquid or gas phase of another. This interaction happens at their interfaces. The absence of a surfactant in the system leads to the formation of two separate layers. Surfactants reduce interfacial tension by adsorbing at the liquid-liquid

interface between oil and water, allowing the formation of a thermodynamically stable emulsion (Aulton, Wells 2002, Aulton, Taylor 2007).

4.5.1.2. Droplet size

Smaller droplets have higher extraction efficiency as well as better breaking resistance compared to larger droplets (Li, Cahn et al. 1983). It is imperative that the emulsification process produces smaller micro-droplets. Li et al (1983) also suggested that if the droplets are small, the emulsion cannot be broken down easily by mechanical methods. This becomes a disadvantage to the ELM process because the ELM must easily break in the demulsification process in order to recover the extracted compound. Therefore the micro-droplet size for the ELM extraction process must be small enough to facilitate efficient extraction but big enough not to create a very stable ELM which cannot be easily demulsified. On the other hand, very large droplets cause the membranes to rupture easily, due to easy coalescence, resulting in poor stability and poor extraction efficiency (Patnaik 1995). Mechanical agitation was used for emulsification because it generates a strong flow field (Ahmad, Kusumastuti et al. 2011). An orbital shaker at a speed of 600 rpm for 40 minutes was used in the current study. Other studies have shown that speeds up to 24 000 rpm for varying time intervals have been used (Bringas, San Roman et al. 2006). Differences in emulsion composition are pivotal in obtaining small micro-droplet diameters at particular speed intervals (Ahmad, Kusumastuti et al. 2011)

Differences in the emulsion composition, as stated by Ahmad et al (2011), are important in obtaining ELMs of small micro-droplets size diameter at particular speeds. The average micro-droplet size using the optical microscope in the current study (see Section 4.4.1.5b) after shaking at a speed of 600 rpm for 40 minutes were 3.1 ± 0.9 µm and 3.4± 0.9 µm for 1:1 ELMs and 3.3 ± 0.5 µm and 2.9 ± 1.0 µm for the 1:2 ELMs for emulsions which contained 20 g/l PIB (Figure 4.3). The Zetasizer produced micro-droplet sizes of 3.83 ± 0.8 µm and 2.34 ± 1.1 µm for 1:1 and 1:2 ELMs respectively after 40 minutes, as shown in Table 4.3. The *t*-test was used to test for the difference between means obtained using the optical microscope and the Zetasizer. The *p* value 0.5465 at 5 % level of significance for 1:1 ELM showed that the the difference between the means for the 1:1 ELM was statistically insignificant, while the *p* value: 0.0009, at 5 % level of significance for 1:2 ELM showed that the difference between the means for the 1:2 ELM was

significant. For highly viscous ELMs formed with 30 g/l PIB, the average micro-droplet size of the 1:1 ELMs were 3.0 ± 0.6 µm, 3.2 ± 0.5 µm and 4.1 ± 0.7 µm and the average diameters of the globules of the 1:2 ELMs are 3.0 ± 0.5 µm; 2.9 ± 0.4 µm and 2.9 ± 1.0 µm (Figure 4.4) using the optical microscope. The Zetasizer produced micro-droplet sizes of 3.36 ± 0.6 µm and 2.84 ± 1.0 µm for 1:1 and 1:2 ELMs respectively after 40 minutes, as shown in Table 4.4. The *p* values 0.105, 0.4287 at 5 % level of significance for 1:1 ELM showed that the difference between the means for the 1:1 ELM was statistically insignificant. The *p* value: 0.6343 and 0.6619 at 5 % level of significance for 1:2 ELM showed that the the difference between the means for the 1:2 ELM was were statistically insignificant. The *p* value of 0.3018 at 5 % level of significance for the difference between mean micro-droplet size for 1:2 ELMs containing 20 g/l and 30 g/l PIB obtained using a Zetasizer after 40 minutes shows that there was statistically no significant difference in micro-droplet size for 1:2 ELMs containing 20 g/l and 30 g/l PIB.

Hence the 1:2 ELM will be used for the extraction of Rh in Chapter 5 because they produced micro-droplets in the range of 0.8-3 µm. ELMs of good stability and rapid extraction have droplets in the range of 0.3-10 µm although the most preferable range is 0.8-3µm (Li, Cahn et al. 1983, Chanukya, Rastogi 2013). These values for optical microscopy were calculated from the micro-droplets with diameters big enough to be measured under the microscope at a magnification of 400x. From Figures 4.3 and 4.4, it is clear that most of the droplets were small and it was not easy to measure them using the optical microscope, hence use of the Zetasizer.

4.5.1.3. Emulsification speed and time.

In the current study, two time intervals of 20 minutes (Figure 4.2) and 40 minutes (Figure 4.3) were used. In Figure 4.2 (a) for 1:1 emulsion, the average droplet diameter was 5.8± 1.5 µm and 5.8 ± 2.9 µm and, from Figure 4.2 (b) for 1:2 emulsions, the average droplet sizes were 3.4 ± 1.0 µm and 3.4 ± 0.8 µm using the optical microscope. Most droplets were so small that it was difficult to measure them as they were below 3 µm, hence the Zetasizer was utilized. As shown in Table 4.3 after 20 minutes of shaking, the micro-droplet sizes were 5.31 ± 2.6 µm and 4.93 ± 1.0 µm. Zetasizer and optical microscope results were comparable for the 1:1 emulsion. In Figure 4.3 (a), which is the globule sizes of a 1:1 emulsion after 40 minutes of shaking, showed small droplet sizes compared to 1:1 emulsion at 20 minutes (Figure 4.2a) and, in Figure 4.3 (b),

which is the globule sizes of a 1:2 emulsion after 40 minutes of shaking, showed smaller droplet sizes than the 1:2 emulsion at 20 minutes. These results were confirmed using the Zetasizer (Table 4.3).

These are in agreement with other studies. It has been reported that emulsification speed and time have a direct effect on the droplet size. Droplet size decreases as the emulsification speed and time increase (Chiha, Samar et al. 2006, Gasser, El-Hefny et al. 2008, Venkatesan, Meera Sheriffa Begum 2009b). In studies on the effect of speed and time of emulsification reported by Venkatesan, Meera Sheriffa Begum (2009b) and Venkatesan, Meera Sheriffa Begum (2009a), w/o ELMs were prepared using a speed of 2 000 – 12 000 rpm at different time intervals of between 2 – 10 minutes, and they obtained an optimum emulsification time of 6 mins at 10 000 rpm. In another study, optimum emulsification time and speed obtained was 5 mins and 7 000 rpm respectively, where w/o ELMs were made using a speed of range of 3 000 rpm – 8 000 rpm from between 2 – 10 minutes (Gasser, El-Hefny et al. 2008). In the current study, a lower speed was used for a longer time, whilst in these cited studies high speeds were used for a shorter time interval. Studies have shown that higher speeds, compared to the 600 rpm used in this study, have been used to produce smaller micro-droplets. A speed of 12 000 rpm for 30 minutes to produce micro-droplets of 3.35, 3.424 and 2.72 µm (Sengupta, Sengupta et al. 2006a, Sengupta, Sengupta et al. 2006b) and in another study, micro-droplets of 2.13 and 1 µm at the speed of 7 000 rpm for 20 minutes were produced (Reis, Carvalho 2004). These differences are due to differences in emulsion compositions.

4.5.1.4. Volume ratio of stripping phase (V_s) to the diluent (V_d)

The ratio of volumes of stripping phase to diluent (V_s/V_d) has been studied and it has a significant impact on the stability of the emulsion and the extraction process (Lee 2011, Goyal, Jayakumar emuet al. 2011, Chanukya, Rastogi 2013). In this study, ratios of 1:1, 1:2, 1:3, and 1:4 (stripping phase: diluent) were examined. The ratio of 1:2 produced ELM with small droplet sizes and hence, by implication, it was more stable and had a better extraction ratio, as discussed in Section 4.5.1.2. The 1:3 and 1:4 produced very large droplets of diameters 11.4 ± 4.6 µm and 14.6 ± 6.7 µm respectively, as can be seen in Figures 4.1 (c) and (d) using the optical microscope. The Zetasizer was used to verify these results. From Table 4.2, the average micro-

droplet diameter for 1:1, 1:2, 1:3 and 1:4 were 5.93 ± 2.8 µm, 4.66 ± 1.9 µm, 5.31 ± 3.7 µm and 5.69 ± 2.9 µm respectively. These results are not comparable to the ones of the optical microscope. But they are still outside the 0.8 to3 µm range which will make a preferable emulsion (Li, Cahn et al. 1983, Chanukya, Rastogi 2013). From Figure 4.1 (b), which is a 1:2, it could be seen that the droplets were smaller and hence 1:2 was preferred. It has been reported that increasing the V_s/V_d decreases emulsion stability. Increasing the volume of the stripping phase leads to the increase in the droplet diameter which in turn leads to easy coalescence of the droplets, reducing the stability of the membrane. Increasing the volume of the stripping phase also leads to leakage of the stripping solution into the external/feed phase (Kumbasar, Şahin 2008, Kumbasar 2009a, Kumbasar 2009b, Kumbasar 2010a). When the volume of the stripping phase is increased beyond a certain critical point, the membrane phase becomes insufficient to cover the disperse phase (Kumbasar 2008) hence the micro-droplets of the stripping phase are not wholly covered by the surfactant, leading to an increase in the interfacial tension resulting in coalescence and membrane instability. It has also been reported that the lower V_s/V_d the more stable the membrane, the higher its resistance is to breakage, the higher the osmotic swelling and entrainment and the less the diffusion process (Wan, Zhang 2002, Mortaheb, Kosuge et al. 2009, Tang, Yu et al. 2010). Less diffusion process, higher osmotic swelling and an increase in entrainment may lead to low extraction efficiency. Hence it is important to select the optimum ratio which is high enough not to impede the diffusion process, high enough not to increase osmotic swelling and entrainment but which is also low enough not to lead to emulsion instability by increasing the droplet sizes and reducing extraction efficiency. For this study, the ratio of 1:2 was used according to the results obtained in Section 4.4.1.6 and Figure 4.4.

4.5.1.5. The choice of a diluent

The choice of the diluent is also important for emulsion stability. The diluent should be compatible with the surfactant and the extractant. Its solubility in the internal and external phase should be negligible and its density should be different to that of the aqueous phase. In this study, kerosene was used because it has been widely and successfully used as a diluent in different studies of ELM (Lee, Hyun 2010, Lee 2011, Bhowal, Bhattacharyya et al. 2012, García, Acosta et al. 2013). Kerosene has been used with TBP as a diluent and has been used with TOA as an extractant (Kumbasar 2010b). Viscosity of the diluent plays an important part in stability of

the membrane. Non-Newtonian modifiers like PIB have been used to increase the viscosity of the diluents (Skelland, Meng 1996, Skelland, (Michael) Meng 1999, Park, Forney et al. 2004, Park 2006). PIB was used in the current study to modify the viscosity of the diluent (kerosene and toluene). Dissolving PIB in a mixture of kerosene and toluene took 24 hours, with shaking at the speed of 100 rpm; hence TBP was replaced by toluene. The other reason for the substitution of TBP was the acid hydrolysis of the TBP molecule, which led to the decrease in ELM stability. Toluene was chosen because it has been successfully used as a diluent in other studies (Kageyama, Matsumiya et al. 2004, Matsumiya, Kageyama et al. 2004, Mortaheb, Kosuge et al. 2009). Hence 30 % of toluene was used and PIB dissolved in 7 hours of shaking at a speed of 100 rpm. For comparison of the effect of viscosity on emulsion droplet size and extraction, ELMs containing concentrations of 20 g/l and 30 g/l of the PIB were used in this study. From Figure 4.4 using 30 g/l of PIB, globule size of a 1:1 emulsion after 40 minutes of shaking were 3.0 ± 0.6 µm, 3.2 ± 0.5 µm and 4.1 ± 0.7 µm. The globule sizes of a 1:2 emulsion after 40 minutes were 3.0 ± 0.5 µm; 2.8 ± 0.4 µm and 2.9 ± 1.0 µm. These values are comparable to the ones obtained in Figure 4.3. This led to the conclusions that there was no significant change in droplet size diameter between ELMs containing 20 g/l and 30 g/l of PIB, as described in Section 4.5.1.2.

4.5.1.6. Surfactant concentration

In this study a concentration of 5 % w/v of SPAN 80 was used as the surfactant. This concentration was chosen based on the literature review of the emulsification process of the ELMs with SPAN 80 as a surfactant. In a study by García, Acosta et al. (2013), the concentration of SPAN 80 was varied from 0 % to 3 % w/v. It was concluded that emulsion stability increases with increases in SPAN 80 concentrations. Optimum extraction was obtained at 2 % w/v SPAN 80. They also stated that 3 % of SPAN 80 formed super stable ELMs which were difficult to break and that very low surfactant concentrations of 0-0.5 % produced unstable ELMs resulting in approximately 0 % extraction of chromium. In a similar study by Chanukya, Rastogi (2013), concentration range of SPAN 80 used was 2-4 %. It was discovered that extraction increases with increases in SPAN 80 concentrations until the concentration of SPAN reaches an optimum, in which case extraction begins to drop. In a different study by Goyal, Jayakumar et al. (2011), 3 % of SPAN 80 resulted in the maximum extraction of chromium. The concentration range of

SPAN 80 used was 1 – 5 %. Above 3 %, the extraction efficiency decreased. Therefore surfactant concentration is vital in the stability and extraction of the membrane. The lower the concentration the more unstable the ELM becomes. When concentration is increased above the critical micelles, aggregate formation takes place in the bulk. Micelles, reverse micelles and surfactant hydration cause breakage and osmotic swelling as they promote the transportation of water from the feed phase to the internal phase. As the surfactant concentration increases the mass transfer resistance is enhanced (Shen, Yin et al. 1996, Venkatesan, Meera Sheriffa Begum 2009a, Ahmad, Kusumastuti et al. 2012).

4.5.1.7. Zeta potential and poly-dispersity index

The zeta potential can be used to predict the physical stability of the emulsion (Müller, Mäder et al. 2000, Mehnert, Mäder 2001, Radomska-Soukharev 2007). For excellent physical stability, a minimum zeta potential of greater than ±60 mV is mandatory and greater than ±30 mV is needed for good physical stability (Freitas, Müller 1998, Heurtault, Saulnier et al. 2003). The ZP of the 1:1, 1:2, 1:3 and 1:4 ranged from + 35 mV to + 55 mV (see Table 4.2) soon after manufacture, meaning that they were relatively stable, and the ZP fell in the range of ±60 mV. Only the 1:4 ELMs had a ZP of +67 mV, which is outside the range and it can be concluded that it was the least stable emulsion. There was no significant difference in the ZP in the study of effect of time on emulsification and micro-droplet size (Section 4.4.1.5). The ZP in the 1:1 emulsion was + 55 and + 47 mV for 20 and 40 minutes respectively and + 47 mV and + 43 mV for 1:2 emulsion for 20 and 40 minutes respectively (Table 4.3). From Table 4.4, the ZP for ELMs prepared using 30 g/l PIB were within the range of stability. Zeta potential decreases with an increase in the energy (light and temperature) of the system due to increased particle kinetic energy thus particle aggregation and gelation (Uner 2006). So to maintain the stability of the emulsion, it was important to keep them in a temperature controlled environment, for example in the fridge. PI is defined as the measurement of the width of the distribution of these particle sizes. In this case, PI is going to be the measurement of micro-droplet sizes. The PI ranges from 0 to 1. In a mono-disperse system, the PI should be 0. PI increases for very broadly distributed particles (Kovacevic, Savic et al. 2011). The PI from Table 4.2 ranges from 0.53 to 0.70. This is an indication that the micro-droplets are not mono dispersed. This means the micro-droplets are of varying sizes. 1:3 ELMs had the largest PI, meaning that, for this emulsion, the difference

between the smallest micro-droplets and the largest micro-droplets was large. In Table 4.3, the PI ranged from 0.43 to 0.54. The ELMs shaken for 40 minutes had a lower PI of 0.3 and 0.47 for 1:1 and 1:2 ELMs respectively. From this it can be concluded that the effect of time on emulsification affects the PI of micro-droplet size. The longer the emulsification time, the better the PI.

4.5.2. Demulsification, ELM carryover and COD

Heat was first used for demulsification. Two temperatures were used: 35 ˚C and 45 ˚C. After 24 hours, demulsification was not achieved, as shown in Figures 4.5 and 4.6. Demulsification efficiency using heat only for ELMs stabilized by SPAN 80 surfactant is very low (Peng, Jiao et al. 2012). Hence there was a need to add a chemical de-emulsifier. The heat was increased to 70˚C and a chemical de-emulsifier, PEG 400, was introduced. Al-Sabagh et al (2013) stated that sometimes a combination of the chemical and the physical approach are necessary for successful demulsification to take place. Hence, in this study, a combination of the chemical approach (PEG 400) and the physical approach (heat) was used. For successful chemical de-emulsification, selection of the chemical de-emulsifier is vital. The quantity and duration of mixing of the de-emulsifier with the emulsion, and the sufficient time to allow the de-emulsifier to coalesce and settle the droplets are also factors to be considered (Al-Sabagh, Nasser et al. 2013). The quantity of the PEG which was optimum for successful demulsification was examined using PEG quantities varying from 1 g -10 g. After 24 hours of heating, the ELMs containing the chemical de-emulsifier were successfully demulsified. But, as shown in Figure 4.8, the diluent which floated on the aqueous phase was orange in colour, which was not the original colour of the diluent. This could have been due to the chemical change of the chemicals composing the diluent resulting from high temperatures and the addition of PEG. The aqueous phase had an orange colour, indicating that, although demulsification was achieved, some of the diluent was still in the aqueous phase. This led to the examination of the amount of carbon content in the aqueous phase using COD. COD is used to indirectly measure the amount of organic compounds in water. This follows the logic that organic compounds are oxidised fully to form carbon dioxide in the presence of a strong oxidising agent under acidic conditions (Pisarevsky, Polozova et al. 2005) .

Another important discovery was that the higher the HLB value for the chemical de-emulsifier the better a de-emulsifier it becomes (Abdel-Azim et al. 1998). The w/o ELMs are formed using surfactants with low HLB values and the o/w ELMs are formed using surfactants with high HLB values. Hence, chemicals with high HLB values are likely to demulsify water in oil ELMs. The HLB of PEG is 11.6, which is higher than that of the SPAN 80 (HLB 4.3) (Block 2001) used as a surfactant in the ELMs. Al-Sabagh et al (2013) stated that chemical de-emulsifiers usually have a high molecular weight and a higher HLB value than the surfactant used to stabilize the emulsion so as to be able to destabilize the emulsion. PEG reduces the stability of the interfacial film, leading to the coalescence of the aqueous phase, hence demulsification. It has been stated that in chemical demulsification, the stability of the interfacial film is reduced by increasing the film-thinning rate by addition of a chemical demulsifier. This chemical demulsifier destabilizes the surfactant-stabilized emulsion films by altering the interfacial rheological properties (Mohammed et al. 1993, Mohammed et al. 1994, Eley et al. 1987). The interfacial activity of the demulsifier must be high enough to suppress the interfacial tension gradient, thus accelerating the rate of film drainage and promoting coalescence (Kim, Wasan 1996a)

The duration of mixing the chemical de-emulsifier with the emulsion is also important to successful demulsification. PEG was mixed with the emulsion for 75 minutes. All these ELMs were heated at 70˚C for 24 hours and all were demulsified, as shown in Figure 4.8. The temperature was then reduced to 50˚C since it was suspected that 70˚C was denaturing the components of the diluent, as it can be seen from Figure 4.11 that the colours of the diluents are different, indicative of the chemical denaturing of the diluent at 70 ˚C. At 50 ˚C the ELM containing 6 g of PEG, had not yet demulsified completely, hence 10 g at 50 ˚C was done. From Figure 4.10, it can be seen that demulsification was successful and the diluent remained its original colour. At 50 ˚C, demulsification was achieved fully when the amount of added PEG was 10 g. This is because the concentration of the demulsifier must be sufficient enough in the droplets to ensure a high enough diffusion flux to the interface (Krawczyk, Wasan et al. 1991, Kim, Wasan 1996b).

It was noted that, as the concentration of the PEG increased in the emulsion, COD values also increased, as shown in Figure 4.9. This is due to the fact that PEG is an o/w surfactant since it has the ability to partition in water as much as it is oil soluble. Hence some PEG is in the water,

increasing the COD. Kim et al (1996) stated that for the chemical de-emulsifier to be good, it has to partition into the aqueous phase (Kim, Wasan 1996b). Other authors in another study of demulsification of Petroleum ELMs using oil-soluble de-emulsifiers reached the same conclusions (Krawczyk, Wasan et al. 1991).

It has to be stated, however, that the carry-over of organic matter is variable. These data were taken into account during the study as the loss of diluent components increases the cost of any developed ELM extraction method for Rh. Prices for the extractant, diluent and the chemical demulsifier vary significantly and, therefore, it is critical to ascertain which one of these components is likely to contribute to the COD concentrations shown in Figure 4.9. The concentration TOA is unlikely to be influenced by the weights of PEG added to the ELM prior to demulsification, as this compound has been shown to be miscible with water and will not influence TOA mass transfer into the aqueous phase. Summation of the TOA and toluene contributions to the COD levels in the stripping phase account for 1 970 mg/l. The remaining COD concentrations most likely originate from oxidation of the PEG molecule, which dissolves in water during chemical demulsification. This also explains the increase of COD with the increase of PEG observed in Figure 4.9.

4.6. CONCLUSIONS

The emulsification process was successfully developed and optimum conditions of emulsification for this study were:

a) The stripping phase: diluent ratio was 1:2
b) The mechanical agitation speed was 600 rpm and the emulsification time was 40 minutes
c) 5 % of the surfactant SPAN 80 was used.
d) The *p* value of 0.3018 at 5 % level of significance for the difference between mean micro-droplet size for 1:2 ELMs containing 20 g/l and 30 g/l PIB obtained using a Zetasizer after 40 minutes showed that there was statistically no significant difference in micro-droplet size for 1:2 ELMs containing 20 g/l and 30 g/l PIB.

The demulsification technique was successfully optimised. Optimum conditions for demulsification were heating the emulsion for 24 hours at a temperature of 50 ˚C. The chemical

de-emulsifier, PEG, used was 10 g and mixed with the emulsion for 75 minutes before heating. The 1:2 ELM containing both 20 g/l PIB and 30 g/l PIB will be used for extraction in Chapter 5.

REFERENCES

AHMAD, A.L., KUSUMASTUTI, A., DEREK, C.J.C. and OOI, B.S., 2011. Emulsion liquid membrane for heavy metal removal: An overview on emulsion stabilization and destabilization. *Chemical Engineering Journal,* **171**, pp. 870-882.

AHMAD, A.L., KUSUMASTUTI, A., DEREK, C.J.C. and OOI, B.S., 2012. Emulsion liquid membrane for cadmium removal: Studies on emulsion diameter and stability. *Desalination,* **287**, pp. 30-34.

AL-SABAGH, A.M., NASSER, N.M. and ABD EL-HAMID, T.M., 2013. Investigation of Kinetic and Rheological Properties for the Demulsification Process. *Egyptian Journal of Petroleum,* **22**, pp. 117-127.

AULTON, M.E. and TAYLOR, K., 2007. *Aulton's pharmaceutics: the design and manufacture of medicines.* Churchill Livingstone Edinburgh. New York, USA.

AULTON, M.E. and WELLS, T., 2002. Pharmaceutics: The science of dosage form design, 2nd ed. Churchill Livingstone Edinburgh., New York, USA, pp. 41-86.

BEHREND, O., AX, K. and SCHUBERT, H., 2000. Influence of continuous phase viscosity on emulsification by ultrasound. *Ultrasonics sonochemistry,* **7**, pp. 77-85.

BHOWAL, A., BHATTACHARYYA, G., INTURU, B. and DATTA, S., 2012. Continuous removal of hexavalent chromium by emulsion liquid membrane in a modified spray column. *Separation and Purification Technology,* **99**, pp. 69-76.

BLOCK, S.S., 2001. *Disinfection, sterilization and preservation,* 5th ed. Wolters Kluwer Health Lippincott Williams & Wilkins, New York, USA.

BRINGAS, E., SAN ROMAN, M.F. and ORTIZ, I., 2006. Separation and recovery of anionic pollutants by the emulsion pertraction technology. Remediation of polluted groundwaters with Cr (VI). *Industrial & Engineering Chemistry Research,* **45**, pp. 4295-4303.

CHANUKYA, B.S. and RASTOGI, N.K., 2013. Extraction of alcohol from wine and color extracts using liquid emulsion membrane. *Separation and Purification Technology,* **105**, pp. 41-47.

CHIHA, M., SAMAR, M.H. and HAMDAOUI, O., 2006. Extraction of chromium (VI) from sulphuric acid aqueous solutions by a liquid surfactant membrane (LSM). *Desalination,* **194**, pp. 69-80.

FLOURY, J., LEGRAND, J. and DESRUMAUX, A., 2004. Analysis of a new type of high pressure homogeniser. Part B. Study of droplet break-up and recoalescence phenomena. *Chemical Engineering Science,* **59**, pp. 1285-1294.

FREITAS, C. and MÜLLER, R.H., 1998. Effect of light and temperature on zeta potential and physical stability in solid lipid nanoparticle (SLN™) dispersions. *International journal of pharmaceutics,* **168**, pp. 221-229.

GARCÍA, M.G., ACOSTA, A.O. and MARCHESE, J., 2013. Emulsion liquid membrane pertraction of Cr(III) from aqueous solutions using PC-88A as carrier. *Desalination,* **318**, pp. 88-96.

GASSER, M., EL-HEFNY, N. and DAOUD, J., 2008. Extraction of Co (II) from aqueous solution using emulsion liquid membrane. *Journal of hazardous materials,* **151**, pp. 610-615.

GOYAL, R.K., JAYAKUMAR, N.S. and HASHIM, M.A., 2011. Chromium removal by emulsion liquid membrane using $[BMIM]^{+}[NTf2]^{-}$ as stabilizer and TOMAC as extractant. *Desalination,* **278**, pp. 50-56.

HEURTAULT, B., SAULNIER, P., PECH, B., PROUST, J. and BENOIT, J., 2003. Physico-chemical stability of colloidal lipid particles. *Biomaterials,* **24**, pp. 4283-4300.

HIEMENZ, P.C. and RAJAGOPALAN, R., 1997. *Principles of Colloid and Surface Chemistry, revised and expanded.* CRC Press. Boca Raton, Florida, USA.

JAFARI, S.M., ASSADPOOR, E., HE, Y. and BHANDARI, B., 2008. Re-coalescence of emulsion droplets during high-energy emulsification. *Food Hydrocolloids,* **22**, pp. 1191-1202.

KAGEYAMA, T., MATSUMIYA, H. and HIRAIDE, M., 2004. Separation of traces of heavy metals from an iron matrix by use of an emulsion liquid membrane. *Analytical and bioanalytical chemistry,* **379**, pp. 1083-1087.

KIM, Y.H. and WASAN, D.T., 1996a. Effect of demulsifier partitioning on the destabilization of water-in-oil ELMs. *Industrial & Engineering Chemistry Research,* **35**, pp. 1141-1149.

KIM, Y.H. and WASAN, D.T., 1996b. Effect of demulsifier partitioning on the destabilization of water-in-oil ELMs. *Industrial & Engineering Chemistry Research,* **35**, pp. 1141-1149.

KOVACEVIC, A., SAVIC, S., VULETA, G., MÜLLER, R. and KECK, C., 2011. Polyhydroxy surfactants for the formulation of lipid nanoparticles (SLN and NLC): Effects on size, physical stability and particle matrix structure. *International journal of pharmaceutics,* **406**, pp. 163-172.

KRAWCZYK, M.A., WASAN, D.T. and SHETTY, C., 1991. Chemical demulsification of petroleum ELMs using oil-soluble demulsifiers. *Industrial & Engineering Chemistry Research,* **30**, pp. 367-375.

KUMBASAR, R. and ŞAHIN, İ., 2008. Separation and concentration of cobalt from ammoniacal solutions containing cobalt and nickel by emulsion liquid membranes using 5, 7-dibromo-8-hydroxyquinoline (DBHQ). *Journal of Membrane Science,* **325**, pp. 712-718.

KUMBASAR, R.A., 2010a. Extraction and concentration of cobalt from acidic leach solutions containing Co–Ni by emulsion liquid membrane using TOA as extractant. *Journal of Industrial and Engineering Chemistry*, **16**, pp. 448-454.

KUMBASAR, R.A., 2010b. Selective extraction of chromium (VI) from multicomponent acidic solutions by emulsion liquid membranes using tributhylphosphate as carrier. *Journal of hazardous materials,* **178**, pp. 875-882.

KUMBASAR, R.A., 2009a. Cobalt–nickel separation from acidic thiocyanate leach solutions by emulsion liquid membranes (ELMs) using TOPO as carrier. *Separation and Purification Technology,* **68**, pp. 208-215.

KUMBASAR, R.A., 2009b. Separation and concentration of cobalt from aqueous thiocyanate solutions containing cobalt–nickel by emulsion liquid membranes using TBP as extractant. *Journal of Membrane Science,* **338**, pp. 182-188.

KUMBASAR, R.A., 2008. Selective separation of chromium (VI) from acidic solutions containing various metal ions through emulsion liquid membrane using trioctylamine as extractant. *Separation and Purification Technology*, **64**, pp. 56-62.

LAMBRICH, U. and SCHUBERT, H., 2005. Emulsification using microporous systems. *Journal of Membrane Science,* **257**, pp. 76-84.

LEE, S.C., 2011. Extraction of succinic acid from simulated media by emulsion liquid membranes. *Journal of Membrane Science*, **381**, pp. 237-243.

LEE, S.C. and HYUN, K., 2010. Development of an emulsion liquid membrane system for separation of acetic acid from succinic acid. *Journal of Membrane Science*, **350**, pp. 333-339.

LI, N., CAHN, R., NADEN, D. and LAI, R., 1983. Liquid membrane processes for copper extraction. *Hydrometallurgy,* **9**, pp. 277-305.

MATOS, M., SUÁREZ, M.A., GUTIÉRREZ, G., COCA, J. and PAZOS, C., 2013. Emulsification with microfiltration ceramic membranes: A different approach to droplet formation mechanism. *Journal of Membrane Science,* **444**, pp. 345-358.

MATSUMIYA, H., KAGEYAMA, T. and HIRAIDE, M., 2004. Multielement preconcentration of trace heavy metals in seawater with an emulsion containing 8-quinolinol for graphite-furnace atomic absorption spectrometry. *Analytica Chimica Acta,* **507**, pp. 205-209.

MEHNERT, W. and MÄDER, K., 2001. Solid lipid nanoparticles: production, characterization and applications. *Advanced Drug Delivery Reviews,* **47**, pp. 165-196.

MOHAN, S. and NARSIMHAN, G., 1997. Coalescence of protein-stabilized ELMs in a high-pressure homogenizer. *Journal of colloid and interface science,* **192**, pp. 1-15.

MORTAHEB, H.R., KOSUGE, H., MOKHTARANI, B., AMINI, M.H. and BANIHASHEMI, H.R., 2009. Study on removal of cadmium from wastewater by emulsion liquid membrane. *Journal of hazardous materials,* **165**, pp. 630-636.

MÜLLER, R.H., MÄDER, K. and GOHLA, S., 2000. Solid lipid nanoparticles (SLN) for controlled drug delivery–a review of the state of the art. *European journal of pharmaceutics and biopharmaceutics,* **50**, pp. 161-177.

PARK, Y., 2006. Development and Optimization of Novel Emulsion Liquid Membranes Stabilized by Non-Newtonian Conversion in Taylor-Couette Flow for Extraction of Selected Organic and Metallic Contaminants. *PhD thesis*, Georgia Institute of Technology, Georgia, USA.

PARK, Y., FORNEY, L.J., KIM, J.H. and SKELLAND, A.H.P., 2004. Optimum emulsion liquid membranes stabilized by non-Newtonian conversion in Taylor–Couette flow. *Chemical Engineering Science,* **59**, pp. 5725-5734.

PATNAIK, P.R., 1995. Liquid emulsion membranes: Principles, problems and applications in fermentation processes. *Biotechnology Advances,* **13**, pp. 175-208.

PENG, W., JIAO, H., SHI, H. and XU, C., 2012. The application of emulsion liquid membrane process and heat-induced demulsification for removal of pyridine from aqueous solutions. *Desalination,* **286**, pp. 372-378.

PERRIER-CORNET, J., MARIE, P. and GERVAIS, P., 2005. Comparison of emulsification efficiency of protein-stabilized oil-in-water ELMs using jet, high pressure and colloid mill homogenization. *Journal of Food Engineering,* **66**, pp. 211-217.

PISAREVSKY, A., POLOZOVA, I. and HOCKRIDGE, P., 2005. Chemical oxygen demand. *Russian journal of applied chemistry,* **78**, pp. 101-107.

RADOMSKA-SOUKHAREV, A., 2007. Stability of lipid excipients in solid lipid nanoparticles. *Advanced Drug Delivery Reviews,* **59**, pp. 411-418.

REIS, M.T.A. and CARVALHO, J.M., 2004. Modelling of zinc extraction from sulphate solutions with bis (2-ethylhexyl) thiophosphoric acid by emulsion liquid membranes. *Journal of Membrane Science,* **237**, pp. 97-107.

SENGUPTA, B., SENGUPTA, R. and SUBRAHMANYAM, N., 2006a. Copper extraction into emulsion liquid membranes using LIX 984N-C®. *Hydrometallurgy,* **81**, pp. 67-73.

SENGUPTA, B., SENGUPTA, R. and SUBRAHMANYAM, N., 2006b. Process intensification of copper extraction using emulsion liquid membranes: Experimental search for optimal conditions. *Hydrometallurgy,* **84**, pp. 43-53.

SHEN, J., YIN, W., ZHAO, Y. and YU, L., 1996. Extraction of alanine using emulsion liquid membranes featuring a cationic carrier. *Journal of Membrane Science,* **120**, pp. 45-53.

SKELLAND, A. and MENG, X.M., 1996. A new solution to emulsion liquid membrane problems by non-Newtonian conversion. *AIChE Journal,* **42**, pp. 547-561.

SKELLAND, A.H.P. and (MICHAEL) MENG, X., 1999. Non-Newtonian conversion solves problems of stability, permeability, and swelling in emulsion liquid membranes. *Journal of Membrane Science,* **158**, pp. 1-15.

SUN, D., DUAN, X., LI, W. and ZHOU, D., 1998. Demulsification of water-in-oil emulsion by using porous glass membrane. *Journal of Membrane Science,* **146**, pp. 65-72.

TANDLICH, R. and ZUMA, B.M., 2012. Mutual relationship of henry's law constants and aqueous phase concentrations for benzene, toluene and o-xylene at 30 degree C. *Fresenius Environmental Bulletin,* **21**(1), pp. 68-75.

TANDLICH, R., 2010. Chapter 8 - Application of Liquid Membranes in Wastewater Treatment. In: VLADIMIR S. KISLIK, ed, *Liquid Membranes.* Amsterdam: Elsevier, pp. 357-400.

TANG, B., YU, G., FANG, J. and SHI, T., 2010. Recovery of high-purity silver directly from dilute effluents by an emulsion liquid membrane-crystallization process. *Journal of hazardous materials,* **177**, pp. 377-383.

TESCH, S. and SCHUBERT, H., 2002. Influence of increasing viscosity of the aqueous phase on the short-term stability of protein stabilized ELMs. *Journal of Food Engineering,* **52**, pp. 305-312.

UNER, M., 2006. Preparation, characterization and physico-chemical properties of solid lipid nanoparticles (SLN) and nanostructured lipid carriers (NLC): their benefits as colloidal drug carrier systems. *Die Pharmazie-An International Journal of Pharmaceutical Sciences,* **61**, pp. 375-386.

VENKATESAN, S. and MEERA SHERIFFA BEGUM, K.M., 2009a. Emulsion liquid membrane pertraction of benzimidazole using a room temperature ionic liquid (RTIL) carrier. *Chemical Engineering Journal,* **148**, pp. 254-262.

VENKATESAN, S. and MEERA SHERIFFA BEGUM, K.M., 2009b. Emulsion liquid membrane pertraction of imidazole from dilute aqueous solutions by Aliquat-336 mobile carrier. *Desalination,* **236**, pp. 65-77.

WAN, Y. and ZHANG, X., 2002. Swelling determination of W/O/W emulsion liquid membranes. *Journal of Membrane Science*, **196**, pp. 185-201.

CHAPTER 5

EXTRACTION OF RHODIUM FROM A MODEL OF METAL SIDE STREAM EFFLUENT AND EFFECTS OF TEMPERATURE ON THE ELM AND EXTRACTION

5.1. INTRODUCTION

Rh is part of the PGM and solvent extraction of Rh has previously been studied (Raju, Kumar et al. 2012, Sun, Lee et al. 2012, Gupta, Singh 2013). Rh extraction has been affected by Rh complexes formed between Rh and various components of the aqueous medium in which it is dissolved. Rh chloride complexes have been studied and the extraction of Rh from hydrochloric acid (HCl) medium has also been studied, using TOA (Levitin, Schmuckler 2003). The most common oxidation states exhibited by Rh are +1 and +3 and the oxidation state of +3 is the most common when it comes to its chloride complexes (Levitin, Schmuckler 2003). Rh chloro complexes exist in chloro/aquo complexes such as $[RhCI_{6-n}(H20)_n]^{(n-3)-}$ where n is 1 or 2 (Levitin, Schmuckler 2003). These complexes range from hexa-chloro-rhodate ($RhCl_6^{3-}$) to hexa-aquo-rhodate $[Rh(H_2O)_6^{3+}]$. The existence of these aquo complexes has mainly to do with the concentration of the chloride ions in the solution and the pH, temperature and age of the solution (Benguerel, Demopoulos et al. 1996). At high concentrations of chlorides, hexa-chloro-rhodate ($RhCl_6^{3-}$) is the main complex and the others which exist are $RhCl_5(H_2O)^{2-}$and $RhCl_4(H_2O)_2^-$. When the solution starts aging substitution of ligands in the complexes occurs, leading to production of a variety of complexes with different extraction rates (Al-Bazi, Chow 1984).The equations below (5.1-5.6) show the stages the ($RhCl_6^{3-}$) complexes undergo during ligand substitution to $Rh(H_2O)_6^{3+}$as the concentration of the chloride decreases:

$$RhCl_6^{3-} + H_2O \rightarrow RhCl_5(H_2O)^{2-} + Cl^- \quad (5.1)$$

$$RhCl_5(H_2O)^{2-} + H_2O \rightarrow RhCl_4(H_2O)_2^- + Cl^- \quad (5.2)$$

$$RhCl_4(H_2O)_2^- + H_2O \rightarrow RhCl_3(H_2O)_3 + Cl^- \quad (5.3)$$

$$RhCl_3(H_2O)_3 + H_2O \rightarrow RhCl_2(H_2O)_4^+ + Cl^- \quad (5.4)$$

$$RhCl_2(H_2O)_4^+ + H_2O \rightarrow RhCl(H_2O)_5^{2+} + Cl^- \quad (5.5)$$

$$RhCl(H_2O)_5^{2+} + H_2O \rightarrow Rh(H_2O)_6^{3+} + Cl^- \quad (5.6)$$

Due to the availability of diffrent aquo/chloro complexes, extraction of Rh is difficult. Solutions must thus be carefully controlled (Levitin, Schmuckler 2003). The main focus of this chapter is to study the extraction of Rh from an acidic environment, using HCl at pH 2 and pH 3. Rh will only be soluble in aqueous environments if the pH of the aqueous phase equals 4.00 or lower. HCl was used as a solvent due to the presence of chloride anions being essential in stabilization of the Rh cations in solution. This extraction will be done using the tertiary amine TOA. The effect of the structure of the rhodium chloride complexes is discussed in Section 5.8.1 of this chapter.

Stability and the morphology of ELM is affected by temperature. Temperature affects the viscocity of the interfacial film of the ELM (Rosen, Kunjappu 2012). It also affects swelling of the membrane, affecting the stability of the membrane and, subsequently, the extraction (Ahmad, Kusumastuti et al. 2011). Effects of increasing temperature of the ELM and how it affects extraction of Rh will be examined in this chapter.

The turbidity of the mixture of the feed and the ELM was examined, as well as the turbidity of the side stream after extraction. Scale-up considerations were also looked at.

5.2. EXPERIMENTALS

5.2.1. Extraction of Rh at pH 2

5.2.1.1. Apparatus and Chemicals

Kerosene (diluent), PIB, Rh and TOA were purchased from Sigma Aldrich (Johannesburg, South Africa). Nitric acid was purchased from SAARCHEM (PTY) LTD South Africa, and Span 80 from Fluka analytical. An Olympus UCMAD3 microscope mounted with an Olympus Ultra 20 soft imaging system UTVX-2 was used for all microscopic work and the circulating water bath serial number 109046004 were from Grant instruments (Cambridge, England). Orbital shaking

was done using the Chiltern Orbital Shaker SS70 (Slough, Berkshire, Chiltern Scientific, United Kingdom). All mass weightings were performed analytically, using the PA1214 analytical balance (Pioneer™, Ohaus Corporation, Johannesburg, South Africa). Incubations of the ELMs were done using Heraeus Model FT 420 (HeraeusKulzer GmbH, Dormagen, Germany).

5.2.1.2. Preparation of the metal refining side-streams model

Model metal refining side-streams were prepared as follows: A solution of 7 mg/l of Rh was prepared by diluting the stock solution with the certified concentration 999 ± 5 mg/l in 0.01 M HCl (pH=1.87) and in 0.001 M HCl (pH = 2.92) respectively. Extraction of Rh with the optimised ELM was performed using the TVC shown in Figure 5.1.

5.2.1.3. Preparation of ELMs

The optimised ELMs with 30 g/l PIB (see Chapter 4 Section 4.4.1.6) was prepared as follows: 7.526g of PIB was dissolved in a mixture of 150 ml of kerosene and 75 ml toluene. 2.6031 g TOA was added. 12.532g of SPAN 80 was added. Kerosene was then added to the 250 ml mark to make 30.104 g/l (m/v) of PIB, 10.412 g/l (m/v) of TOA and 50.128 g/l (m/v) of Span 80. This diluent was mixed with 2 M nitric acid in the ratios 1:2 (125 ml of the nitric acid: 250 ml of diluent) to form 1:2 ELM in 500 ml Erlenmeyer flasks. The flasks were shaken for 40 minutes using an orbital shaker at 600 rpm.

The ELMs with 20 g/l PIB were prepared as follows: 5g PIB was dissolved in 150 ml of Kerosene and 75 ml of toluene was added and 2.539g of TOA was added. 12.4936g of SPAN 80 was added. Kerosene was then added up to the 250 ml mark, making 20 g/l (m/v) of PIB, 10.156 g/l (m/v) TOA and 49.972 g/l (m/v) of Span 80. This diluent was mixed with 2 M nitric acid in the ratio of 1:2 (125 ml of the nitric acid: 250 ml of diluent) to form 1:2 ELM in 500 ml Erlenmeyer flasks. The flask was shaken for 40 minutes using an orbital shaker at 600 rpm.

5.2.1.4. Extraction of Rh in the TVC

The optimised ELM was mixed with the model side-stream in a ratio of 1:5 (10 ml ELM: 50 ml model mining side-stream). The solution was stirred in the TVC at 250 rpm and the temperature

was held at 21 ± 1°C. After the extraction process had been completed, the ELM/side-stream mixture was removed from the TVC. It was placed into a conical flask and left to stand, allowing separation of the aqueous phase (model of mining side stream) from the ELM. The ELM was then removed and demulsified. The extraction procedure was done at pH = 1.87 for stirring times of 5, 7, 15, 25 and 30 minutes. The ELMs used contained 20 g/l PIB and 30 g/l PIB.

5.2.1.5. Chemical Demulsification of ELM

Demulsification of the ELM in question was completed by adding 10 g of PEG 400 to the loaded ELM. The mixture was subsequently shaken at 600 rpm on an orbital shaker for 75 minutes and placed into a UFE 700 oven at 50 ± 1°C for 24 hours. The bottom layer was pipetted and analysed for Rh, using the ICP-AAS.

5.2.2. Extraction of Rh at pH 3

5.2.2.1. Extraction Rh in the TVC

The models of the metal refining side-streams containing Rh and the ELM were put into the TVC in the ratio of 1:5 as above, in Section 5.2.1.4. The mixture in the TVC was treated as above (section 5.2.1.4). The procedure was performed for 5, 10, 15, 20 and 30 minutes.

5.2.2.2. Chemical Demulsification of ELM

The ELM was then removed and demulsified using a combination of thermal and chemical demulsification as described in Section 5.2.1.5. The aqueous phase of the ELM was analysed for Rh using ICP. The remaining side stream after extraction was also analysed for Rh using ICP.

5.2.2.3. Percentage Extraction

Percentage extraction was calculated using the Equation 5.7 below:

$$\%\ Extraction = \frac{C_{elm} \times V_{elm}}{C_{in} \times V_{in}} x\ 100 \qquad (5.7)$$

5.3. MASS BALANCE

Masss balance is a concept based on the principle of the conservation of matter - i.e. matter is neither created nor destroyed. It is a concept widely used in manufacturing processes in pharmaceutical industries (Baertschi, Pack et al. 2013). The concept can be simplified by the equation below:

$$\text{Input} = \text{Output} \tag{5.8}$$

Mass balance was calculated using Equation 5.9 below:

$$\%\ Mass\ Balance = \frac{[C_{elm} \times V_{elm} + C_{ww} \times V_{ww}\ ]}{C_{in} \times V_{in}} \times 100 \tag{5.9}$$

Where C_{elm} and V_{elm} is the concentration of Rh recovered in the stripping phase of the ELM and the volume of the stripping phase after demulsification respectively and C_{ww} and V_{ww} are the concentrations of Rh remaining in the side stream and the volume of the side stream left after extraction, respectively. C_{in} and V_{in} are the initial concentration of Rh and initial volume of the side stream before extraction. Mass balance was calculated using Equation 5.9 which took into consideration the extracted Rh and Rh in the remaining side stream after extraction. Hence the mass balance Equation 5.9 can be simplified as follows:

$$Mass\ balance = Rh_{ww} + Rh_{extracted} \tag{5.10}$$

Where Rh_{ww} represents Rh remaining in the waste water side stream after extraction

Figure 5.1 shows the schematic representation of TVC used for extraction in the current study, with its dimensions included.

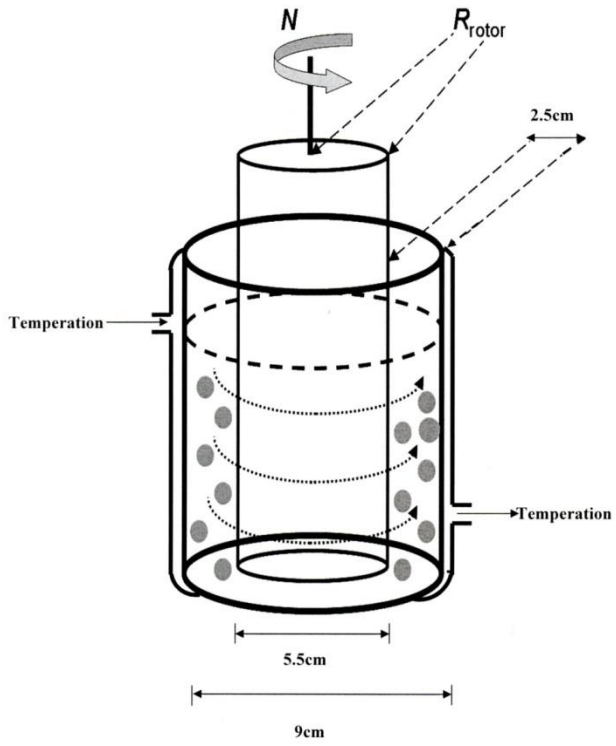

Figure 5.1: *The TVC. The diameters of internal and external cylinders and the thickness of the external cylinder are shown in the diagram. The membrane globules (●) are dispersed in the feed phase of the system via the rotation of the inner cylinder of the TVC. The dotted arrows around the internal cylinder represent the stirring pattern due to the rotation of the inner cylinder, and point out the even distribution of energy in the entire volume of the ELM-side stream mixture*

5.4. EFFECT OF TEMPERATURE ON THE ELMs

5.4.1. Examining the Heat Conductivity of the TVC

The TVC was connected to the circulating water bath as shown in Figure 5.2 below. The TVC was filled with water. The water bath was set at 40 ± 1 ˚C.

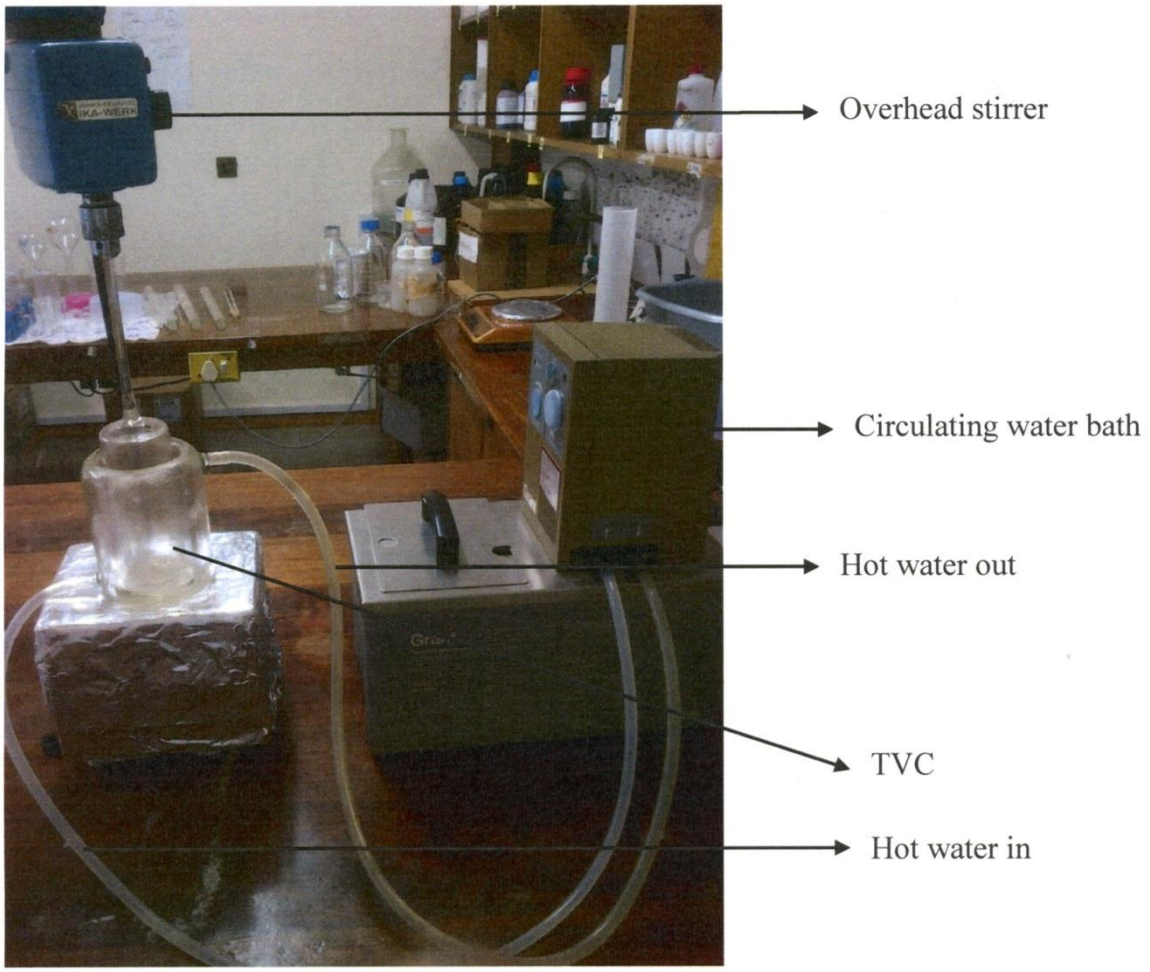

Figure 5.2: *The TVC connected to the circulating water bath and overhead stirrer*

The water from the water bath, which was 40 ± 1 ˚C, was pumped through the temperation of the TVC to heat the column. Temperature in the TVC was measured after 30 minutes, 1 hour, 2 hours and again after 24 hours. The process was repeated at 50± 1 ˚C.

5.4.2. Effect of Increasing Temperature on the ELMs

5.4.2.1. Micro-droplet size at 40 ± 1 ˚C

Ten millilitres (10 ml) of the ELM was put in the empty TVC which had been temperated to 40 ± 1 ˚C. It was left for 5 minutes. It was removed and the micro-droplet diameters were examined under an electron microscope. The procedure was repeated for 10, 15, 20 and 30 minutes.

5.4.2.2. Micro-droplet Size at 50 ± 1 ˚C

The above procedure (Section 5.4.2.1) was repeated at 50 ± 1 ˚C for the same time intervals.

5.4.3. Extractions at 40 ± 1 ˚C and 50 ± 1 ˚C

5.4.3.1. Extractions at pH 2

A solution of 7 mg/l of Rh metal was prepared in 0.01M (pH = 2.04) of hydrochloric acid (HCl) to prepare a model of metal refining side-streams. Fifty millilitres (50 ml) of the side stream was placed in the TVC which had been temperated to 40 ± 1 ˚C and 10 ml of the ELM was added. The ELM used contained 20 g/l PIB. The solution was stirred in the TVC at a speed of 250 rpm for 5 minutes. The mixture was taken out of the column and placed in a conical flask and left to stand, allowing separation of the aqueous phase. The procedure was repeated for 10, 15, 20 and 30 minutes. The aqueous phase was removed and the ELMs demulsified.

The whole procedure was repeated at 50 ± 1 ˚C.

5.4.3.2 Extractions at pH 3

A solution of 7 mg/l of Rh was prepared by diluting the stock solution with the certified concentration of 999 ± 5 mg/l in 0.001 M HCl (pH = 3.14) to prepare a model of mining side stream. Fifty millilitres (50 ml) of the side stream was placed in the TVC which had been temperated to 40 ± 1˚C and 10 ml of the ELM was added. The ELM used contained 20 g/l PIB. The solution was then stirred in the TVC at 250 rpm for 5 minutes. The mixture was then removed from the column and placed in a conical flask and left to stand to allow separation of the aqueous phase. The procedure was repeated for 10, 15, 20 and 30 minutes. The aqueous phase was removed and the ELMs were demulsified.

The whole procedure was repeated at 50 ± 1 ˚C.

5.4.3.3. Chemical Demulsification of ELM

Ten grams (10 g) of PEG was added to each ELM after extraction and the emulsion was shaken at 600 rpm on an orbital shaker for 75 minutes. The ELMs were placed in an oven at 50˚C for 24 hrs. The bottom layer was pipetted and analysed for Rh metal using induced coupled plasma (ICP).

5.4.4. Threefold Extraction Process

The model of the metal refining side-streams containing Rh was placed into the TVC and the ELM was added to make a ratio of 1:5 (10 ml: 50 ml) ELM to metal refining side-streams. The solution was stirred in the TVC using a speed of 250 rpm for 30 minutes. This mixture was then taken from the column and placed in a conical flask and then left to stand to allow separation of the aqueous phase (model mining side stream) from the ELM. The ELM was removed and demulsified. For the second extraction, the side stream from the first extraction was put back into the TVC. A new ELM was added and the procedure repeated for 30 minutes. The mixture was treated as above. For the third extraction, the side stream was put back into the TVC and a new ELM was added. After demulsification, the stripping phase was analysed using ICP. The ELMs used contained 30 g/l PIB. The procedure is shown in Figure 5.3 below:

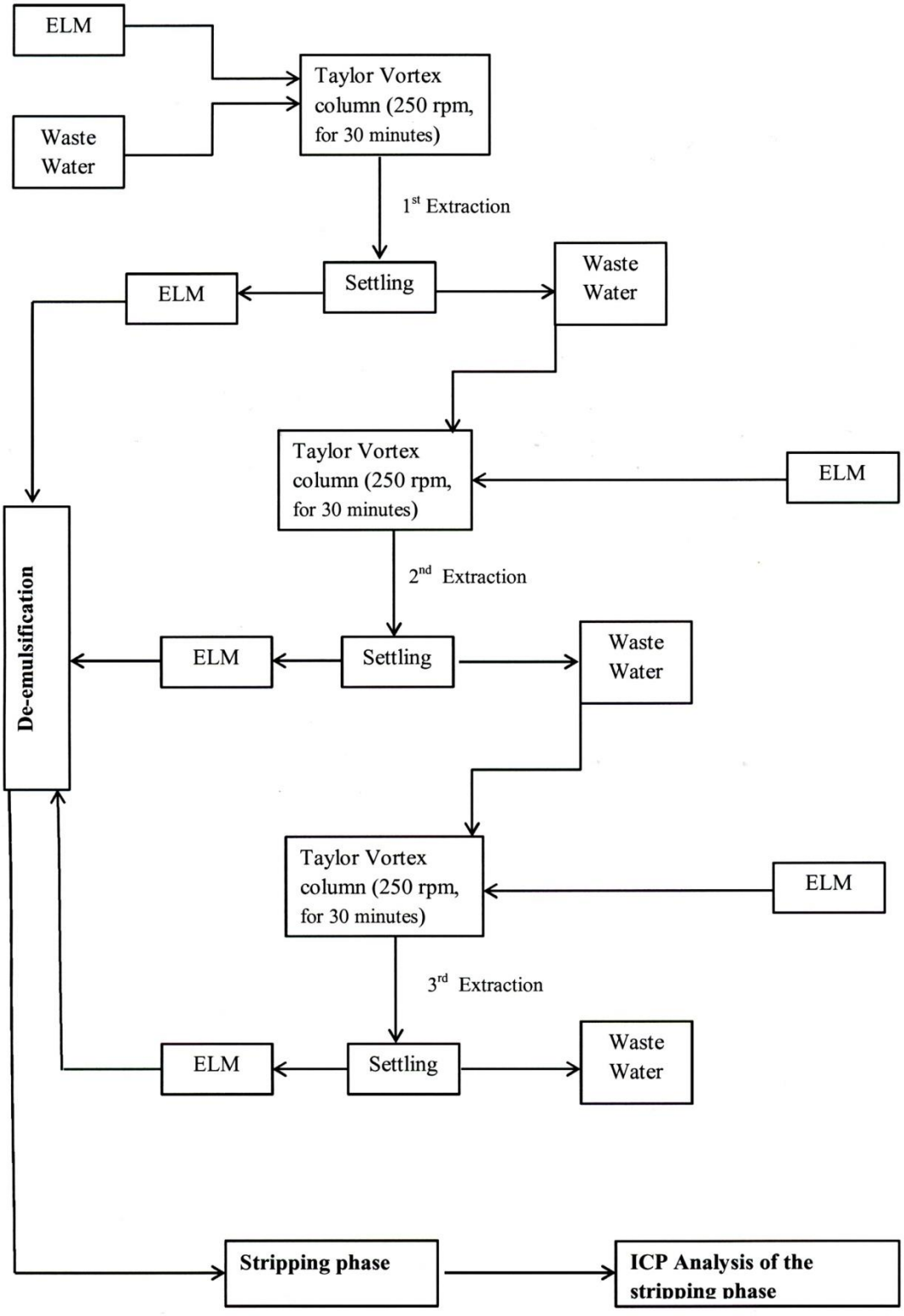

Figure 5.3: *Schematic representation of the three folds extraction of Rh at room temperature.*

5.5. MEASUREMENTS OF TURBIDITY

Turbidity was done in order to assess the extent of mixing of the liquid membrane and the feed phase. The colloidal matter of the ELM during the extraction process will cause turbidity. Hence it was necessary to assess turbidity after the ELM had separated from the feed after extraction. This also helped assess if there were some residues of the ELM carryover remaining in the waste water. Turbidity is defined as the cloudiness of water due to the presence of suspended or dissolved matter (Davies-Colley, Smith 2001). ASTM-International, 2003 cited in Guttler et al 2013, states that turbidity is an expression of the optical properties of a liquid which cause light rays to be scattered and absorbed rather than transmitted in straight lines through a sample. NWEA, 2000 cited in Guttler et al 2013, explains turbidity as a relative measurement, comparing the amount of light scattered by a sample with the amount scattered by a standard. The more light deflected, the higher the turbidity of the sample. Results are shown in Table 5.2.

5.5.1. Turbidity at pH 2

The model of the mining side stream containing 7 mg/l of Rh metal was prepared (as in section 5.2.1.2) with 0.01 M (pH = 2.04) of hydrochloric acid (HCl) and put into the TVC. The ELM was added to make a ratio of 1:5 (10 ml: 50 ml) ELM to metal refining side-streams. The solution was then stirred in the TVC using a speed of 250 rpm for 30 minutes at room temperature (20 $\pm$ 2 ˚C). The mixture was then removed and placed in a conical flask and left to stand to allow separation of the aqueous phase (model of metal refining side-streams) from the ELM. The turbidity of the side stream after complete separation from the ELM was measured. The above procedure was repeated at 40 ± 1 ˚C and 50 ± 1 ˚C.

5.5.2. Turbidity at pH 3

The model of the metal refining side-streams containing7 mg/l of Rh metal was prepared in 0.01 M (pH = 3.14) of hydrochloric acid (HCL) and put into the TVC (Figure 5.1). ELM was added to make a ratio of 1:5 (10 ml: 50 ml) ELM to mining side stream. The solution was then stirred in the TVC at 250 rpm for 30 minutes at room temperature 50 $\pm$ 2 ˚C. The mixture was then taken out of the TVC and placed in a conical flask. It was left to stand to allow separation of the

aqueous phase (model of metal refining side-streams) from the ELM. The turbidity of the side stream after complete separation from the ELM was measured. The above procedure was repeated at 40 ± 1 ˚C and 50 ± 1 ˚C.

5.6. RESULTS

5.6.1. Demulsification of ELM

The ELMs were cracking and the two phases were already separating after the addition of the required amount of PEG and shaken for 75 minutes. After incubation at 50 ± 1 ˚C, complete demulsification of the ELM was achieved, as shown in Figure 5.4

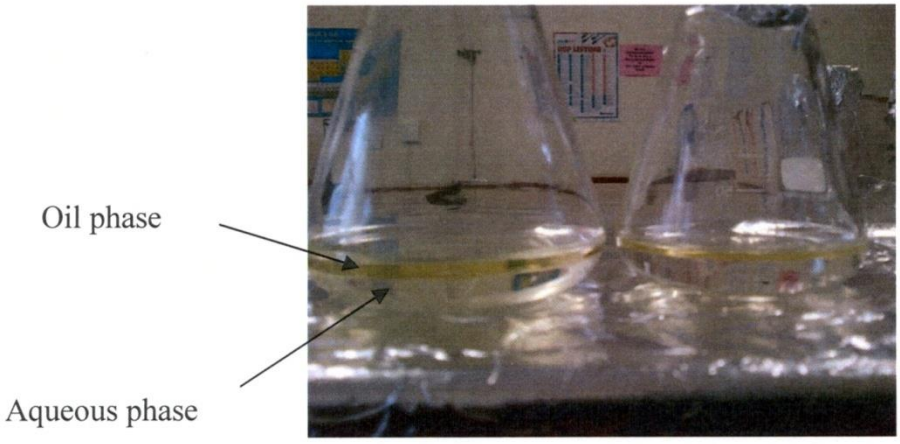

Figure 5.4: *Emulsion with 10 g of PEG after incubation for 24 hours at 50 ± 1 ˚C*

5.6.2. Extraction of Rh at using the ELM containing 20 g/l PIB

A maximum recovery of 41.7 % of Rh was extracted after stirring in the TVC for 30 minutes at pH = 1.87. At pH 2.92, 46.2 % was extracted.

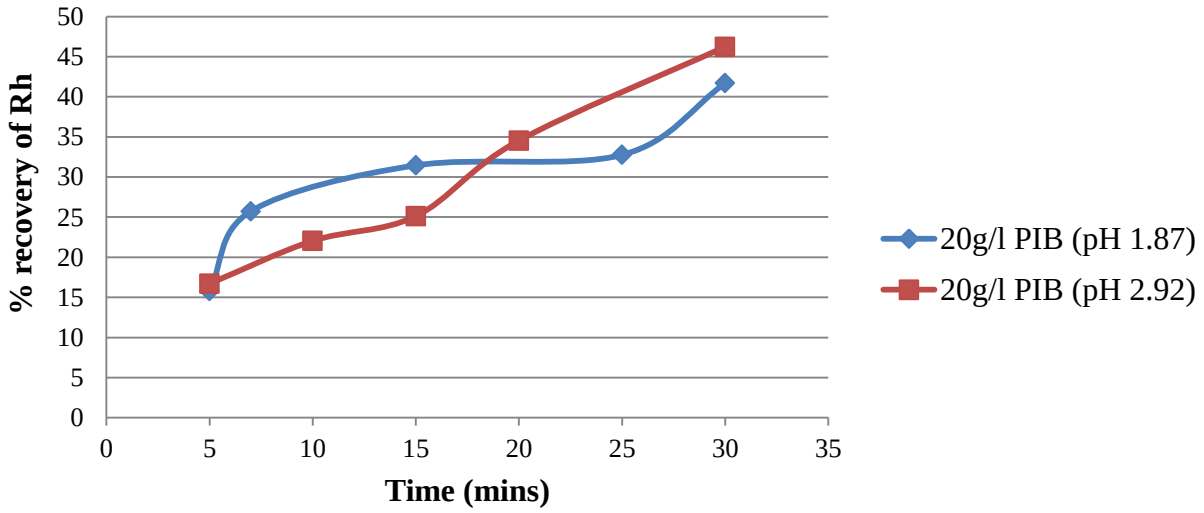

Figure 5.5: *Percentage recovery of Rh from the aqueous phase of the ELM containing 20 g/l PIB after demulsification at pH 1.87 and pH 2.92.*

5.6.3. Extraction of Rh using the ELM containing 30 g/l PIB

5.6.3.1. Percentage recovery of Rh

A maximum recovery of 52.4 % of Rh was extracted after stirring in the TVC for 30 minutes at pH 1.87 and 53.5 % of the Rh was extracted at pH 2.92, as shown in Figure 5.6.

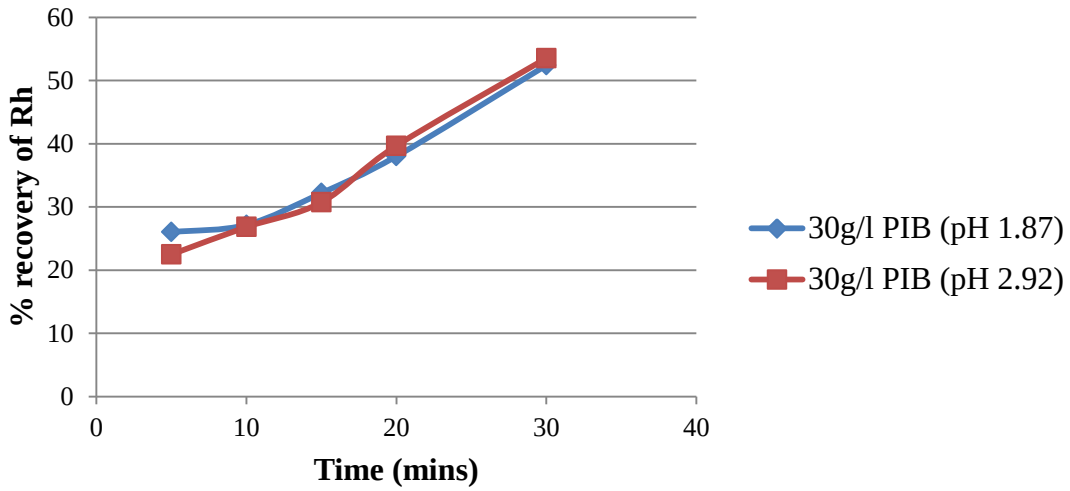

Figure 5.6: *Percentage recovery of Rh from the aqueous phase of the ELM containing 30 g/l PIB after demulsification at pH 2 and pH 3.*

5.6.3.2. Rh Remaining in the Side Stream Effluent

Figure 5.7 shows the percentage of Rh left in the side stream effluent after extraction. As it can be seen from the figure, at pH 1.87 and pH 2.92 using the ELM with 20 g/l PIB, 22 % and 25.7 % of the Rh was left in the side stream after extraction respectively. When using the ELM with 30 g/l PIB 22.2 % and 28.2 % of Rh at pH 1.87 and pH 2.92 respectively remained unextracted from the side stream.

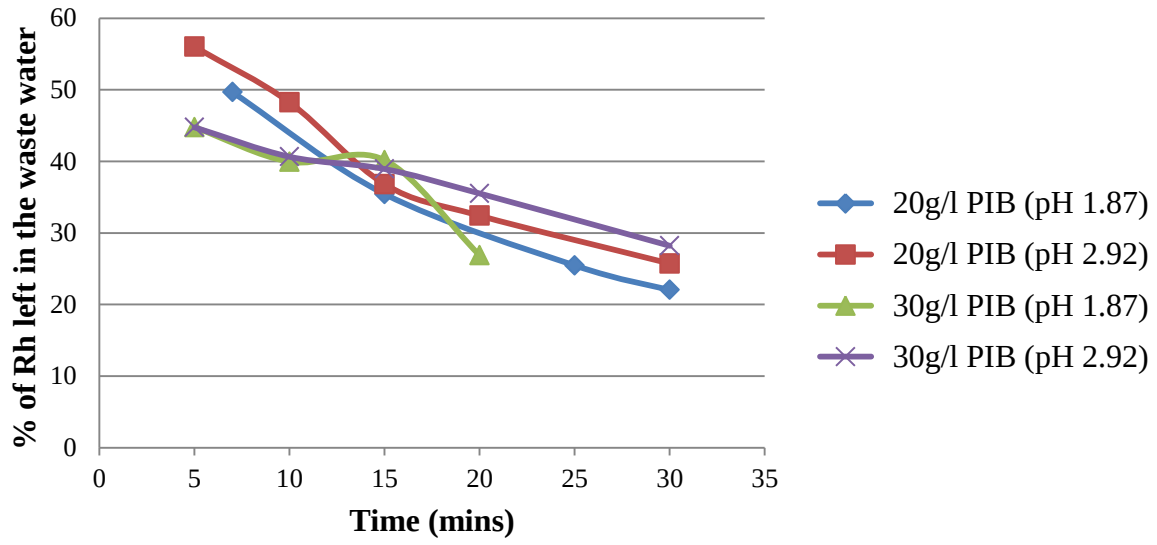

Figure 5.7: *Percentange of Rh left in the side stream effluent after extraction using the ELMs containg 20 g/l PIB and 30 g/l PIB and pH 2 and pH 3*

5.6.3.3. Mass Balance

Figure 5.8 shows the mass balance as calculated using Equation 5.9:

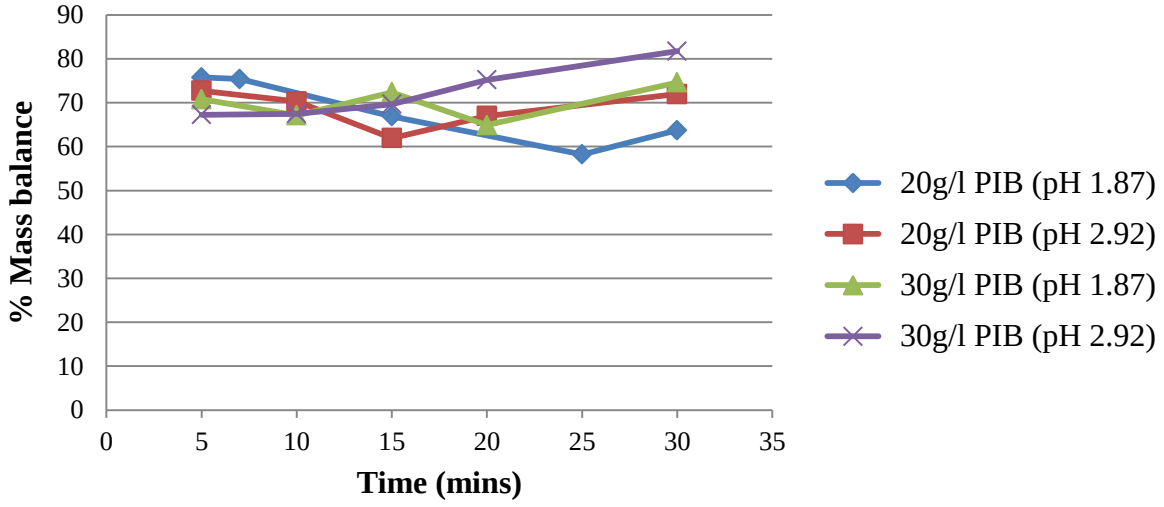

Figure 5.8: *Percentage mass balance of Rh after extraction using the ELMs containing 20 g/l PIB and 30 g/l PIB at pH 2 and pH 3*

Figure 5.8 shows the percentage mass balance of Rh after extraction. As can be seen from the figure, at pH 1.87 and pH 2.92, using the ELM with 20 g/l PIB, the mass balance was 63.7 % and 72 %. When using the ELM with 30 g/l PIB, the mass balance was 74.6 % and 81.7 % at pH 1.87 and pH 2.92 respectively.

5.6.4. Effect of temperature on the ELM

5.6.4.1. Examining the Heat Conductivity of the TVC

When the temperature of the water bath was 40 ± 0.5˚C, the temperature of the water in the TVC was 39 ± 0.5˚C after 30 minutes. After 1 hour, 2 hours and 24 hours, the temperature of the water bath was the same as the temperature of water in the TVC.

5.6.4.2. Effect of Increasing Temperature on the ELMs

Figure 5.9 below shows the micro-droplet sizes of ELM at 40 ± 1 ˚C after 5 minutes:

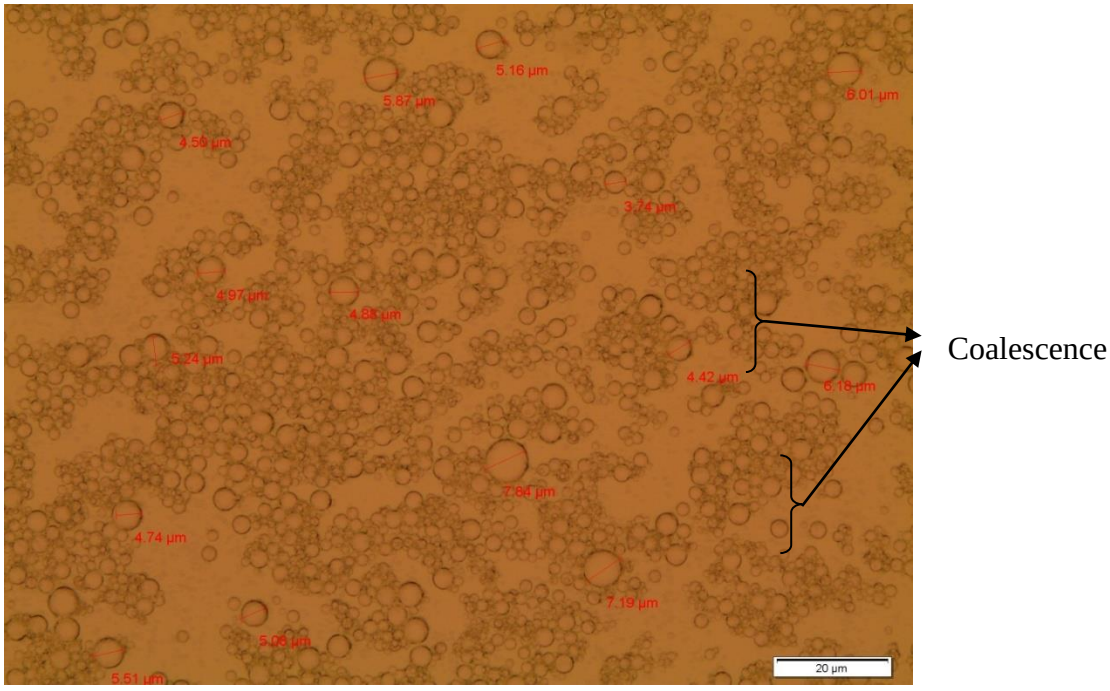

Figure 5.9: *The micro-droplet sizes of ELM at 40 ± 1 ˚C after 5 minutes (see Appendix V for other photographs of the ELM at 50 ± 1 ˚C)*

Figure 5.10 below shows the micro-droplet sizes of ELM at 50 ± 1 ˚C after 5 minutes:

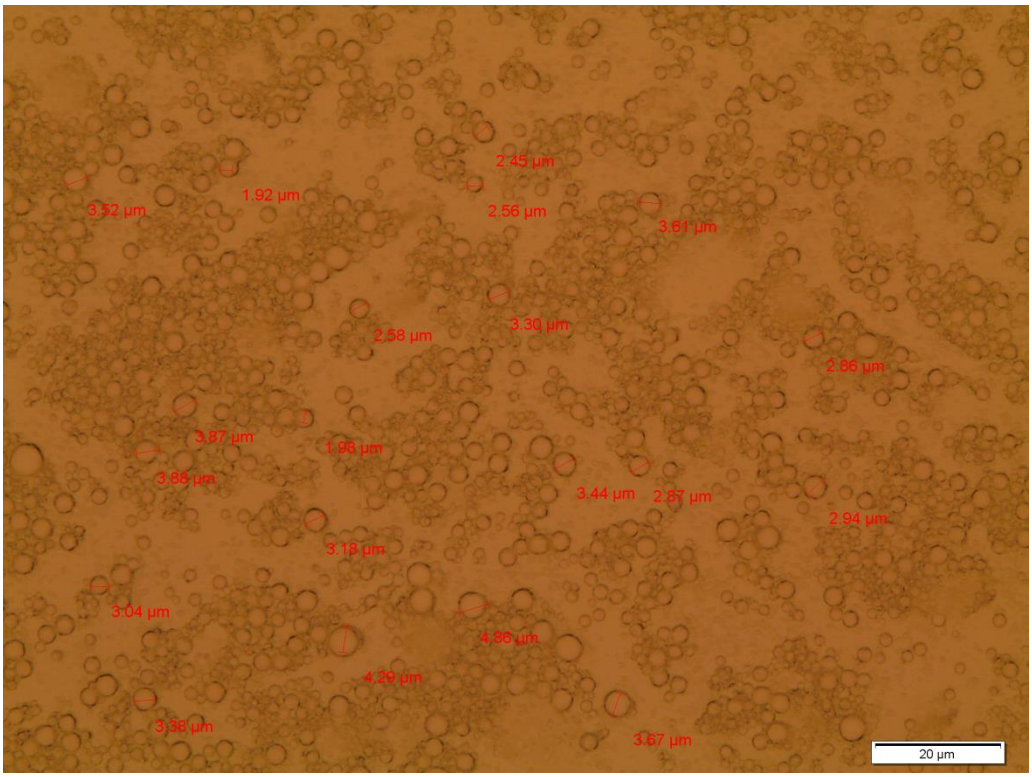

Figure 5.10: *The micro-droplet sizes of ELM at 50 ± 1 ˚C after 5 minutes (see Appendix V for other photographs of the ELM at 50 ± 1 ˚C)*

5.6.4.3. Extraction of Rh at 40 ± 1 ˚C and 50 ± 1 ˚C

A maximum recovery of 38.1 % and 37 % of Rh was extracted at pH 2.04 and pH 3.14 respectively after stirring in the TVC for 30 minutes using an ELM containing 20 g/l PIB at 40 ± 1 ˚C. 39 % and 38 % was extracted at pH 2.04 and pH 3.14 respectively using ELM containing 20 g/l PIB at 50 ± 1 ˚C, as shown in Figure 5.11.

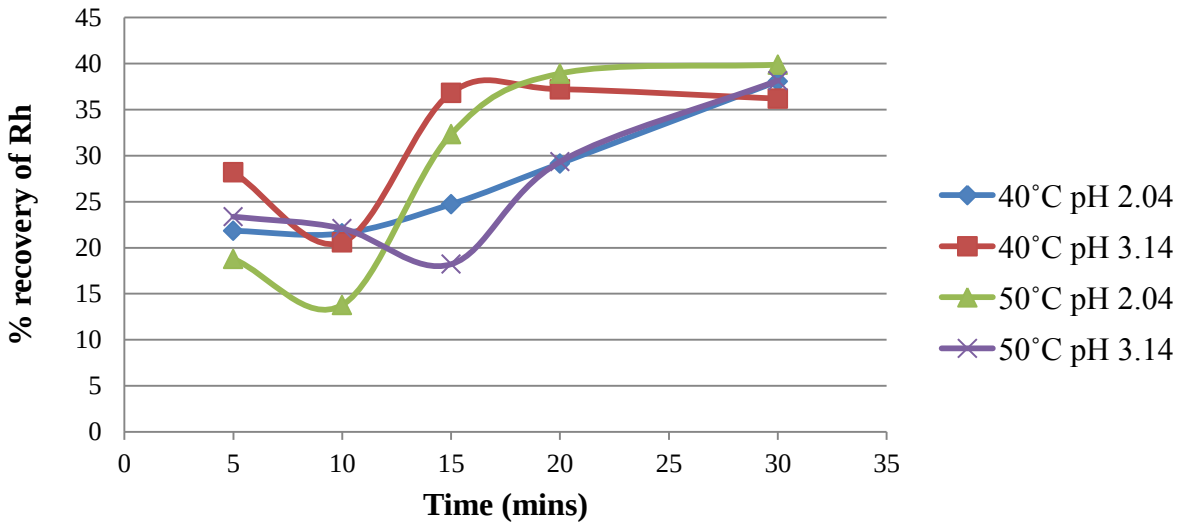

Figure 5.11: *Percentage extraction of Rh at 40 ± 1 ˚C and 50 ± 1 ˚C using the ELMs containing 20 g/l PIB and pH 2.04 and pH 3.14*

5.6.4.4. Rh Remaining in the Side Stream Effluent After Extraction at 40 ± 1 ˚C and 50 ± 1 ˚C

Figure 5.12 below shows the percentange of Rh remaining in the side stream effluent after extraction at 40 ± 1 ˚C and 50 ± 1 ˚C using ELMs containing 20 g/l PIB and pH 2.04 and pH 3.14. As can be seen from the figure, at pH 2.04 and pH 3.14 at 40 ± 1 ˚C, 23.8 % and 27.2 % of the Rh was left in the side stream after extraction. At 50 ± 1 ˚C, 23.2 % and 26.6 % of Rh at pH 2.04 and pH 3.14 respectively remained unextracted from the side stream.

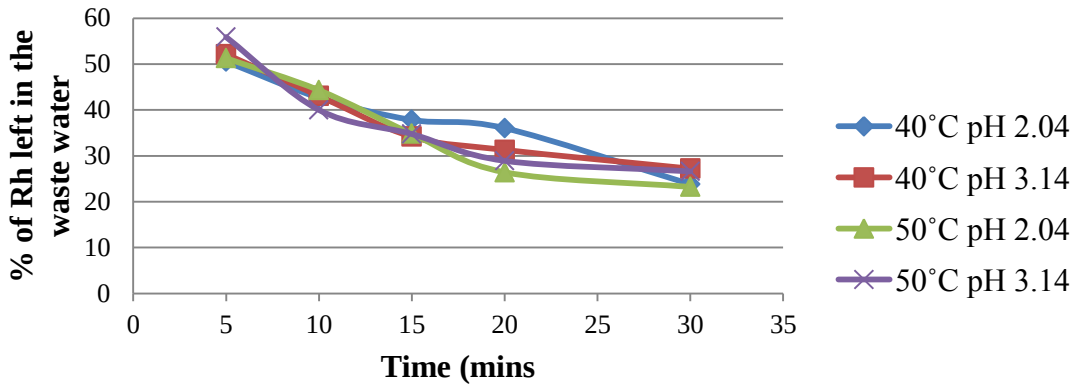

Figure 5.12: *Percentange of Rh left in the side stream effluent after extraction at 40 ± 1 ˚C and 50 ± 1 ˚C using ELMs containing 20 g/l PIB at pH 2.04 and pH 3.14*

5.6.4.5. Mass Balance

Figure 5.13 shows the percentage mass balance of Rh after extraction at 40 ± 1 ˚C and 50 ± 1 ˚C at pH 2 and pH 3. As can be seen in the figure, at pH 2.04 and pH 3.14 at 40 ± 1 ˚C, the mass balance was 61.8 % and 62.4 %. At 50 ± 1 ˚C at pH 2.04 and pH 3.14 respectively, the mass balance was 63.1 % and 64.8 %.

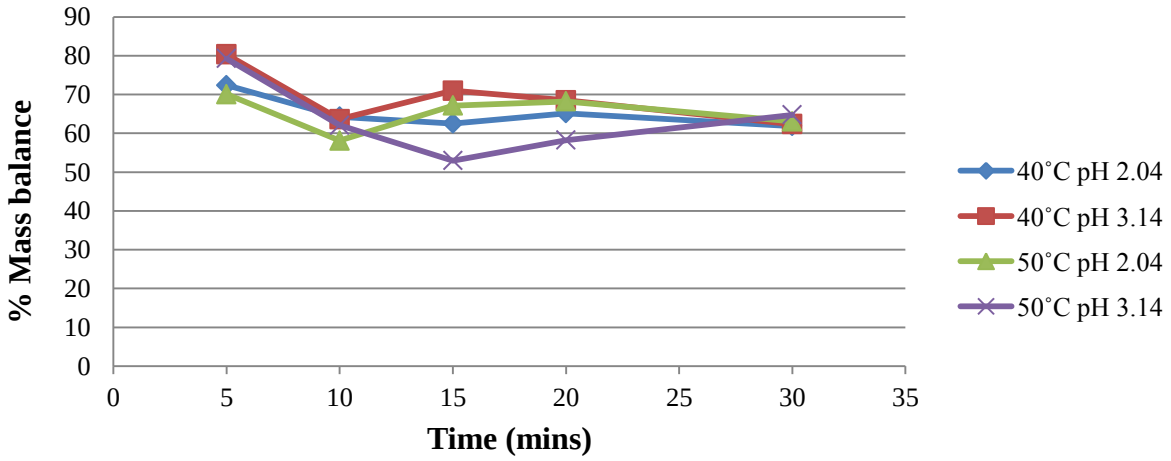

Figure 5.13: *Percentage mass balance of Rh after extraction at 40 ± 1 ˚C and 50 ± 1 ˚C, using ELMs containing 20 g/l PIB at pH 2.04 and pH 3.14*

5.6.5. Threefold Extraction Process

Table 5.1 below shows the amount of Rh extracted at pH 2.01 and pH 3.08, using the ELM containing 30 g/l PIB.

Table 5.1: Extraction efficiency of Rh at varying pH values of the spent side stream for consecutive ELM extractions in the TVC:

pH[a]	C_0(Rh)[b] (μg/ ml)	M_0(Rh)[c] (μg)	M_1(Rh)[d] (μg)	M_2(Rh)[e] (μg)	M_3(Rh)[f] (μg)	P_2(Rh)[g] (%)	P_3(Rh)[h] (%)
2.01	7.00	350	205	366	376	104.4	107.3
3.08	7.00	350	185	345	380	98.7	108.7

[a] Initial pH value of the treated side stream
[b] Initial Rh concentration in the treated side stream
[c] Initial Rh amount
[d] Rh amount extracted after one extraction
[e] Rh amount extracted after two extractions
[f] Rh amount extracted after three extractions
[g] Percentage Rh amount extracted after two extractions
[h] Percentage Rh amount extracted after three extractions

5.6.6. Measurements of Turbidity

Table 5.2: Turbidity (NTUs) of the side stream after separation and removal of ELM after 30 minutes at pH 2.01 and pH 3.08 at different temperatures

pH	20 ± 1 ˚C	40 ± 1 ˚C	50 ± 1 ˚C
2.01	130	114	122
3.08	124	117	126

The higher the value the higher the turbidity.

5.7. SCALE-UP CONSIDERATIONS

Figure 5.1 contains a detailed description of the TVC used in the extraction experiments. Based on the discussion above, a scaled-up form of this instrument would optimally run at 20 °C. Given the nature of the apparatus, the mass balances and the percentage of Rh extracted in a single-step extraction, the scaled-up process will have to be run as a sequential arrangement of two to three single ELM based extractions. Such experiments are currently underway and will be reported upon in the final report of the project. Any scale up will be simple from the constancy of the Taylor criterion (Ta) as defined in Equation (5.11):

$$T_a = \frac{2\pi\, N\, (R_{rotor})^{\frac{1}{2}}\, (d_{ag})^{\frac{3}{2}}}{V} \qquad (5.11)$$

In Equation (5.11), where R_{rotor} is the radius of the inner cylinder of the Taylor column, that is, rotor (m), N is the rotational speed (s-1), dag is the diameter of the space between the inner and outer cylinders of the TVC (m). Given the information in Figure 5.1 and assuming that the kinematic viscosity of the ELM is equal to that of kerosene, the Ta for the system used in this study will be equal to 24.1. Parameters that will change with scale-up are the energy requirements. These originate from the mixing during ELM preparation and demulsification, stirring during the extraction process and the heating of the loaded ELM during demulsification and Rh recovery. Energy requirements for the scaled-up version of the TVC in Figure 5.1 will be as follows:

$$P = \frac{[V_{scale-up}]}{[V_{laboratory}]} \times (P_{shaker} \times t_{shaker} + P_{stirrer} \times t_{stirrer} + P_{oven} \times t_{oven}) \qquad (5.12)$$

In Equation (5.12), the terms P stand for the work done by a given instrument (Watts) and the terms *t* represent the time required to perform a given operation (hours). The first fraction in Equation (5.12) stands for the size factor, with V representing the volume of the operation (dm^3). Subscript of scale-up stands for volume of the treated side-stream in the scaled-up version of the

TVC, while the subscript laboratory stands for the volume in its laboratory version. Stirrer stands for the extraction apparatus, oven for the demulsification oven and the shaker for the shaking.

The energy requirements for 50 ml of the model side-stream are based on the following values: 115 minutes/1.92 hours for the shaking, 24 hours for the oven and 30 minutes for the stirrer. The respective work values are 60 Watts for the shaker and the stirrer and 250 W for the oven. Energy consumption for the 50 ml of the model side-stream is equal to 145 Wh. Using Equation (5.11), the energy consumption for the extraction of 10000 litres can be estimated at 2.9 × 104 kWh.

5.8. DISCUSSION

5.8.1. Extraction using TOA and mass balance

TOA reacts with the HCl in the feed as follows Equation 5.13:

$$R_3N + HCl \rightarrow R_3NH^+Cl^- \quad (5.13)$$

Where R_3N represents TOA. The extraction of metals using amines can be represented by the equations:

$$3R_3NH^+Cl^- + MCl_6^{3-} \rightarrow (R_3NH)_3.MCl_6 + 3Cl^- \quad (5.14)$$

However, Benguerel et al. (1996) state that due to the speciation of Rh in the chloride solutions, extraction using amines will be difficult due to the presence of different aquo/chloro complexes. Extraction is represented by Equation (5.15) below:

$$2(R_4NH)_2.[RhCl_5(H_2O)] \rightarrow (R_4N)_3.[Rh_2Cl_9] + R_4N^+Cl^- \quad (5.15)$$

The $RhCl_5(H_2O)$ complex is hydrophilic. Hence it does move freely into the aqueous phase. But the $Rh_2Cl_9^{3-}$ anion is bound to the hydrophobic ammonium cation and stripping becomes difficult. In this study, 41.7 % and 46.2 % of Rh were extracted using the ELM with 20 g/l PIB as shown in Figure 5.5 and 52.4 % and 54.5 % of Rh was extracted using ELM with 30 g/l PIB, as shown in Figure 5.6. There is a knowledge gap on the extraction of Rh using ELMs from the literature hence these results were compared to those of solvent extraction of Rh. The results of

the extraction using ELM with 20 g/l PIB at pH 1.87 are comparable to the studies on solvent extraction using kerosene as the diluent and tri-iso-octylamine as the extractant (Lee, Rajesh Kumar, Kim, Park, & Yoon, 2009). In their study, the extracted Rh was 36 % while in the current study it was 41.7 %. However Kumar et al system did not have the non-Newtonian modifier PIB. The amount of Rh left in the side stream was also examined and results are shown in Figure 5.7. For all ELMs, the amount of Rh decreased with time. This was due to the fact that extraction of the Rh by the ELMs increased with time. Mass balance was then calculted using equation 5.15. Extraction efficiency of the ELM containing 30 g/l PIB was higher than that of the ELM containing 20 g/l PIB. This can be explained by the higher viscosity caused by the 30 g/l PIB. Increased viscosity leads to reduced movement of microdroplets - hence reduced coalscence.

To account for all the rhodium initially used at the beginning of the extraction process, based on Equation 5.8, that states that input should be equal to output, Equation 5.16 was used:

$$Input\ \left(Rh_{(INITIAL)}\right) = \ Output\ (Mass\ balance + \ Rh_{(trapped)}) \qquad (5.16)$$

Where $Rh_{(INITIAL)}$ represents the initial concentration of Rh used before extraction and $Rh_{(trapped)}$ represents Rh trapped in the organic phase of the ELM after the extraction process. Substituting Equation 5.10 in Equation 5.16, Equation 5.17 is formed:

$$Rh_{(INITIAL)} = \ Rh_{ww} + \ Rh_{extracted} + \ Rh_{(trapped)} \qquad (5.17)$$

The mass balance of Rh after the single extraction using the ELM with 20 g/l PIB, as shown in Figure 5.8, was approximately 64 % at pH 1.87 and approximatey 71 % at pH 2.92 after 30 minutes of extraction. Using Equation 5.17, about 30 % of the Rh might have been trapped in the organic phase of the ELM. The mass balance using ELM with 30 g/l PIB was found to be 72 % and 74 % at pH 1.87 and pH 2.92 respectively (Figure 5.8). Rh trapped in the ELM could be explained as follows: Rh forms aquo/chloro complexes in HCl ranges from $[Rh(H_2O)_6]^{3+}$ to $[RhCl_6]^{3-}$. The speciation of Rh is affected by the increase in the concentration of the chloride ion. Studies by Levitin et al. (2003) and Benguerel et al. (1996) concluded that in 1M HCl, Rh complexes exist as$[RhCl_5(H_2O)]^{2-}$. In the presence of TOA, which was used as an extractant in this study, the following reaction occurs:

$$2R_3NH^+Cl^- + [RhCl_5(H_2O)]^{2-} \leftrightarrow 2(R_3NH)_2[RhCl_5(H_2O)] + 2Cl^- \quad (5.18)$$

The Rh ion pair $2(R_3NH)_2[RhCl_5(H_2O)]$ converts gradually into a dimer $(R_3NH)_3[Rh_2Cl_9]$ which is hydrophobic:

$$2(R_3NH)_2[RhCl_5(H_2O)] \leftrightarrow (R_3NH)_3[Rh_2Cl_9] + R_3NHCl + 2H_2O \quad (5.19)$$

Because of its hydrophobicity, stripping becomes a major problem and it has a tendency of staying in the hydrophobic phase. In our study, we used lower concentrations of 0.01 and 0.001 HCl to avoid this problem. However, we still had some Rh trapped in the Hydrophobic phase.

In the three fold extraction explained in Section 5.4.4, complete extraction of Rh was achieved.

5.8.2. The Effect of Temperature

Effects of temperature on ELM have also been studied during the current study. Extraction was done at an elevated temperature of 40 ± 1 ˚C. From the results in Figure 5.11, after the single extraction using the ELM with 20 g/l PIB, 38.1 % at pH 2.04 and 37.3 % at pH 3.14 of Rh was extracted after 30 minutes at 40 ± 1 ˚C. The percentage extraction was found to be 39.9 % and 38.1 % was extracted at pH 2.04 and pH 3.14 respectively at 50 ± 1 ˚C (Figure 5.11). The extraction efficiency dropped compared to the extractions done at 21 ± 1 ˚C where 41.7 % and 46.2 % of Rh at pH 1.92 and pH 2.92 respectively (Figure 5.5) was extracted using the ELM with 20 g/l PIB and 52.4 % and 53.5 % was extracted at pH 1.92 and pH 2.92 respectively, using the ELM with 30 g/l PIB (Figure 5.6). This is because temperature increases affect the size of the emulsion droplets. Temperature changes cause alterations to the viscocity of the interfacial film, leading to a change in interfacial tension between the two phases. They also affect the solubility of the surfactant in the two phases (Rosen, Kunjappu 2012).When temperature increases, there is an increase in the kinetic energy of the droplets. This in turn increases in the chance of coalescence, leading to an increase in emulsion microdroplet size and a subsequent decrease of the extraction efficiency. Increases in temperature also lead to reduced viscosity (Pérez, Zambrano et al. 2002). If viscosity of the oil phase is reduced, the motion of the droplets also increases, increasing the chances of the droplets bumping onto each other and leading to coalscence. With the increase in droplet size, coalescence and droplet aggrigation increase, as can be seen in Figures 5.8 and 5.9. Increases in the instability of the membrane lead to its easy

breaking and poor extraction efficiency. A study by Hempoonsert *et al.* (2010) concluded that temperature had a significant effect on droplet size. But as can be seen from Figure 5.11, there was no significant difference in the percentage recovery of Rh at 40 ± 1 ˚C and 50 ± 1 ˚C. This is because the ELM at 40 ± 1 ˚C and 50 ± 1 ˚C are fairly stable, even though coalsescence is occuring. From the studies of demulsification in Chapter 4, it was noted that the ELM did not completely demulsify at 45 ˚C, showing that, at this temperature, they are fairly stable for 24 hours. Only creaming occured. This explains the lack of differences between the extractions at 40 ± 1 ˚C and 50 ± 1 ˚C. The study was only done for 30 minutes, ensuring the stability of the ELM.

5.8.3. The Stirring Speed (Extraction Speed)

In this study the stirring speed used in extraction in the TVC was 250 rpm. This speed was chosen based on the literature review of the extraction of metals using ELMs. In a study by Hasan *et al.* (2009), it was concluded that extraction increased with speed. The stirring speeds used in their study ranged from 200-600 rpm. At 600 rpm the extraction of chromium (IV) was at optimum. It was concluded from this study that increase in stirring speed increased the number of emulsion globules, increasing the surface area of the membrane (Hasan, Selim et al. 2009). In another study, a stirring speed of between 300-600 rpm was used. It was observed that increases in the stirring speed increased the extraction rate up to 500 rpm. This is because increase in speed increases the interfacial area and leads to an increase in the mass transfer coefficient. They also observed that an increase from 500 rpm to 600 rpm led to a drop in the extraction efficiency (Kumbasar, Tutkun 2008). This was confirmed by a study done by Kumbasar (2009), in which their stirring speed ranged from 250 rpm to 400 rpm. Increase to 400 rpm led to a decrease in the extraction efficiency. Their optimum speed for the extraction of Cd was 300 rpm (Kumbasar 2009). Increase in agitation from 200 rpm to 400 rpm led to a decrease in the extraction degree from 90 % at 250 rpm to 50 % at 400 rpm (Othman, Mat et al. 2006). It was concluded that stirring speed must be increased to an optimum at which beyond this optimum, further increase in speed will break the emulsion droplets, leading to a reduced extraction rate (Othman, Mat et al. 2006, Kumbasar, Tutkun 2008, Kumbasar 2009). Increase in the stirring speed also leads to increase in swelling, due to the transport of water from the external phase to the internal phase (Othman, Mat et al. 2006).

5.8.4. Turbidity

In Table 5.3, turbidity of the side stream after separation from the ELM was assessed. This was done to check whether the emulsion had separated completely from the side stream. The turbidity from Table 5.3 was low at both pHs. This indicated that a lot of the ELM had separated from the side stream and less colloidal matter of the ELM during the extraction process was left in the side stream. Therefore much of the ELM was available for demulsification.

5.9. CONCLUSIONS

The extraction of Rh was successful. Single extraction processes failed to extract Rh completely, as reported in Sections 5.6.2.1 and 5.6.3.1. Hence a threefold extraction process was performed, as explained in Section 5.4.4 and schematically shown in Figure 5.3. Complete extraction of Rh was achieved using the threefold extraction process. After single extraction processes, mass balance calculations indicated that some of the Rh may be trapped in the organic phase of the ELM. This was explained in Section 5.8.1. It can also be concluded that the contact time between the ELM and the external phase increases the amount of trapped Rh as well as it increaseses the amount of Rh extracted. The ELM must thus be changed at a particular time to ensure that the lesser Rh complexes are trapped in the organic phase of the ELM. Hence, in the current study, the ELMs were changed after 30 minutes in the threefold extraction. Another potential problem caused by increased contact time during stirring is that the membrane raptures due to shear, compromising the extraction process. It is therefore important to change the membrane after some time to ensure effective extraction.

REFERENCES

AHMAD, A.L., KUSUMASTUTI, A., DEREK, C.J.C. and OOI, B.S., 2011. Emulsion liquid membrane for heavy metal removal: An overview on emulsion stabilization and destabilization. *Chemical Engineering Journal,* **171**, pp. 870-882.

AL-BAZI, S. and CHOW, A., 1984. Platinum metals-solution chemistry and separation methods (ion-exchange and solvent extraction). *Talanta,* **31**, pp. 815-836.

BAERTSCHI, S.W., PACK, B.W., HOAGLUND HYZER, C.S. and NUSSBAUM, M.A., 2013. Assessing mass balance in pharmaceutical drug products: New insights into an old topic. *TrAC Trends in Analytical Chemistry,* **49**, pp. 126-136.

BENGUEREL, E., DEMOPOULOS, G. and HARRIS, G., 1996. Speciation and separation of rhodium (III) from chloride solutions: a critical review. *Hydrometallurgy,* **40**, pp. 135-152.

DAVIES-COLLEY, R. and SMITH, D., 2001. Turbidity suspended sediment, and water clarity: A review1. *JAWRA Journal of the American Water Resources Association,* **37**, pp. 1085-1101.

GUPTA, B. and SINGH, I., 2013. Extraction and separation of platinum, palladium and rhodium using Cyanex 923 and their recovery from real samples. *Hydrometallurgy,* **134–135**, pp. 11-18.

HASAN, M.A., SELIM, Y.T. and MOHAMED, K.M., 2009. Removal of chromium from aqueous waste solution using liquid emulsion membrane. *Journal of hazardous materials,* **168**, pp. 1537-1541.

HEMPOONSERT, J., TANSEL, B. and LAHA, S., 2010. Effect of temperature and pH on droplet aggregation and phase separation characteristics of flocs formed in oil–water emulsions after coagulation. *Colloids and Surfaces A: Physicochemical and Engineering Aspects,* **353**, pp. 37-42.

KUMBASAR, R.A., 2009. Extraction and concentration study of cadmium from zinc plant leach solutions by emulsion liquid membrane using trioctylamine as extractant. *Hydrometallurgy,* **95**, pp. 290-296.

KUMBASAR, R.A. and TUTKUN, O., 2008. Separation of cobalt and nickel from acidic leach solutions by emulsion liquid membranes using Alamine 300 (TOA) as a mobile carrier. *Desalination,* **224**, pp. 201-208.

LEE, J., RAJESH KUMAR, J., KIM, J., PARK, H. and YOON, H., 2009. Liquid–liquid extraction/separation of platinum (IV) and rhodium (III) from acidic chloride solutions using tri-iso-octylamine. Journal of Hazardous Materials, vol. 168, no. 1, pp. 424-429.

LEVITIN, G. and SCHMUCKLER, G., 2003. Solvent extraction of rhodium chloride from aqueous solutions and its separation from palladium and platinum. *Reactive and Functional Polymers,* **54**, pp. 149-154.

OTHMAN, N., MAT, H. and GOTO, M., 2006. Separation of silver from photographic wastes by emulsion liquid membrane system. *Journal of Membrane Science,* **282**, pp. 171-177.

PÉREZ, M., ZAMBRANO, N., RAMIREZ, M., TYRODE, E. and SALAGER, J., 2002. Surfactant-oil-water systems near the affinity inversion. XII. Emulsion drop size versus formulation and composition. *Journal of Dispersion Science and Technology,* **23**, pp. 55-63.

RAJU, B., KUMAR, J.R., LEE, J., KWONC, H., KANTAM, M.L. and REDDY, B.R., 2012. Separation of platinum and rhodium from chloride solutions containing aluminum, magnesium and iron using solvent extraction and precipitation methods. *Journal of hazardous materials,* **227–228**, pp. 142-147.

ROSEN, M.J. and KUNJAPPU, J.T., 2012. Surfactants and interfacial phenomena. John Wiley & Sons.

SUN, P.P., LEE, J.Y. and LEE, M.S., 2012. Separation of platinum(IV) and rhodium(III) from acidic chloride solution by ion exchange with anion resins. *Hydrometallurgy,* **113–114**, pp. 200-204.

CHAPTER 6

DAPHNIA PULEX TOXICITY TESTING OF ETHYLENEDIAMINETETRAACETIC ACID TETRASODIUM SALT DIHYDRATE AND THE WASTE WATER EFFLUENT FROM EXTRACTION OF RHODIUM

6.1. INTRODUCTION

Ethylenediaminetetraacetic acid tetrasodium salt dihydrate (EDTA) is a mono- to tetradentate ligand, depending on the pH of the aqueous phase (Kari, Giger 1996, Repo, Malinen et al. 2011). It has a high affinity for heavy metals (e.g., Cu, Fe, Pb and Co) widely used in industries and agriculture (Wu, Zhou et al. 2011). EDTA is used to prevent the precipitation of metals at high pH through chelation (Kołodyńska, Hubicka et al. 2008). This includes Rh, as it is precipitated when the pH of the aqueous phase increases above 4.00 (Barbosa, Tandlich et al. 2007). EDTA may affect metal toxicity, which will be considered in data evaluation from the *D. pulex* acute test (Bergers, de Groot 1994, Guilhermino, Diamantino et al. 1997). However, it is impossible to use standard microbial toxicity tests, such as Microtox and Biotox, to assess the toxicity of the final effluent/spent side-stream after the ELM extraction of Rh from this matrix. Presence of EDTA is necessary in any toxicity test as some metals, e.g. Rh are unstable in solution at neutral pH values – conditions required by the organism necessary for the test.

D. pulex is a Cladocera crustacean belonging to the Arthropoda phylum, subphylum Crustacea, Branchiopoda class, and subclass Phyllopoda (Christie, McCoole et al. 2011, Liu, Kong et al. 2013). They are commonly known as water fleas (Liu, Kong et al. 2013) and inhabit lakes, eutrophic ponds and rock pools (Hebert 1978, Chen, Stillman 2012). *Daphnia* is very sensitive environmental changes (Miyakawa, Imai et al. 2010, Liu, Kong et al. 2013) and has the ability to physiologically, morphologically and behaviourally adapt to the environmental changes (Hunter, Pyle 2004, Zeis, Lamkemeyer et al. 2009, Connelly, Moeller et al. 2009, Mirza, Pyle 2009, Miyakawa, Imai et al. 2010). The ease of laboratory culture, sexual and asexual

(parthenogenetic) reproduction make *daphnia* a model organism in ecotoxicology (Christie, McCoole et al. 2011, Chen, Stillman 2012) and in monitoring levels of water pollution (Liu, Kong et al. 2013). *D. pulex* has been successfully used in various studies to assess the toxicity of metals such as cadmium, zinc, nickel and arsenic (Clifford, McGeer 2009, Kozlova, Wood et al. 2009, Clifford, McGeer 2010, Caumette, Koch et al. 2012). In a different study, the toxicity of copper, lead, zinc and arsenic from fresh water was successfully assessed using *Daphnia* (Theegala, Suleiman et al. 2007, De Samber, De Schamphelaere et al. 2009, Caumette, Koch et al. 2012). The present study is the first to address rhodium toxicity using *D. pulex.*

At the same time, mammalian (including human) toxicity of EDTA is low as it has low absorptivity and is not carcinogenic (Kari, Giger 1996, Sorvari, Sillanpää 1996). Thus, even though the toxicity of the spent side-stream after the ELM extraction process will be affected by the EDTA, if this influence is quantified and taken into account, a general estimate about the Rh toxicity to the environmental compartments it is discharged into should be feasible. Preliminary toxicity assessments of the Rh spent side-stream, in this chapter, are performed using the acute *D. pulex* toxicity test. There is insufficient data in literature that indicates that Rh is toxic to human beings. Some studies have shown the sensitizing activity to humans of the hexachlororhodiate ($RhCl_6^{3-}$) (Bingham, Cohrssen, & Powell, 2001) and the cytogenetic of rhodium Chloride (RhCl (III)) has been reported (Migliore, Frenzilli, Nesti, Fortaner, & Sabbioni, 2002). The appropriateness of acute testing is that most metal refinery operations aim to work on the zero-discharge principle, i.e. any spillage of Rh-bearing materials and side-streams into the environmental result from industrial accidents.

The principle of the test method is as follows: *Daphnids* are exposed to the test substance, added to water at a range of concentrations, for 48 hours. This is because *daphnids* are highly sensitive and have a short generation time. Under identical test conditions and with an adequate range of test substance concentrations, different concentrations of a test substance exert different average degrees of effect on the swimming ability of *Daphnia*. Different concentrations result in different percentages of *Daphnia* being no longer capable of swimming by the end of the test. Immobility of daphnids is used as the end point for toxicity testing. The concentrations causing zero or 100

% immobilizations are derived directly from test observations, whereas the 48-hour EC_{50} is determined by calculation if possible (He, Yu et al. 2012, Ton, Chang et al. 2012).

6.2. CHEMICALS AND TEST ORGANISM

EDTA and standardised Rh were purchased from Sigma-Aldrich (Johannesburg, South Africa), while the *D. pulex,* chemicals, and consumables for the 48 hour acute *D. pulex* toxicity test were purchased from the Institute for Water Research at Rhodes University (Grahamstown, South Africa). For the acute 48-hour toxicity testing, *D. pulex* was cultivated in the dilution water described in ISO 6341 in the temperature of 20 ± 2°C in the light rhythm of 16 hours light and 8 hours dark. The green alga *Chlorella* sp. was used as a food source. Cultures were prepared in 2 L containers, with an initial population density of one daphnid per 100 ml. Neonates were separated and used for toxicity determination. Organisms were not fed during the experiments.

6.3. STABILIZATION OF RH AT NEUTRAL PH

The milli Q water used in the work presented in this chapter was prepared by reverse osmosis, using a Milli-RO® 15 water purification system (Millipore®, Bedford, MA, USA), consisting of a Super-C carbon cartridge, two Ion-X® ion-exchange cartridges and an Organex-Q® cartridge. This water was filtered through a 0.22 μm Millipak® stack filter (Millipore®, Bedford, MA, USA). Preliminary experiments indicate that Rh was unstable in solutions when the pH of the aqueous phase increased above 3.14. This confirmed the literature data (see section 6.1 for details). On the other hand, the *D. pulex* acute toxicity test is conducted at neutral pH values. Thus the first partial task in the toxicity testing was to stabilise concentrations of Rh in aqueous solutions around pH 7.00. For this purpose, solutions of EDTA (purchased from Sigma-Aldrich, Johannesburg, South Africa) in Milli Q water, with EDTA concentrations ranging from 0 to 3 g/L, were prepared by dissolving between 0.0000 and 0.7500 g of EDTA in 100 ml of 0.01 M HCl and transferred into a 250 ml volumetric flask. The volume was made up to the mark with 0.01 M HCl and 50 ml of this solution was put into an Erlenmeyer flask before adding 5 ml of 1000 mg/L standardised Rh solution.

The solution was stored at 20 ± 2°C for 72 hours and ICP readings were taken from this solution for Rh concentration, and any precipitation was observed visually. Another solution was prepared in the above-stated fashion, but the pH of the final solution was adjusted to 8.4 with 2.5 M NaOH. The solution was incubated at 20 ± 2 °C for up to 3 days. Precipitation and Rh concentrations were assayed periodically over the 72-hour timeframe. No precipitation was observed in any of the solutions and Rh concentration only remained stable within 20 % of the initial value when EDTA concentrations equalled 3 g/L. The solution prepared in this manner was therefore considered suitable for use in the acute *D. pulex* test.

6.4. PREPARATION OF THE MODEL MINING SIDE-STREAM

The first model mining side-stream was a solution of 7 mg/L of Rh (purchased from Sigma-Aldrich, Johannesburg, South Africa) prepared in 0.01 M HCl (pH 1.87) by dilution of the standardised Rh solution, with an initial concentration of 999 ± 5 mg/L. A second model mining side-stream was prepared in the same fashion, but 0.001 M HCl (pH = 2.92) was used as the solvent. The model mining side-streams containing Rh were mixed with the optimised ELM with 30.000 g/L PIB (see Chapter 5 section 2.12 for details) and both were put into the Taylor-vortex column in the ratio 1:5 (10 ml ELM : 50 ml the model mining side-stream). The solutions were then stirred in the Taylor vortex column (Fig 5.1 in Chapter 5) using a speed of 250 rpm for 30 minutes. The ELM/feed phase mixture was then taken out of the column and placed in a conical flask. It was allowed to stand at 21 ± 2 °C until phase separation was observed between the spent model mining side-stream and the loaded ELM. The spent mining effluent was put aside and stored at 5 ± 2 °C until the ICP mass balance analyses and toxicity testing could be conducted. This procedure was repeated until 250 ml of the aqueous phase was collected for both model mining side-streams. All samples were analysed within 72 hours of production.

6.5. TOXICITY OF EDTA

Approximately 1 g; 1.5 g and 3 g of Ethylenediaminetetraacetic acid (EDTA) were analytically weighed, using a PA1214 analytical balance (Pioneer™, Ohaus Corporation, Johannesburg, South Africa), and placed in 1000 ml volumetric flasks. They were then dissolved in 500 ml of

MilliQ water. Each volumetric flask was then filled to the mark to make 1 g/l, 1.5 g/l and 3 g/l of EDTA respectively. pH was adjusted using 5 M hydrochloric acid (HCl) up to a pH of around 7.4. All glassware was purchased from Sigma-Aldrich (Johannesburg, South Africa).

6.5.1. Preparation of test concentrations

All glassware used in this section was purchased from Sigma-Aldrich (Johannesburg, South Africa). The test concentration was made by pipetting 25ml of the 1g/l EDTA stock solution into a 200 ml volumetric flask. The solution was filled to the mark using the growth medium to make a concentration of 12.5 % of the stock solution. This mixture was hand shaken for mixing. The procedure was repeated with 50ml, 100ml, 125ml, 175ml and 200ml to make test concentrations of 25%, 50%, 62.5%, 87.5% and 100% respectively.

6.5.2. Acute toxicity of EDTA

a) Each test concentration was divided into four batches of 50 ml each and poured into 100 ml beakers. 5 *daphnids* were put into each solution.
b) The *daphnids* were exposed for 48hrs. *Daphnid* survival was inspected after 24 hours of exposure and again after 48 hours.

The above procedure was repeated using stock solutions of 1.5 g/l and 3 g/l of EDTA.

6.6. STOCK SOLUTIONS FOR THE *D. PULEX* TOXICITY DETERMINATION

For each of the model mining side-streams, 200 ml of the spent effluent was brought to room temperature and transferred into a 1000 ml acid-washed glass beaker. 1 g of EDTA was then added to each of the solutions and salt crystals were completely dissolved. The volume was made up to approximately 900 ml with Milli Q water and pH was adjusted to 6.8 using 2.5 M NaOH. Solutions were then transferred into the acid-washed 1000 ml volumetric flask and the volume was made up to the mark with Milli Q water. Each of the two solutions had a final pH of around 6.90. Both solutions were then stored at 5 ± 2 ° C for 120 hours. They were examined under an optical microscope at magnification of 400 x for any traces of crystals forming, and ICP readings

were taken to confirm the concentration. No crystal formation was observed and the Rh concentration remained within 20 % of the initial value.

Toxicity of the mining effluents had to be evaluated in comparison to the EDTA baseline. Therefore, 1000 ml of a 1 g/L EDTA solution in MilliQ water was prepared. pH was adjusted to 6.90 with 5 M HCl and this value remained stable at 5 ± 2 ° C for 120 hours. It was thus used in additional toxicity testing without any further modifications.

The test concentration of both mining effluents and the EDTA solution, 25 ml of each of the stock solutions (see previous section), was pipetted into an acid-washed 200 ml volumetric flask. All three solutions were then made up to the mark using the *D. pulex* growth medium to make a concentration of 12.5 % of stock solution. Resulting mixtures were hand-shaken to achieve complete mixing and then further subdivided into four batches of 50 ml each. Each of the 50 ml aliquots was poured into a separate 100 ml beaker and 5 *Daphnids* were placed in each solution. This procedure was repeated using 25 %, 50 %, 62.5 %, 87.5 % and 100% of each of the spent mining effluent solutions. Next, all *Daphnids* were exposed to the test solutions for 48 hours. Their survival was inspected after 24 hours of exposure and again after 48 hours, when counting of results was again performed. A control experiment was set up in an analogical fashion, but the *D. pulex* growth medium was the only medium common to all toxicity experiments.

6.7. RESULTS AND DISCUSSION

6.7.1. Acute toxicity of EDTA

Table 6.1: The percentage survival of *D. pulex* after 24 hours and 48 hours of exposure to 1 g/l EDTA

Test concentration (%)	% survival after 24hrs	% survival after 48hrs
12.5	100	100
25	100	100
50	95	95
62.5	100	100
87.5	100	90
100	100	65
Control	100	100

Table 6.2: The percentage survival of *D. pulex* after 24 hours and 48 hours of exposure to 1.5 g/l EDTA

Test concentration (%)	% survival after 24hrs	% survival after 48hrs
12.5	90	90
25	100	100
50	100	100
62.5	90	95
87.5	100	90
100	100	75
control	100	100

Table 6.3: The percentage survival of *D. pulex* after 24 hours and 48 hours of exposure to 3 g/l EDTA

Test concentration (%)	% survival after 24hrs	% survival after 48hrs
12.5	100	100
25	100	100
50	95	95
62.5	95	80
87.5	75	5
100	75	0
control	100	100

From Tables 6.1 and 6.2, it can be seen that the EDTA was not toxic to *D. pulex* for lower test concentrations at 1 g/l and 1.5 g/l. There was considerable die-off at the highest concentration of 35 % and 25 % at 1 g/l and 1.5 g/l respectively. At higher concentrations of 3 g/l EDTA, the data clearly shows that the addition of 3 g/L EDTA led to minor toxicity to *D. pulex*, as only the undiluted solution led to complete die-off of the Daphnids (see Table 6.3 for details). It can be concluded from these results that increases in the concentration of EDTA in test concentrations leads to the death of *D. pulex.*

6.7.2. Acute toxicity of mining water side-stream

Results for the EDTA solution and spent mining effluents are shown in Tables 6.4-6.5. The Daphnids were well adapted to the test conditions, as 100 % survival was observed in the control experiment. All test organisms died after 48 hours of exposure to the mining effluent with the original pH = 1.87, while 10-60 % survival rates were observed at the mining spent effluent with the original pH of 2.92 if the strength of the effluent ranged from 12.5 to 62.5 % (see Tables 6.4 and 6.5).

Table 6.4: The percentage survival of D. pulex after 24 hours and 48 hours of exposure to aqueous phase effluent of mining side-streams made by a solution of Rh at pH = 1.87 after extraction of Rh using the ELM.

Test concentration (%)	% survival after 24 hrs	% survival after 48 hrs
12.5	85	0
25	90	0
50	70	0
62.5	45	0
87.5	15	0
100	0	0
control	100	100

Table 6.5: The percentage survival of D. pulex after 24 hours and 48 hours of exposure to aqueous phase effluent of mining side-streams made by a solution of Rh at pH = 2.92 after extraction of Rh using the ELM

Test concentration (%)	% survival after 24 hrs	% survival after 48 hrs
12.5	100	65
25	90	45
50	65	20
62.5	45	10
87.5	15	0
100	0	0
Control	100	100

The other studies revealed that other heavy metals like copper, mecury, zinc, cadmium, iron and manganese are also toxic to daphnia (Sorvari & Sillanpää, 1996). In addition some organic

components of the ELM, most probably toluene, the molecules carried over into the spent mining effluent may have also contributed to the observed die off. This was probably observed to a higher extent at pH of 1.87 than at pH of 2.92, providing an explanation of the results in Tables 6.4 and 6.5. It has been reported that the presence of EDTA reduces the toxicity of the metal (Sorvari & Sillanpää, 1996). This is because the toxicity of the metal is related to the free uncomplexed ions (Foster & Morel, 1982). However in the study of the complexation of the metals with EDTA and DTPA, it was concluded that the concentration of free ions is not the only reason for the explanation of toxicity to daphnia, this was because metals like mercury still showed high toxicity levels even after chelation. The results also showed that there was no significant difference in the toxicity of metals chelated using EDTA and DTPA except for mercury and iron. In the curreny study we found that the increase of EDTA for chelation of the metal may result in the die off of daphnia, hence a minimum amount of EDTA which will not cause die off should be used. Other studies have reported that the presence of EDTA may introduce errors in the study of the ecotoxicity of metals (Bergers & de Groot, 1994; Huebert & Shay, 1992). In the current study 1 g/L of EDTA was used because there was minimum die off caused by EDTA.

6.8. CONCLUSIONS

Considering that the side stream was diluted as described in section 2.6 before toxicity testing and there was a considerable die off, it can be concluded that the very dilute water side streams are toxic hence the discharge of the spent Rh side-stream should thus be discouraged and prevented at all costs. It can be concluded that some components of the ELM carried over into the stripping phase and might have contributed to the observed die off. Rh compounds should be treated as highly carcinogenic and toxic.

REFERENCES

BARBOSA, V., TANDLICH, R. and BURGESS, J., 2007. Bioremediation of trace organic compounds found in precious metals refineries' wastewaters: A review of potential options. *Chemosphere*, **68**, pp. 1195-1203.

BERGERS, P.J.M. and DE GROOT, A.C., 1994. The analysis of EDTA in water by HPLC. *Water research*, **28**, pp. 639-642.

BINGHAM, E., COHRSSEN, B. and POWELL, C.H., 2001. Patty's toxicology. Volume 2: toxicological issues related to metals, neurotoxicology and radiation metals and metal compounds. John Wiley and Sons.

CAUMETTE, G., KOCH, I., MORIARTY, M. and REIMER, K.J., 2012. Arsenic distribution and speciation in Daphnia pulex. *Science of The Total Environment*, **432**, pp. 243-250.

CHEN, X. and STILLMAN, J.H., 2012. Multigenerational analysis of temperature and salinity variability affects on metabolic rate, generation time, and acute thermal and salinity tolerance in Daphnia pulex. *Journal of thermal biology*, **37**, pp. 185-194.

CHRISTIE, A.E., MCCOOLE, M.D., HARMON, S.M., BAER, K.N. and LENZ, P.H., 2011. Genomic analyses of the Daphnia pulex peptidome. *General and comparative endocrinology*, **171**, pp. 131-150.

CLIFFORD, M. and MCGEER, J.C., 2010. Development of a biotic ligand model to predict the acute toxicity of cadmium to Daphnia pulex. *Aquatic Toxicology*, **98**, pp. 1-7.

CLIFFORD, M. and MCGEER, J.C., 2009. Development of a biotic ligand model for the acute toxicity of zinc to Daphnia pulex in soft waters. *Aquatic Toxicology*, **91**, pp. 26-32.

CONNELLY, S.J., MOELLER, R.E., SANCHEZ, G. and MITCHELL, D.L., 2009. Temperature effects on survival and DNA repair in four freshwater cladoceran Daphnia species exposed to UV radiation. *Photochemistry and photobiology*, **85**, pp. 144-152.

DE SAMBER, B., DE SCHAMPHELAERE, K., VANBLAERE, S., JANSSEN, C., SZALOKI, I., FALKENBERG, G., APPEL, K. and VINCZE, L., 2009. Investigation of Daphnia magna genotypes with different Zn tolerance using micro-XRF under cryogenic conditions.

FOSTER, P. and MOREL, F.M., 1982. Reversal of cadmium toxicity in a diatom: An interaction between cadmium activity and iron. Limnol.Oceanogr.;(United States), vol. 27, no. 4.

GUILHERMINO, L., DIAMANTINO, T.C., RIBEIRO, R., GONÇALVES, F. and SOARES, A.M.V.M., 1997. Suitability of Test Media Containing EDTA for the Evaluation of Acute Metal Toxicity toDaphnia magnaStraus. *Ecotoxicology and environmental safety*, **38**, pp. 292-295.

HE, H., YU, J., CHEN, G., LI, W., HE, J. and LI, H., 2012. Acute toxicity of butachlor and atrazine to freshwater green alga Scenedesmus obliquus and cladoceran Daphnia carinata. *Ecotoxicology and environmental safety,* **80**, pp. 91-96.

HEBERT, P.D., 1978. The population bilogy of daphnia (crustacea, daphnidae). *Biological Reviews,* **53**, pp. 387-426.

HUEBERT, D.B. and SHAY, J.M., 1992. The effect of EDTA on cadmium and zinc uptake and toxicity in Lemna trisulca L. Archives of Environmental Contamination and Toxicology, vol. 22, no. 3, pp. 313-318.

HUNTER, K. and PYLE, G., 2004. Morphological responses of Daphnia pulex to Chaoborus americanus kairomone in the presence and absence of metals. *Environmental toxicology and chemistry,* **23**, pp. 1311-1316.

KARI, F.G. and GIGER, W., 1996. Speciation and fate of ethylenediaminetetraacetate (EDTA) in municipal wastewater treatment. *Water research,* **30**, pp. 122-134.

KOŁODYŃSKA, D., HUBICKA, H. and HUBICKI, Z., 2008. Sorption of heavy metal ions from aqueous solutions in the presence of EDTA on monodisperse anion exchangers. *Desalination,* **227**, pp. 150-166.

KOZLOVA, T., WOOD, C.M. and MCGEER, J.C., 2009. The effect of water chemistry on the acute toxicity of nickel to the cladoceran Daphnia pulex and the development of a biotic ligand model. *Aquatic Toxicology,* **91**, pp. 221-228.

LIU, A., KONG, L., ZHANG, M., WU, D., WANG, D. and ZHAO, Y., 2013. Cloning, expression and cellular localization of Daphnia pulex senescence-associated protein, DpSAP. *Gene,* . 39172. Article in press. Accessed 12/12/2013 [http://0-www.sciencedirect.com.wam.seals.ac.za/science/article/pii/S0378111913014558]

MIGLIORE, L., FRENZILLI, G., NESTI, C., FORTANER, S. and SABBIONI, E., 2002. Cytogenetic and oxidative damage induced in human lymphocytes by platinum, rhodium and palladium compounds. Mutagenesis, vol. 17, no. 5, pp. 411-417.

MIRZA, R. and PYLE, G., 2009. Waterborne metals impair inducible defences in Daphnia pulex: morphology, life-history traits and encounters with predators. *Freshwater Biology,* **54**, pp. 1016-1027.

MIYAKAWA, H., IMAI, M., SUGIMOTO, N., ISHIKAWA, Y., ISHIKAWA, A., ISHIGAKI, H., OKADA, Y., MIYAZAKI, S., KOSHIKAWA, S. and CORNETTE, R., 2010. Gene up-regulation in response to predator kairomones in the water flea, Daphnia pulex. *BMC developmental biology,* **10**, pp. 45.

REPO, E., MALINEN, L., KOIVULA, R., HARJULA, R. and SILLANPÄÄ, M., 2011. Capture of Co(II) from its aqueous EDTA-chelate by DTPA-modified silica gel and chitosan. *Journal of hazardous materials,* **187**, pp. 122-132.

SORVARI, J. and SILLANPÄÄ, M., 1996. Influence of metal complex formation on heavy metal and free EDTA and DTPA acute toxicity determined by Daphnia magna. *Chemosphere,* **33**, pp. 1119-1127.

THEEGALA, C.S., SULEIMAN, A.A. and CARRIERE, P.A., 2007. Toxicity and biouptake of lead and arsenic by Daphnia pulex. *Journal of Environmental Science and Health Part A,* **42**, pp. 27-31.

TON, S., CHANG, S., HSU, L., WANG, M. and WANG, K., 2012. Evaluation of acute toxicity and teratogenic effects of disinfectants by Daphnia magna embryo assay. *Environmental Pollution,* **168**, pp. 54-61.

WU, P., ZHOU, J., WANG, X., DAI, Y., DANG, Z., ZHU, N., LI, P. and WU, J., 2011. Adsorption of Cu–EDTA complexes from aqueous solutions by polymeric Fe/Zr pillared montmorillonite: Behaviors and mechanisms. *Desalination,* **277**, pp. 288-295.

ZEIS, B., LAMKEMEYER, T., PAUL, R.J., NUNES, F., SCHWERIN, S., KOCH, M., SCHÜTZ, W., MADLUNG, J., FLADERER, C. and PIROW, R., 2009. Acclimatory responses of the Daphnia pulex proteome to environmental changes. I. Chronic exposure to hypoxia affects the oxygen transport system and carbohydrate metabolism. *BMC physiology,* **9**, pp. 7.

CHAPTER 7

SORPTION OF TRIOCTYLAMINE AND TRIHEXYLAMINE TO KAOLINITE

7.1. INTRODUCTION

The mining metallurgical industry is one of the main industries contributing to environmental pollution due to increasing use of reagents which ensure higher efficiencies in the mining process, such as those used in floatation processes (Sales, Magriotis et al. 2013) and solvent extraction. Organic chemicals have been used in these processes. Amines, such as etheramine, are used as collectors in the process of reverse flotation and are highly toxic and corrosive to aquatic organisms (Araujo, Viana et al. 2005). In a study of the solvent extraction of platinum and palladium (PGMs), a tertiary amine, alamine 336 (tertiary amine of mixed tri-octyl/decyl amine) was used as the organic extractrant due to its effectiveness as a platinum extractant (Yin, Nikoloski et al. 2013). TOA has been used commercially in the extraction of platinum (Jha, Gupta et al. 2013). TBP diluted in kerosene has also been used as an extractant in the solvent extraction and recovery of platinum and palladium (Lee, Raju et al. 2010). Di (2-ethylhexyl) phosphoric acid (D2EHPA) have been used as extractants in the solvent extraction of cadmium and copper and it is also reported that cadmium has been successfully extracted in many industrial and experimental works using D2EHPA (Bidari, Irannejad et al. 2013). Another organic extractant which has been used successfully in the solvent extraction of zinc, cadmium and chromium is g 7-(4-ethyl-1-methyloctyl)-8-hydroxyquinoline-Kelex 100®, where kerosene was used as the diluent (Mellah, Benachour 2006). Hydroxy-5-nonylacetophenone oxime has also been used in other liquid extraction studies (Panigrahi, Parhi et al. 2009, Rout, Sarangi 2014).

Liquid membranes are relatively old and present an alternative to the solvent extraction process (Kislik 2010). Although LM technology use at an industrial scale is limited due to various disadvantages, the use of organic chemicals such as TOA (Levitin, Schmuckler 2003, Kumbasar, Tutkun 2008), D2EHPA (Vernekar, Jagdale et al. 2013), methyl iso-butyl ketone (Kargari,

Kaghazchi et al. 2004) , tri-n-octylmethylammonium chloride (Goyal, Jayakumar et al. 2011), ti-octylphosphine oxide (Hasan, Selim et al. 2009), tri-dodecyl amine (Othman, Zailani et al. 2011) and other tertiary amines (Jha, Gupta et al. 2013) as extractants, or as carriers, in liquid membrane studies in the extraction of metals from metal waste water effluents has been suggested. The potential use of these chemicals as extractants on an industrial scale poses danger to the environment. Some cases of accidental industrial spillages of organic chemicals leading to seepage of these chemicals underground, resulting in the contamination of groundwater, has been reported (Kistemann, Hundhausen et al. 2008, Bonaparte, Neto et al. 2010, Hu, Qi et al. 2011). Accidental spillages of organic chemicals such as trichloro ethylene, tetrachloro-ethylene, gasoline and coal tar have been reported and have led to the formation of non-aqueous phase liquids (NAPLs) (Yang, Niemi et al. 2013, Goldstein, Prasher et al. 2007). Such risks also arise from the release of water used in the metal processing effluents in the mining metallurgical industry into water sources such as rivers. NAPLs are hydrophobic contaminants which do not readily dissolve in water. They do not mix with water, but float (Yang, Niemi et al. 2012), depending on the density of these organic chemicals. NAPLs get trapped in the rock matrix as they migrate to the subsurface and tend to partition into underground water, causing long-term pollution problems to groundwater (Goldstein, Prasher et al. 2007). Exposure to the environment may also be due to leaks from waste disposal sites (Mackay, Freyberg et al. 1986, Barber, Thurman et al. 1988, Kistemann, Hundhausen et al. 2008). The NAPLs may become a dissolution medium and a potential contamination source/depot of tertiary amines accidentally released/spilled into the environment. The influence of organic solvents such as NAPL on the fate of tertiary amines in the soil environments has been understudied.

Due to increased industrial use of hydrophobic organic chemicals (Bearden, Schultz 1997, Ren, Schultz 2002), there is a rise of persistent organic pollutants, POPs and NAPLs. Quality of water - the basic need of life - is being compromised (Dou, Zhou et al. 2012). This will lead to increased water scarcity, which is already a global concern (Pereira, Oweis et al. 2002, Rijsberman 2006). It is estimated that by 2025, two thirds of the world's population will lack access to fresh water (Rosegrant, Cai et al. 2002, Lindblom, Nordell 2006). By 2004 it was estimated that about 20 % of cultivated land is irrigated and of this land comes 40 % of food for consumption. Increased agricultural activity in the twentieth century to meet the food demand of the growing population has led to a fivefold increase in irrigation (Rosegrant, Cai et al. 2002,

Lindblom, Nordell 2006). Because of this, the use of underground water for irrigation becomes a possibility. Mining and metal processing use large quantities of water for transportation of ore and waste, minerals separation, dust suppression, washing of equipment and human consumption and, because of this, use both surface and underground water. This has a big impact on ecosystems and the environment (Bridge 2004, van Berkel 2007, Mudd 2008). Processes like floatation are used in concentrating minerals and this uses large amounts of water (Magriotis, Leal et al. 2010). This contributes to the water scarcity problem and increases competition for access to water with other users (Kemp, Bond et al. 2010). Mining industries recycle water after the extraction of the mineral of interest. Waste rock dumps and conventional tailings facilities are the most commonly used methods to manage mining waste waters. If these fail, it leads to devastating results like polluting of local water resources like dams (Plumlee, Morton et al. 2000, Coumans 2002, Kemp, Bond et al. 2010). There are also instances where mining waste water is accidentally released into rivers, oceans and lakes. This direct disposal can lead to widespread water contamination, like the Chilean example of the El Salvador Mine (UNEP, 1997 cited in Kemp et al. 2010) (Kemp, Bond et al. 2010).

There is a need to investigate and develop methods to reduce the impact of hydrophobic organic chemicals released into the environment from mining metallurgical industry and metal processing waste water effluents. The current study focused on the sorption of the extractant TOA and another tertiary amine, THA, using kaolinite - a low cost adsorbent from kerosene. Due to its abundance and low cost, kaolinite is used in the ceramic, paint, pesticide, paper, cement, pharmaceutical, plastic and textile industries, among others. It has also been used in the environmental area for the treatment of industrial effluents such as heavy metals (Angove, Johnson et al. 1997, Alkan, Kalay et al. 2008), organic pollutants (Peng, Wang et al. 2009) and dyes (Nandi, Goswami et al. 2009, Karaoğlu, Doğan et al. 2010). It is therefore important to understand the sorption characteristics of TOA and THA, and their relationship to the sorbent soil (kaolinite) and its sorption characteristics. The process of sorption in natural solids of organic chemicals is complex. It is a function of the sorbent properties such as mineral content and organic matter content of the soil/sediment (Delle Site 2001). Sorption is the process of interaction between the solute and the solid/sorbent, leading to the uptake of the sorbate by the sorbent matrix. Apparent sorption equilibrium is reached after a certain period of time when the liquid phase and the sorbed concentrations no longer change with time. Sorption is divided into

adsorption and absorption, depending on the extent of interaction between the solute and the sorbent (Weber, McGinley et al. 1991). Adsorption is the physical adherence or bonding of ions and molecules onto the surface of the sorbent matrix (Weber, McGinley et al. 1991, Huang, Peng et al. 2003). On the other hand, absorption is incorporation/partitioning of the sorbate into the matrix of the sorbent (Weber, McGinley et al. 1991, Huang, Peng et al. 2003). Figure 1 shows the schematic representation of TOA and THA. To the best of the author's knowledge, there are currently no studies focusing on the sorption of tertiary amines from hydrophobic/hydrophilic media onto clays or clay soils. To address this knowledge gap, the current study seeks to examine the sorption behaviour of TOA and THA on kaolinite as a function of the conditions and characteristics of the sorbent matrix.

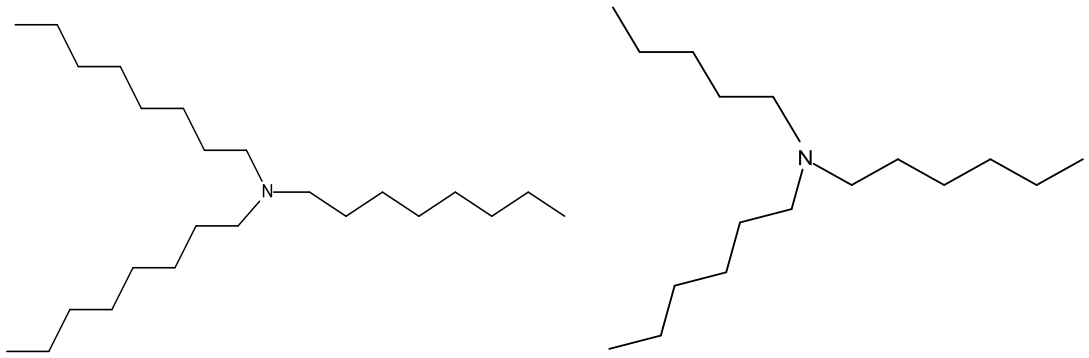

(a) **(b)**

Figure 7.1: Schematic representation of (a) TOA and (b) THA

7.2. METHOD

7.2.1. Apparatus and chemicals

TOA, THA, calcium chloride ($CaCl_2$), potassium chloride (KCl), ammonia, and kerosene were purchased from Sigma Aldrich (Johannesburg, South Africa). Perchloric acid, potassium hydrogen phthalate (KHP), ammonium per-sulphate, sulphuric acid and ethylene glycol mono-ethyl ether (EGME) were purchased from Merck (Pty.) Ltd (Johannesburg/Cape Town, South Africa). All masses were measured using a PA1214 analytical balance (Pioneer™, Ohaus Corporation, Johannesburg, South Africa). Fluka Sieve Standard, (Sigma-Aldrich, Johannesburg, RSA) were used for particle size.

7.2.2. Kaolinite characterisation

7.2.2.1. Loss on ignition (LOI)

In calculating the dry mass (W_s) of kaolinite, Equation 7.1 below was used. Porcelain high form crucibles purchased from Sigma-Aldrich (Johannesburg, South Africa), capacity 15 ml, were acid washed and dried in an oven at 105 °C for 24 hours. They were removed from the oven (UFE 700 oven, Memmert, Schwabach, Germany) and placed in a desiccator containing silica gel for 24 hours. The mass of the dried crucibles (M_0) was determined. Five grams (5 g) of the soil sample was weighed in the dried crucibles(M_1). The total mass of the crucible containing approximately 5 g of dried kaolinite was determined (M_2). The dry mass of kaolinite soil was calculated using the equation below (Margesin, Schinner 2005):

$$W_s = \frac{M_2 - M_0}{M_1 - M_0} \tag{7.1}$$

The crucibles containing the soil samples were ignited at 400 ^{o}C in a muffle furnace (Gallenkamp App 9B 4152 SP, Leicestershire, United Kingdom) until a constant weight was reached. The experiment was conducted in triplicates and a control which did not contain any soil sample was included. LOI was calculated using the following equation (7.2) below:

$$\Delta m\ (g) = M_S - M_C \tag{7.2}$$

Percentage LOI can be calculated using the following equation (7.3) below:

$$LOI\ (\%) = \frac{\Delta m\ (g)}{M_S(g)} \times 100 \tag{7.3}$$

Where $\Delta m(g)$ *is* loss of mass after ignition, M_S is kaolinite dry weight at 105 ^{o}C and M_C is mass of kaolinite after ignition at 400 ^{o}C.

7.2.2.2. Specific surface area measurements

7.2.2.2.1. Drying the sample

The specific surface area of the kaolinite was determined using the modified ethylene glycol mono-ethyl ether / calcium chloride (EGME/$CaCl_2$) method (Tandlich, Baláž 2011). Small glass

jars (50 ml) purchased from Sigma-Aldrich (Johannesburg, South Africa) were oven dried at 105 °C for 24 hours and their masses were determined. A sample approximately 1.1 g of kaolinite was weighed into each glass jar and the jars were placed into a desiccator, overnight, with open lids, over $CaCl_2$ to dry the soil samples. The desiccator lid was closed. After this period, the individual glass jars were covered with lids and weighed to determine the dry weight of each sample. This procedure was repeated until the mass of the glass jar and the soil sample remained constant (Ws). Samples were stored in the desiccator until the measurement, with lids on. As a control, an empty jar was treated the same way as the jars containing the soil sample.

7.2.2.2.2. Preparation of CaCl2/EGME solvate

Approximately 110 g $CaCl_2$ was ground, sieved through a 400 µm sieve and baked at 160 °C overnight. 100 g of hot $CaCl_2$ was removed from the oven and directly mixed into an aliquot volume of 100 ml of EGME to obtain the $CaCl_2$/EGME solvate (Tandlich, 2004). This solvate was used as it is sufficient to achieve constant pressure of EGME inside the desiccator used (Tandlich, 2004).

7.2.2.2.3. Measurement of specific surface area

The $CaCl_2$/EGME solvate was immediately placed into an empty desiccator (to create a stable EGME atmosphere over the clay samples) and the clay samples were allowed to equilibrate, with lids off, for 30 minutes. The desiccator was then evacuated at approx. 6.7 Pa using a vacuum pump for 45 minutes. After evacuation was completed, the desiccator was sealed and samples were allowed to equilibrate with the EGME atmosphere for 2 to 4 hours. At the appropriate time, the desiccator was re-pressurized and samples were weighed with the lids on. As the last step of the experimental procedure, the desiccator content was again evacuated under conditions analogical to those above. The operations were repeated until a constant weight of the samples was obtained (0.0001g precision). The specific surface area was then calculated using equation 7.4 (Cerato, Luteneggerl 2002).

$$SSA = \frac{W_a}{0.000286 x Ws} \quad (7.4)$$

Where W_s is the weight (g) of the soil added initially (dry weight) and W_a is the quantity (g) of EGME preserved by the sample and it is the difference between the equilibrated samples and the sample's dry weight (Equilibrated mass of the soil$-$ W_s) and 0.000286 is a constant representative of the mass of EGME needed for the formation of a monolayer of a square meter of a surface.

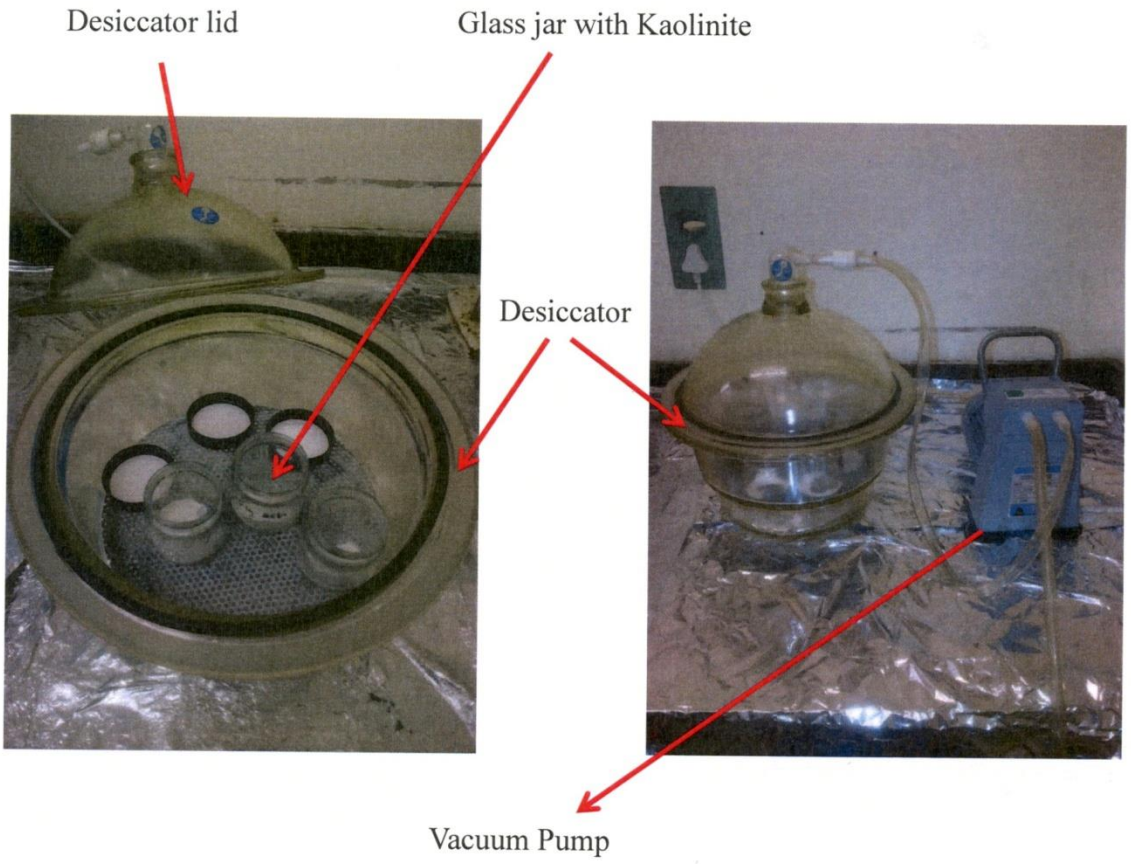

Figure 7.2: *EGME method of finding SSA of kaolinite*

7.2.2.3. Scanning electron microscopy (SEM)

The SEM (Tescan, VEGA LMU, Czechoslovakia) was used to analyse the surface morphology of the soil particles. Soil samples were placed on a double-sized carbon stub which was then

placed on a disc carrier of 3 mm height and 10 mm diameter. This was gold coated under a vacuum (0.25 Torr). The samples were imaged using a 20kV electron beam.

7.2.2.4. X-ray diffraction (XRD)

XRD patterns were recorded using a Bruker D8 Discover machine equipped with the PSD LynxEye detector, using Cu-K radiation (λ = 1.5405 Å, nickel filter). Samples were placed on the zero background (511) silicon wafer embedded in a generic sample holder and data recorded within the range $2\theta = 10^{\circ}$ to 100°, scanning at 1° min^{-1} with a filter time constant of 2.0 s per step at room temperature. A slit width of 6.0 mm was used in the measurements. The data was fitted using evaluation (Eva) curve fitting software.

7.2.2.5. Infrared Spectra (IR))

The IR spectra of solids can be prepared and recorded either by incorporating the sample into a disc composed of Potassium Bromide (KBr), by making a Nujol mull of the compound or by dissolving the solid compound in solvent, most commonly carbon tetrachloride. The KBr method was used to obtain the IR spectrum of kaolinite using a Perkin-Elmer® Precisely FT-IR spectrometer Spectrum 100 (Perkin-Elmer® Pty Ltd, Beaconsfield, England). Scans were performed in a range of 4000-650 cm^{-1}.

7.2.3. Measurement of sorption using batch equilibration

TOA was dissolved as follows in kerosene: 1.021 g of TOA was added to 95 ml of kerosene in a 100 ml volumetric flask. It was hand mixed by vigorous shaking and then kerosene was added to the mark to make a concentration of 10.21 g/l (m/v) TOA in kerosene. Ten grams of kaolinite and 50 ml of 10.21 g/l of TOA in kerosene prepared as described above were added to 250 ml Erlenmeyer flasks. The flasks were closed with aluminium foil and agitated using desk orbital shakers (using the Chiltern orbital shaker SS70 Slough, Berkshire, Chiltern Scientific, United Kingdom) at room temperature (21 ± 2 $^{\circ}$C) at 100 rpm for 30 minutes. The process was repeated for time intervals of 1 hour, 2, 4, 8, 16, 24, 36, 48, 60, 72, 96, 120, 144, 168 hours. The time interval for shaking was 30 minutes to 168 hours. Twenty five millilitres (25 ml) aliquots were taken at known time intervals from each flask, centrifuged at 3000 rpm using the Allegra X-15

benchtop centrifuge (Beckman Coulter, Johannesburg, South Africa) for 10 minutes and the concentration of the TOA in the supernatant was determined using non aqueous titrations method by Kar (2007). Standardised 0.0975 M perchloric acid (see Chapter 3 Section 3.6) was used as the titrant. This was done until the concentration of TOA in the aliquot was constant (168 hours), signifying that equilibrium has been reached. Experiments were repeated using 20 g of kaolinite. The percentage removal efficiency of TOA and THA adsorbed was determined by the differences of the initial and final TOA/THA concentrations using the equation below:

$$Removal\ efficiency = \left(\frac{M_0 - M_f}{M_O}\right) \times 100 \qquad (7.5)$$

M_0 is a starting concentration of the tertiary amine TOA and THA in kerosene before sorption and M_f is a final concentration of the tertiary amine in kerosene after sorption. A graph of % removal vs time was plotted. TOA sorption capacities were assessed for different kaolinite particle sizes: 101-400 µm and 65-100 µm. All the experiments were done in triplicates. Titrations were done until the concentration of TOA in the supernatant was constant (after 168 hours), signifying that equilibrium has been reached, and the experiments were then terminated. Control experiments were done by incubating a solution of TOA under the same conditions as the kinetics of sorption, but with no kaolinite added. Sorption of THA was done in the same way and the mass used for THA was 1.046 g.

7.3. RESULTS AND DISCUSSION

7.3.1. Loss on ignition (LOI)

Average LOI (%) of kaolin samples was 0.0086 $\pm$ 0.004 % (see Table 1 in Appendix III for the calculation). This was higher that what was found in a study done by Tandlich and Balaz (2011) in which they stated that their LOI after combustion of kaolinite was less than 0.001% (Tandlich, Baláž 2011). The binding of the organic compound to soil is affected by the total concentration of SOM which also includes soil organic carbon (SOC) which has to be above 0.01–0.2 % to affect sorption (McGroddy et al. 1998, Perminova, Grechishcheva et al. 1999, Huang, Peng et al. 2003, Chiou). The value of soil organic matter found using LOI in the current study is smaller than 0.2%, therefore it will have no influence on sorption of THA and TOA.

7.3.2. Specific surface area measurements

The SSA was 18.21 ± 0.8 m^2 g^{-1}. This is in agreement with the literature values of SSA of kaolinite. In different studies done using kaolinite from different locations it was found that the specific surface area of Kaolinite was 25.5 m^2g^{-1}(Yukselen, Kaya 2006), 5.9 m^2g^{-1} (Churchman, Burke et al. 1991) and 15 m^2 g^{-1}(Cerato, Luteneggerl 2002). It has been stated in literature that non-expanding soils like kaolinite has the SSA values ranging from 10 m^2 $g^{-1}$to 40 m^2 g^{-1}(Cerato, Luteneggerl 2002b). Kaolinite is a natural occurring inorganic polymer. It consists of siloxane and gibbsite layers. And its chemical formula is $Al_2[Si_2O_5](OH)_4$. It consists of 1:1 octahedral alumosilicate sheet with aluminium cations bonded to another tetrahedral sheet with silicon cations (Elbokl, Detellier 2008, Cheng, Liu et al. 2012). These sheets are stacked on top of each other and the adjoining layers form van der Waals forces and hydrogen bonds because of the availability of an OH group and an oxygen atom in the two adjacent layers (Cheng, Liu et al. 2012). The hydroxyl functional groups on kaolinite are the most reactive (Letaief, Diaco et al. 2008, Cheng, Liu et al. 2012). They may take part in various chemical reactions including ion exchange processing. Lack of expanding potential of the kaolin crystalline structure due to hydrogen bonds (Tandlich, Baláž 2011) means that its internal surface area is negligible as compared to the total specific surface area (Jaynes, Boyd 1991), leading to the conclusions that sorption of HOC takes place mostly on the outer surface of kaolinite (Gianotti, Benzi et al. 2008). Hence it can be concluded that the sorption of TOA and THA took place on the outer surface of kaolinite.

7.3.3. Scanning Electron Microscopy (SEM)

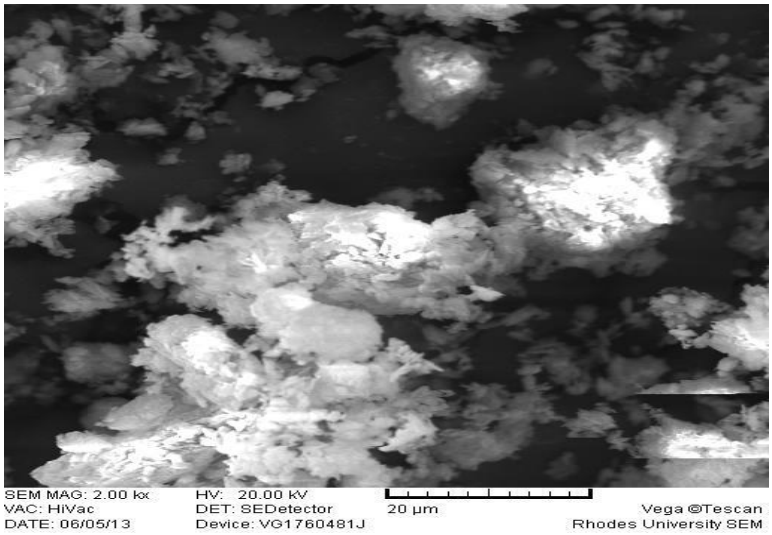

(a)

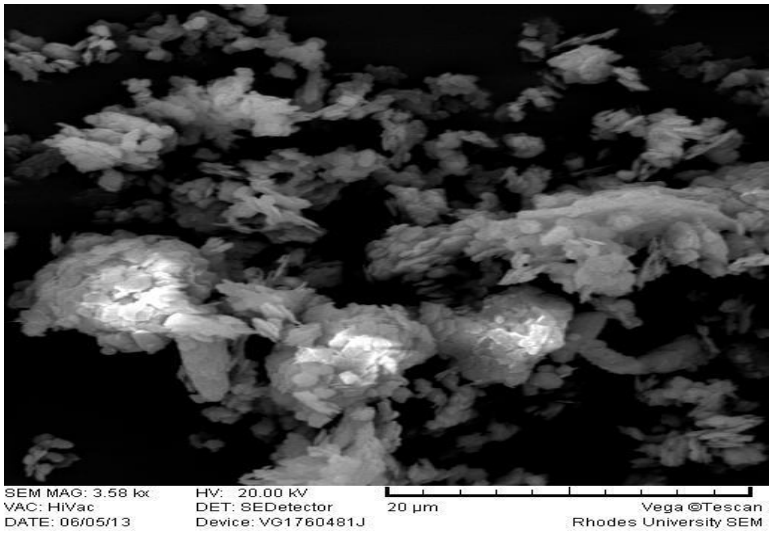

(b)

Figure 7.3: *SEM photomicrographs of kaolinite at different time intervals during batch equilibration: (a) control sample which was not exposed to kerosene, TOA and THA; (b) kaolinite patterns after 24 hours; (c) 72 hours and; (d) 168 hours*

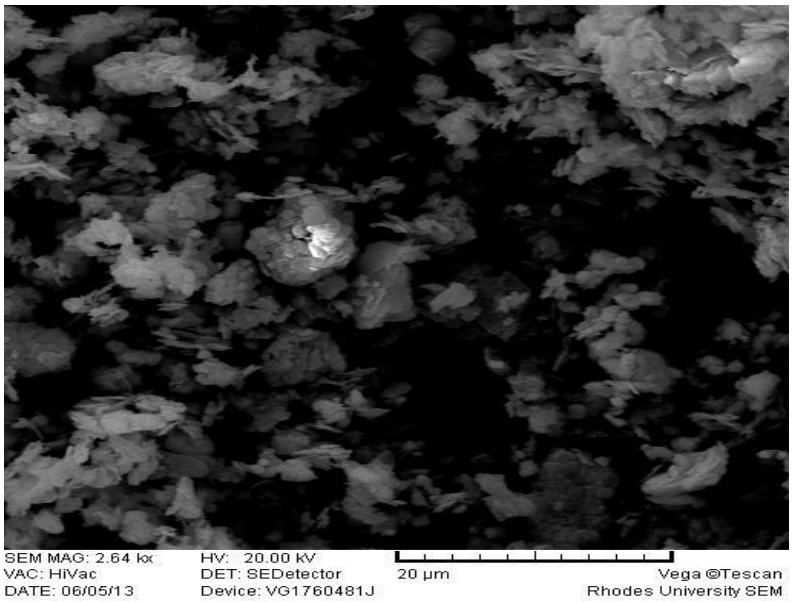

(c)

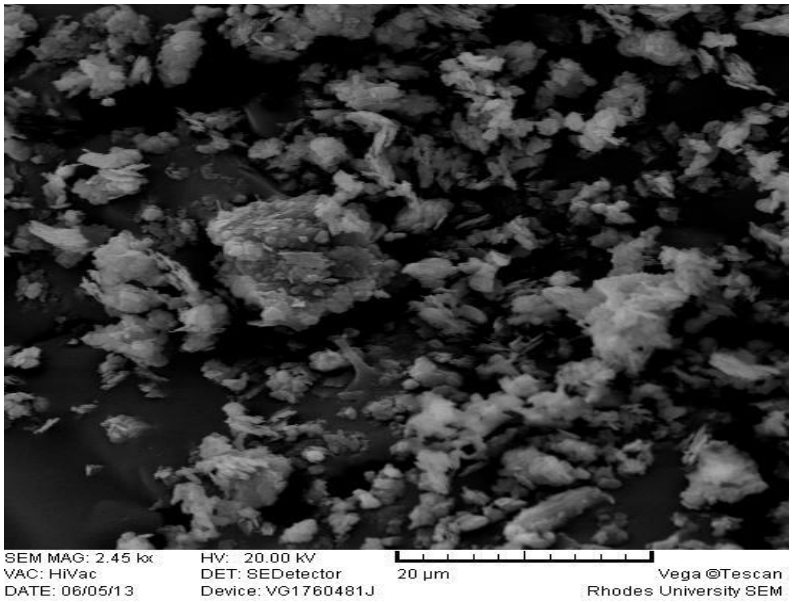

(d)

Figure 7.3: (continued)

Figure 7.3 shows the SEM micrographs of the kaolinite samples. SEM photomicrographs indicate that small soil particles adhere to each other, forming clusters. This may reduce the surface area of sorption. It can also be seen that the shape of the kaolinite particles is hexagonal,

which agrees with the findings purported by other studies (Xu, Van Deventer 2002). The surfaces of the kaolinite flakes show that they are a composite of particles greater than 20 µm.

7.3.4. X-ray diffraction (XRD)

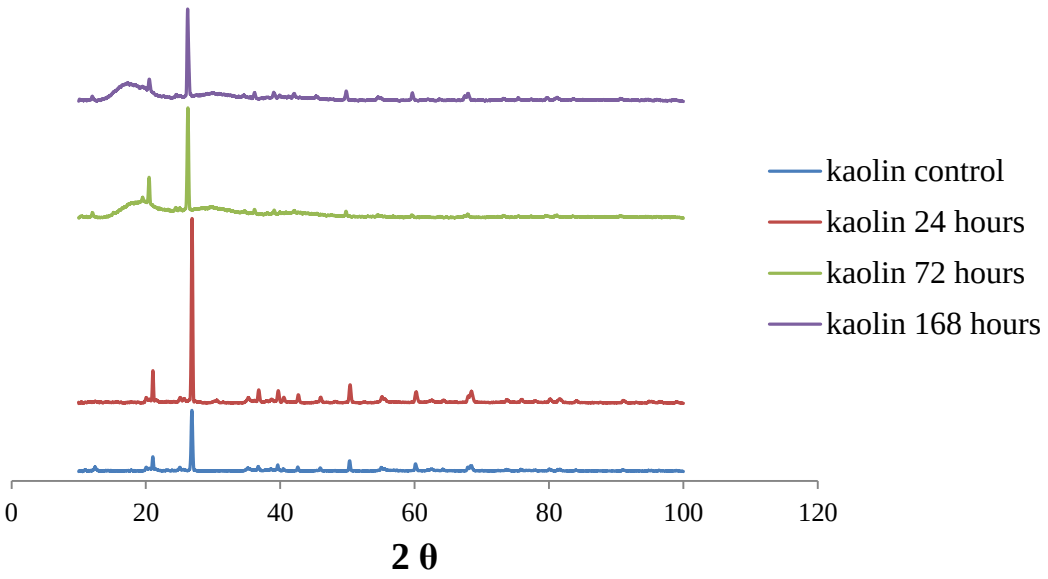

Figure 7.4*:XRD patterns of kaolinite at different time intervals (24 hours, 72 hours and 168 hours) during batch equilibration. The control sample was not exposed to kerosene, TOA and THA.*

XRD spectrums show that the crystalline nature of kaolinite is dominant throughout 168 hours of exposure to kaolinite. But there are small peaks indicating the presence of mica, quartz and minor microcline. From the XRD spectrum, using an XRD background of 2θ = 10˚ to 100˚, it can be seen that the structure of kaolinite was not altered by the presence of kerosene and tertiary amine during the duration of the batch equilibration experiments. All the major peaks of kaolinite at the diffraction peak of 1.5405 Å were observed for the control sample and were still observed after 168 hours of exposure to kerosene and tertiary amine during batch equilibration sorption experiments. The intensity of the largest peak at 2θ = 27˚ increased after 24 hours and reduced after 72 hours and 168 hours. The XRD spectrums show that the position of the major peaks conforms to previous literature data reported by Kakali et al (2001) and He et al (1994).

XRD backgrounds used in these studies were 2θ = 20˚ to 30˚ with diffraction peaks of 3.58 Å (He, Makovicky et al. 1994, Kakali, Perraki et al. 2001).

7.3.5. IR of kaolinite

Figure 7.5 represents the IR spectra of untreated samples.

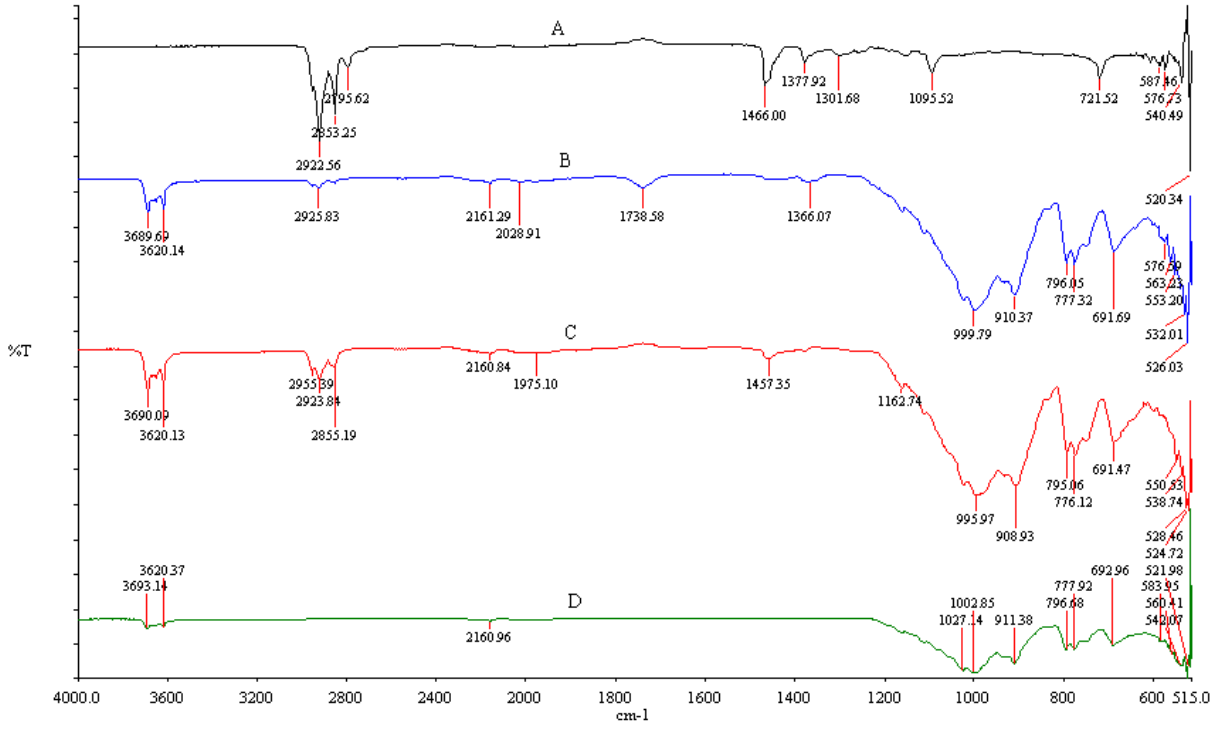

Figure 7.5: *(A) Infrared emission spectra of TOA; (B) Infrared emission spectra of dried kaolinite after 168 hours after batch equilibration; (C) Infrared emission spectra of kaolinite after 168 hours after batch equilibration before drying; and (D) Infrared emission spectra of the original sample of kaolinite.*

The bands between 3 700-3 620 cm^{-1} correspond to the well-crystallized structure of kaolinite (Kakali, Perraki et al. 2001). Cheng at al. (2011) contradicted with Suraj *et al.* (1997) when the bands at 937 and 914 were attributed to OH bending vibrations and bands at 983 and 1035 were attributed to the Si–O–Si in-plane vibrations (Cheng, Yang et al. 2011). As described above, the

Si-O-Si represents the siloxane bonds which are hydrophobic and will have a bearing on the sorption of HOC. Table 7.1 below shows the spectral wave lengths of kaolinite as studied by Suraj *et al.* (1997).

Table 7.1: Band assignments for kaolinite soil (Suraj, Iyer et al. 1997).

Wavelength (cm^{-1})	Assignments
3700	Inner surface -OH stretching vibration
3620	Inner -OH stretching vibration
1114, 1035, 1010	Si-0 bending vibrations
938, 918	AI-OH bending vibration
792, 754	Si-O-Al compounded vibrations
692	Si-O stretching vibration

From the current study, the bands of 3 693-3 620 cm^{-1} were observed for kaolinite before and after the batch equilibration experiments. These bands correspond to the inner surface -OH stretching vibration. Bands 1 027- 1 02 cm^{-1} were also seen for the original sample (D), corresponding to Si-O bending vibrations. For spectra (B) and (C), these were shifted to 999 cm^{-1} and 995 cm^{-1}. These results signified potential interaction between TOA and the Si-O bonds. Bands of 911 (D), 908 (C), 910 (B) were observed, which are likely to correspond to AI-OH bending vibrations. Spectra 796 and 692 were observed, corresponding to Si-O-Al compounded vibrations and Si-0 stretching vibration respectively. These bands existed after the batch experiments (B) and (C). The bands of TOA 2 922 cm^{-1}, 2 955 cm^{-1}, 1 457 cm^{-1} and 1 366 cm^{-1} were observed in spectra (B) and (C), showing that some TOA traces were detected on the kaolinite soon after batch experiments and after the kaolinite had been dried. This proved that TOA sorbed to kaolinite. It can be seen from the original sample of kaolinite that these bands did not exist before introduction of TOA.

7.3.6. Batch Experiments

Table 7.2 below shows the removal efficiencies of THA and TOA after the sorption experiments were completed after 168 hours. Calculation tables are shown in Appendix IV.

Table 7.2: TOA and THA removal efficiencies and sorption capacities at equilibrium after 168 hours

		TOA		**THA**	
Mass of kaolinite (g)	**Particle size (µm)**	**Removal efficiency (%)**	**Sorption capacity (g/g)**	**Removal efficiency (%)**	**Sorption capacity (g/g)**
10	65-100	18.1	0.92	-	-
	101-400	17.5	0.88	-	-
20	65-100	35.8	0.93	29.3	0.73
	101-400	33.3	0.87	28.9	0.75

After apparent equilibrium was established after 168 hours, the removal efficiency of TOA for 10 g of kaolin and particle size 65 µm-100 µm and 101 µm-400 µm was 18.1 % and 17.4 % (Table 1 Appendix IV for calculations) respectively, while sorption capacities were 0.92 g/g and 0.88 g/g respectively. Figure 7.6 below shows the comparison of sorption of TOA to kaolinite of particle size 101-400 µm using 10 g and 20 g of kaolinite. It can be seen from the graph that an increase in the amount of sorbent kaolinite results in increases in the amount of the tertiary amine sorbed.

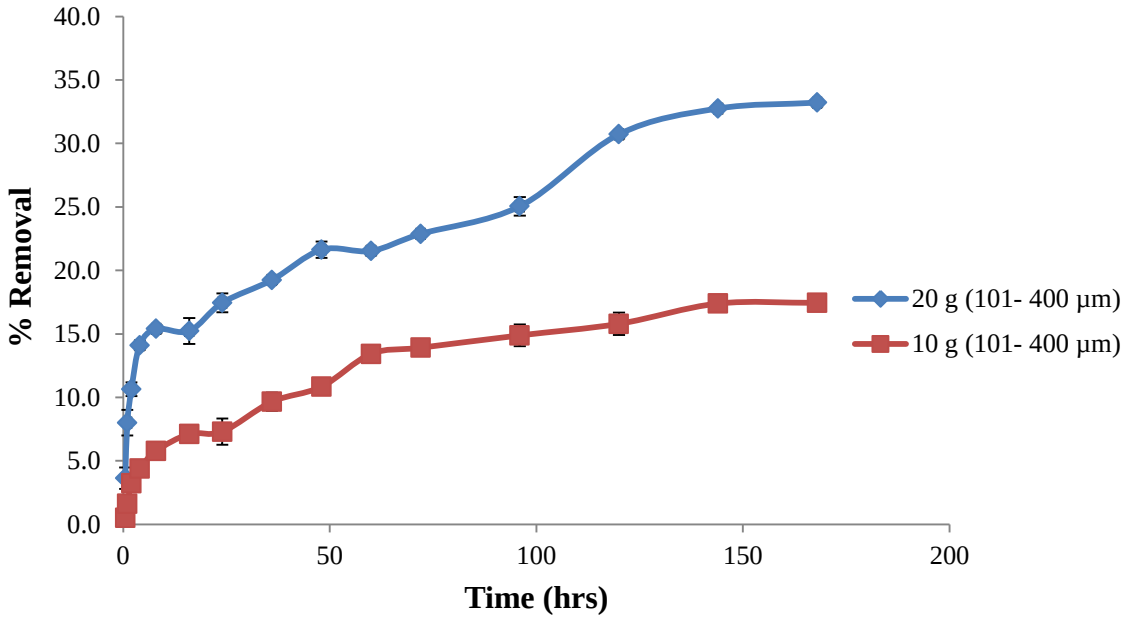

Figure 7.6: *Comparison of sorption of TOA onto kaolinite of particle size 101-400 µm using 10 g and 20 g of kaolinite.*

When 20 g of kaolin was used, the removal efficiency was 35.8 % and 33.2 %, as shown in Figure 7.7 below, and sorption capacities were 0.93 g/g and 0.87 g/g respectively. The R^2 values obtained for Freundlich and Langmuir were 0.9757 and 0.9819 respectively as shown in Figure 7.9 and 7.10 for particle size 101 µm-400 µm. For particle size 101 µm-400 µm, the R^2 values obtained for Freundlich and Langmuir were 0.9719 and 0.9491 respectively.

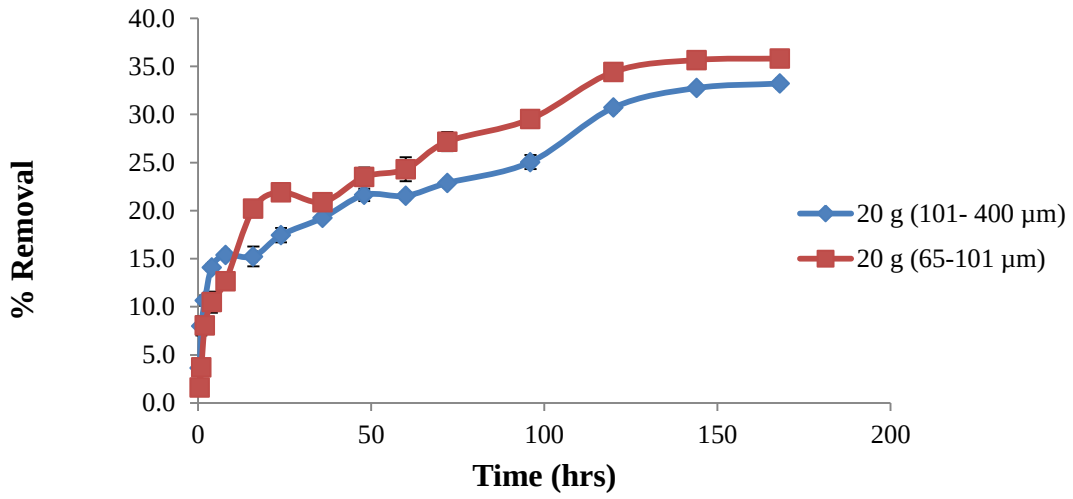

Figure 7.7: *Sorption of TOA onto 20 g of kaolinite of particle sizes 65-100 µm and 101- 400 µm*

This showed that sorption was higher in kaolinite with smaller particle size. As the results show, smaller sized particles have a higher sorption capacity compared to larger particles. This is due to increases in the surface area of the soil resulting from the decrease of particle size (Wang, Keller 2008). Results of the current study in relationship to particle size are also supported by the study by Zhou *et al.* (2004). They reported a relationship between sorption of phenanthrene and particle size. The isotherm data followed the Freundlich isotherm. They reported that as particle sizes decreased, K_f values increased. This is due to higher total organic carbon associated with the finer particles of the soil and the sediment. Mesh sizes of 120, 240, and 360 gave a Freundlich exponent *n* of 0.91, 0.93, and 0.61 and the corresponding K_f values were 51.2 $\mu g g^{-1}$, 83.6 $\mu g g^{-1}$ and 96.4 $\mu g g^{-1}$using Beizhai kaolinite soil samples. This proved there is a relationship between particle size and sorption (Zhou, Liu et al. 2004). Removal efficiency for THA of particle sizes 101 µm-400 µm and 65 µm-100 µm was 28.8 % and 29.3 % respectively, while sorption capacities were 0.73 g/g and 0.75 g/g respectively. The R^2 values obtained for Freundlich and Langmuir were 0.957 and 0.989 respectively as shown in Figure 7.9 and 7.10 for particle size 101 µm-400 µm. For particle size 65 µm- 100 µm, the R^2 values obtained for Freundlich and Langmuir were 0.9751 and 0.9713 respectively. Figure 7.8 shows a comparison in the sorption of THA and TOA. It can be seen that more TOA (35.8 %) was sorbed compared to the 29.3 % THA sorbed using 20 g kaolinite of particle sizes 65- 100 µm. This could have

been related to the hydrophobicity of TOA and THA, since the organic content of kaolinite was negligible (see section 7.3.1) and is not expected to influence sorption.

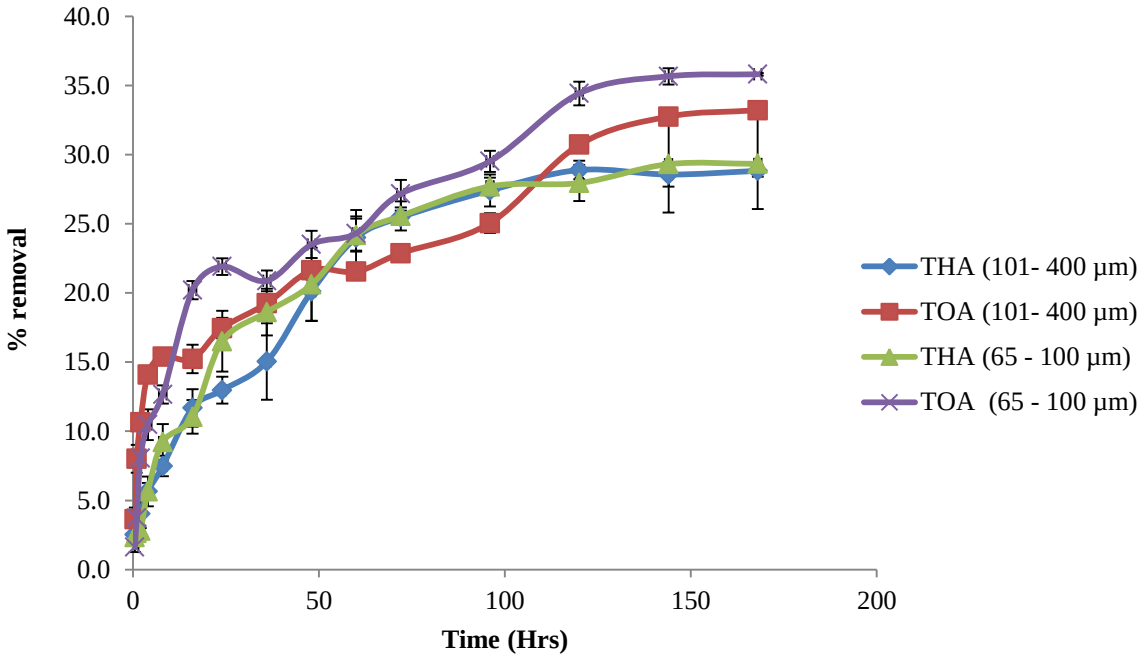

Figure 7.8: *Comparison of sorption of TOA and THA onto 20 g kaolinite of particle sizes 65-101 µm and 101- 400µm.*

Hydrophobicity is often referred to as log $\boldsymbol{K_{ow}}$, where $\boldsymbol{K_{ow}}$ refers to octanol/water partition coefficients. Octanol is a model of the hydrophobic phase and the organic matter found in soils and sediments has been equated to that of an organic phase in solvent extraction in some studies (Delle Site 2001). The log $\boldsymbol{K_{ow}}$ of TOA is 10.81 while that of THA is 7.761. This implies that TOA is more hydrophobic than THA. Since sorption was from a hydrophobic medium - kerosene to kaolinite - the better sorption of TOA to kaolinite can be attributed to the presence of hydrophobic siloxane groups (Cheng, Liu et al. 2010). Jaynes et al (1991) studied the nature of siloxane groups and their hydrophobicity. From their results, they concluded that organic compounds adsorbed to siloxane surfaces, demonstrating the hydrophobicity of the siloxane surfaces in smectites (Jaynes, Boyd 1991). In another study on the adsorption of poly(ethylene oxide) on smectites, they conclude that an interaction between siloxane groups of smectites with the -CH_2-CH_2- of poly(ethylene oxide) occurred while the poly(ethylene oxide) hydrophilic ether group formed a hydrogen bond with the OH structures on smectite. This showed that the hydrophobic part of poly(ethylene oxide) had a higher affinity for the siloxane groups in the

smectite soils (Su, Shen 2009). From this, it can be concluded that the longer the hydrophobic tail, the higher the affinity for siloxane groups. TOA has a longer hydrophobic chain than THA and it can hence be concluded that it has a higher affinity for siloxane groups of kaolinite. Kaolinite crystalline lattice is neutral compared to other clay soils. Its two well-defined layers, alumina and silica surfaces, provide different potential surfaces of adsorption because of the hydroxyl groups and the silica-oxygen bridged surfaces (van Duin, Larter 2001). Kaolinite has a high affinity for organic compounds compared to other clay surfaces, especially illite (Saada, Siffert et al. 1995, Bantignies, Cartier Dit Moulin et al. 1997). According to Van Duin et al. (2001) this could be due to the neutrality of the kaolinite lattice and due to the close proximity of charged counter-balancing ions to the illite surfaces, rendering it a low affinity for less polar organic compounds (van Duin, Larter 2001). Saada et al. (1995) focused on the hydrophilicity and hydrophobicity of illites and kaolinite. They reported only 25 % of the kaolinite surface to be hydrophilic and the remaining part is either neutral or hydrophobic when compared to illites, which are 40 % hydrophilic (Saada, Siffert et al. 1995). They stated that the surface of kaolinite is more oleophilic and is hence easily wetted by oils (Saada, Siffert et al. 1995). So kaolinite surfaces would easily be wetted by kerosene, making kaolinite more hydrophobic. This explains why the kaolinite surface would be more hydrophobic in kerosene. Together with the log $\boldsymbol{K_{ow}}$ value of TOA, this provides an explanation for the TOA having stronger sorption than THA.

The Collander equation can be used to relate hydrophobicity with sorption:

$$log\, K_1 = a\, log\, K_2 + b \tag{7.6}$$

Where K_1 and K_2 represent organic solvent-water partition coefficients calculated using equation (7.7) and a and b are constants calculated with the knowledge of the concentration in the two organic solvents:

$$P = \frac{C_o}{C_w} \tag{7.7}$$

Where C_o represents the concentration of the organic solvent and C_W represents the concentration in the aqueous phase. Collander observed that the relationship between partition

coefficients of various organic solvents in a two phased system of water/organic solvent and the partition coefficients of the same solutes in a different organic solvent/water system are linear and, using the logarithmic scale, he obtained the equation designed to colander (Madeira, Teixeira et al. 2008, Silvério, Rodriguez et al. 2010, Han, Qiao et al. 2012).

7.3.7. Adsorption Isotherms

Figure 7.9 below shows the Freundlich isotherm of TOA and THA to kaolinite particles sizes of 65 -100 µm and 101-400 µm

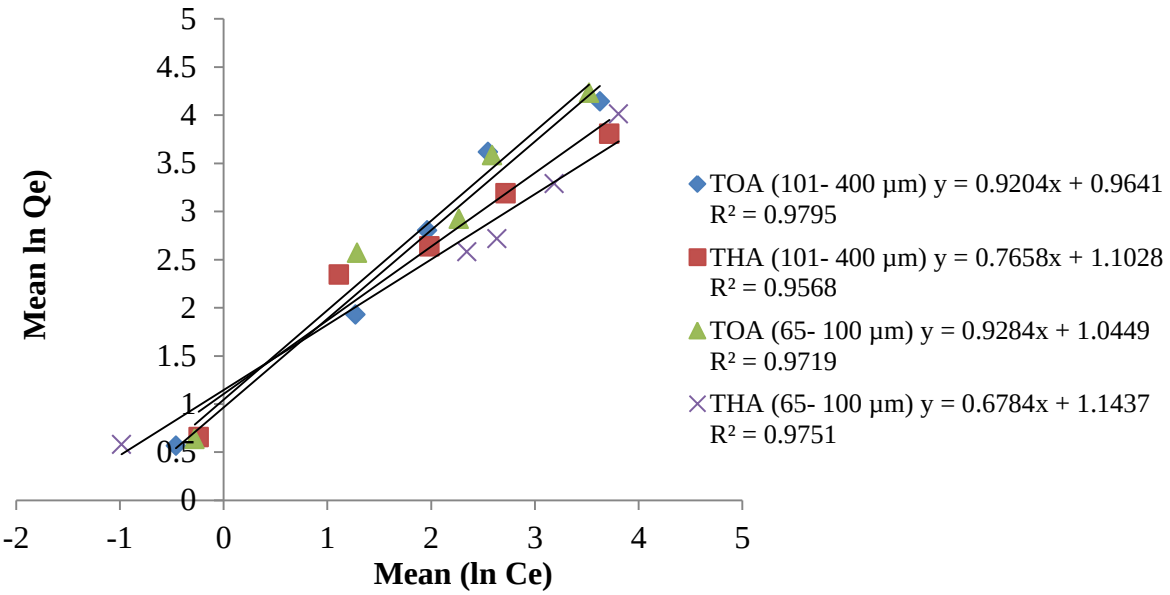

Figure 7.9: *The Freundlich isotherm of TOA and THA to kaolinite particle sizes 65-101 µm and 101- 400µm.*

The Freundlich isotherm, as shown in equation 7.8 below:

$$lnq_e = lnk_f + \frac{1}{n}(lnC_e) \qquad (7.8)$$

Where q_e is the amount of solute adsorbed at equilibrium time (µg/g), C_e is the equilibrium concentration of the solute in solution (µg/ ml), and K_f and n are isotherm constants indicating the capacity and intensity of the adsorption, respectively. The Freundlich isotherm assumes adsorption takes place on heterogeneous surfaces (Arami, Limaee et al. 2006). It has been shown

to demonstrate that the ratio of the amount of solute adsorbed onto a given mass of the adsorbent to the amount of concentration of the solute in solution is not constant at different solution concentrations (Mall, Srivastava et al. 2006).

Figure 7.10 below shows the Langmuir isotherm of TOA and THA to kaolinite particle sizes of 65 – 100 µm and 101- 400 µm.

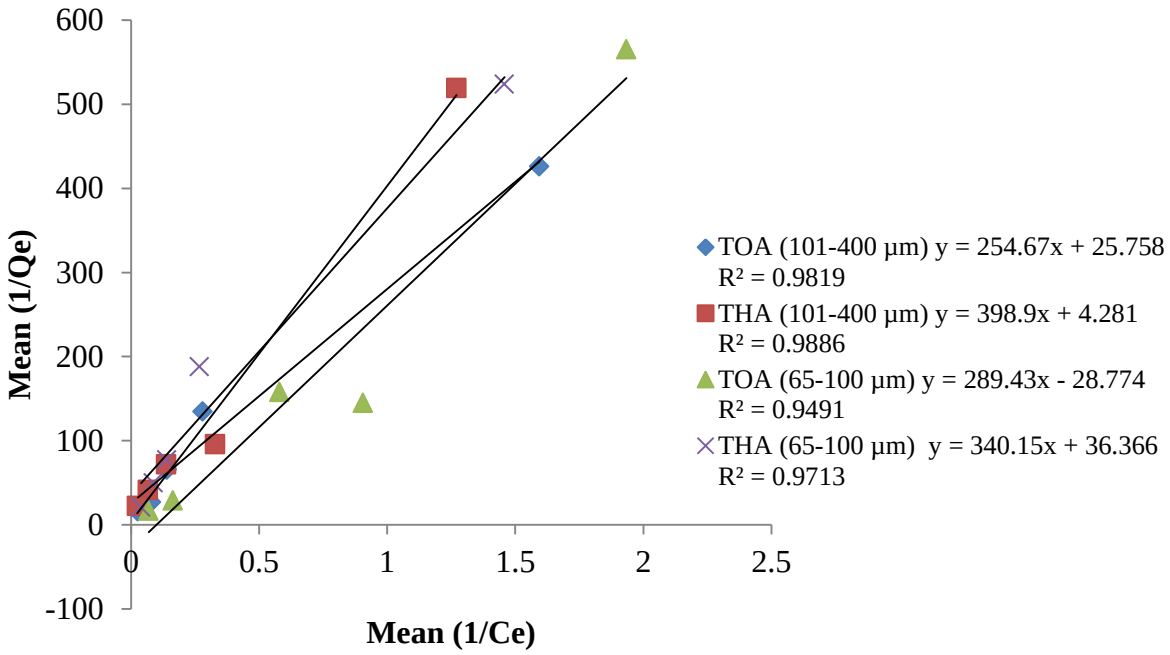

Figure 7.10: *Langmuir isotherm of TOA and THA onto kaolinite particles sized 65-101 µm and 101- 400µm.*

The Langmuir isotherm assumes that adsorption takes place at specific homogenous adsorption sites within the adsorbent (Almeida, Debacher et al. 2009, Clark Ehlers, Forrester et al. 2010). Assumptions of this theory are that, once a solute molecule occupies a site, no further adsorption can take place at that site (monolayer adsorption) (Ng, Losso et al. 2002, Almeida, Debacher et al. 2009). It is explained by the equation below:

$$\frac{C_e}{q_e} = \frac{C_e}{q_m} + \frac{1}{K_{ads} q_m} \qquad (7.9)$$

Where K_{ads} is the equilibrium adsorption coefficient (ml/g), q_m is the maximum adsorption capacity (mg/g), q_e is the amount of solute adsorbed at equilibrium time (µg/g), and C_e is the equilibrium concentration of the solute in solution (µg/ml). Table 7.3 below shows the sorption parameters of TOA and THA.

Table 7.3: Sorption parameters of TOA and THA on kaolinite.

		Freundlich Model			Langmuir Model
		K	***n***	R^2	R^2
TOA	101 – 400 µm	2.622	1.086	0.9795	0.9819
	65 – 100 µm	2.843	1.077	0.9719	0.9491
THA	101 – 400 µm	2.151	1.307	0.956	0.9886
	65 – 100 µm	3.138	1.474	0.9751	0.9713

From the table, it can be seen that $\frac{1}{n} < 1$ for the Freundlich isotherm for both TOA and THA. This implies that with increases of surface concentration, the marginal sorption energy decreases (Giles, Smith et al. 1974, Farrell, Reinhard 1994). It also indicates that there is less competition for binding sites by the solvent. This could be due to the planar shape of the absorbate molecule. From the R^2 values shown in Table 7.3, the sorption of TOA using particle size of 101 – 400 µm was best described by the Langmuir model and the particle size of 65 – 100 µm was best described by the Freundlich model. THA sorption of using particle size of 101 – 400 µm was best described by the Langmuir model and the particle size of 65 – 100 µm was best described by the Freundlich model. Using the K_f it can be seen that for both THA and TOA, the K_f for smaller particle sized kaolinite (65 – 100 µm) was higher signifying that the smaller sized particles had a higher sorption capacity. This can be attributed to a larger surface area associated with smaller sized particles.

7.4. CONCLUSIONS

From the results it was concluded that sorption of larger particle size for both TOA and THA was best described by the Langmuir isotherm model and the smaller sized particles were best described by the Freundlich isotherm model. Hydrophobicity of the tertiary amine and organic carbon content of kaolinite, the structure of kaolinite and the presence of hydrophobic siloxane bonds play a crucial role in its adsorption. In this study, the organic carbon content was negligible and the sorption of the tertiary amine was not attributed to the carbon content. The hydrophobic medium, kerosene, also has an effect on the structure of kaolinite. The oleophilic nature of kaolinite makes it easily wetted by organic chemicals, such as kerosene. This increases its hydrophobicity. It is also concluded that the hydrophobicity of the tertiary amine affected its sorption to kaolinite. TOA, which is more hydrophobic than THA, due to the length of its alkyl chains, had better sorption efficiency compared to THA. Smaller sized particles proved to have the highest adsorption capacity and better removal efficiency. This suggests that Kaolinite carries a potential for being used in the remediation of metal processing wastewaters containing hydrophobic extractants.

REFERENCES

ALKAN, M., KALAY, B., DOĞAN, M. and DEMIRBAŞ, Ö., 2008. Removal of copper ions from aqueous solutions by kaolinite and batch design. *Journal of hazardous materials,* **153**, pp. 867-876.

ALMEIDA, C., DEBACHER, N., DOWNS, A., COTTET, L. and MELLO, C., 2009. Removal of methylene blue from colored effluents by adsorption on montmorillonite clay. *Journal of colloid and interface science,* **332**, pp. 46.

ANGOVE, M.J., JOHNSON, B.B. and WELLS, J.D., 1997. Adsorption of cadmium(II) on kaolinite. *Colloids and Surfaces A: Physicochemical and Engineering Aspects,* **126**, pp. 137-147.

ARAMI, M., LIMAEE, N.Y., MAHMOODI, N.M. and TABRIZI, N.S., 2006. Equilibrium and kinetics studies for the adsorption of direct and acid dyes from aqueous solution by soy meal hull. *Journal of hazardous materials,* **135**, pp. 171-179.

ARAUJO, A.C., VIANA, P.R.M. and PERES, A.E.C., 2005. Reagents in iron ores flotation. *Minerals Engineering,* **18**, pp. 219-224.

BANTIGNIES, J.L., CARTIER DIT MOULIN, C. and DEXPERT, H., 1997. Wettability contrasts in kaolinite and illite clays: characterization by infrared and X-ray absorption spectroscopies. *Le Journal de Physique IV,* **7**, pp. 2-2.

BARBER, L.B., THURMAN, E.M., SCHROEDER, M.P. and LEBLANC, D.R., 1988. Long-term fate of organic micropollutants in sewage-contaminated groundwater. *Environmental science & technology,* **22**, pp. 205-211.

BEARDEN, A.P. and SCHULTZ, T.W., 1997. Structure-activity relationships for Pimephales and Tetrahymena: A mechanism of action approach. *Environmental toxicology and chemistry,* **16**, pp. 1311-1317.

BIDARI, E., IRANNEJAD, M. and GHARABAGHI, M., 2013. Solvent extraction recovery and separation of cadmium and copper from sulphate solution. *Journal of Environmental Chemical Engineering,* **1**, pp. 1269-1274.

BONAPARTE, L.V.C., NETO, A.T.P., VASCONCELOS, L.G.S., BRITO, R.P. and ALVES, J.J.N., 2010. Remediation procedure used for contaminated soil and underground water: A case study from the chemical industry. *Process Safety and Environmental Protection,* **88**, pp. 372-379.

BRIDGE, G., 2004. Contested terrain: mining and the environment. *Annu.Rev.Environ.Resour.,* **29**, pp. 205-259.

CERATO, A.B. and LUTENEGGERL, A.J., 2002a. Determination of Surface Area of Fine-Grained Soils by the Ethylene Glycol Monoethyl Ether. *Geotechnical Testing Journal,* **25**,.

CERATO, A.B. and LUTENEGGERL, A.J., 2002b. Determination of Surface Area of Fine-Grained Soils by the Ethylene Glycol Monoethyl Ether. *Geotechnical Testing Journal,* **25**,.

CHENG, H., LIU, Q., YANG, J., ZHANG, Q. and FROST, R.L., 2010. Thermal behavior and decomposition of kaolinite–potassium acetate intercalation composite. *Thermochimica Acta,* **503**, pp. 16-20.

CHENG, H., YANG, J., FROST, R.L., LIU, Q. and ZHANG, Z., 2011. Thermal analysis and Infrared emission spectroscopic study of kaolinite–potassium acetate intercalate complex. *Journal of thermal analysis and calorimetry,* **103**, pp. 507-513.

CHENG, H., LIU, Q., YANG, J., MA, S. and FROST, R.L., 2012. The thermal behavior of kaolinite intercalation complexes-A review. *Thermochimica Acta,* **545**, pp. 1-13.

CHIOU, C.T., MCGRODDY, S.E. and KILE, D.E., 1998. Partition characteristics of polycyclic aromatic hydrocarbons on soils and sediments. *Environmental science & technology,* **32**, pp. 264-269.

CHURCHMAN, G., BURKE, C. and PARFITT, R., 1991. Comparison of various methods for the determination of specific surfaces of sub soils. *Journal of Soil Science,* **42**, pp. 449-461.

CLARK EHLERS, G.A., FORRESTER, S.T., SCHERR, K.E., LOIBNER, A.P. and JANIK, L.J., 2010. Influence of the nature of soil organic matter on the sorption behaviour of pentadecane as determined by PLS analysis of mid-infrared DRIFT and solid-state 13C NMR spectra. *Environmental Pollution,* **158**, pp. 285-291.

COUMANS, C., 2002. *Submarine tailings disposal toolkit. Mining Watch Canada & Project Underground,* .

DELLE SITE, A., 2001. Factors affecting sorption of organic compounds in natural sorbent/water systems and sorption coefficients for selected pollutants. A review. *Journal of Physical and Chemical Reference Data,* **30**, pp. 187.

DOU, Z., ZHOU, Z., HUANG, Y. and WU, W., 2012. Numerical study of non-aqueous phase liquid transport in a single filled fracture by lattice boltzmann method. *Journal of Hydrodynamics, Ser.B,* **24**, pp. 130-137.

ELBOKL, T.A. and DETELLIER, C., 2008. Intercalation of cyclic imides in kaolinite. *Journal of colloid and interface science,* **323**, pp. 338-348.

FARRELL, J. and REINHARD, M., 1994. Desorption of halogenated organics from model solids, sediments, and soil under unsaturated conditions. 1. Isotherms. *Environmental science & technology,* **28**, pp. 53-62.

GIANOTTI, V., BENZI, M., CROCE, G., FRASCAROLO, P., GOSETTI, F., MAZZUCCO, E., BOTTARO, M. and GENNARO, M., 2008. The use of clays to sequestrate organic pollutants. Leaching experiments. *Chemosphere,* **73**, pp. 1731-1736.

GILES, C.H., SMITH, D. and HUITSON, A., 1974. A general treatment and classification of the solute adsorption isotherm. I. Theoretical. *Journal of colloid and interface science,* **47**, pp. 755-765.

GOLDSTEIN, L., PRASHER, S.O. and GHOSHAL, S., 2007. Three-dimensional visualization and quantification of non-aqueous phase liquid volumes in natural porous media using a medical X-ray Computed Tomography scanner. *Journal of contaminant hydrology,* **93**, pp. 96-110.

GOYAL, R.K., JAYAKUMAR, N.S. and HASHIM, M.A., 2011. Chromium removal by emulsion liquid membrane using [BMIM]+[NTf2]− as stabilizer and TOMAC as extractant. *Desalination,* **278**, pp. 50-56.

HAN, S., QIAO, J., ZHANG, Y., LIAN, H. and GE, X., 2012. Determination of n-octanol/water partition coefficients of weak ionizable solutes by RP-HPLC with neutral model compounds. *Talanta,* **97**, pp. 355-361.

HASAN, M.A., SELIM, Y.T. and MOHAMED, K.M., 2009. Removal of chromium from aqueous waste solution using liquid emulsion membrane. *Journal of hazardous materials,* **168**, pp. 1537-1541.

HE, C., MAKOVICKY, E. and OSBÆCK, B., 1994. Thermal stability and pozzolanic activity of calcined kaolin. *Applied Clay Science,* **9**, pp. 165-187.

HEILMAN, M., CARTER, D. and GONZALEZ, C., 1965. The ethylene glycol monoethyl ether (EGME) technique for determining soil-surface area. *Soil Science*, **100**, pp. 409-413.

HU, Y., QI, S., ZHANG, J., TAN, L., ZHANG, J., WANG, Y. and YUAN, D., 2011. Assessment of organochlorine pesticides contamination in underground rivers in Chongqing, Southwest China. *Journal of Geochemical Exploration,* **111**, pp. 47-55.

HUANG, W., PENG, P., YU, Z. and FU, J., 2003. Effects of organic matter heterogeneity on sorption and desorption of organic contaminants by soils and sediments. *Applied Geochemistry,* **18**, pp. 955-972.

JAYNES, W. and BOYD, S., 1991. Hydrophobicity of siloxane surfaces in smectites as revealed by aromatic hydrocarbon adsorption from water. *Clays Clay Miner,* **39**, pp. 428-436.

JHA, M.K., GUPTA, D., LEE, J., KUMAR, V. and JEONG, J., 2013. Solvent extraction of platinum using amine based extractants in different solutions: A review. *Hydrometallurgy,* .

KAKALI, G., PERRAKI, T., TSIVILIS, S. and BADOGIANNIS, E., 2001. Thermal treatment of kaolin: the effect of mineralogy on the pozzolanic activity. *Applied Clay Science,* **20**, pp. 73-80.

KAR, A., 2007. *Pharmaceutical drug analysis.* New Age International, New Delhi, India.

KARAOĞLU, M.H., DOĞAN, M. and ALKAN, M., 2010. Kinetic analysis of reactive blue 221 adsorption on kaolinite. *Desalination,* **256**, pp. 154-165.

KARGARI, A., KAGHAZCHI, T., SOHRABI, M. and SOLEIMANI, M., 2004. Batch extraction of gold(III) ions from aqueous solutions using emulsion liquid membrane via facilitated carrier transport. *Journal of Membrane Science,* **233**, pp. 1-10.

KEMP, D., BOND, C.J., FRANKS, D.M. and COTE, C., 2010. Mining, water and human rights: making the connection. *Journal of Cleaner Production,* **18**, pp. 1553-1562.

KISTEMANN, T., HUNDHAUSEN, J., HERBST, S., CLAßEN, T. and FÄRBER, H., 2008. Assessment of a groundwater contamination with vinyl chloride (VC) and precursor volatile organic compounds (VOC) by use of a geographical information system (GIS). *International journal of hygiene and environmental health,* **211**, pp. 308-317.

KUMBASAR, R.A. and TUTKUN, O., 2008. Separation of cobalt and nickel from acidic leach solutions by emulsion liquid membranes using Alamine 300 (TOA) as a mobile carrier. *Desalination,* **224**, pp. 201-208.

LEE, J.Y., RAJU, B., KUMAR, B.N., KUMAR, J.R., PARK, H.K. and REDDY, B.R., 2010. Solvent extraction separation and recovery of palladium and platinum from chloride leach liquors of spent automobile catalyst. *Separation and Purification Technology,* **73**, pp. 213-218.

LETAIEF, S., DIACO, T., PELL, W., GORELSKY, S.I. and DETELLIER, C., 2008. Ionic conductivity of nanostructured hybrid materials designed from imidazolium ionic liquids and kaolinite. *Chemistry of Materials,* **20**, pp. 7136-7142.

LEVITIN, G. and SCHMUCKLER, G., 2003. Solvent extraction of rhodium chloride from aqueous solutions and its separation from palladium and platinum. *Reactive and Functional Polymers,* **54**, pp. 149-154.

LINDBLOM, J. and NORDELL, B., 2006. Water production by underground condensation of humid air. *Desalination,* **189**, pp. 248-260.

MACKAY, D.M., FREYBERG, D., ROBERTS, P. and CHERRY, J., 1986. A natural gradient experiment on solute transport in a sand aquifer: 1. Approach and overview of plume movement. *Water Resources Research,* **22**, pp. 2017-2029.

MADEIRA, P.P., TEIXEIRA, J.A., MACEDO, E.A., MIKHEEVA, L.M. and ZASLAVSKY, B.Y., 2008. "On the Collander equation": Protein partitioning in polymer/polymer aqueous two-phase systems. *Journal of Chromatography A,* **1190**, pp. 39-43.

MAGRIOTIS, Z.M., LEAL, P.V.B., SALES, P.F., PAPINI, R.M. and VIANA, P.R.M., 2010. Adsorption of etheramine on kaolinite: A cheap alternative for the treatment of mining effluents. *Journal of hazardous materials,* **184**, pp. 465-471.

MALL, I.D., SRIVASTAVA, V.C. and AGARWAL, N.K., 2006. Removal of Orange-G and Methyl Violet dyes by adsorption onto bagasse fly ash—kinetic study and equilibrium isotherm analyses. *Dyes and Pigments,* **69**, pp. 210-223.

MARGESIN, R. and SCHINNER, F., 2005. *Manual for Soil Analysis—Monitoring and Assessing Soil Bioremediation. Soil Biology, Vol. 5.* Springer Verlag, Berlin.

MELLAH, A. and BENACHOUR, D., 2006. Solvent extraction of heavy metals contained in phosphoric acid solutions by 7-(4-ethyl-1-methyloctyl)-8-hydroxyquinoline in kerosene diluent. *Hydrometallurgy,* **81**, pp. 100-103.

MUDD, G.M., 2008. Sustainability reporting and water resources: a preliminary assessment of embodied water and sustainable mining. *Mine Water and the Environment,* **27**, pp. 136-144.

NANDI, B.K., GOSWAMI, A. and PURKAIT, M.K., 2009. Removal of cationic dyes from aqueous solutions by kaolin: Kinetic and equilibrium studies. *Applied Clay Science,* **42**, pp. 583-590.

NG, C., LOSSO, J.N., MARSHALL, W.E. and RAO, R.M., 2002. Freundlich adsorption isotherms of agricultural by-product-based powdered activated carbons in a geosmin–water system. *Bioresource technology,* **85**, pp. 131-135.

OTHMAN, N., ZAILANI, S.N. and MILI, N., 2011. Recovery of synthetic dye from simulated wastewater using emulsion liquid membrane process containing tri-dodecyl amine as a mobile carrier. *Journal of hazardous materials,* **198**, pp. 103-112.

PANIGRAHI, S., PARHI, P.K., SARANGI, K. and NATHSARMA, K.C., 2009. A study on extraction of copper using LIX 84-I and LIX 622N. *Separation and Purification Technology,* **70**, pp. 58-62.

PENG, X., WANG, J., FAN, B. and LUAN, Z., 2009. Sorption of endrin to montmorillonite and kaolinite clays. *Journal of hazardous materials,* **168**, pp. 210-214.

PEREIRA, L.S., OWEIS, T. and ZAIRI, A., 2002. Irrigation management under water scarcity. *Agricultural Water Management,* **57**, pp. 175-206.

PERMINOVA, I.V., GRECHISHCHEVA, N.Y. and PETROSYAN, V.S., 1999. Relationships between structure and binding affinity of humic substances for polycyclic aromatic

hydrocarbons: relevance of molecular descriptors. *Environmental science & technology,* **33**, pp. 3781-3787.

PLUMLEE, G.S., MORTON, R.A., BOYLE, T.P., MEDLIN, J.H. and CENTENO, J.A., 2000. *An Overview of Mining-related Environmental and Human Health Issues, Marinduque Island, Philippines: Observations from a Joint US Geological Survey-Armed Forces Institute of Pathology Reconnaissance Field Evaluation, May 12-19, 2000.* US Department of the Interior, US Geological Survey.

REN, S. and SCHULTZ, T.W., 2002. Identifying the mechanism of aquatic toxicity of selected compounds by hydrophobicity and electrophilicity descriptors. *Toxicology letters,* **129**, pp. 151-160.

RIJSBERMAN, F.R., 2006. Water scarcity: Fact or fiction? *Agricultural Water Management,* **80**, pp. 5-22.

ROSEGRANT, M.W., CAI, X. and CLINE, S.A., 2002. *World water and food to 2025: dealing with scarcity.* Intl Food Policy Res Inst.

ROUT, P.C. and SARANGI, K., 2014. Separation of vanadium using both hollow fiber membrane and solvent extraction technique – A comparative study. *Separation and Purification Technology,* **122**, pp. 270-277.

S KISLIK, V., 2010. Chapter 2 - Carrier-Facilitated Coupled Transport Through Liquid Membranes: General Theoretical Considerations and Influencing Parameters. In: VLADIMIR S. KISLIK, ed, *Liquid Membranes.* Amsterdam: Elsevier, pp. 17-71.

SAADA, A., SIFFERT, B. and PAPIRER, E., 1995. Comparison of the hydrophilicity/hydrophobicity of illites and kaolinites. *Journal of colloid and interface science,* **174**, pp. 185-190.

SALES, P.F.D., MAGRIOTIS, Z.M., ROSSI, M.A.D.L.S., TARTUCI, L.G., PAPINI, R.M. and VIANA, P.R.M., 2013. Study of chemical and thermal treatment of kaolinite and its influence on the removal of contaminants from mining effluents. *Journal of environmental management,* **128**, pp. 480-488.

SILVÉRIO, S.C., RODRIGUEZ, O., TEIXEIRA, J.A. and MACEDO, E.A., 2010. Solute partitioning in polymer–salt ATPS: The Collander equation. *Fluid Phase Equilibria,* **296**, pp. 173-177.

SU, C.C. and SHEN, Y.H., 2009. Adsorption of poly (ethylene oxide) on smectite: Effect of layer charge. *Journal of colloid and interface science,* **332**, pp. 11-15.

SURAJ, G., IYER, C.S.P., RUGMINI, S. and LALITHAMBIKA, M., 1997. The effect of micronization on kaolinites and their sorption behaviour. *Applied Clay Science,* **12**, pp. 111-130.

TANDLICH, R. and BALÁŽ, Š., 2011. Biphenyl sorption to different soil clay minerals. *African Journal of Agricultural Research,* **6**, pp. 2321-2328.

Tandlich, R. PCB biodegradation and binding to soil components. PhD thesis, North Dakota State University, Fargo, ND, USA. 2004

VAN BERKEL, R., 2007. Eco-efficiency in the Australian minerals processing sector. *Journal of Cleaner Production,* **15**, pp. 772-781.

VAN DUIN, A.C.T. and LARTER, S.R., 2001. Molecular dynamics investigation into the adsorption of organic compounds on kaolinite surfaces. *Organic Geochemistry,* **32**, pp. 143-150.

VERNEKAR, P.V., JAGDALE, Y.D., PATWARDHAN, A.W., PATWARDHAN, A.V., ANSARI, S.A., MOHAPATRA, P.K. and MANCHANDA, V.K., 2013. Transport of cobalt(II) through a hollow fiber supported liquid membrane containing di-(2-ethylhexyl) phosphoric acid (D2EHPA) as the carrier. *Chemical Engineering Research and Design,* **91**, pp. 141-157.

WANG, P. and KELLER, A.A., 2008. Particle-Size Dependent Sorption and Desorption of Pesticides within a Water− Soil− Nonionic Surfactant System. *Environmental science & technology,* **42**, pp. 3381-3387.

WEBER, W.J., MCGINLEY, P.M. and KATZ, L.E., 1991. Sorption phenomena in subsurface systems: Concepts, models and effects on contaminant fate and transport. *Water research,* **25**, pp. 499-528.

XU, H. and VAN DEVENTER, J.S.J., 2002. Microstructural characterisation of geopolymers synthesised from kaolinite/stilbite mixtures using XRD, MAS-NMR, SEM/EDX, TEM/EDX, and HREM. *Cement and Concrete Research,* **32**, pp. 1705-1716.

YANG, Z., NIEMI, A., FAGERLUND, F. and ILLANGASEKARE, T., 2012. Effects of single-fracture aperture statistics on entrapment, dissolution and source depletion behavior of dense non-aqueous phase liquids. *Journal of contaminant hydrology,* **133**, pp. 1-16.

YANG, Z., NIEMI, A., FAGERLUND, F., ILLANGASEKARE, T. and DETWILER, R.L., 2013. Dissolution of dense non-aqueous phase liquids in vertical fractures: Effect of finger residuals and dead-end pools. *Journal of contaminant hydrology,* **149**, pp. 88-99.

YIN, C., NIKOLOSKI, A.N. and WANG, M., 2013. Microfluidic solvent extraction of platinum and palladium from a chloride leach solution using Alamine 336. *Minerals Engineering,* **45**, pp. 18-21.

YUKSELEN, Y. and KAYA, A., 2006. Comparison of methods for determining specific surface area of soils. *Journal of Geotechnical and Geoenvironmental Engineering,* **132**, pp. 931-936.

ZHOU, Y., LIU, R. and TANG, H., 2004. Sorption interaction of phenanthrene with soil and sediment of different particle sizes and in various $CaCl_2$ solutions. *Journal of colloid and interface science,* **270**, pp. 37-46.

CHAPTER 8
CONCLUSIONS AND RECOMMENDATIONS

8. CONCLUSIONS

8.1. Emulsion liquid membranes and extraction of rhodium

Results show that complete extraction of Rh is possible from model side-streams, namely hydrochloric acid (HCl) solutions containing 7 mg/L of Rh. This is achieved by use of optimised ELMs with a diluent that was a 30 % solution of toluene in kerosene with other component concentrations as follows: 30.000 g/L (w/v) PIB, 10.870 g/L (m/v) of TOA and 51.001 g/L (m/v) of SPAN 80 while the optimised ELM containing 20.000 g/l of PIB, was made of 10.268 g/l TOA and 50.024 g/l of SPAN 80. This diluent phase was then mixed with 2 M HNO_3 (stripping phase) in a ratio of 2:1. The volumetric ratio of the treated side-stream and the ELM was 5:1. Three extraction runs were made and 98.7 to 108.7 % of the initial Rh amount was recovered in the stripping phase after chemical demulsification. Chemical demulsification was performed with polyethylene glycol with a molecular weight of 400 g/mol (PEG) at 50 ± 1°C for 24 hours. Major carry-over of the diluent components into the stripping phase and side-stream was observed. Using the COD digestion stoichiometry, the aqueous solubility and the measured ELM component concentrations, it is estimated that the carry-over was mostly from TOA, toluene and PEG. Summation of the TOA and toluene contributions to the COD levels in the stripping phase account for 1 970 mg/l. TOA accounted for 560 mg/L of COD while toluene accounted for 1 410 mg/L of COD. The remaining COD concentrations most likely originate from oxidation of the PEG molecule, which dissolves in water during chemical demulsification. This also explains the increase of COD with the increase of PEG observed. The final spent side-stream discharged into the environment was tested for ecotoxicity using *Daphnia pulex*. Considering that the side stream was diluted, as described in section 6.6, before toxicity testing and that there was a considerable die-off, it can be concluded that the highly diluted water side-streams are toxic - hence the discharge of the spent Rh side-stream should be discouraged and prevented at all costs.

8.2. Recommendations for ELMs

Commercial use of ELMs in extraction processes is often hindered by the instability of the stripping phase micro-droplets, due to the absorption of water from the feed phase into the ELM matrix. The classical solution is to increase the surfactant concentration in the ELM. While this increases the stability of the micro-droplets, it also leads to a decrease in mass transfer rates during metal extraction. A novel solution must thus be found to address this problem. One of the solutions listed in literature for the extraction of base metals is the use of non-Newtonian liquids as ELMs. The simplest way to construct a non-Newtonian liquid is the addition of a polymer such as polyisobutylene (PIB) to the ELM diluent. Shear stress is further decreased by the extraction contactor - the Taylor-vortex column.

Limitations of the results from this project include the lack of competitive studies, more in depth examination of Rh extraction from the real mining/metal refinery effluents and the lack of distribution of an isotherm of Rh in the ELM/side-stream system. Competition studies will have to be performed with other PGMs before any scale-up or any industrial application of the optimised ELM and Taylor-vortex column can be launched. Competition studies are currently underway and should be completed in the near future, as will the distribution isotherm of Rh in the ELM/side-stream treatment system. Preliminary experiments indicate the extraction efficiency of Rh from side-streams is going to be influenced by the high concentrations of chloride anions and the sorption of Rh-chloro complexes on the glass matrices of the extraction vessels. The nature of this effect should be addressed if future projects with similar scope are funded.

8.3. Sorption of TOA and THA

This study focused on the use of kaolinite as a sorbent of TOA and THA of waste water effluents resulting from metal processing. This is due to the use of TOA as an extractant in the liquid membrane extraction techniques suggested in literature. The SSA of kaolin was 18.21 $\pm$ 0.8 m^2 g^{-1} and Loss on ignition was 0.0086 $\pm$0.004 %. This LOI value was too low to exert an effect on sorption. The total concentration of SOM which also includes soil organic carbon (SOC) which has to be above 0.01–0.2 % to affect sorption (Chiou et al. 1998, Huang et al. 2003, Perminova et al. 1999). The initial TOA and THA used in the sorption studies was 10 g/L in kerosene.

Removal efficiency of TOA for 10 g of kaolin and particle size 65 µm-100 µm and 101 µm-400 µm was 18.1 % and 17.5 % respectively, while sorption capacities were 0.92 g/g and 0.88 g/g respectively. When 20 g of kaolin was used, removal efficiency was 35.8 % and 33.3 % and sorption capacities were 0.93 g/g and 0.87 g/g respectively. The R^2 values obtained for Freundlich and Langmuir were 0.9757 and 0.9819 respectively as shown in Figure 7.8 and 7.9 for particle size 101 µm-400 µm. For particle size 101 µm-400 µm, the R^2 values obtained for Freundlich and Langmuir were 0.9719 and 0.9491 respectively.The n and K_f for Freundlich isotherm were 1.086 and 2.622. Removal efficiency for THA for particle sizes 101 µm-400 µm and 65 µm-100 µm was 28.9 % and 29.3 % respectively, while sorption capacities were 0.73 g/g and 0.75 g/g respectively. The R^2 values obtained for Freundlich and Langmuir were 0.957 and 0.989 respectively as shown in Figure 7.9 and 7.10 for particle size 101 µm-400 µm. For particle size 65 µm- 100 µm, the R^2 values obtained for Freundlich and Langmuir were 0.9751 and 0.9713 respectively. The n and K_f for Freundlich isotherm were 1.307 and 2.151. Smaller sized particles proved to have the highest adsorption capacity and better removal efficiency. This suggests that kaolinite could potentially be used in remediation of metal wastewaters containing hydrophobic extractants. The larger particle size for both TOA and THA was best described by the Langmuir isotherm model and the smaller sized particles were best described by the Freundlich isotherm model.: The higher the value of $\frac{1}{n}$ the more favourable the adsorption (Ng et al. 2002). If, $\frac{1}{n} = 1$, it indicates a linear adsorption. This implies that the adsorption sites have equal adsorption energies. This is a common phenomenon at very low solute concentrations and low sorbent loading. When the sorption energy is directly proportional to surface concentration that is increase in marginal sorption energy cause an increase in the surface concentration, then $\frac{1}{n} > 1$. In the present study, $\frac{1}{n} < 1$ for the Freundlich isotherm for both TOA and THA. This indicates that with increases in the surface concentration, marginal sorption energy decreases and also indicates that there is less competition for binding sites by the solvent (Giles et al. 1974, Farrell et al. 1994).

SEM photomicrographs indicate that small soil particles adhere to each other, forming clusters. This may reduce the surface area of sorption. The XRD spectrum revealed that the crystalline nature of kaolinite is dominant throughout the 168 hours of exposure to kerosene. The surface of

kaolinite is more oleophilic hence it's easily wettable by oils (Saada et al. 1995). Hence kaolinite surface would easily be wetted by kerosene making kaolinite more hydrophobic. This explains why the kaolinite surface would become more hydrophobic in kerosene. . This together with the log K_{ow} value of the tertiary amine will provide an explanation for the adsorption of the tertiary amine to kaolinite. It will also provide an explanation for the TOA having stronger sorption as compared to THA. The IR spectrum (figure 7.5) showed that TOA traces were detected on the kaolinite soon after batch experiments and after the kaolinite had been dried. This proved that TOA sorbed to kaolinite. Some of the bands of TOA observed on kaolinite were 2 922 cm^{-1}, 2 955 cm^{-1}, 1 457cm^{-1} and 1 366 cm^{-1} .

REFERENCES

CHIOU, C.T., MCGRODDY, S.E. and KILE, D.E., 1998. Partition characteristics of polycyclic aromatic hydrocarbons on soils and sediments. *Environmental Science & Technology*, **32**, pp. 264-269.

FARRELL, J. and REINHARD, M., 1994. Desorption of halogenated organics from model solids, sediments, and soil under unsaturated conditions. 1. Isotherms. *Environmental Science & Technology*, **28**, pp. 53-62.

GILES, C.H., SMITH, D. and HUITSON, A., 1974. A general treatment and classification of the solute adsorption isotherm. I. Theoretical. *Journal of Colloid and Interface Science*, **47**, pp. 755-765.

HUANG, W., PENG, P., YU, Z. and FU, J., 2003. Effects of organic matter heterogeneity on sorption and desorption of organic contaminants by soils and sediments. *Applied Geochemistry*, **18**, pp. 955-972.

NG, C., LOSSO, J.N., MARSHALL, W.E. and RAO, R.M., 2002. Freundlich adsorption isotherms of agricultural by-product-based powdered activated carbons in a geosmin–water system. *Bioresource Technology*, **85**, pp. 131-135.

PERMINOVA, I.V., GRECHISHCHEVA, N.Y. and PETROSYAN, V.S., 1999. Relationships between structure and binding affinity of humic substances for polycyclic aromatic hydrocarbons: relevance of molecular descriptors. *Environmental Science & Technology*, **21**, 3781-3787.

SAADA, A., SIFFERT, B. and PAPIRER, E., 1995. Comparison of the hydrophilicity/hydrophobicity of illites and kaolinites. *Journal of Colloid and Interface Science*, **174**, pp. 185-190.

APPENDIX I: MICRO-DROPLET DIAMETER USING OPTICAL MICROSCOPY (CHAPTER 4)

Table 1.1: Microdroplet diameter (Chapter 4: section 4.4.1.4)

Micro-droplet number	ELM Micro-droplet diameter (µm)			
	1:1	**1:2**	**1:3**	**1:4**
1	11.97	2.52	14.49	21.84
2	8.46	2.52	6.09	22.89
3	13.44	3.15	6.3	9.03
4	10.71	5.25	14.07	14.7
5	10.71	3.15	10.29	12.18
6	8.61	2.31	21.42	10.5
7	8.19	2.73	7.56	9.87
8	5.46	2.94	10.08	7.56
9	11.76	3.36	13.02	5.04
10	14.91	3.36	10.29	22.68
11	6.93	4.41		24.15
12	11.97	5.04		23.73
13	11.34	6.93		8.61
14	11.34	6.72		15.96
15	15.75	6.09		10.08
Average	**10.77**	**4.03**	**11.36**	**14.59**
S.d.*	**2.84**	**1.59**	**4.63**	**6.74**
Mode	**11.97**	**2.52**	**10.29**	

*Standard deviation

Table 1.2: Microdroplet diameter (Chapter 4: section 4.4.1.5a)

Micro-droplet number	ELMMicro-droplet diameter (µm)			
	1:1[a]	**1:1**[b]	**1:2**[c]	**1:2**[d]
1	5.25	3.36	3.99	3.57
2	4.62	3.36	2.94	4.2
3	6.3	1.68	2.52	2.31
4	7.35	4.2	2.94	4.41
5	3.99	7.77	2.94	2.94
6	4.2	8.19	2.94	2.94
7	6.51	2.73	4.2	4.41
8	5.04	5.67	5.46	2.94
9	7.77	6.72	3.78	2.94
10	7.35	2.73	1.89	2.31
11	7.98	8.19	2.1	4.41
12	7.35	8.19	3.36	2.73
13	5.67	9.24	3.15	2.52
14	4.62	9.45	4.62	3.99
15	3.57	5.04	4.2	3.15
Average	**5.84**	**5.77**	**3.40**	**3.32**
s.d. *	**1.49**	**2.64**	**0.97**	**0.78**
mode	**7.35**	**8.19**	**2.94**	**2.94**

*Standard deviation

[a] Microdroplet size of the 1:1 ELM after storage at 22 ± 1°C for 12 hours.
[b] Microdroplet size of the 1:1 ELM after re-shaking and storage at 5 ± 2 °C for up to 24 hours
[c] Microdroplet size of the 1:2 ELM after storage at 22 ± 1°C for 12 hours.
[d] Microdroplet size of the 1:2 ELM after re-shaking and storage at 5 ± 2 °C for up to 24 hours

Table 1.3: Microdroplet diameter (Chapter 4: section 4.4.1.5b)

Micro-droplet number	ELMMicro-droplet diameter (µm)			
	1:1[a]	**1:1**[b]	**1:2**[c]	**1:2**[d]
1	3.15	4.41	4.2	4.62
2	2.52	3.78	2.31	2.1
3	3.36	2.52	3.57	2.73
4	2.52	3.57	3.15	4.41
5	2.73	2.1	3.36	3.57
6	2.73	3.57	2.73	1.89
7	2.31	4.41	3.36	1.68
8	4.62	4.62	2.94	2.73
9	5.04	2.23	3.57	3.36
10	2.31	3.31	2.73	2.1
11	2.73	5.67	3.99	2.52
12	2.36	3.42	3.36	2.53
13	3.17	2.76	3.36	3.87
14	3.3	2.13	2.94	2.14
15	2.93	4.15	3.36	2.93
Average	**3.05**	**3.51**	**3.26**	**2.88**
s.d.*	**0.80**	**1.04**	**0.49**	**0.91**
mode	**2.73**	**4.41**	**3.36**	**2.10**

*Standard deviation

[a] Microdroplet size of the 1:1 ELM after storage at 22 ± 1°C for 12 hours.
[b] Microdroplet size of the 1:1 ELM after re-shaking and storage at 5 ± 2 °C for up to 24 hours
[c] Microdroplet size of the 1:2 ELM after storage at 22 ± 1°C for 12 hours.
[d] Microdroplet size of the 1:2 ELM after re-shaking and storage at 5 ± 2 °C for up to 24 hours

Table 1.4: Microdroplet diameter (Chapter 4: section 4.4.1.6)

Micro-droplet number	Micro-droplet diameter (μm)					
	1:1[a]	**1:1**[b]	**1:1**[c]	**1:2**[d]	**1:2**[e]	**1:2**[f]
1	3.57	3.78	3.57	2.73	2.94	3.15
2	1.68	2.52	3.99	2.94	2.94	4.2
3	2.73	4.2	3.15	3.78	3.78	2.73
4	2.73	2.52	3.36	2.73	2.31	3.57
5	3.57	2.73	3.99	3.15	2.52	3.36
6	2.73	3.36	3.37	2.31	2.31	3.36
7	2.94	3.15	5.46	2.73	2.31	2.31
8	2.94	2.73	5.04	3.57	2.73	3.36
9	2.73	3.78	3.15	2.73	3.15	3.36
10	2.73	3.57	3.57	3.15	2.73	2.31
11	2.31	2.94	4.62	3.57	3.15	3.36
12	3.36	2.94	4.2	3.36	2.73	3.78
13	2.52	3.57	4.2	1.89	3.15	1.89
14	3.15	2.78	4.2	3.78	2.52	2.31
15	3.78	3.78	5.46	2.73	2.73	2.73
16	2.94	2.94	4.2	3.78	3.15	2.73
17	4.41	2.73	3.78	2.94	3.15	2.52
18	2.73			3.15	3.57	2.73
19	2.94			2.1	2.73	2.73
20				2.73	2.1	3.15
Average	**2.97**	**3.18**	**4.08**	**2.99**	**2.84**	**2.98**
s.d.*	**0.59**	**0.52**	**0.73**	**0.54**	**0.43**	**0.58**
mode	**2.73**	**3.78**	**4.20**			

*Standard deviation, [a] Microdroplet size of the 1:1 ELM right after manufacture, [b] Microdroplet size of the 1:1 ELM right after the 12 hour storage at 21 ± 2°C and reconstitution, [c] The changes

of the microdroplet diameter distribution after the storage of the reconstituted ELM at 5 ± 2°C for 24 hours of the 1:1 ELM, [d] Microdroplet size of the 1:2 ELM right after manufacture,
[e] Microdroplet size of the 1:2 ELM right after the 12 hour storage at 21 ± 2°C and reconstitution,
[f]The changes of the microdroplet diameter distribution after the storage of the reconstituted ELM at 5 ± 2°C for 24 hours of the 1:1 ELM

APPENDIX II: CONVERSION OF POTASSIUM HYDROGEN PHTHALATE TO COD CONCENTRATIONS

The KHP concentrations were converted to COD concentrations using the stoichiometry shown in equation below**.**

$$KC_8H_5O_4 + 7.5\ O_2 \longrightarrow KOH + 8\ CO_2 + 2\ H_2O$$

$$\frac{n(KHP)}{n(O_2)} = \frac{1}{7.5}$$

$$n(KHP) \times 7.5 = n(O_2)$$

$$\frac{n(KHP) \times 7.5}{m(KHP)} = \frac{n(O_2)}{m(O_2)}$$

$$\frac{n(KHP) \times 7.5 \times m(O_2)}{m(KHP)} \times \frac{1}{V} = n(O_2) \times \frac{1}{V}$$

V = Volume of solution

$$\frac{c\ (KHP) \times 7.5\ \times m(O_2)}{m\ (KHP)} = COD$$

$$c(KHP) = \frac{COD \times m(KHP)}{m(O_2) \times 7.5}$$

$$c(KHP) = \frac{204.22 \times COD}{32 \times 7.5}$$

$$c(KHP) = 0.85092 \times COD$$

$$c(KHP) = 0.85092 \times 100 mg/L = 85.1\, mg/L$$

$$c(KHP) = 0.85092 \times 500 mg/L = 425.5\, mg/L$$

$$c(KHP) = 0.85092 \times \frac{800 mg}{L} = 680.7 mg/L$$

Table 2.1: COD concentration equivalents to KHP

Concentration of COD	Concentration of KHP
100	85.1
500	425.5
800	680.7
1000	850.9
1500	1276.4
2000	1701.8

COD CALIBRATION CURVE

Table 2.2: The UV-Vis absorbances of for the calibration curve of COD

Concentration (mg/l)	A 1[a]	A 2[b]	A 3[c]	Mean A[d]	SD[e]
0.00				0.00	
100.00	0.14	0.12	0.14	0.13	0.01
500.00	0.35	0.45	0.33	0.37	0.07
800.00	0.56	0.48	0.47	0.50	0.05
1000.00	0.57	0.56	0.59	0.57	0.02
1500.00	0.75	0.76	0.77	0.76	0.01
2000.00	0.95	0.84	0.97	0.92	0.07

[a] First experiment of absorbance, [b] Second experiment of absorbance, [c] Third experiment of absorbance, [d] Average of absorbance and [e] Standard deviation

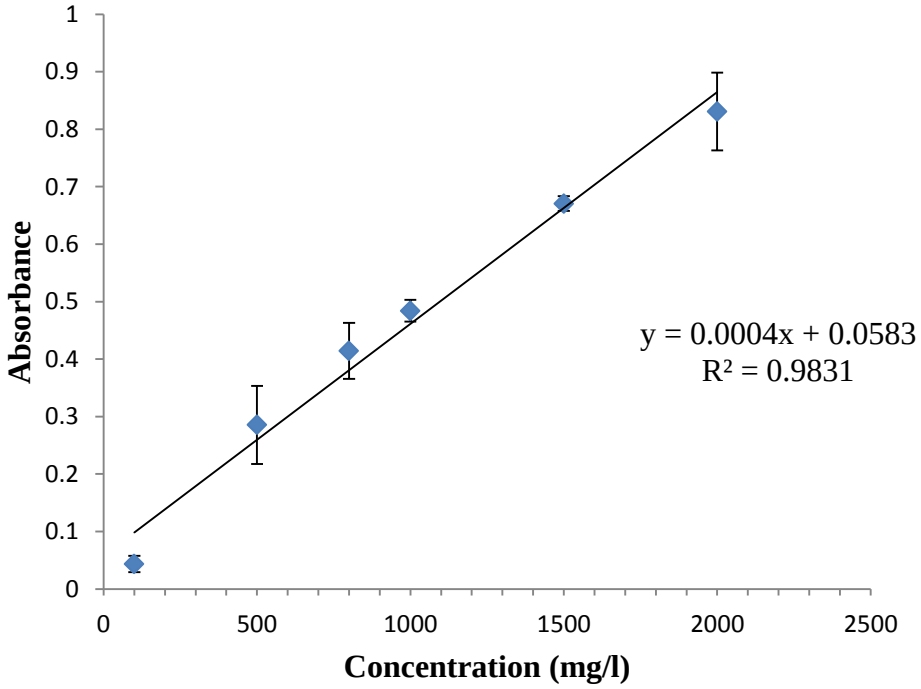

Table 2.3; Absorbance values of the aqueous phase of the emulsions containing 20 g/l PIB

Emulsion	PEG added (g)	Absorbance	COD concentrations (mg/L)
1	0	0.454	989.25
2	1	0.910	2129.25
3	2	1.244	2964.25
4	4	1.780	4304.25
5	6	2.630	6429.25
6	10	2.43	5929.25

Table 2.4: Absorbance values of the aqueous phase of the emulsions containing 30 g/l PIB

Emulsion	PEG added (g)	Absorbance	COD concentrations (mg/L)
1	0	0.422	909.25
2	1	1.215	2891.75
3	2	1.310	3129.25
4	4	1.930	4679.25
5	6	2.41	5879.25
6	10	1.810	4379.25

APPENDIX III: LOSS ON IGNITION (CHAPTER 7)

Loss on ignition (LOI)

Masses of the crucibles and the soil are recorded in table 1

Table 3.1: Change in mass of Kaolin during LOI procedure

Crucible no'	**Control**	**1**	**2**	**3**
Crucible	17.3318	19.4819	18.1345	19.8553
Crucible + soil/g	17.3318	24.4638	22.1351	24.8575
Crucible + soil after 105^{o}C /g	17.3317	24.4139	22.0896	24.8029
Crucible + soil after 400^{o}C/g	17.3317	24.4163	22.0889	24.7997
Mass of air-dried soil/g	0	4.9819	4.0006	5.0022
$^{a}m_s$/g	0	4.9344	3.9551	4.9476
$^{b}m_c$/g	0	4.9320	3.9544	4.9444
$^{c}\Delta m$/g	0	0.0024	0.0007	0.0032
LOI (%)	0	0.0098	0.0032	0.0129

[a] M_S is kaolinite dry weight at 105 ^{o}C ,

[b] M_C is mass of kaolinite after ignition at 400 ^{o}C.

[c]$\Delta m(g)$ *is* loss of mass after ignition,

$$Average\ LOI = \frac{0.0098 + 0.0032 + 0.0129}{3} = 0.0086 \pm 0.004$$

APPENDIX IV: BATCH EQUILIBRATION (CHAPTER 7)

1. Sorption of TOA

Table 4.1: Sorption of TOA onto 10 g of kaolinite of particle size 101-400 µm

Time (Hours)	% Removal Batch 1	% Removal Batch 2	% Removal Batch 3	Average % Removal	Standard deviation
0.5	0.3	0.5	0.7	0.5	0.2
1	1.7	1.8	1.4	1.6	0.2
2	3.2	3.6	2.9	3.2	0.3
4	4.3	3.9	5.0	4.4	0.5
8	5.8	5.4	6.2	5.8	0.4
16	7.2	6.5	7.7	7.1	0.6
24	7.1	6.4	8.4	7.3	1.0
36	9.8	8.9	10.3	9.7	0.7
48	10.7	10.6	11.3	10.8	0.4
60	13.0	13.8	13.5	13.4	0.4
72	14.3	13.9	13.5	13.9	0.4
96	15.3	13.9	15.5	14.9	0.9
120	16.6	14.9	15.9	15.8	0.9
144	17.1	17.3	17.8	17.4	0.4
168	17.5	17.7	17.1	17.4	0.3

Table 4.2: Sorption of TOA onto 20g of kaolinite of particle size 101- 400 µm

Time (Hours)	% Removal Batch 1	% Removal Batch 2	% Removal Batch 3	Average % Removal	Standard deviation
0.5	3.4	4.6	2.9	3.6	0.8
1	7.1	7.8	9.1	8.0	1.0
2	10.1	11.1	10.8	10.7	0.5
4	14.0	14.5	13.8	14.1	0.4
8	15.4	15.7	15.1	15.4	0.3
16	14.1	15.5	16.1	15.2	1.0
24	18.0	16.6	17.8	17.5	0.7
36	18.9	19.2	19.6	19.2	0.3
48	21.9	20.9	22.1	21.6	0.6
60	21.2	21.5	21.9	21.5	0.3
72	23.0	22.9	22.7	22.9	0.2
96	25.7	25.1	24.3	25.0	0.7
120	31.1	30.4	30.7	30.7	0.3
144	33.0	32.8	32.5	32.8	0.2
168	33.3	32.9	33.5	33.2	0.3

Table 4.3: Sorption of TOA onto 20 g of kaolinite of particle size 65-100 µm

Time (Hours)	% Removal Batch 1	% Removal Batch 2	% Removal Batch 3	Average % Removal	Standard deviation
0.5	1.7	1.2	1.9	1.6	0.4
1	3.7	3.5	4.0	3.7	0.2
2	8.7	7.6	7.9	8.1	0.5
4	10.6	11.5	9.3	10.5	1.1
8	13.0	13.1	11.9	12.7	0.7
16	19.6	20.9	20.1	20.2	0.6
24	21.9	21.3	22.5	21.9	0.6
36	21.0	21.6	20.1	20.9	0.8
48	23.8	22.4	24.3	23.5	1.0
60	23.0	25.5	24.4	24.3	1.2
72	26.0	27.7	27.8	27.2	1.0
96	30.4	28.9	29.3	29.5	0.8
120	35.0	33.5	34.8	34.4	0.9
144	35.0	36.1	35.9	35.7	0.6
168	35.8	35.7	35.9	35.8	0.1

2. Sorption of THA

Table 4.4: Sorption of THA onto 20 g of kaolinite of particle size 101- 400 µm

Time (Hours)	% Removal Batch 1	% Removal Batch 2	% Removal Batch 3	Average % Removal	Standard deviation
0.5	2.0	3.1	2.5	2.5	0.5
1	2.6	2.8	4.0	3.1	0.7
2	3.0	5.1	4.0	4.0	1.0
4	4.4	6.1	6.4	5.6	1.1
8	7.2	6.9	8.3	7.5	0.7
16	11.3	13.2	10.6	11.7	1.4
24	13.4	13.6	11.9	13.0	1.0
36	14.3	18.1	12.7	15.0	2.8
48	21.4	21.3	17.7	20.1	2.1
60	25.1	25.1	21.7	24.0	2.0
72	25.7	25.8	24.9	25.5	0.5
96	28.6	27.2	26.3	27.4	1.2
120	28.7	28.3	29.6	28.9	0.7
144	28.6	27.7	29.4	28.6	0.9
168	28.6	28.6	29.3	28.8	0.4

Table 4.5: Sorption of THA onto 20 g of kaolinite of particle size 65- 100 µm

Time (Hours)	% Removal Batch 1	% Removal Batch 2	% Removal Batch 3	Average % removal	standard deviation
0.5	2.1	2.4	2.5	2.4	0.2
1.0	2.6	2.5	2.8	2.6	0.2
2.0	2.8	2.6	3.0	2.8	0.2
4.0	5.8	6.2	5.0	5.6	0.6
8.0	9.3	10.5	7.9	9.2	1.3
16.0	10.0	12.4	10.8	11.0	1.2
24.0	14.4	18.8	16.4	16.5	2.2
36.0	17.0	20.4	18.5	18.6	1.7
48.0	19.4	18.8	23.6	20.6	2.7
60.0	22.9	24.3	25.3	24.2	1.2
72.0	24.4	26.0	26.4	25.6	1.1
96.0	27.1	28.4	27.7	27.7	0.6
120.0	27.7	26.8	29.4	27.9	1.3
144.0	33.0	29.0	26.0	29.3	3.5
168.0	32.8	28.8	26.4	29.3	3.3

APPENDIX V: EFFECT OF TEMPERATURE ON THE ELMS

Effect of increasing temperature on the ELMs

1. micro-droplet size at 40 ± 1 ˚C

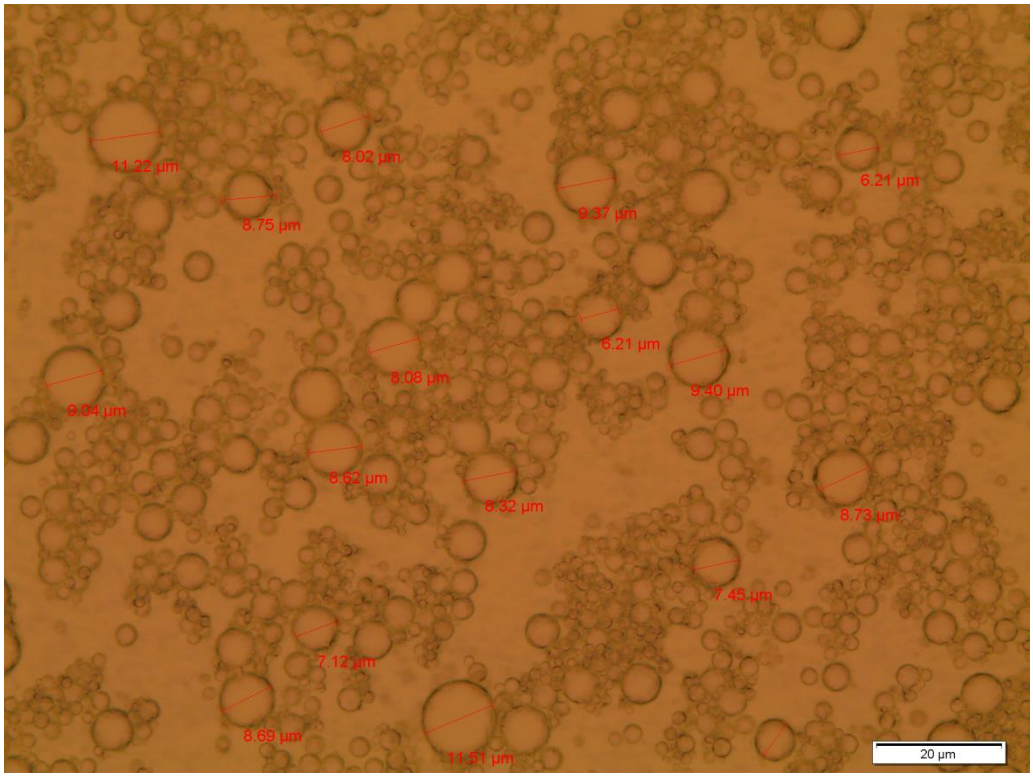

(b)

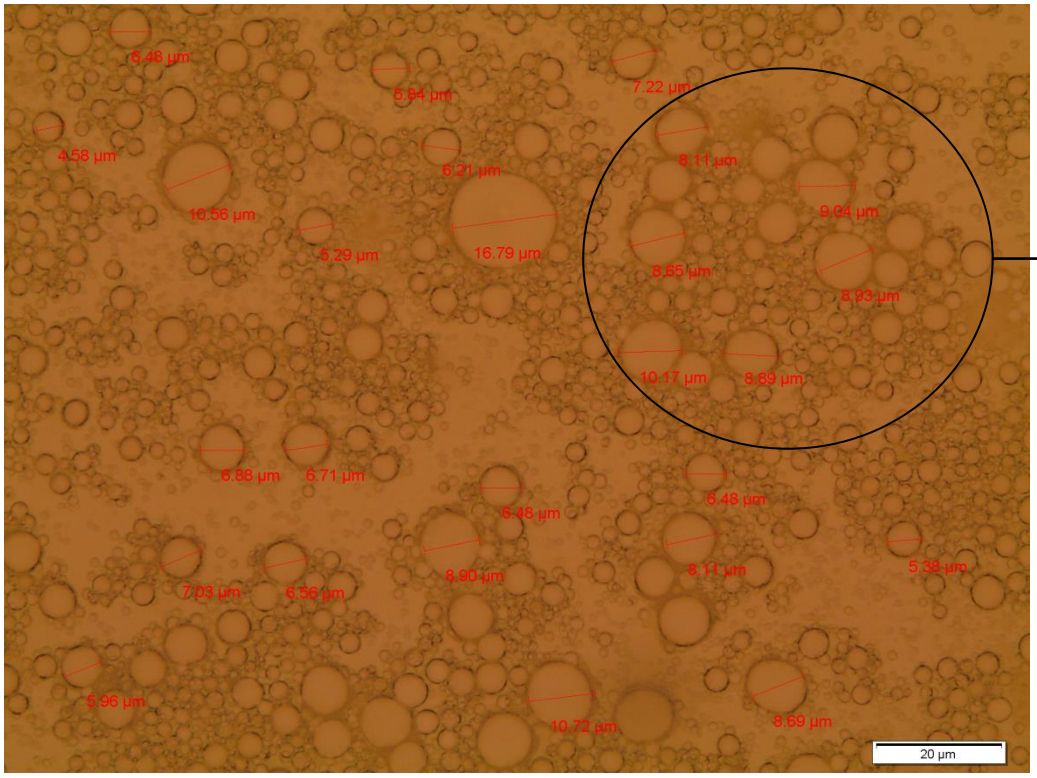

Coalescence

(c)

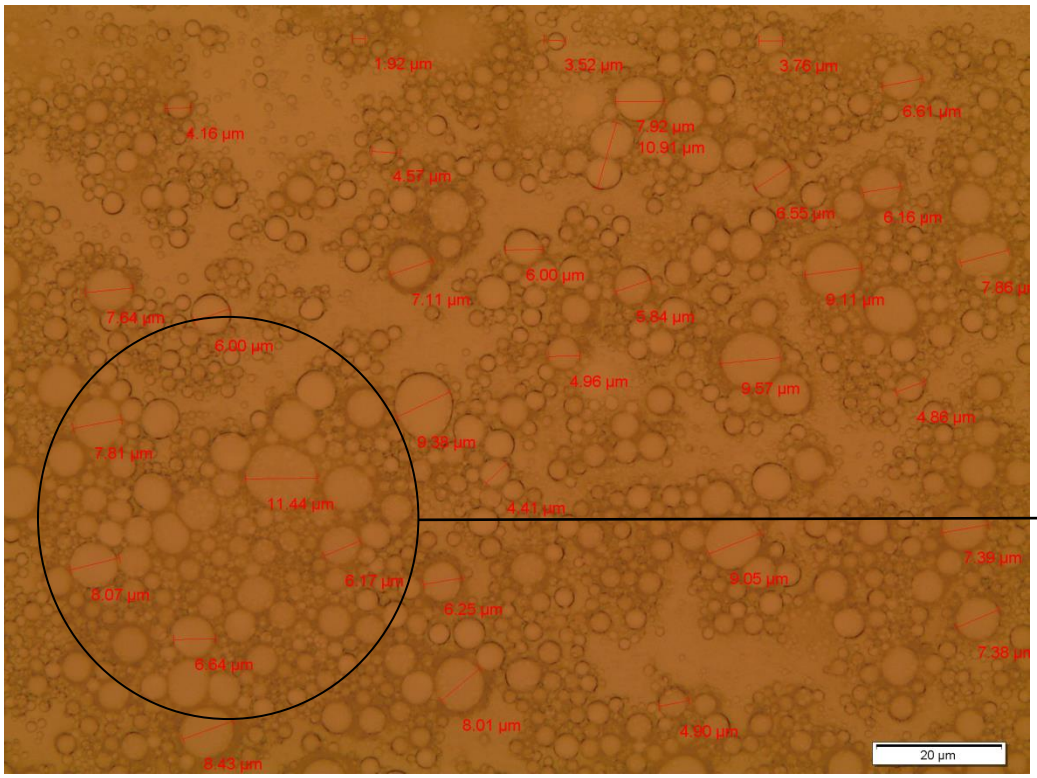

Coalescence

(d)

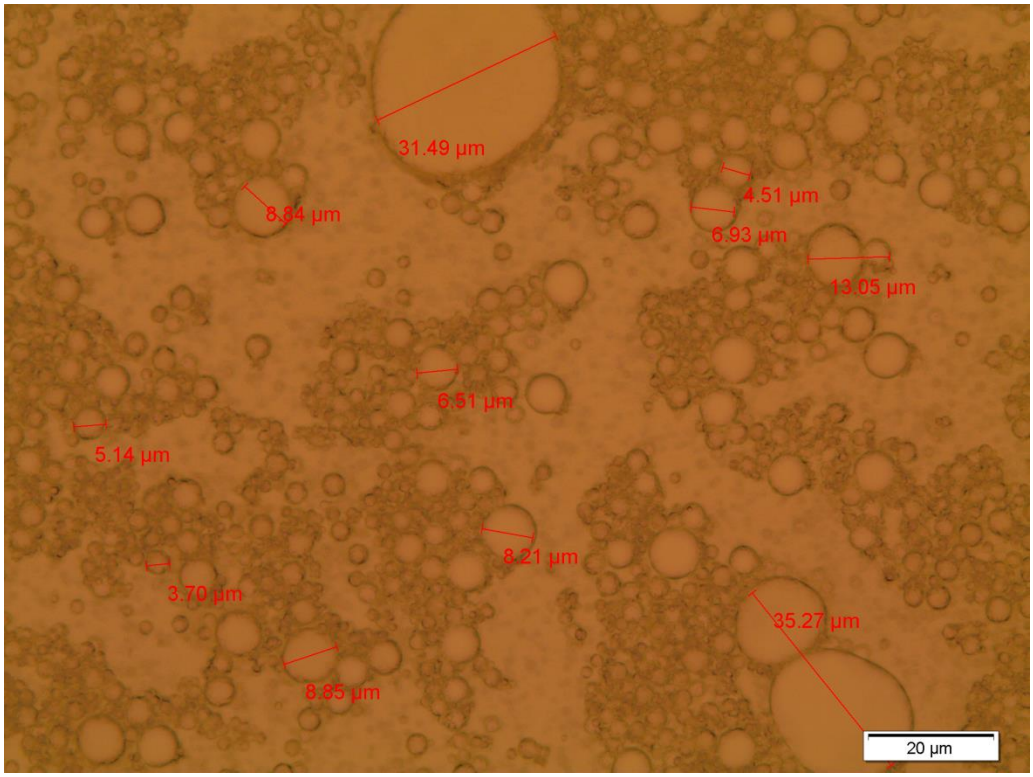

(e)

Fig AP 1; (b) The micro-droplet sizes of ELM at 40 ˚C after 10 minutes (c) The micro-droplet sizes of ELM at 40 ˚C after 15 minutes (d The micro-droplet sizes of ELM at 40 ˚C after 20 minutes (e) The micro-droplet sizes of ELM at 40˚C after 30 minutes

2. micro-droplet size at 50˚C ± 1 ˚C

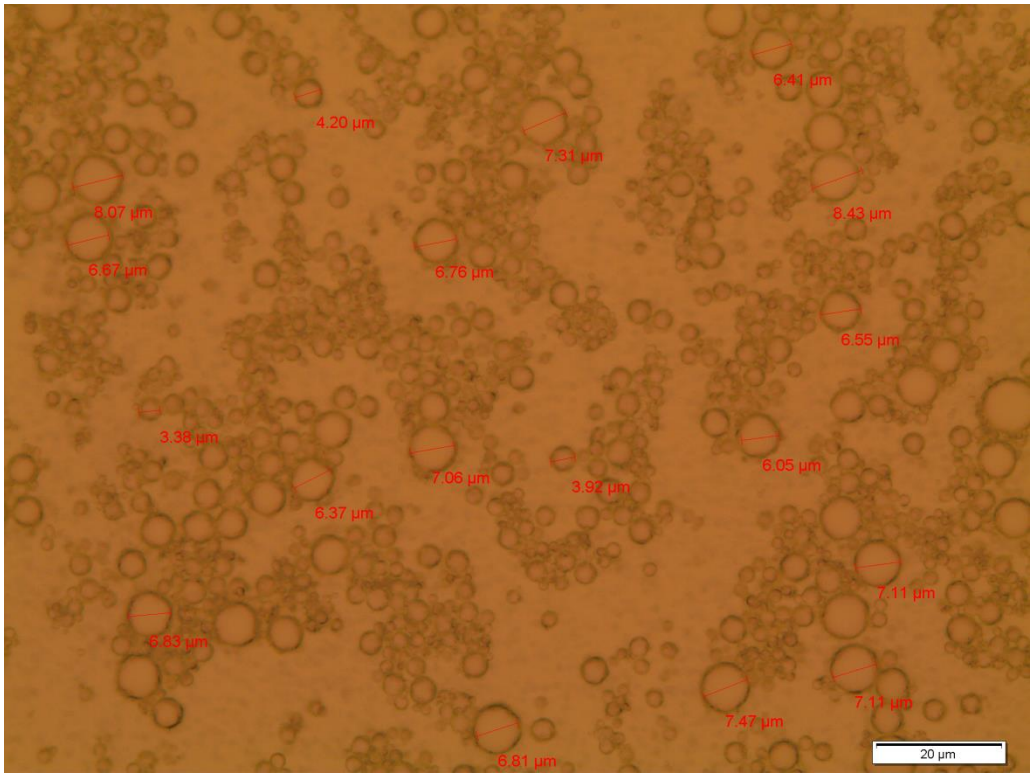

(b)

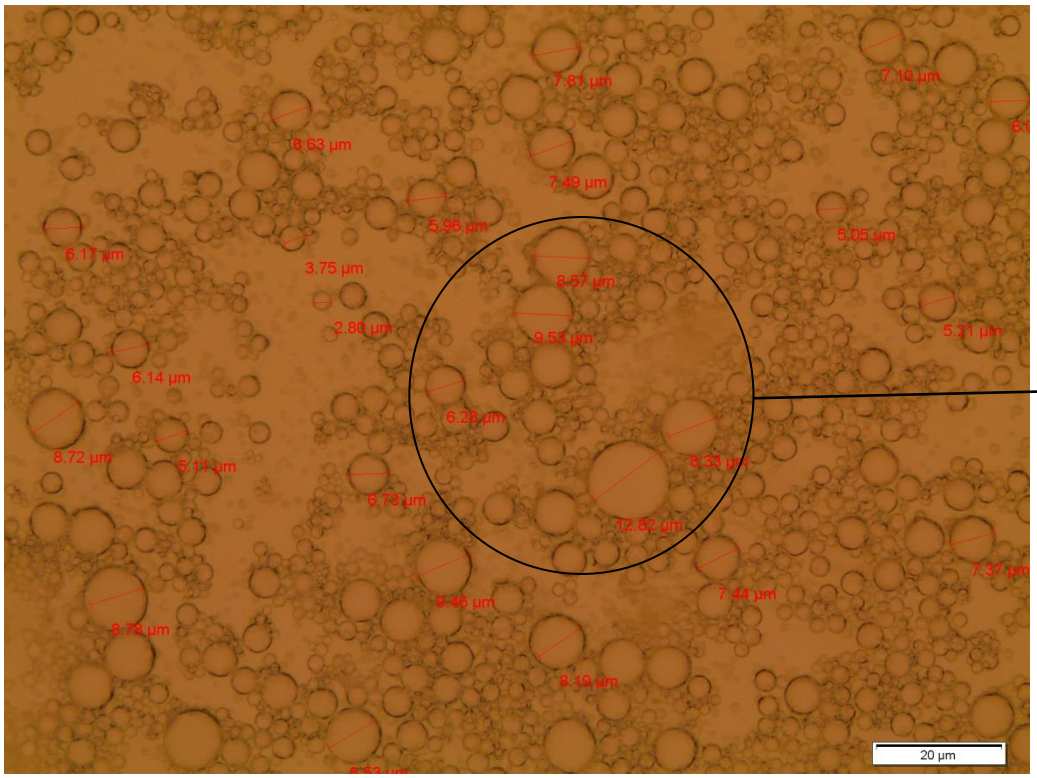

Coalescence

(c)

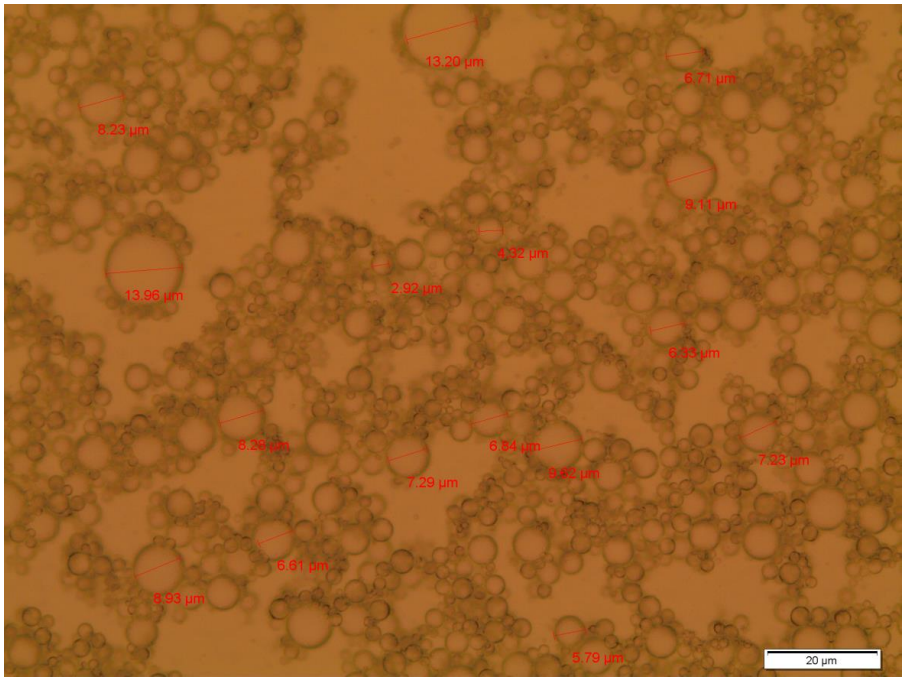

(d)

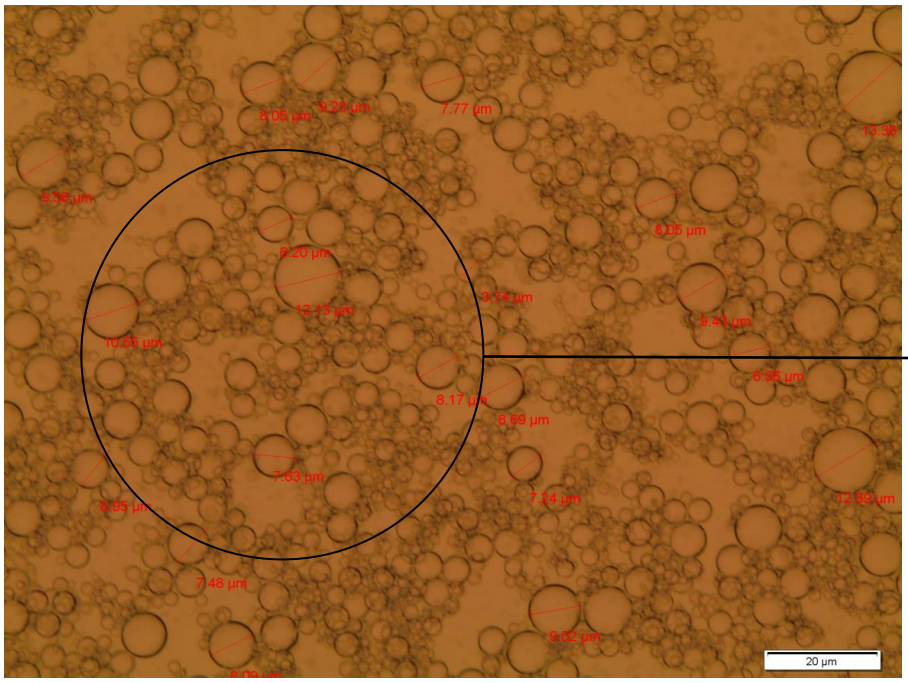

Coalescence

(e)

Fig AP 2 (b) The micro-droplet sizes of ELM at 50 ˚C after 10 minutes (c) The micro-droplet sizes of ELM at 50 ˚C after 15 minutes (d The micro-droplet sizes of ELM at 50˚C after 20 minutes (e) The micro-droplet sizes of ELM at 50 ˚C after 30 minutes